Seismic response analysis of steel plate shear wall systems using detailed and simplified models

Arghya Kamal Chatterjee

A Thesis
in
The Department of
Building, Civil & Environmental Engineering

Presented in Partial Fulfillment of the Requirements
for the Degree of Master of Applied Science (Civil Engineering) at
Concordia University Montreal, Quebec Canada

April, 2013

CONCORDIA UNIVERSITY
School of Graduate Studies

This is to certify that the thesis prepared

By: Arghya Kamal Chatterjee

Entitled: Seismic response analysis of steel plate shear wall systems using detailed and simplified models

and submitted in partial fulfillment of the requirements for the degree of

MASc Civil Engineering

complies with the regulations of the University and meets the accepted standards with respect to originality and quality.

Signed by the final examining committee:

Dr. Khaled Galal Chair

Dr. Rama Bhat Examiner

Dr. Lucia Tirca Examiner

Dr. Ashutosh Bagchi and Dr. Anjan Bhowmick Supervisor

Approved by _____
Chair of Department or Graduate Program Director

_____
Dean of Faculty

Date _____

ABSTRACT

Seismic response analysis of steel plate shear wall systems using detailed and simplified models

Arghya Kamal Chatterjee

Ductile Steel Plate Shear Walls (SPSWs) have been accepted widely as a very effective lateral load resisting system. However, their use in retrofit works is very limited because of the design inefficiency arising from the use of thicker than required commercially available infill plates. Consequently the ductility demand for the surrounding framing members is higher than required. SPSWs utilizing light-gauge cold-formed infill plates could be a viable alternative for rehabilitation of seismically deficient buildings. This thesis presents a numerical study using finite element models on the behavior of unstiffened light-gauge steel plate shear walls with welded infill plate connection. The detailed finite element models include both material and geometric non-linearity. This research describes in detail the validation of the key finite element models by comparing the results with that from the available experimental studies. Excellent correlation between the test results and the finite element analysis results has been achieved.

For seismic performance evaluation of a multi-storey building with SPSWs, detailed finite element models or a strip model can be used to represent the SPSW components. However, development and analysis of such models often require undesirable effort and excess time for

high-to-medium rise buildings. A simplified model is developed in this research to study the behavior of SPSW system. In the simplified model, discrete elements are used for the framing members and the behavior of the infill plate is represented by equivalent diagonal bracing members. The simplified model, Equivalent Braced Model, is developed through repeated static and dynamic validations with experiment and detailed finite element models. The proposed Equivalent Braced Model would facilitate a simplification to the structural modeling of large buildings with SPSWs in order to evaluate the seismic performance using regular structural analysis tools and can prove to be a potential aid in performance-based seismic design of SPSW buildings. Finally, the developed equivalent braced model and the detailed finite element model are used to analyze three multi-storey light-gauge SPSWs (four-storey, six-storey and ten-storey) designed according to the capacity design approach.

ACKNOWLEDGEMENTS

To begin with this chapter of thanks I would like to pay my gratitude to my supervisors, Dr. Ashutosh Bagchi and Dr. Anjan Bhowmick. Without their endless help this research would have never started or taken into shape. All through my stay as a part of Concordia University, both on and off the record, their support and supervision has helped me complete this great chapter in my life. I am thankful to them for their endless time and enlightening lectures that helped me to widen my area of interest and knowledge.

I am also thankful to Concordia University team of professors who made my stay as a student in this university an unforgettable one. Special thanks to my course instructors Dr. Kinh H. Ha, Dr. Lan Lin and Dr. Jassim Hassan. Their support in class particularly related to Finite Element Methods acted as pillars on my research background.

Nothing would have been possible without the endless love and support of my parents. They are the foundation to whatever I have done and will do in future. Their words of wisdom and love always kept me going. Whenever things seemed impossible, it's their encouragement and mental support that showed a new way out. Thank you for being so optimistic and I will be in eternal debt for whatever I have derived so far from you all. Also, thanks to my extended family for all the indirect help and support that I have derived so far. I feel lucky to have a big family support comprising you all. Love you all.

Last, but not the least, thanks to all my colleagues and friends, especially Ram Adhikari, Rasha Ibrahim and Gurinderbir Singh Sooch, for making my graduate studies so memorable. Wish you all the best in your future endeavors. Hope to stay in touch with you all and derive help as always.

TABLE OF CONTENTS

List of Figures

List of Tables

List of Symbols

L_1	Centre to centre length of SPSW panel
H	Centre to centre height of SPSW panel
b	Thickness of plate
A_c	Cross-sectional area of column
I_c	Second moment of inertia of column
W	Gravity load on SPSWs
W_y	Axial yield load of SPSWs
δ	Top displacement
V	Shear load on SPSWs
V_y	Shear yield capacity of SPSWs
σ_{yc}	Column yield stress
ε_{yc}	Column yield strain
σ_y	Infill-plate yield stress
ε_y	Infill-plate yield strain
E	Young's modulus of steel
Δ_{imp}	Maximum imperfection of infill-plate
α	Angle of orientation of tension strips (tension field) with vertical
A_b	Cross-sectional area of beams
I_b	Second moment of inertia of beams
S	Width of tension field
h	Height of infill plate

l	Length of infill plate
φ	Angle of diagonal brace with horizontal
A_d	Area of diagonal brace
A_{ver}	Area of vertical boundary member in braced model
L_d	Length of brace connecting centre to centre of beam column joints
d_c	Depth of column section
I_{pl}	Second moment of inertia of infill-plate
I_m	Modified second moment of inertia of infill-plate
A_{pl}	Cross sectional area of infill plate
Q	Static moment of area with respect to neutral axis
α_b	Ratio of post-buckling stiffness to pre-buckled stiffness of infill plate in bending
α_s	Ratio of post-buckling stiffness to pre-buckled stiffness of infill plate in shear
σ_{norm}	Nominal stress
ε_{norm}	Nominal strain
σ_{true}	True stress
R_d	Ductility related force modification factor
R_o	Over-strength force modification factor
β_1	Ratio of thickness of plate to the diagonal length of the plate
β_2	Aspect ratio of plate
M	Slope of line relating α_s and β_1
M	Poisson's ratio
I	Second moment of inertia for transverse section of infill plate
G	Shear modulus

K	Stiffness of the member
L	Diagonal length of infill plate
α_m	Capacity increase factor of infill plates for the presence of boundary members
β_3	Column flexibility parameter
A_1, B_1, C_1	Polynomial constants
X_1, X_2, X_3	Polynomial constants
F_{buckle}	Force at which infill plate buckles
Δ_{buckle}	Top displacement of infill plate corresponding to buckling load
γ	Angle of inclination of the brace with vertical column
α_{bal}	Balancing factor for inter-storey forces
E_{brace}	Modified Young's modulus for braces
Δh_b	Length of plastic elongation in brace
Δh_p	Length of maximum plastic elongation of infill plate
β_4^i	Ratio of web thickness of bean to that of connecting infill plates for i^{th} storey
α_k	Ratio of maximum plastic deformation of brace to that of infill plate

Chapter 1. Introduction

1.1 General Overview

Through decades of research Steel Plate Shear Wall systems have proved to be an effective method for dissipation of energy due to lateral forces. Use of SPSW has gained ground with development on its efficient design techniques. It has proved to be more efficient and economical than a regular moment-resisting frame (Timler et al. 1998). Primarily, an SPSW consists of bounding beams and columns, collectively known as boundary members, and infill plate. Fish-plates are normally used in connecting the thin infill plates to the boundary. Like any other normal shear wall, there is no restriction to the number of connected panels being constructed as SPSW systems.

A notable feature in SPSW system is the infill plate buckling with application of very small lateral load. This is primarily due to imperfections introduced during construction. However, research has indicated that even after buckling infill plates have sufficient capacity to develop tension fields and provide lateral strength to the structure. The main efficiency of SPSW lies in tension yielding of infill plates allowing sufficient dissipation of energy during extreme load events like intense earthquakes. High redundancy and robustness of infill-plate allows the development of load path even though some other part of the plate has failed. This significantly increases the capacity and ductility of SPSW systems. According to National Building Code of Canada (NBCC 2010), SPSW system has the highest ductility amongst commonly used structural lateral load resisting systems. High strength to weight ratio makes the SPSW system a preferred

choice in industries as compared to reinforced concrete shear wall systems. SPSW application has extended from new buildings to rehabilitation of an existing steel or reinforced concrete buildings.

1.2 Motivation and Background

Design philosophy developed for SPSW system was initially based on prevention of buckling by using very thick plate, which gave rise to uneconomic design sections. However, it was replaced by a new concept where similarity of SPSW system was observed with vertical plate girder. The bounding columns were to represent flanges of similar girder and the plate was considered as the web of the girder. Beams at every storey height were approximated as transverse stiffeners connecting the flanges of web girder. To this new concept post-buckling strength of plates was incorporated. Due to buckling the load transfer mechanics in infill plate changes from in-plane forces to inclined forces responsible for the formation of tension field in the infill plate. Thus SPSW does not lose its load carrying capacity and the shear is resisted by the inclined tension field. Introduction of post-buckling strength in design of SPSW systems involved lot of experimental and analytical research. With time and more research it has been repeatedly reported that stable hysteretic curves and consistent pushover curves are achievable with steel plate shear wall system. This indicated a wider acceptability of SPSW in construction of earthquake resistant design. Canadian Standard on Limit State Design of Steel Structures (CSA-S16-09) has also provided guidelines for analysis and design of ductile SPSW system.

To have the optimum performance advantage on use of infill plates in any SPSW system, yielding of the plate should be completed before yielding of any boundary member starts. Thus, the maximum energy will be dissipated by infill-plate of a SPSW system. To allow complete development of tension fields in infill plate, CSA-S19-09 indicates that the boundary members should have sufficient capacity. If plates thicker than design specifications are put to use then it will not just be uneconomical but also the desired yielding sequence of members might change i.e. instead of plate yielding first, boundary member might start to yield. For high rise buildings the desired thickness of infill plate in upper stories is so small that hot-rolled plates of desired thickness are normally not available (Berman et al., 2005). Thus, either cold-rolled steel is preferred or areas of weakness are introduced in thicker plates by cutting holes. CSA-S16-09 also imposes some restriction on the area cutouts of infill-plate. With the same purpose of maintaining a proper yielding sequence, some researchers have indicated the use of reduced beam sections. Out of all mentioned solutions the simplest one is to use of light-gauge steel as infill-material. Limitation with use of light-gauge steel is mainly in welding of plates to its boundary and also, lack of study done so far in properly establishing the design acceptability. Neilson (2010) worked out a solution on the welding problem and some experimental study has already been performed (Kharrazi 2005). However, limitation on availability of research in numerical study of SPSWs using light-gauge steel as infill plate still exists.

Several numerical modeling techniques have been suggested to achieve the design requirements of SPSW system. One of the first and most successful modeling techniques

was proposed by (Thronburn et al., 1983), known as strip model. Since the behavior of buckled infill plate is similar to a bunch of similar parallel strips, in strip model, the infill-plate can be replaced by parallel tension strips of pre-calculated stiffness. Till date a lot of modeling technique has been proposed by research communities which are both very approximate and not necessarily reliable or are computationally very expensive. Demand of more research in this area of simplified modeling for SPSW systems is directly implicated in current scenario.

1.3 **Objectives and Scope**

Limited availability of research in the field of Steel Plate Shear Wall systems, opens up a wide area of interest for researchers. Broadly speaking there are two highlighted areas where more research is demanded. Firstly, to test numerically the acceptability of light-gauge steel infill plates in SPSW systems based on currently available design techniques. Secondly, develop simplified model for analysis of SPSW systems. Establishment of the second objective will also facilitate in completion of the first objective, since several repeated numerical study is expected to successfully come up with reliable results and indicate the acceptability of available design techniques in light gauge steel late shear wall systems.

Developed design provisions for SPSW systems, currently available in standard codes, is primarily based on research on hot-rolled sections. Though some recent experimental work on light-gauge has been reported, they are just not enough for incorporation in the standard. Lot more research mainly numerical has to be carried out to

comment on the feasibility of acceptable design technique. Change in the nature of steel from hot-rolled to cold-rolled light-gauge for the infill plate may or may not have an effect in real SPSW systems. Almost, reported experiments were limited to static tests on single storey structures. Owing to experimental limitations for carrying out several test on multi-storey structures, numerical tests needs to be carried out. Through this research some multi-storey structure designed as per available code guidelines has been made but instead of hot-rolled steel, light-gauge steel was used as infill plate. The structures were also subjected to dynamic tests by applying several scaled ground motions. Finally, it has been determined whether the structural behavior is acceptable based on provisions given in NBCC2010.

One of the expected problems for the previous set of analysis would be the length of time required for each analysis. To test several multi-storey SPSW structures with several ground motions numerically, analysis time becomes a big criterion when every analysis is performed with detailed modeling technique. So, a simplified numerical modeling technique needs to be established which not only helps in research but also in industries where repeated analysis is involved. As already mentioned, several simplified modeling technique has already been attempted. But most of them are either very approximate or more time consuming. Also, hardly any attempt on simplified modeling technique has been done where the model is suitable for dynamic analysis using real time ground motion records. So, a reliable, relatively accurate modeling technique with which even time history analysis can be performed needs to be developed. Through this research a statistical attempt has been made such that a braced model with modified properties of

the braces can successfully represent the complex plate model. Several validations have been carried out to judge the acceptability of the new proposed modeling technique.

1.4 Thesis Organization

The work on this thesis is primarily segmented into seven chapters beginning with the introduction of Steel Plate Shear Wall systems. A brief description of the current problem scenario on SPSW design along with the scope and objective of this thesis is described through chapter one.

Chapter two presents the literature review part in which the background of research objective is made. The state of the art research in light-gauge steel plate shear walls and simplified modeling of SPSW have been discussed in details. In terms of simplified modeling technique development, the limitations and workability of so far available models will be highlighted.

Chapter three describes the methodology for the development of the new modeling technique. Outline on the finite element modeling technique that will be used in this study have also been mentioned in this chapter.

Chapter four discusses in details the development of detailed FE model. Validation of the detailed FE model against available experimental results is presented in this chapter. Also, a series of time history analysis is carried out using the discussed modeling technique.

Development of simplified braced model is presented in chapter five. A detailed parametric study, as presented in this chapter, is conducted to develop the braced model. A brief study on existing models is also carried out in this chapter.

In Chapter six, a detailed validation on the newly developed simplified model of SPSWs is carried out. The braced model is first validated for available quasi-static tests. In addition, a series of light gauge steel shear walls are designed and analyzed using both the detailed and the simplified equivalent braced model. Results from the detailed FE model are compared with the results obtained from simplified braced model.

In chapter seven, both the finite element model and the equivalent braced frame model are utilized to study a set of multi-storey SPSW structures with light-gauge steel infill plates. The results from nonlinear static and seismic analysis are used to assess the applicability of seismic design guidelines of ductile SPSWs for light-gauge steel shear walls.

Finally, in chapter eight, a summary and key conclusions, as well as recommendations for future research, are presented.

Chapter 2. Literature Review

2.1 General Overview

Research on steel plate shear walls has been going on for the last forty years. Around 1960s Japan first introduced steel plates to use in buildings as shear walls. At that time owing to the limitation of research in this new area, highly stiffened steel plates were used since under design loads buckling was considered as failure of the plates. With time several analytical and experimental studies have been carried out to investigate the behavior of Steel Plate Shear Wall (SPSW) systems. With development in research it was concluded that buckling is not the ultimate failure of plates. The tension field developed in plates after bucking is also capable to resist shear. This usable post-buckling strength widened the applicability of SPSWs and soon SPSW became a more popular structural system in construction particularly in USA and Japan. Particularly places where dissipation of lateral forces is a concern, SPSW made its way. For high seismic region, where higher ductility is the prime requirement for the lateral load resisting system use of SPSW in structures can be at a very effective and economic solution.

Proper technique for utilizing the post buckling strength and a methodical approach for analysis of SPSW was first suggested by Thorburn et al. (1983). When buckling starts in steel plate the in plane tension field becomes inclined tension field i.e. from linear behavior the plate behavior changes to geometrically non-linear behavior. The concept and formulation introduced by Thorburn has later been acknowledged by Canadian Steel Design Standards (CAN/CSA-S16-01) and was accepted as a standard method for analysis. This concept of diagonal tension field being formed in buckled plates under shear was first introduced by Wagner (1931). Wagner's

theory indicated that the capacity of thin plate being supported by relatively stiff boundary members depend largely on the parallel tension fields being developed. Other researchers like Kuhn et al. (1952) tried to establish a proper relation on how the flexibility of boundary members limited the complete development of tension fields in plates. Their work was mainly on plate girders. Research indicated similarity in behavior of plate girders and SPSW systems. Initial proposal for design technique of SPSW was based on the assumption that columns of SPSW system behave as flanges of a plate girder and the infill plate as web of the girder. Also, beams in SPSW system act as stiffener plates connecting the two flanges and attached to web of girder. The modern design technique is an evolution from this theory. However, with time even more complicated models of Finite Element Method (FEM) came up (like Elgaaly et al., 1993, Driver et.al, 1997) which are normally more accurate and reliable but time expensive technique. For cyclic load test or test of structure with several ground motions where performance based design philosophy is involved, none of the models described so far (Thorburn et al. (1983), Elgaaly (1998), Mohammad et al. (2003), Bhowmick et al. (2010), Kharrazi et al. (2004), Topkaya and Atasoy (2009)) in this area of research is very effective.

Berman et al. (2005) indicated that for low rise structures and for the upper stories of high rise structures the infill plate thickness required for the seismic design loads is less than 1mm. Practically, achieving this thickness with hot rolled steel becomes impossible. Also, handling and welding demands a higher thickness. If the thickness of infill plate is increased, then instead of plates yielding first, the boundary members start to yield when design loads are exceeded. This contradicts the capacity design philosophy. Vian et al., (2005) proposed a solution to this problem by introducing areas of weakness within the plates like quarter circle corner cutoffs and

openings. Using cold rolled steel is another solution to the thickness problem, since cold rolled steel can be made thinner. The main problem faced with cold rolled steel was welding of such thin plates. Neilson (2010) documented the welding requirements while using cold-rolled SPSW of thickness less than 1mm. There have been some experimental tests on light gauge thin-walled SPSW systems (Kharrazi (2005), Neilson (2010)) but hardly any analytical study to determine the acceptability of light gauge infill plate in SPSW system design is available. If a convenient, fast, reliable and easy to use modeling technique is available to determine the acceptability of SPSW systems on case specific basis then its industrial acceptability is expected to widen up. A brief review relating to research works done in relation to modeling of SPSW systems analytically and use of light gauge thin plate shear wall, around the world has been presented in the following.

2.2 **Establishing property of SPSW systems**

To develop any new modeling technique or comment on the acceptability of available design techniques for steel plate shear walls, it is necessary that a detailed study on all the parameters responsible for the complete behavior of SPSW systems is carried out. Analyzing individual parametric properties of SPSW systems as reported through earlier studies by various authors on basis of experimental or numerical studies creates the background for the objective of this research.

Thorburn et al. (1983) works can be regarded as one of the first to give a comprehensive estimate on the behavior of unstiffened steel plate shear wall systems. Through this research it was indicated clearly that buckling does not indicate the ultimate failure of infill plates in SPSW

system. Wagner's (1931) theory in development of tension field was utilized to explain the tension strip development in panels. Strength of infill plates prior buckling was considered negligible in comparison to the strength that the tension strips can provide. In other words, rather than considering the buckling as failure of plates, shear strength prior to buckling of plate was neglected. The tension fields that dominate the post-buckling strength were considered to be the only load transferring path and thus came up a strip model that can estimate the SPSW behavior. A parametric study with the basic parameters like plate thickness, aspect ratio, column flexibility, etc. was conducted. It was concluded that the parameters are interdependent on one another and their interactions are complex. This exposed bigger challenges for upcoming researchers through next few decades. Following the works of Thorburn et al. (1983), several other attempts were made to establish a set of independent parameters that can predict the behavior of SPSW systems. Tromposch and Kulak (1987) made an important conclusion based on their experimental work that eccentricity involved in fixing fish plate had no significant effect on performance of SPSW specimen. They also attempted to investigate the effect of beam column connection and concluded that the experimental model was somewhere in between fixed and pinned connection. It was also concluded that increasing the connections to rigid beam-column has a significant increase in energy absorption capacity of the system.

With the objective of evaluating the overall in-plane performance of shear wall under extreme cyclic loading Driver et al. (1997, 1998) tested a half-scale four-storey unstiffened steel plate shear wall (Figure 2.2). All connections in the specimen were made rigid and the infill plate was welded to the boundary framing members using a fish plate. For pre-stressing the members constant gravity load was applied on top of columns. Cyclic load of constant magnitude was

applied at every floor level. Also, the cyclic test was carried out according to the requirements of ATC-24 (Applied Technology Council 1992). First storey displacement was used as control point for the loading. Initially the first yield displacement load was applied and then in consecutive cycles the yield displacement was increased. Up to a maximum of five times the first yield displacement the structure could resist increasing loads. Gradual and stable strength reduction was observed after ultimate strength (3080 KN) was achieved. The maximum deflection attained by the lowest storey, beyond which the structure failed, was nine times the yield deflection. A total of 30 cycles of load were applied out of which almost 20 were in the inelastic range. Hysteretic curves are also observed to be very stable throughout the experiment (Figure 2.1). It was concluded from the experiment that rigid beam column connections are capable of dissipating more energy than that of shear beam to column connections (Thromposch and Kulak 1987), since severe shear pinching of hysteretic loops were significantly less with rigid connections. This research also inferred that for specimens tested the angle of inclination of tension field strips ranged between 42^0 and 50^0. In that short range of inclination angles little effect on the final push-over curves so, a parametric study to observe the behavior further was suggested.

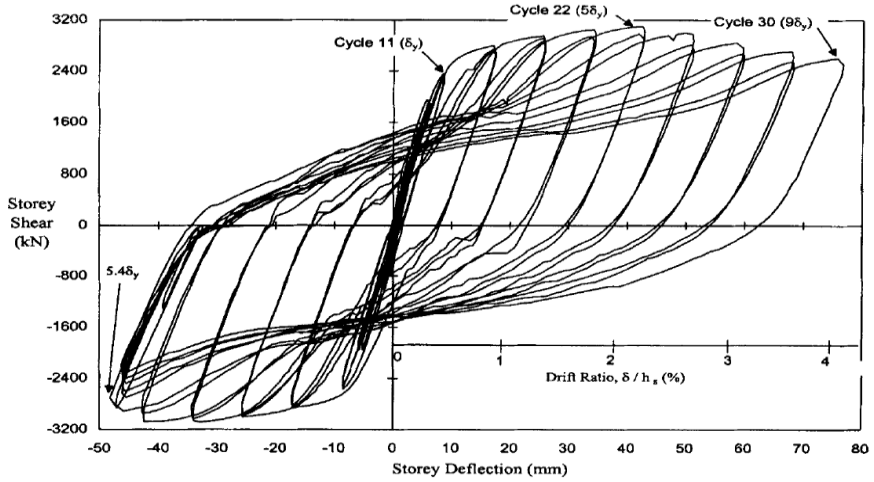

Figure 2.1: Storey shear vs storey deflection of panel-1 (Driver et al., 1998)

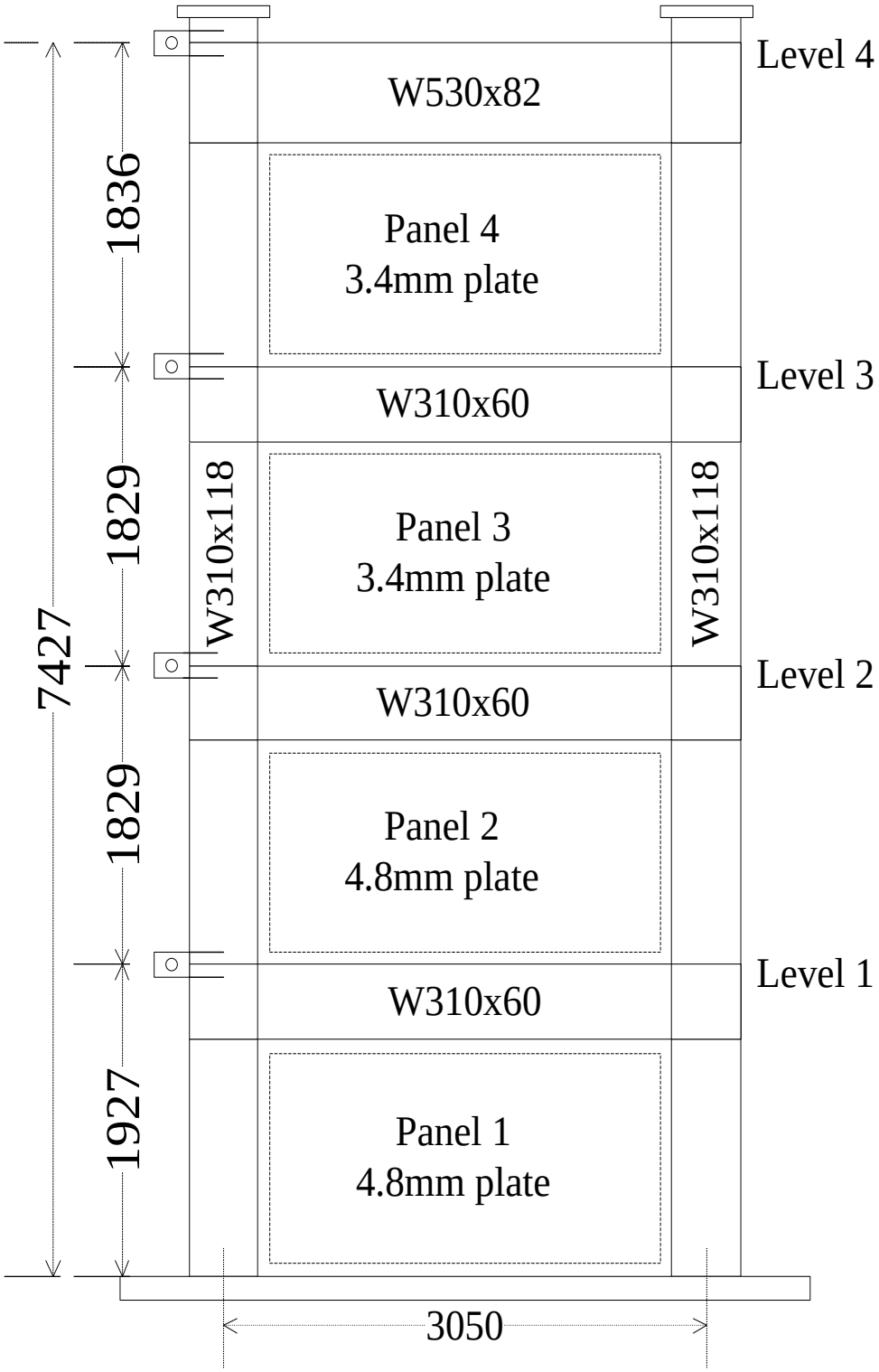

Figure 2.2: Four Storey specimen tested by Driver et al. (1998)

Lubell et al. (2000) tested three quarter scale unstiffened SPSW specimens. Two single storey (SPSW-1 and SPSW-2) and one four storey (SPSW-4) SPSW system were tested under quasi-static cyclic loading. An aspect ratio of one was maintained all through the design. The center line spacing in horizontal and vertical directions was 900mm. S75x8 section for both beams and columns and a plate thickness of 1.5mm was chosen. All materials were hot rolled. Specimen one (SPSW-1) represented the first storey of the four storey structure. Specimen two (SPSW-2) was basically specimen one with just one more top beam of same S75x8 section above the existing frame (Figure 2.3). The purpose of an additional beam was to allow better tension field development in the specimen. All connections were rigid weld connection. In the four storey specimen (SPSW4) the top beam was S200x34. An initial out of plane deformation i.e. initial imperfection up to 26mm has been reported for the first specimen (SPSW1). Quasi-static loading cycles following the guidelines given by Applied Technology Council (ATC-1992) were applied to all three specimens. The single storeys had their load control points at the top of the storey and for the four storey, all the storey were loaded together with the same load as in case of single storey. A gravity load, created by additional steel masses attached at desired portions, of 13.5 KN was maintained at all floor levels.

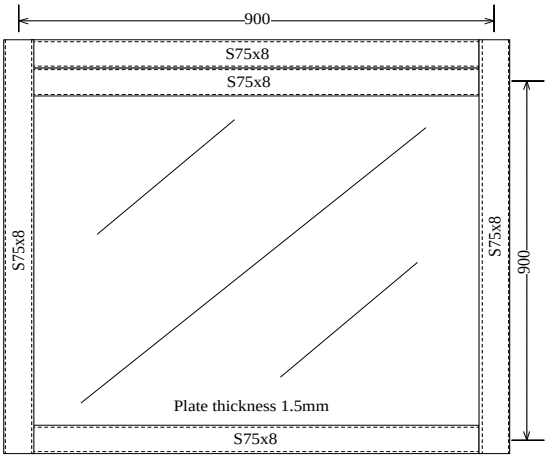

(a) Schematic diagram of SPSW-2

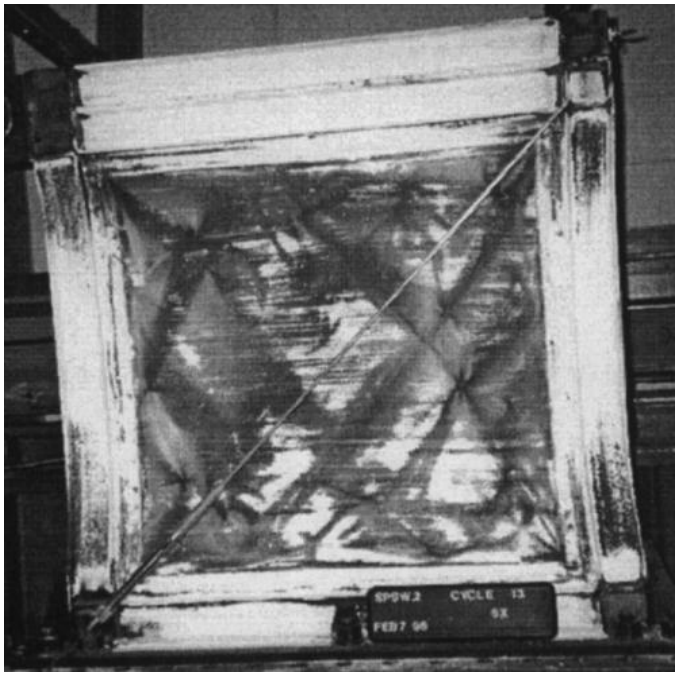

(b) Deformation and yield pattern for specimen SPSW-2

Figure 2.3: Specimen SPSW-2 tested by Lubell et al. (2000)

Stable S-shaped hysteresis was observed from the test (Figure 2.4). From envelope of hysteresis curves it was concluded that all the structures had sufficient initial stiffness and good displacement ductility. Comparing SPSW2 with that of SPSW1, a significant increase in stiffness and capacity has been reported in SPSW2. This was expectedly because of the stiffer beams and less imperfection involved in specimen SPSW2. For SPSW1 and SPSW2 the plate yielded significantly before the boundary members started to yield but for SPSW4 it was the columns where yielding started before any significantly noticeable yielding of plates. The yield sequence of SPSW4 is not desirable in practical design. The possible justification for it was the influence of overturning moments and small aspect ratio of panels. This yielding of columns caused instability and restricted the experiment to a ductility ratio of about one and half times the yield displacement. The boundary members considered through the set of experiments were

significantly light and places of incomplete tension field development have been reported. Specimen SPSW2 inward column deformation resulted in the formation of plastic hinges at top and bottom of column. The experimental outcomes have been discussed in more details by other research groups like Montgomery and Medhekar (2001) and reported that these experiments had inadequate column stiffness. Thus, the importance of strength of boundary members for acceptable behavior of SPSW systems has been indicated through the experimental work of Lubell et al. (2000).

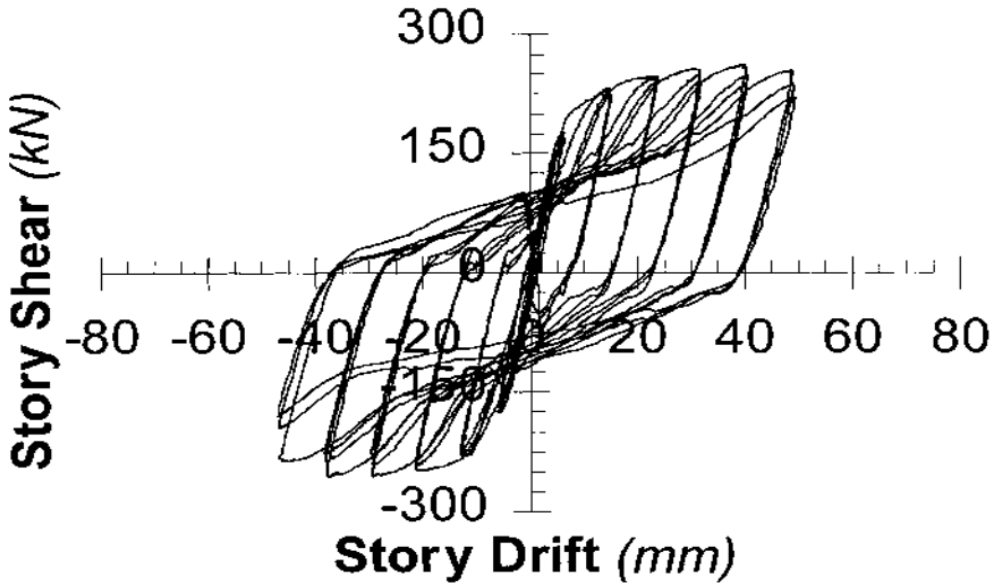

Figure 2.4: Hysteretic curves generated with specimen SPSW2 by Lubell et al. (2000)

Lubell et al. (2000) also concluded that with increase of panel height while all other parameters remain constant, the influence of flexural behavior increases and over turning moment dominated mainly the upper stories in tall buildings. Through this observation it was concluded that in case of SPSW systems the full structure needs to be analyzed as a whole and not as single panel, since the single panel behavior differed significantly from the behavior of the

full multi-panel structure. Modification to the then available design guidelines were indicated through this work by concluding that the available design guidelines may show good co-relation in post yielding character of the structure but may significantly over estimate the elastic stiffness under certain conditions. Also, inefficiency in available design provisions for multi-storey structures was highlighted. Particularly the possible large over turning moment created undesirable yielding sequence in SPSW components, as observed with their experimental study.

Mohammad et al. (2003) carried out experimental and numerical study on unstiffened SPSW. They summarized a set of ten independent parameters which could be used to characterize the behavior of SPSW systems. The specimen test by Mohammad et al. (2003) was very similar to the one tested by Driver at al. (1998a), only with bottom panel removed. Thus, full scale single bay three storey sample was used for experimental test (Figure 2.5). The material properties were assumed to be the same as in case of Driver at al. (1998a), since there was no additional scope to test the material properties of a fabricated sample. Large Initial imperfection (maximum of 39mm) has been reported through this study. All the stories were pushed laterally by hydraulic jacks with same force and second storey displacement was the control point for the setup. The cyclic loading sequence followed ATC-24 guidelines. Rupture in the first level beam at top flange and web of the beam-to-column connection was observed even before the ultimate strength was reached. To achieve the ultimate capacity of plates and to observe the behavior of boundary members under extreme loading, the rapture was fixed and the experiment continued. The hysteric curves indicated a stable behavior. Ultimate strength of the specimen was observed when the maximum second storey displacement was seven times the yield displacement. Beyond this displacement limit, the lower-storey infill plate started to show

tears and thus gradual strength degradation was noticed. Like most other experimental research work, this one also showed excellent ductility and stable hysteric loops (Figure 2.6). High initial stiffness, high degree of redundancy and also reported through this study.

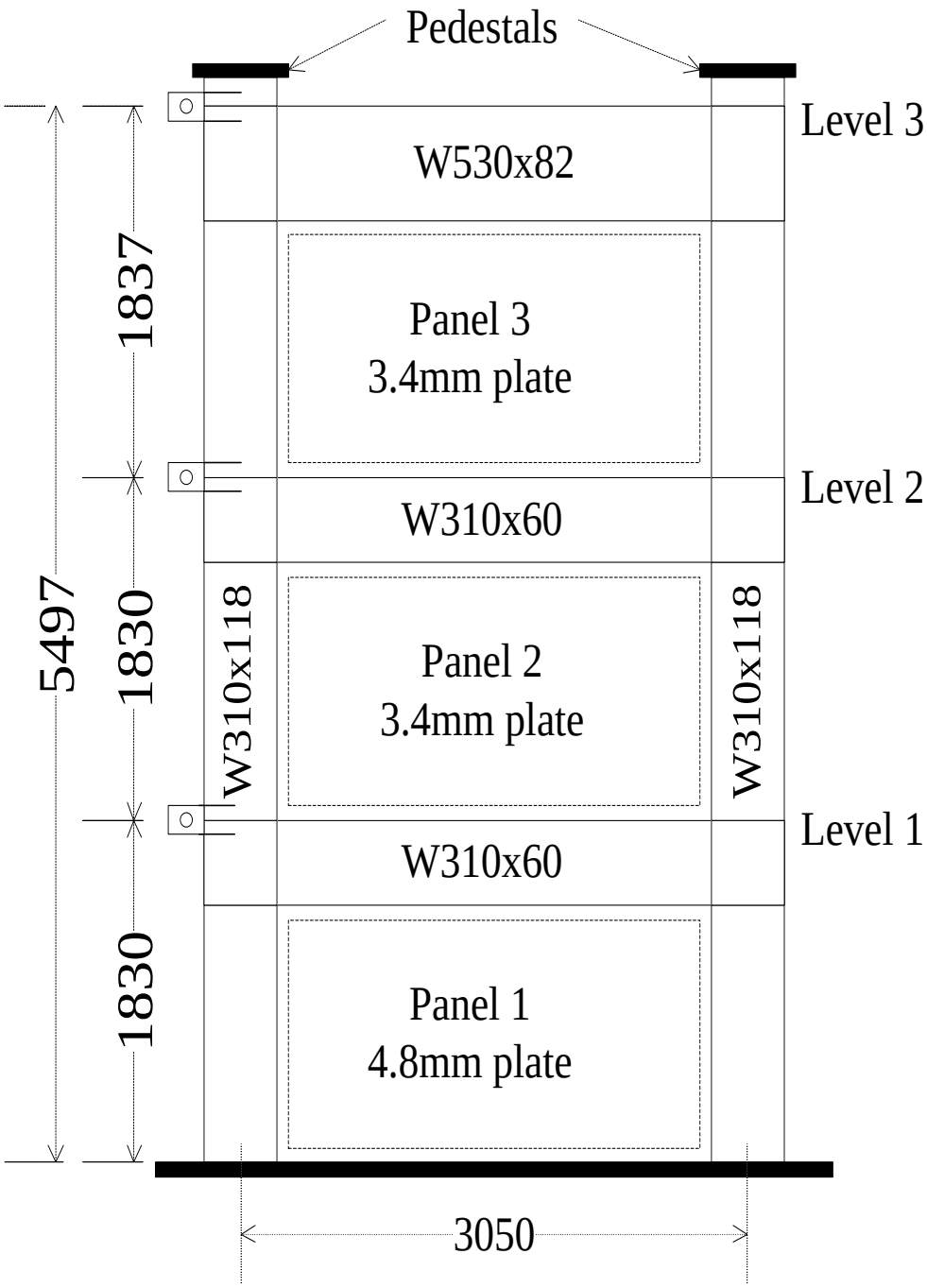

Figure 2.5: Three Storey specimen tested by Mohammad et al. (2003)

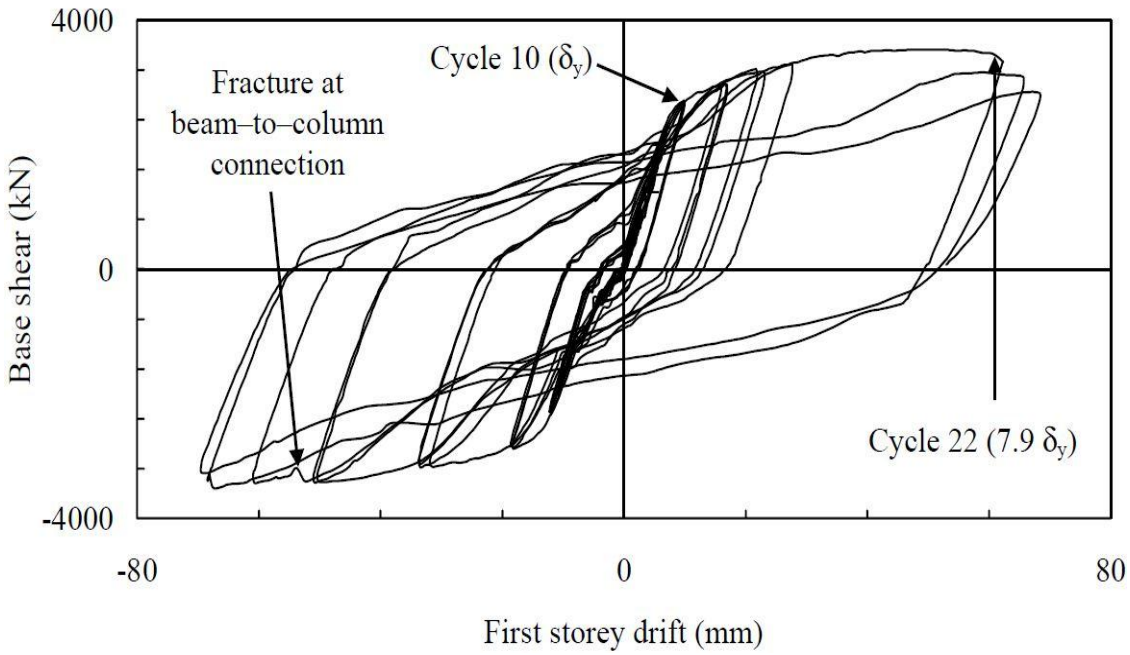

Figure 2.6: Base Shear versus first storey drift (Mohammad et al. 2003)

A numerical model based on Finite Element Method (FEM) was used by Mohammad to validate the experimental work and carry out parametric study. A set of ten non-dimensional parameters were shorted out for parametric study (Table 2.1). Keeping one parameter variable and all others constant several numerical analyses was carried out using a single storey FE model. Effect of parameters like column flexibility, aspect ratio, ratio of axial stiffness of infill plate to that of column, etc. on the overall performance of the SPSW system was indicated. Things like increase of column flexibility will affect the bending deformation of the columns and will introduce non-uniform tension field, resulting in reduced stiffness and capacity was one of the conclusions derived from the parametric study. Imperfection was also one such parameter that affects the capacity and stiffness of SPSW systems, but with imperfection less than $0.01\sqrt{(lh)}$, the effect is negligible. Gravity load and over turning moment is also observed to have a negative effect in the elastic stiffness, normalized capacity and ductility of SPSW systems.

With this parametric study the gross behavior of SPSW was summarized into the influential variables.

Table 2.1: Dimensionless parameters responsible for SPSW behavior

No.	Parameter	Details
β_1'	L_1/H	Aspect ratio
β_2'	$\frac{b*L_1}{2A_c}$	Ratio of axial stiffness of plate to that of columns
β_3'	$0.7 * \sqrt[4]{\frac{H^4*b}{2L_1*I_c}}$	Column flexibility parameter
β_4'	W/W_y	Ratio of gravity load (W) to axial yield load (W_y) or normalized gravity load
β_5'	δ/H	Drift index, δ being the top displacement
β_6'	V/V_y	Ratio of shear load (V) to the shear yield capacity (V_y) or normalized base shear
β_7'	$\frac{\sigma_{yc}}{E} = \varepsilon_{yc}$	Column yield strain, σ_{yc}, ε_{yc} being stress and strain of column material
β_8'	$\frac{\sigma_y}{E} = \varepsilon_y$	Plate yield strain, σ_y, ε_y being stress and strain of plate material
β_9'	$\frac{\Delta_{imp}}{\sqrt{L_1*H}}$	Imperfection ratio, Δ_{imp} being the maximum pre-existing imperfection in plate
β_{10}'	$\frac{(A_c)^2}{I_c}$	Local buckling index

To establish any simplified model or determine the workability of SPSW system all properties of SPSW systems indicated through the selected reports presented above has to be kept in mind. Though there are several other researches that have been reported relating to the SPSW systems, only the ones related to this thesis were shorted out.

2.3 **Works on Light-gauge SPSW**

All experimental and numerical works mentioned so far used to obtain behavior of SPSW systems, was based on hot rolled steel. There is very little research that has been carried out with cold rolled steel as infill panel. Kharrazi (2005) is one of those who performed experimental works with light-gauge SPSW systems. He conducted quasi-static and dynamic test on two light gauge thin walled single storey SPSW specimens (DSPW-1 and DSPW-2) and a moment resisting frame (SF-1). The moment resisting frame had identical boundary frame as in case of DSPW-1 and DSPW-2. To avoid local effect on column, HSS sections were used to design columns but the beams were chosen as W-shapes (Figure 2.7(a)). A 22-gauge cold rolled steel sheet was used for infill plates. The only difference in DSPW-1 and DSPW-2 was in the material property of the plates. DSPW-1 had tensile yield strength of 200MPa whereas DSPW-2 has tensile yield strength of 150MPa. The two HSS 102x102x8 sections used in columns were connected to the light gauge infill plate by an intermediate fishplate (Figure 2.7(b)).

Three cycle cyclic loading was applied with increasing storey drift, unless the load carrying capacity deteriorated significantly. At around 4% drift plastic hinges were observed at top and bottom of columns. At 5.8% drift for specimen DSPW-1, fracture along the weld line of fish late and infill plate was observed. Bram column connections showed to have fracture at

around 7.5% drift. The experiment ended with complete separation of fish plate to infill plate along with complete rupture of beam-column connection. Up to top displacement of twelve times the yield displacement, the specimen showed ductile behavior but beyond this limit the rupture has been reported to be brittle. DSPW-2 had very close behavior to that of DSPW-1 but the weld tearing at fish plate to infill plate was earlier in DSPW-2. At nearly 4% drift, the crack stretched around 400mm and more crack were significantly noticeable. Beyond 6% drift the strength degradation was even more significant. The cyclic load – displacement curves generated from the three samples are shown in Figure 2.8. Energy dissipation in the inelastic region and ductile behavior is well observed. Through conclusion of the research, a comparison amongst the three samples has been done in regards to energy absorption capacity in each cycle of load (Figure 2.9). Dynamic shake table test was performed on another set of sample specimen DSPW-3 (identical to DSPW-1) and SF-2 (identical to SF-1). The shake table test could hardly pass the elastic range owing to the huge capacity of the specimen. The overall behavior reported through this study was not observed to be very different from the one expected in hot-rolled steel infill panel. Berman and Bruneau (2005) also performed similar experiments with light gauge SPSW systems. Their results also indicated a very close behavior as one would expect in use of hot-rolled steel infill plates. Notably, both the experiments with light gauge steel infill panel were single storey experiment. No attempt was made to test the performance in case of multi-storey structures. Also, from practical point of view one major difficulty in use of light-gauge infill plate is welding such a thin plate to the boundary members.

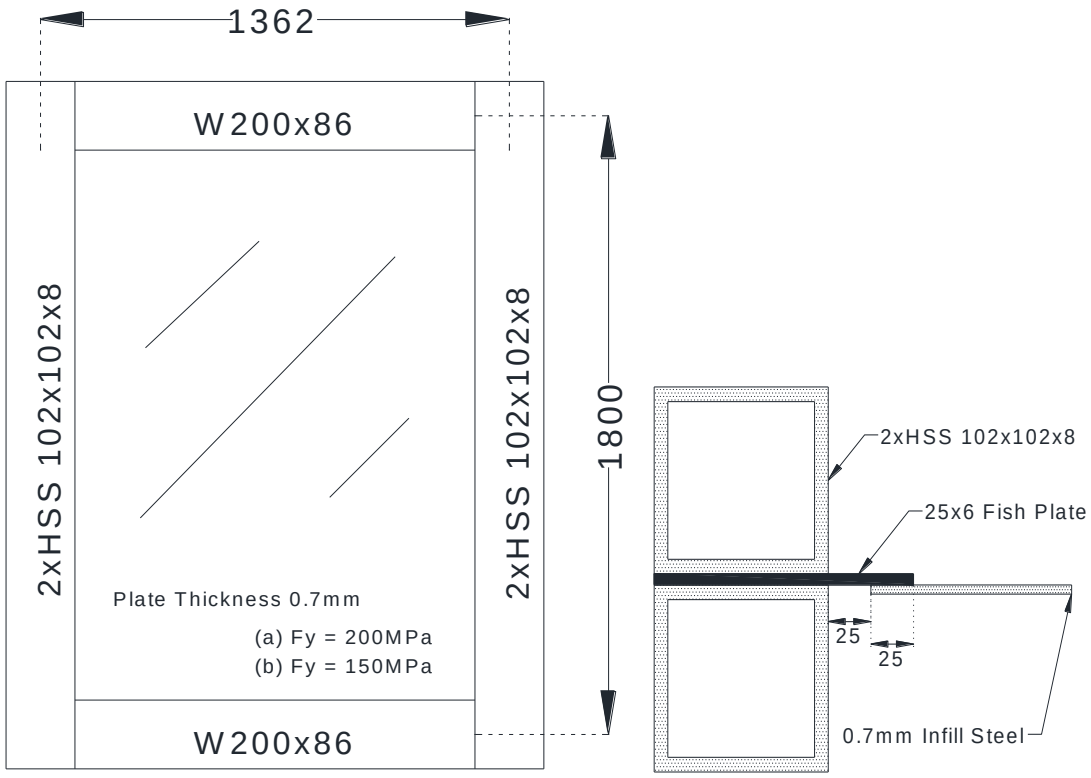

(a) (b)

Figure 2.7: (a) Sketch of single storey specimen (b) Sectional view of column plate arrangement (Kharrazi 2005)

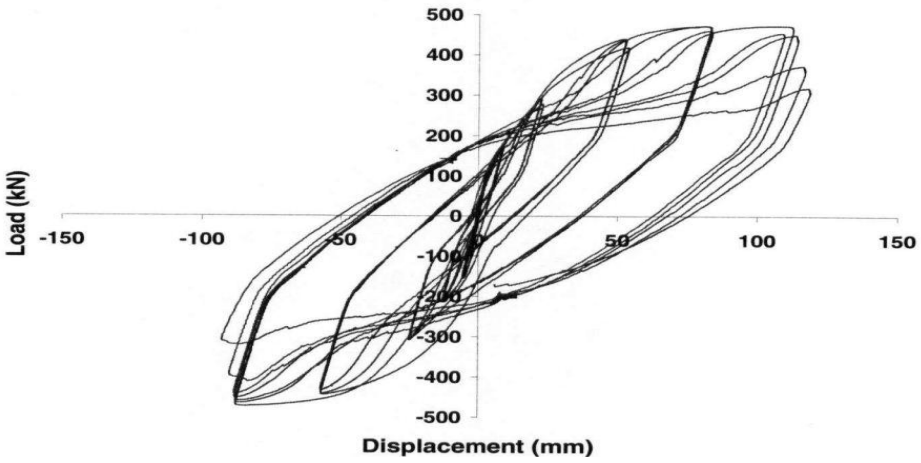

(a) DSPW-1

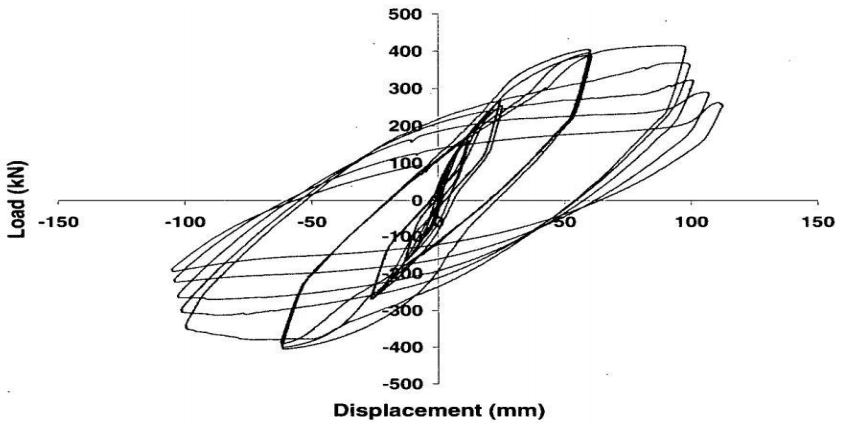

(b) DSPW-2

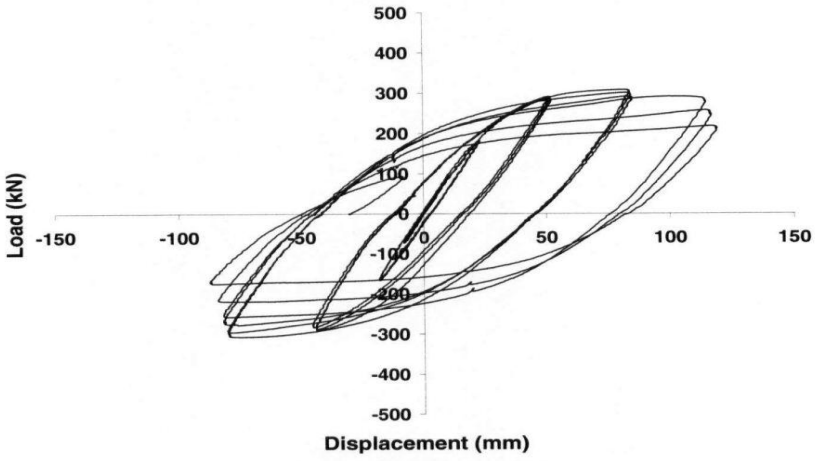

(c) SF-1

Figure 2.8: Load-displacement cycles for samples tested by Kharrazi, 2005

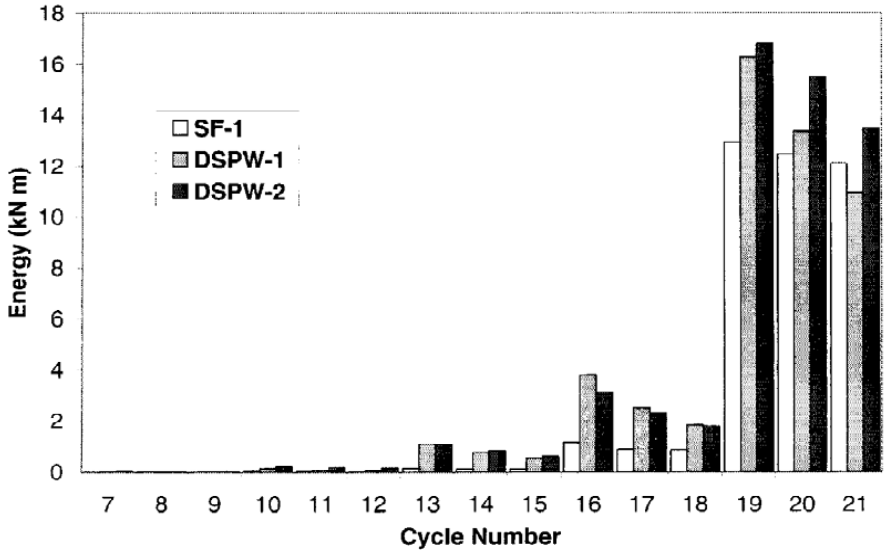

Figure 2.9: Hysteretic energy dissipation of DSPW-1, DSPW-2, SF-1 (Kharrazi, 2005)

Neilson (2010) studied the connection of light gauge steel plate shear wall with its boundary members. The main objective of the work was to develop welding procedure that will be simple to fabricate and at the same time can achieve good cyclic performance. Parameters such as joint geometry, material properties, welding process, electrode and shielding gas were selected for study. Arc welding was selected in making the experimental specimen. An ER70S-6 electrode was selected due to its strength, high toughness and deoxidizer content. Two shielding gases were used, namely, 75Ar – 25CO_2 and pure CO_2. Pure CO_2 was selected as it produced welds with the best arcing, wetting, and profile characteristics. Four possible configurations for the infill panel-to-boundary element connection and two possible configurations for the infill panel splice test have been reported. Configurations differed depending on whether one or two welds were used in the lap joint, and whether a chill strip was placed behind the thin sheet steel during welding to reduce the probability of burn-through and magnitude of distortion. All the configurations were subjected to a set of three quasi-static monotonic load and three cyclic loadings. Once the best configuration was shorted out, it was implemented on a single-storey large scale SPSW specimen (Figure 2.10). Loading of specimen was done based on ATC-24 (ATC, 1992) standards and a peak load of 630KN was achieved in 16 cycles. At the 17^{th} cycle storey drift of 3.5% and a fracture at the model base was reported. The infill panel to fish plate welding has been reported to be stable throughout the test out than some out of plane displacements. No detectable loss of integrity or strength degradation for loss of connection has been reported through the SPSW test. Finally, care on alignment of the weld has been indicated through the study. Thus, the limitation on use of light-gauge infill panel in SPSW system was successfully resolved.

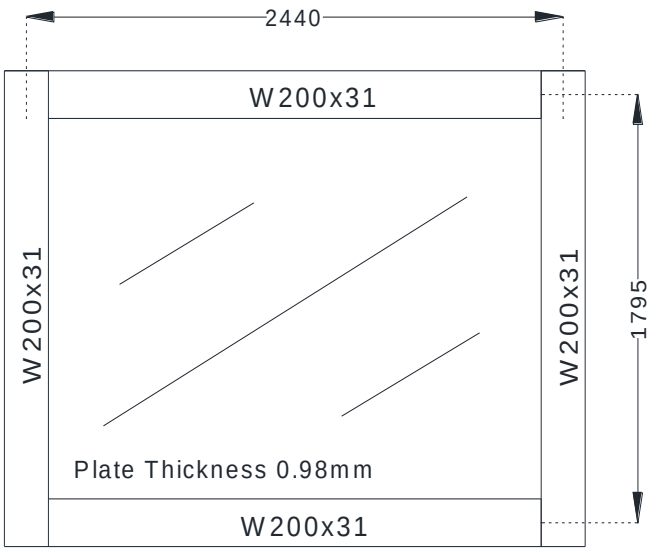

Figure 2.10: Schematic diagram of sample tested by Neilson (2010)

Almost all the experimental research in SPSW systems have attempted to validate with a numerical model. Numerical models are really convenient and cost effective way of carrying out analysis when large scale study with repeated analysis is involved. Several modeling technique has been discussed by researchers so far each having their own set of advantages and disadvantages. The most popular two methods worth mentioning are the strip model and the detailed Finite Element model. Some of these popular models have been discussed through this study.

2.4 **Strip model**

Though SPSWs are being used for decades, the consideration on contribution of post buckling strength in its design and thus modeling accordingly is relatively new. Thorburn et al. (1983) introduced a design technique where the post buckling strength was used. They introduced “strip model”, which proved to be a reasonably acceptable method for analysis of

SPSW systems. In this model, the plate has been analyzed as a number of pin-ended discrete strips capable of taking tension only and oriented along the principal tension direction, which is found by the principle of the least work. Each strip was assigned an area equal to the width of the strip times the thickness of the plate. Inclination of strips with vertical was calculated based on principle of least work (Equation 2.1). For the development of the strip model, the beams were assumed to be infinitely rigid in bending in order to reflect the presence of opposing tension fields above and below the modeled panel. A possible configuration of strips in an interior panel is shown in Figure 2.11. Material properties were assumed to be same as that of original infill plate, like the tensile yield stress in plates is same as that of strips. Since, only post-buckling behavior was considered effective shear strength of plate prior buckling was neglected. This research also indicated a minimum of ten strips per panel is required for analysis. For cyclic and dynamic analysis where the load is not unidirectional the strips need to be oriented in both the directions, this made the modeling technique a bit more complex. Also, this model has been later criticized for under-estimating the stiffness (Driver, 1997). However, owing to its reliability Canadian steel design standard, CAN/CSA-S16-09 (CSA, 2009) accepted this model as a design tool for SPSW systems. A normal plane frame analysis using Finite Element (FE) can be carried out to get the relevant outputs from strip model. However, this method becomes more complicated when cyclic push-pull load (like earthquake load) are applied to the structure. For cyclic loadings, the orientation of strips in both tension and compression direction are necessary. This makes the model more complex and time consuming when repeated analysis is necessary. Elgaaly (1998) modified the strip-model by introducing gusset plates which connect the boundary element with the strips (Figure 2.12). In this modified strip model, orientation of truss strips were assumed to be 45^0 and the truss material was assumed to be elastic, elastic-plastic and

perfectly plastic. Empirical relations were used to compute the reduced young's modulus and second yield stress after first yielding has occurred. A significant observation was reported that the strains at the ends of the diagonal strips near the supported boundaries are higher than the strains at the middle near the center of the plate panel. It was based on this observation that use of gusset plate in modeling technique was recommended. Since the gusset plate is expected to yield in shear before buckling, the dimension of square gusset was derived by equating shear yield stress of plate material with buckling shear stress of the equivalent square plate. Though this model was more accurate than strip model but it was by far more complicated.

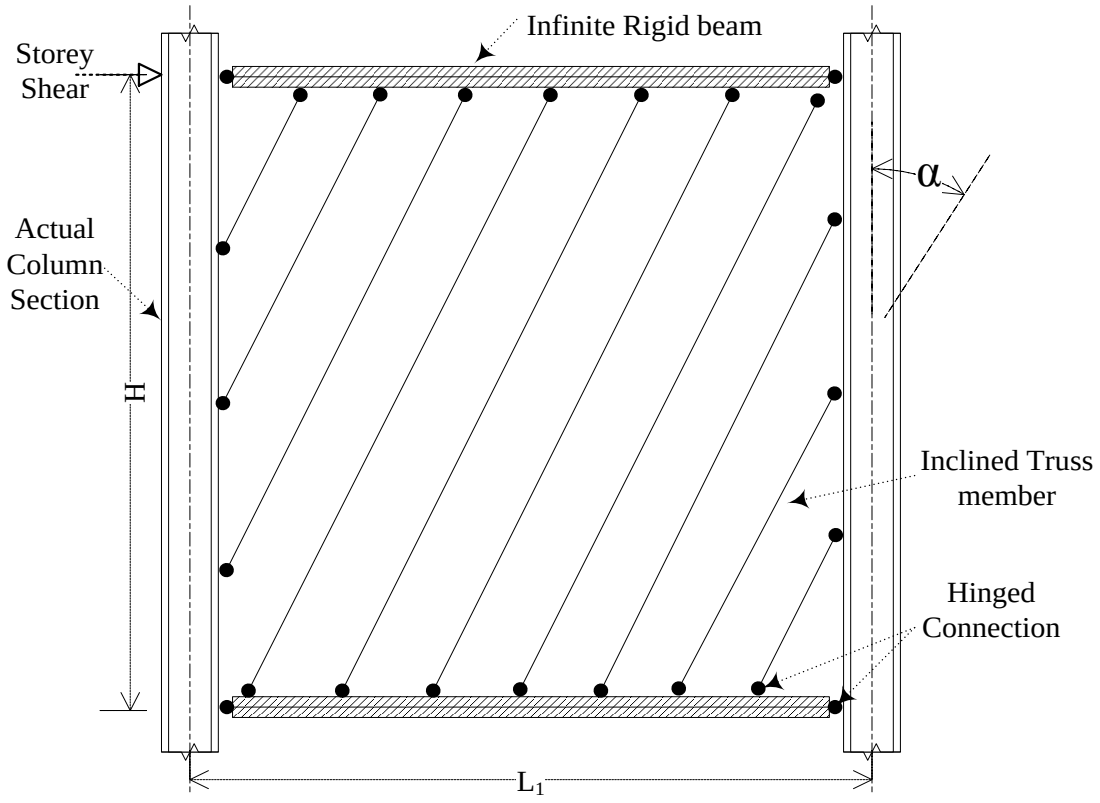

Figure 2.11: Strip model (Thorburn at al. 1983)

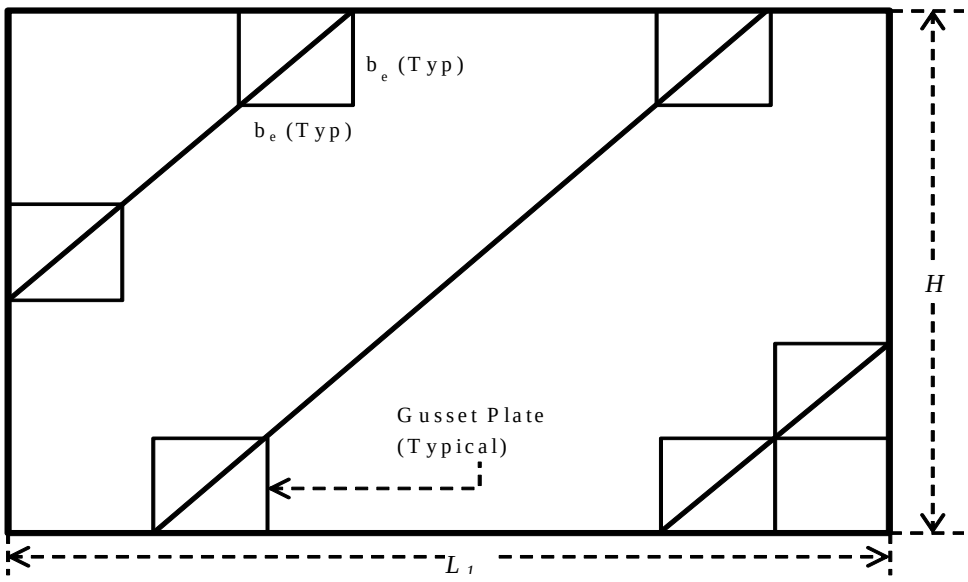

Figure 2.12: Model proposed by Mohamed Elgaaly (1998)

$$tan\alpha = \sqrt[4]{\frac{1 + \frac{L_1 * b}{2A_c}}{1 + \frac{H * b}{A_b}}} \tag{2.1}$$

where, α is the angle of inclination of tension field (Figure 2.11), b is infill plate thickness, L_1 and H are the width and height of panel, A_b and A_c are the cross-sectional area of the beam and column, respectively. The relation of $tan\alpha$ was later modified by Timler and Kulak (1983) as in Equation 2.2.

$$tan\alpha = \sqrt[4]{\frac{1 + \frac{L_1 * b}{2A_c}}{1 + b * H * \left(\frac{1}{A_b} + \frac{H^3}{360 * L_1 * I_c}\right)}} \quad (2.2)$$

where, I_c is the moment of Inertia of the columns and other symbols are as introduced before.

There have been several experimental tests to evaluate the performance of strip-model like Tromposch and Kulak (1987) conducted large scale test with two-storey structure laid horizontally on supports (Figure 2.13 and Figure 2.14). The beam to column connections were bolted connections. Before applying a cyclic load test, gravity load was applied to generated pre-existing stresses on the structure. Owing to the limitation of the loading machine, only 67% of the ultimate load was the maximum applied quasi-static load in cyclic test. This cyclic test was followed by a monotonic loading test where load up to the ultimate capacity of the specimen was applied. The main objective of the test was to validate the strip model proposed by Thorburn et al. (1983). Pinching effect for the presence of 3.25mm plate and flexible boundary elements was significantly noticeable. Also, the ductile behavior of SPSW system was indicated through the experimental study. Nonlinear pushover analysis was conducted using the strip model. The pushover curve had good agreement with envelope of hysteresis loops from test (Figure 2.15). It was also concluded that the strip model gave conservative estimates of both initial stiffness and ultimate capacity of Steel Plate Shear Walls.

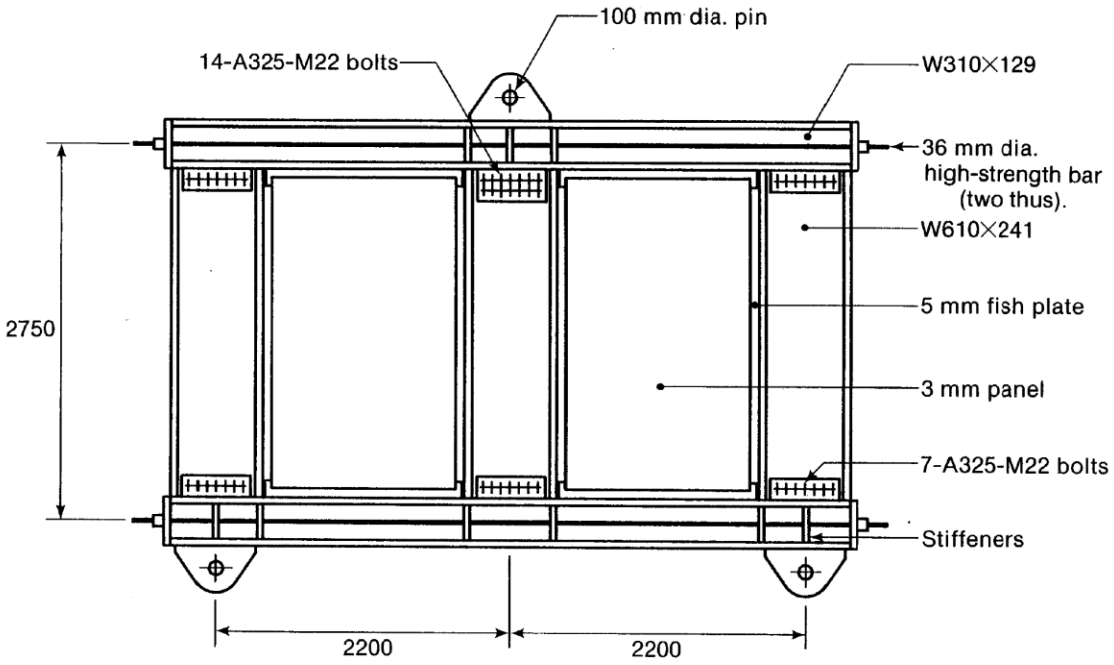

Figure 2.13: Sample tested by Tromposch and Kulak (1987).

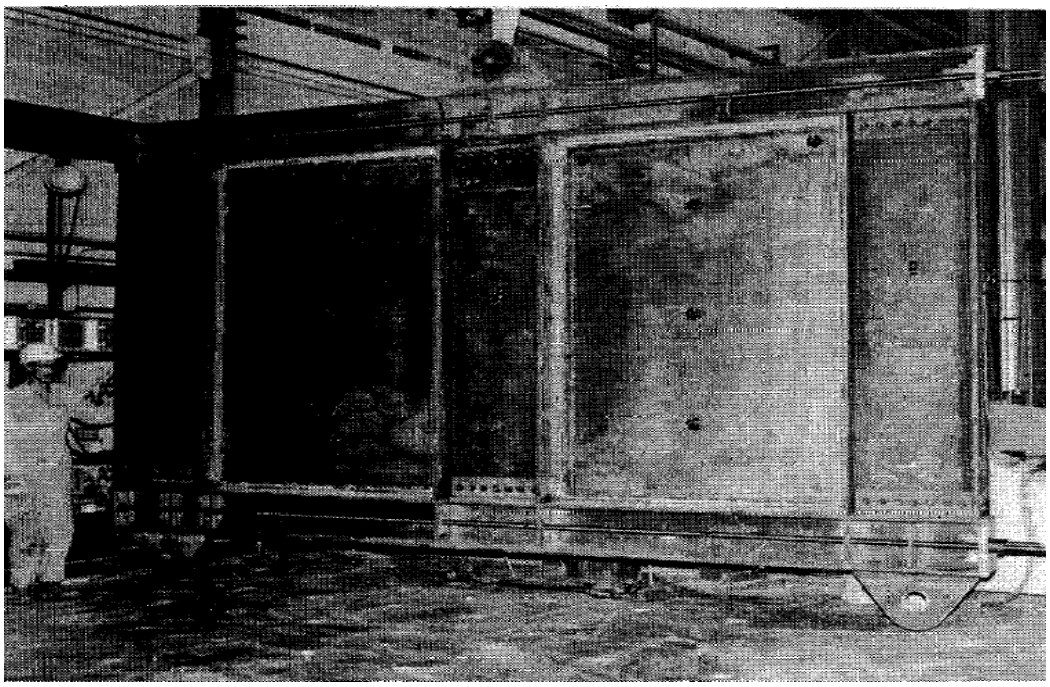

Figure 2.14: Experimental setup of Tromposch and Kulak (1987).

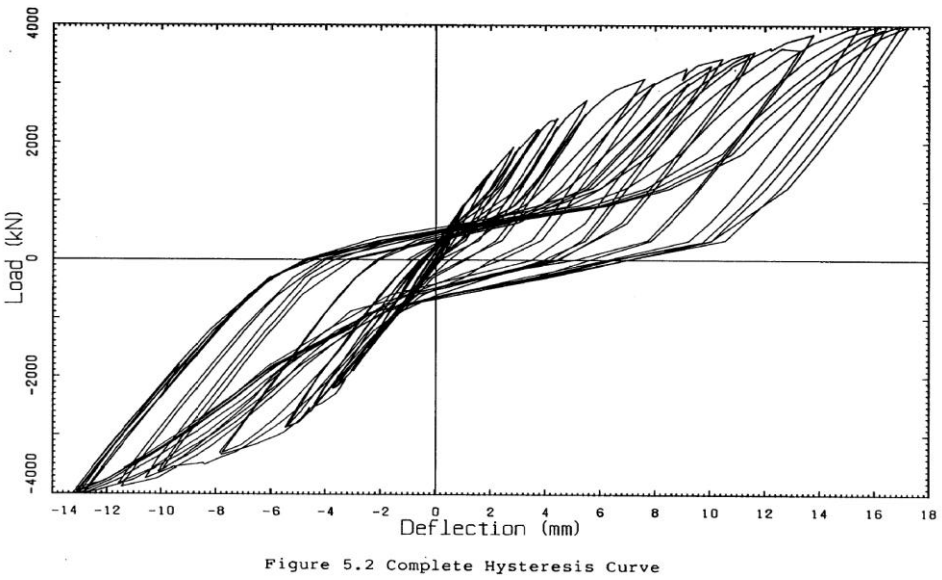

Figure 2.15: Hysteretic curves generated by Tromposch and Kulak (1987).

Driver et al. (1997, 1998) also used the strip model to get the pushover curve and compare with that of experimentally obtained hysteric loops. Ten pin ended strips with area as suggested by Thorburn et al. (1983) was used to replace the infill plate. For calculating the inclination of angle of tension field in the infill plate, the modified relation suggested by Timler and Kulak (1983) was used (Equation 2.2). The strip model was analyzed by a plane frame model using elastic analysis. Incremental load was applied and the strips yielded were removed from the model and tensile yield force from the strip was applied in the direction of the strip at the point where the strip was connected. When the column and beam reached its plastic moment capacity, a true hinge was placed with a constant moment at hinge joint. So, the analysis was carried out in several steps. Gravity load and P-Δ effects were also introduced into the model for analysis. Finally, it was concluded that though the ultimate strength is well estimated but the initial stiffness is slightly under estimated. The underestimation of stiffness was justified by several possible reasons like formation of localized compression field in the diagonally opposite

corners of the frame that form acute angles in the deformed structure where compressed length of plate is short. Other possible reasons can be additional axial stiffness of the tension column arising from the presence of infill plate connected to it. It was also reported that increasing the number of strips from ten to twenty had no significant influence in the final outcome. A new hysteric model was proposed, based on the strip model that explicitly divides the SPSW into two components (the moment resisting frame and the infill panel). This hysteric model has shown good predictions for cyclic behavior.

Following the recommendations in design standard for strip model, Lubell et al. (2000) analyzed his test specimens using non-linear frame analysis software.. Unlike their real experiment the analytical models had rigid beams to simulate floor action. For samples SPSW1 and SPSW4 in their experiment the initial stiffness was significantly over predicted by the analytical study using strip model. However, the ultimate strength in all the models was close enough. It was justified that the flexural modes caused by columns of low stiffness, aspect ratio and panel height significantly influenced the system behavior. The yielding sequence and inelastic characteristics was influenced by high axial and flexural co-efficient developed for excess over turning moment in columns. Thus, presence of excess over-turning moment in columns affects the accuracy in results that can be obtained from strip-model.

As explained before, strip model has some limitations. However, it still remains as one of the most widely accepted method for analysis of SPSW systems. A modeling technique simpler than strip model and yet equally reliable (if not more) is still in nascent stage amongst researchers.

2.5 **Detailed finite element model**

Finite Element Analysis (FEA) proved to be the acceptably accurate way of modeling SPSW (Elgaaly et al., 1993, Driver et.al, 1997). Strictly speaking strip-model and equivalent braced model are also finite element models. But those are simplified model made with several assumptions. Under the topic of detailed FE model, complex behavior of shell-plate element can be discussed. Through FEA it is possible to introduce both geometric non-linearity and material non-linearity. Shell elements representing the plate gave a better estimate of the stiffness and strength. However, the accuracy of FEA model depends greatly on the choice of modeling techniques used. Several modeling FEA modeling techniques like Mohammad et al. (2003), Bhowmick et al. (2010) have been suggested in past, where the efforts were mostly directed to developing a method for predicting more accurate behavior of SPSWs.

Successful finite element modeling technique was introduced by Driver et al. (1997, 1998b) to predict the behavior of SPSW system and compare the model with their experimental results. Quadratic beam elements were used to model the boundary members and quadratic shell element for the plate. Initial imperfections were introduced in the model based on first buckling mode and experimentally obtained residual stresses were included in the boundary members. The dimensions and material properties in FE model was specified as is in case of experimental specimen. Elastic perfectly plastic material curve with kinematic hardening model introduced material non-linearity in the model along with geometric non-linearity for initial imperfection. With a monotonic load pushover curve was generated which gave correct estimate of the ultimate strength but slightly over estimated the initial stiffness of the specimen. Cyclic load

analysis failed to capture the pinching effect and re-distribution of tension fields. More research in FE modeling was recommended by authors.

Analytical study was carried out by Mohammad et al. (2003) using FE software package (Abaqus/Explicit). Material and geometric non-linearity included in the FE model made the model more robust. A kinematic hardening material model was used to simulate Bauschinger effect for cyclic analysis of the SPSW. Also, to make the model displacement control, the concept of loading frame was used. Monotonic and cyclic load test was carried out using the FE model to validate both the experimented three-storey model and the previous four-storey model tested by Driver et al. (1998a). To avoid numerical instability dynamic explicit analysis was carried out with sufficiently small time step so that the final results remain reliable. The FE model and the experimental ones showed good match (12% under estimate in three-storey and 7.8% under estimate in four storey capacity), even the pinching effect was almost accurately captured.

FE modeling is considered to be the acceptably accurate from of analysis for SPSW systems. Wherever highly accurate results are demanded, a detailed FE analysis with shell-plate element representing the infill should be used. However, research have indicated that even with this complicated method the pinching effect is at times not correctly estimated (Driver et al. 1998b). The reason FEA with shell elements is commercially not a practical choice is for it's over complicacy in modeling, particularly for high rise buildings huge time is required for analysis. Speeding up the analysis without compromising accuracy significantly is particularly important when a multi-storey model is analyzed under cyclic or dynamic loading due to

earthquakes. Such structures may need to be analyzed for a suite of seismic ground motions in order to carry out a performance-based design.

2.6 **M-PFI model**

Very few attempts have been made in developing a technique where analysis can be made faster and reasonably accurate. Modified Plate-Frame Interaction method (M-PFI) is one such method developed by Kharrazi et al. (2004). The model was based on the critical observation of the ductile load-displacement curve of SPSW systems. The three main parts of the load-displacement curve, namely elastic buckling, post-buckling and yielding, is treated separated and then combined into the M-PFI model. Initial steps of the model involved the shear analysis of infill plate and frame separately, through which a relation of shear and load-displacement for each infill plate and bounding frame were obtained. These individual relations were super imposed to obtain the shear behavior of SPSW system. In the next step, bending analysis was conducted where the infill plate and frame was considered as a single structural unit. Finally, the interaction of bending and shear was developed and that concluded the M-PFI model. Through the set of equations described in M-PFI model, certain points on the load-displacement curve can be obtained, thus indicating the behavior of the ductile SPSW system. Through this model, with sufficient hand calculations, it is possible to evaluate design parameters (such as the shear load-displacement values, strength, stiffness and limiting elastic displacement for the steel plate and plate-frame interaction) and their effect on the overall SPSW capacity.

To establish the numerical model with proper validation, Kharrazi et al. (2004) used the experimental results from Driver et al. (1998a). For simplicity the model assumed the tension

field developed has an inclination of 45^0. The push-over curve obtained from M-PFI model gave a good estimate of the envelope of cyclic test (Figure 2.16). However, it was reported that the approximate model overestimated the initial stiffness by 5% and under estimated he ultimate capacity by 10%. The main limitation of this model is in describing the ductility of SPSW specimen or the actual failure mechanism. Also, nothing about obtaining the member forces was mentioned through this study.

The main advantage of this model is in its incorporation of bending effect for high rise buildings and is suitable incorporating practical seismic design provisions. However, cyclic load test or time history analysis is not possible through this model. This restricts the applicability of M-PFI method in performance based design.

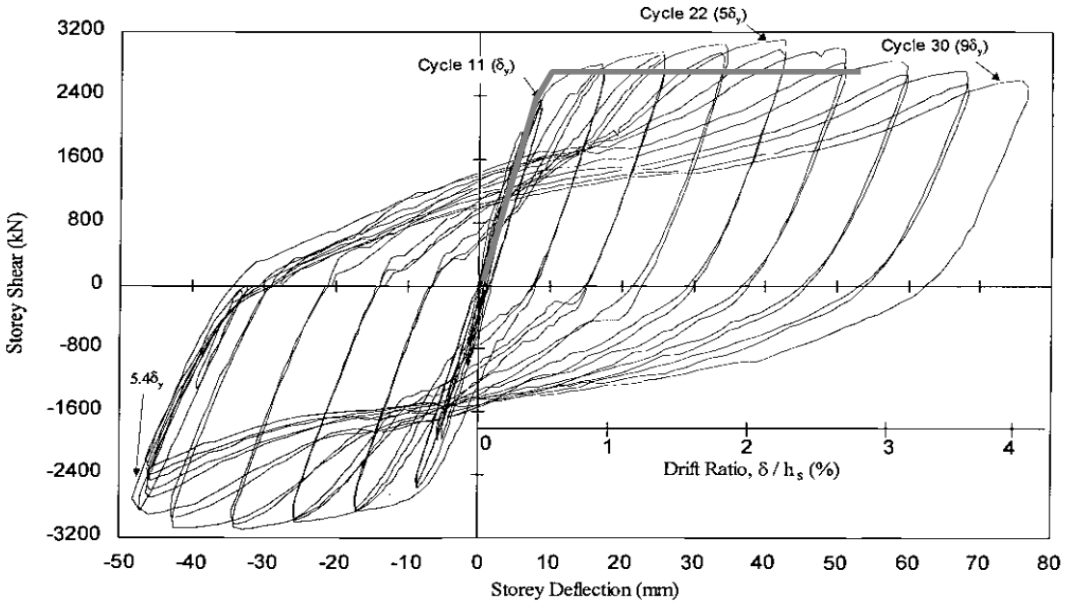

(a) Driver et al., 2000

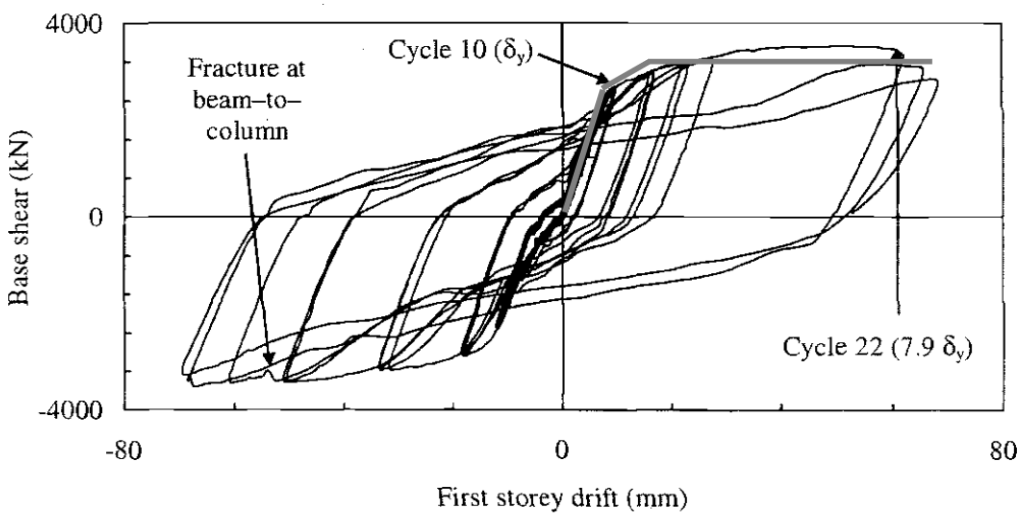

(b) Mohammad et al., 2003 by Kharrazi (2004)

Figure 2.16: Test of M-PFI model with experimental results from

2.7 **Existing braced models**

In this modeling technique truss members representing non-concentric braces along with beam member representing the boundary frame is modeled. Property of the braced and bounding members are so established that as a whole the braced frame represents the original SPSW system. The main advantage with this model over other modeling technique is that it takes the accuracy of FEA and yet very simple to model and most importantly requires very less time for analysis. Also, real time dynamic analysis can be easily performed. However, the accuracy depends greatly on how the properties of the members are established. Thus, the challenge in establishing the material and geometric property of truss braces such that they are capable of representing the behavior of SPSW systems opens up an area of interest amongst researchers. From the very beginning of research with SPSW, attempt has been made to develop an equivalent truss model that can accurately predict the behavior of SPSW. Thorburn et al. (1983) was one of the first to attempt it. Diagonal braces connected at beam column joints by pin

connection, capable of taking tensile force and remaining frame members were same as in actual SPSW was used to develop the truss model. Thorburn's formulation had the objective of determining the area of the diagonal braces (A_d) such that the truss model and their strip model gave same top displacement under shear. They assumed the boundary members to be rigid for the calculation of A_d. For modeling in finite element beam is always considered rigid and actual member dimensions are used as columns. By principle of least work and equating the stiffness of the plate with that of the brace in tension, they came up with significant area of the plate through which the effective tension field works (Figure 2.17), which can ultimately be related to Ad (Equation 2.3). Most of Thorburn's work was based on geometric distribution of tension field. This method of formulation does not necessarily always yield accurate results, thus making the model unreliable.

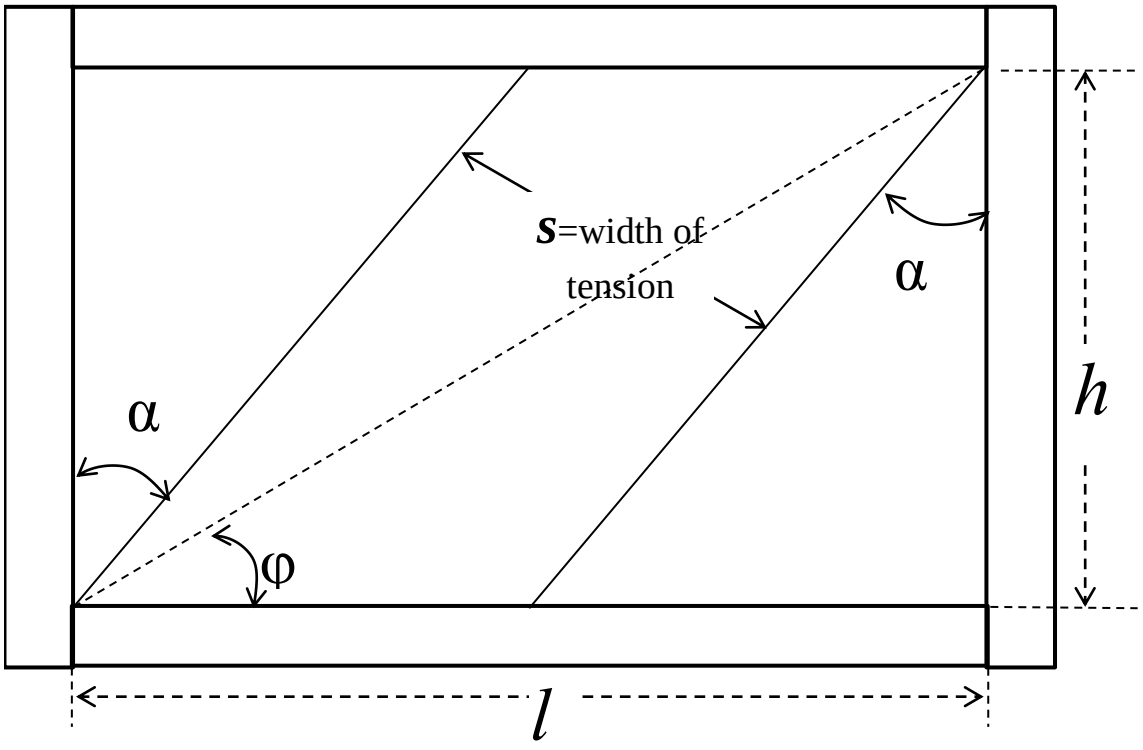

Figure 2.17: Truss model by Thorburn et al. (1983)

$$A_d = \frac{l * b * \sin^2(2 * \alpha)}{2 * \sin(90 - \varphi) * \sin(180 - 2\varphi))} \quad (2.3)$$

where, l is the width of plate, b is thickness of the plate and φ is the angle of brace with the beam (as in Figure 2.17)

Topkaya and Atasoy (2009) came up with a new method for computing the area of equivalent brace model. In their model the beams are the only rigid members. Also, the beams are assumed to be connected to columns by pinned joints (Figure 2.18). By using some empirical and analytical equations primarily developed for hand calculation method, they could come up with an area for the truss braces (A_d). An enhancement of area of the vertical boundary member (A_{ver}) was also recommended thought their study (Equation 2.4 and Equation 2.5). This recommendation for increasing the boundary member's area gave a good estimate for the initial stiffness of SPSW systems. All their computations are restricted within elastic limit. For tall multi-storey structures, the braced model is observed to overestimate the initial stiffness as well. Their work also introduced a parameter α_s which is the ratio of the post-buckled stiffness of the plate to the pre-buckled original stiffness (Figure 2.19). Unlike other parameter, a representative table indicating the possible values of α_s based on slenderness and aspect ratio of plates has also been provided. However, no proper statistically developed mathematical relation has been indicated to estimate the value of α_s. The truss model is workable on computers allowing repeated analysis with cyclic loadings. Validation with acceptable range of accuracy, on the stiffness predicted from both these two models, has been done with some available experimental results, some Finite Element models and some strip model results as well. Through their

calculations and study it has also been indicated that due to presence of stiff boundary members, the buckling of plate under bending does not significantly influence the overall inertia. Thus, for development of a simplified approximate model the bending effect can be safely neglected.

$$A_d = \frac{L_d^3\left({I_{pl}}^2/\beta_m\right)}{2.6h * (l + d_c)^2} \tag{2.4}$$

$$A_{ver} = \frac{I_m}{0.5 * (l + d_c)^2} \tag{2.5}$$

where, h and l are height and width of plate respectively, L_d is diagonal length of plate, d_c is the depth of column section, I_{pl} is the moment of inertia of the plate and I_m is the modified moment of inertia of the plate given by Equation 2.6. β_m represents the sum of contribution of shear stresses in column (β_1) and infill plate (β_2) as represented by approximate Equation 2.7. Also, the contribution of shear stress from plate is enhanced by coefficient α_s for considering geometric non-linearity.

$$I_m = 2I_c + 0.5A_c(l + d_c)^2 + \alpha_b I_{pl} \tag{2.6}$$

$$\beta_m = \int \frac{Q^2}{b^2} dA_{pl} \approx \beta_1 + \left(\beta_2/\alpha_s\right) \tag{2.7}$$

where, Q is static moment of the area with respect to neutral axis, b is width of section, I_{pl} and A_{pl} are second moment of inertia and area of steel plate wall respectively, I_c and A_c are second

moment of inertia and area of cross section for column respectively. α_b is the ratio of post-buckled stiffness of the plate under bending to the original pre-buckled stiffness. Significance of α_b is also reported to negligible in most cases.

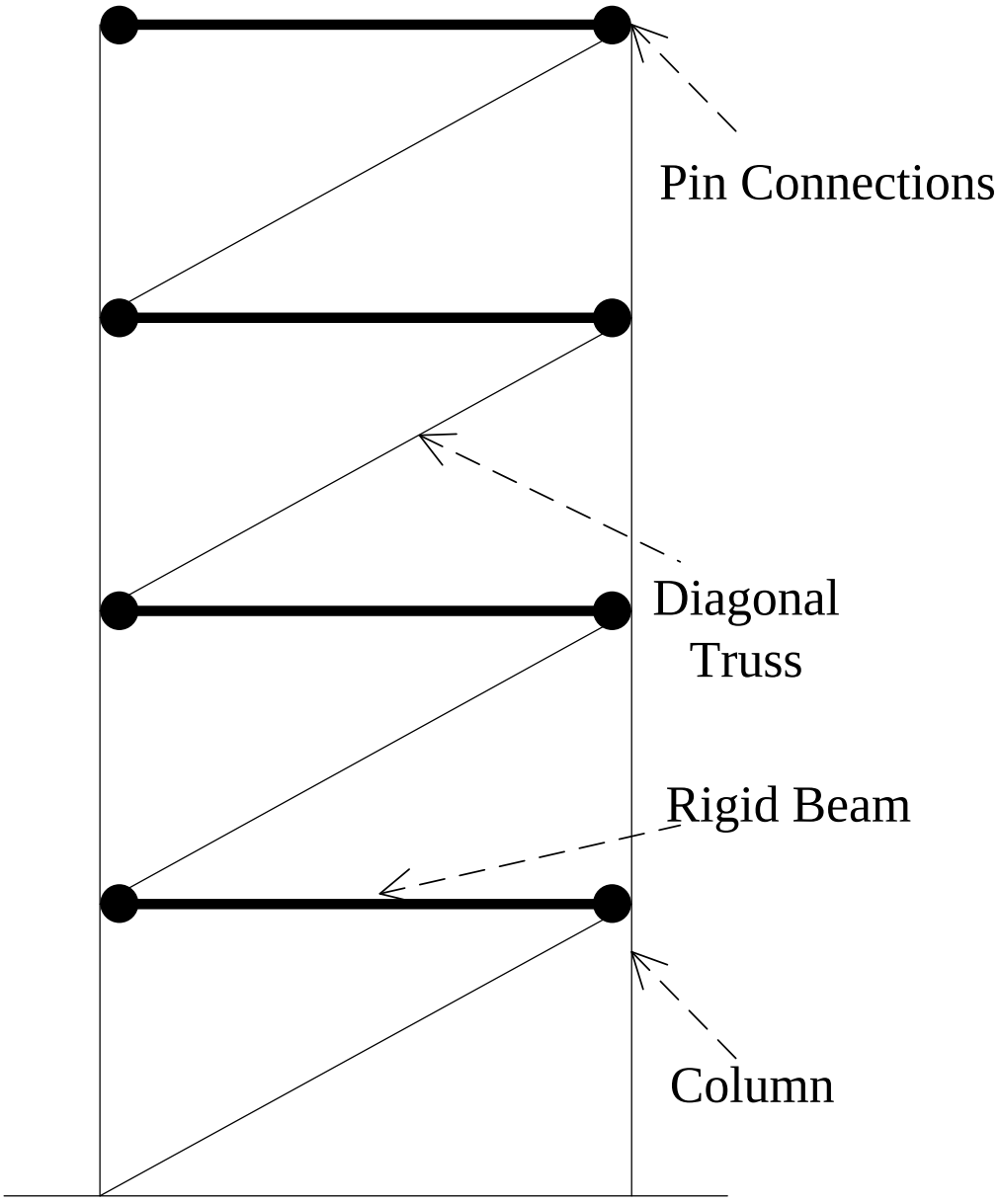

Figure 2.18: Diagonal truss model proposed by Topkaya and Atasoy (2009)

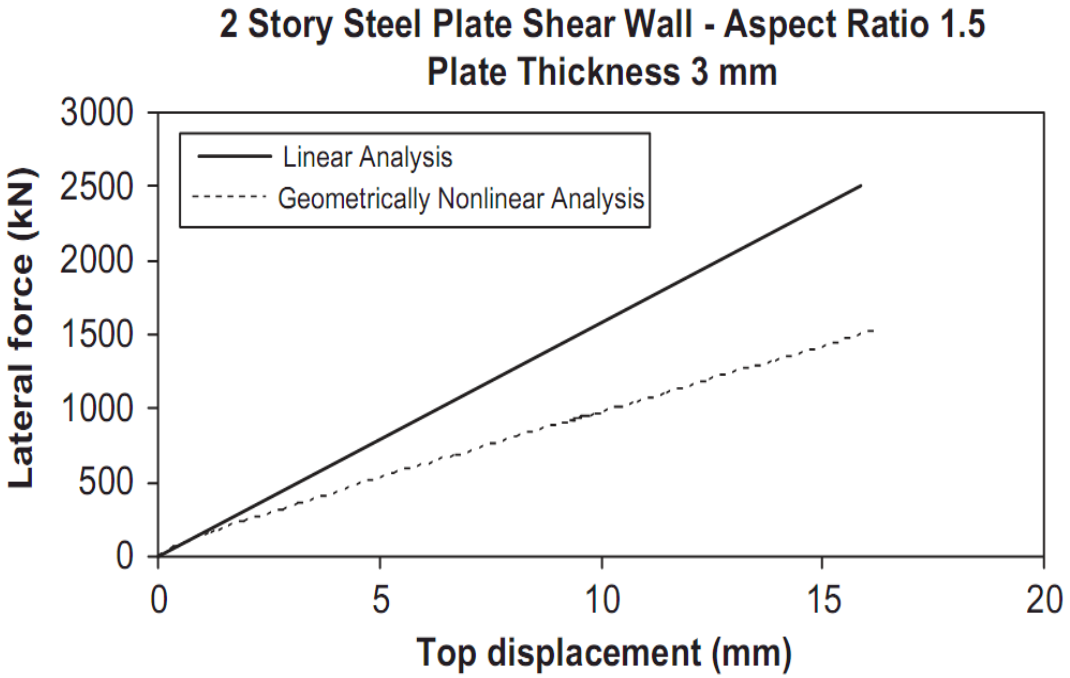

Figure 2.19: A typical Load displacement response of SPSW comparing the change of stiffness for buckling of infill plates by Topkaya and Atasoy (2009)

2.8 **Some other modeling technique**

Tromposch and Kulak (1987) also developed hysteretic model based on research by Mimura and Akiyama (1977) (Figure 2.20). Frame stiffness effect of low panel buckling strength was incorporated in their model. This was one of the beginning level models that could estimate the cyclic load-displacement curve. However, owing to its approximation and complicacy in computation it was not observed to be that popular amongst researchers in this area.

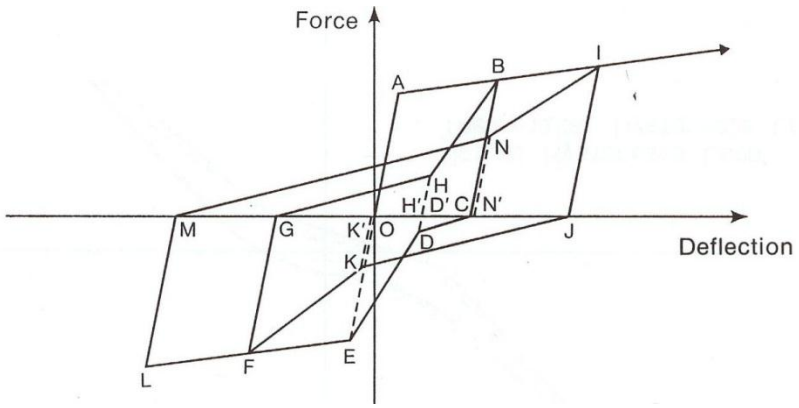

Figure 2.20: Hysteresis model proposed by Tromposh and Kulak (1987)

Topkaya and Atasoy (2009) performed a series of numerical study to develop an approximate hand calculation method to estimate the top displacement of SPSW systems. Modifying the classical deep beam theory based on some parameters as found suitable for the SPSW system under pure shear and pure bending action. Parameters like geometric non-linearity has been implemented into the model by repeated analysis with varying geometric properties in Finite element model. This hand calculation model incorporated some analytical system of equations merged with empirical relations developed by parametric study using FEA model. An example solution for hand calculation method has also been presented by Topkaya and Atasoy. The hand calculation and truss model methods have reported an average of 8% and 6% stiffer in comparison to strip model. A comparison of normalized stiffness for different cases of samples tested by the author has been indicated (Figure 2.21). The model is good for making prior estimate on expected top deflection of SPSW before carrying out final design. Though, this model gives a reasonably accurate estimate of stiffness but only within linear elastic limit of the material. Also, for repeated analysis this model is cumbersome and time consuming. Restrictions with cyclic load test and dynamic tests like time history analysis is also a significant limitation.

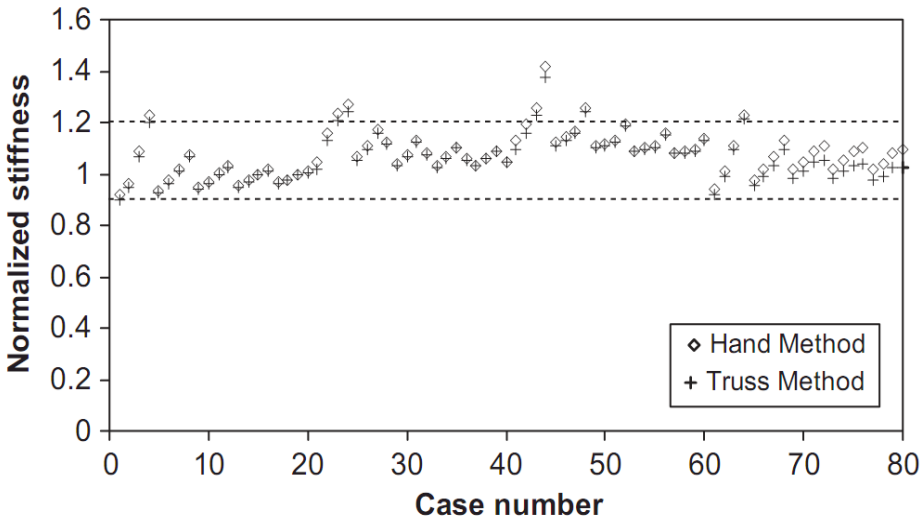

Figure 2.21: Comparison of results for hand and strip methods of analysis with existing methods reported by Topkaya and Atasoy (2009)

2.9 **Summary**

Research on Steel Plate Shear Wall system has been continuing through decades. Almost all literatures, indicated its effectiveness in overall increased structural ductility, stable hysteric behavior, enhanced stiffness and ability to dissipate energy during earthquakes. Thus, steel plate shear wall is gaining more popularity in construction industries specially, in zones of high seismicity where ductility demand of structure is very high. This opens up a demand on more sophisticated and precise design techniques. Involvement of light-gauge infill panels in modern SPSW system is also expected to have more importance in near future. As indicated through this study, research on light gauge SPSW has been very limited (Kharrazi (2005), Berman and Breunau (2003), Neilson (2010)). Even with the welding technique being properly established (Neilson, 2010), all it remains is a proper analytical study. It should be noted here that currently

no design guidelines are available for seismic design of light-gauge SPSWs. Thus, a numerical study will be conducted in this research to assess the applicability of the capacity based design approach, currently used for design of ductile SPSWs, for seismic design of light gauge SPSW systems.

While carrying out this objective with repeated analysis of several multi-storey structures, a bigger realization comes to play i.e. a demand for simplified modeling technique need to be established. From the study of literatures done so far it can be inferred that there is a deficiency in an established simplified model that is reliable and at the same time very fast computationally. Also, the new modeling technique to be established should be capable of carrying out real time time history analysis very fast. It has also been observed that capacity based design technique has already been discussed by several researchers (Bhowmick et al. (2009); Berman and Bruneau (2008)), no study on performance based design is currently available. This is probably due to the limitation of available modeling techniques. Presently available models are either not reliable or far too complex for repeated dynamic analysis. Thus attempt will be made to establish simplified and reliable modeling technique using equivalent bracing system that can be used for performance based seismic design of steel plate shear walls.

Chapter 3. Methodology

3.1 Introduction

To achieve the objectives as indicated in previous chapters, a detailed methodology must be established. Both modeling techniques namely, simplified plane frame model in two dimensions and three dimensional models with shell elements need to be developed prior to the testing of multi-storey SPSW systems. Finite element modeling involves significant prior knowledge and are complicated enough for user to introduce human error or any other fundamental error. Also, the accuracy involved depends greatly on the choice of modeling technique. So wherever possible, cross validation with experimental results or with some other pre-established results need to be performed. The first step of this study would thus involve validation of detailed Finite Element model with reported experimental results. Once an acceptable validation is accomplished with detailed FE model, plane frame models without any infill will be developed in two dimensional platforms such that it's results agrees with identical models developed in already established three dimensional modeling technique. This will create an acceptable background for working with reliable solution techniques for simplified two dimensional modeling. In the process of simplification on analysis of SPSW systems, simplified two dimensional models will be of good use for developing equivalent braced frame model.

After validation the work is divided into two segments. In one side, using the detailed FE model, a thorough study on light-gauge steel plate is carried out. This part of the study would involve not only static analysis like developing pushover curves but also time history analysis for

multi-storey structures. The performance of the buildings will be judged based the structure's fulfillment in criteria imposed by capacity design approach of NBCC 2010. Since, this is a detailed study so both geometric and material non-linearity has to be incorporated in the model. On the other part, an attempt to develop an Equivalent Braced Frame model (EQ.BF model) will be carried on. The primary purpose of this model is to reduce the analysis time to a significant amount. The equivalent braced frame model is expected to have identical behavior as that of SPSW systems. A detailed study on the significance of each parameter in the overall performance of an SPSW needs to be carefully observed. Based on the observations some selected parameters are shorted out and a detailed parametric study is carried out to quantify different parameters of the EQ.BF model. The main achievement expected from the developed EQ.BF model is its efficiency in computation time at no or least compromise on accuracy of final results. The EQ.BF model is finally tested with available experimental data and with results obtained from detailed model analysis. Both static and dynamic results need to be separately validated with available results. Finally, with this simplified EQ.BF model, taller multi-storey structures where infill-plate is made from cold rolled light-gauge steel can be easily tested. Based on those set of results, an estimate on performance of light gauge SPSW systems can be made. Thus, from this research not just the performance of multi-storeyed light gauge SPSW systems will be analyzed but also a simplified modeling technique will be established, which can be further used to develop performance based design strategy for SPSW.

3.2 Development of detailed FE modeling technique

As already indicated, a detailed finite element model needs to be developed in this research to study the behavior of light-gauge steel plate shear walls. With advancement in the technology of computers, finite element analysis is gaining popularity among the structural design engineers. Results from FE analysis are reliable and can be made very precise based on modeling technique. To capture accurate behavior of any structural member with FE model, proper selection of geometry, element and solution strategy is required. Element degrees of freedom should be a correct representative of the member degrees of freedom required to express the deformation of a practical member. Selection of analysis type is another important task since it can influence the accuracy of the analysis results. Among two choices, e non-linear and linear analysis, nonlinear analysis is preferable as it can include the P-Delta effect in analysis. . The material model to be incorporated in the FE model needs to be selected carefully. The material model is usually obtained from results from sample coupon test.. Details of the development of the Finite element model including its validation are presented in the next chapter. Abaqus (Hibbitt, 2011), a commercially available FE package, has been used for development of the detailed FE model.

3.3 Development of Equivalent Braced Frame Modeling Technique

The detailed finite element model though acceptably accurate requires longer analysis time. This makes the model not efficient for design engineers. Thus, there is a timely need for developing a simplified model. One of the simplest forms of model that is expected to represent

the complicated behavior of SPSW system is an equivalent bracing system. Strictly speaking the target braced model will also be a finite element model. However, Equivalent Braced Frame model (EQ.BF model) will be a much simpler model in terms of modeling and analysis time. First step for achieving this simplicity has been carried out by restricting the EQ.BF model to be constructed in a two dimensional environment rather than a conventional three dimensional plate-frame model. This two dimensional modeling part has been carried out in Opensees (Mazzoni et al. 2007). Opensees is an open source software package that works mainly in combination with the tcl/tk programming language. Using Opensees for this variety of problem is way easier for a future user inexperienced in this area than working with Abaqus. Also, being open source software, Opensees is not just getting more popular amongst researcher but also in industries. Few advantages with open source software are the full manual control on the analysis, introducing script or additional parts to the main program for repeated analysis or parametric study or some particular display configuration, etc. To begin work on a new platform with a new program once again the modeling technique need to be established and validation needs to be carried out. Since, braced model is not yet developed and shell-plate cannot be used in two dimensional studies so, results from some bare frame models in Opensees were compared with similar models made in Abaqus. For the bare frame models in Abaqus, exactly same modeling technique has been used as already described for the detailed model with just the infill plate missing. Since, Abaqus models are validated with published experimental results and Opensees is being validated with results from reliable Abaqus models so, it can be said that in Opensees an indirect validation is being planned to be carried out.

3.4 **Modeling in Opensees**

Two dimensional models in Opensees followed the center line geometry for any structure. Height of each floor represented the height of element representing column and bay width represents the length of element representing beam. In other words, there were no intermediate nodes at any storey height. The non-concentric cross-braces have also been connected at the beam column joints. Reducing the total number of nodes reduces the size of the global stiffness matrix since the total number of degree of freedom reduces, thus making the model computationally more efficient in terms of time. Beam-column joints have been limited to be rigid connection. So, any model where the member connections are not rigid, this EQ.BF model is not expected to give very correct results. Non-rigid connection effect on the EQ.BF model is not considered within the limited range of applicability of the model. This can be considered as an area for future work. Opensees library has a huge collection of commonly used elements in its library and it also provides option for user to develop their own set of element based on their needs. For the purpose of this study no new element was developed. Nonlinear-beam-column element was used for bounding beams and columns. Braces were modeled as truss member. Each of these elements has been assigned eight gauss integration points which didn't have an observable effect in analysis time but yet produced results of desired accuracy. An aggregate section comprising both flexural and axial material property is assigned in beams and columns. The material property, geometry and other configuration in boundary members have been kept identical in EQ.BF model as in designed SPSW system. The material property and cross-sectional area of truss to be assigned to the cross braces needs to be calibrated in such a way that the braced model, which is essentially a strut and tie model, represents the SPSW

system in a global sense. A uniaxial hysteretic material model as shown in Figure 3.1 is assigned to the truss braces. Also, another advantage of using hysteretic material model is its ability to take into account material pinching effect for cyclic or dynamic loading, which has been reported for SPSW systems in some experimental research like Mohammad et al. (2003). Gravity loads and P-delta effect are assigned to the columns where ever applicable. Unlike in model in Abaqus, for dynamic analysis no leaning effect was assumed in EQ.BF model. This is primarily because P-delta effect due to eccentricity of gravity load and mass is not observed to be very significant in SPSW systems unless the structure under consideration is very tall (Bhowmick et al. 2010). The tallest structure under consideration for this study is ten-storey with floor to floor height of 3800 mm for which additional effect due to leaning column can be safely neglected. Also, one must keep in mind that result from EQ.BF model is approximate representation of detailed SPSW system and should lie within allowable engineering error (less than 5% in overall). However, when result of higher accuracy is demanded, it is always recommended to conduct a detailed FE analysis.

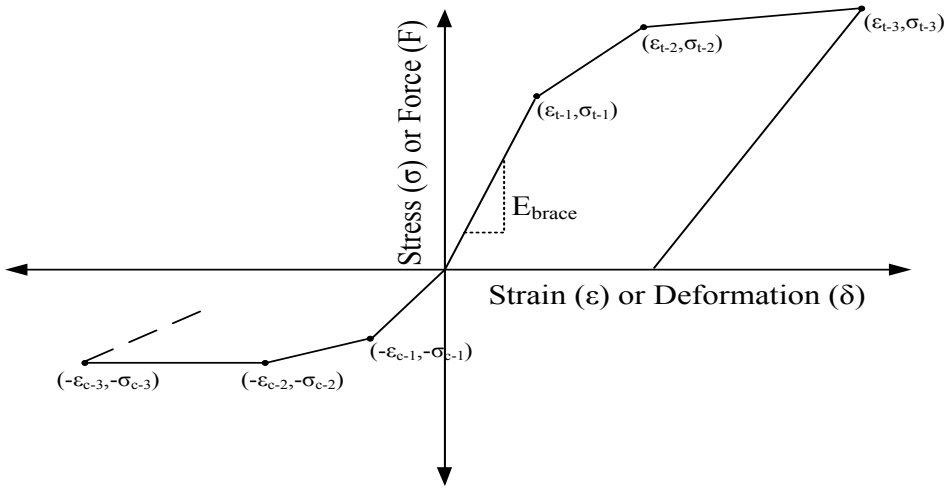

Figure 3.1: Uniaxial Hysteretic material for braces

3.5 **Parametric method on development of EQ.BF model**

To establish the section properties in braces such that EQ.BF model is capable of representing full scale SPSW systems, one has to identify the important parameters which influence the behavior and strength of infill plate. Mohammad et al. (2003) conducted a dimensionless parametric study to identify the parameters which influence the behavior of a SPSW. The parameters (involving both geometric and material properties) which are directly relevant to strength and stiffness of infill-plate are aspect ratio, (β_1'), column flexibility parameter (β_3'), imperfection. These parameters are considered for the development of the EQ.BF model. Some additional parameters like the ratio of diagonal length to the thickness of plate are also expected to have significant influence in development of EQ.BF model. For all parametric studies, detailed modeling technique in Abaqus is used.

Since it is targeted not to change any boundary member, all properties relating to truss braces in EQ.BF model needs to be carefully studied. Particularly, the effect of those properties in the overall behavior of the model needs to carefully observe. Change in any of these properties can be considered as the "cause" that will have a significant "effect" in the final performance of the structure. With an objective to match the final performance of EQ.BF model with the SPSW system that it represents, "cause" that affect the performance of the EQ.BF model needs to be adjusted. Thus, a proper methodology needs to be established through which the "cause" can be calibrated based on the "effect". Figure 3.2 gives a representative diagram showing all the properties that needs to be adjusted ("cause") to achieve the desired behavior ("effect") from

EQ.BF model. Properties of the truss member that can be adjusted are the geometric property i.e. the cross sectional area and the material properties like tension and compression yield stress and yield stain. Since, in case of SPSW systems the yielding of plate is progressive at least a tri-linear curve is required to describe the progressive failure of braces which is supposed to represent the infill plate. Thus, at least two points on the stress-strain curve in tension needs to be calibrated through the modeling process. But for strength in compression a bilinear curve should be adequate since, for SPSW system the infill plate buckles from its perfect geometry almost at an instance. It is expected that the compressive stress in truss braces, i.e. the compression strut in the EQ.BF model will not have a very significant effect in performance of the model. Only the initial stiffness might be slightly affected by it. However, to make the model complete it is an important part that needs to be standardized. Also, some other material property like pinching effect needs to be established independently and thus it is not shown as a part of cause-effect diagram in Figure 3.2.

Once the parameters are identified and established, the very next step is to calibrate them. A kind of reverse strategy in parametric study is used since, the effect is known from the SPSW performance and now the cause needs to be calibrated. An outline of the method that has been planned to establish the selected parameters is outlines in a flowchart in Figure 3.3. Initially to establish the cross-sectional area of the truss brace a linear shear stiffness relation of infill plate may be equated with that of shear stiffness in braces. Then to introduce geometric non-linearity for buckling of plates additional parameters may be introduced. Further modification of the area is expected to be required, since the strength of infill plate is greatly influenced by strength of the

bounding members. It can be observed here that an approximation has already been considered where the bending effect on infill plate is neglected. This is an assumption of the EQ.BF model.

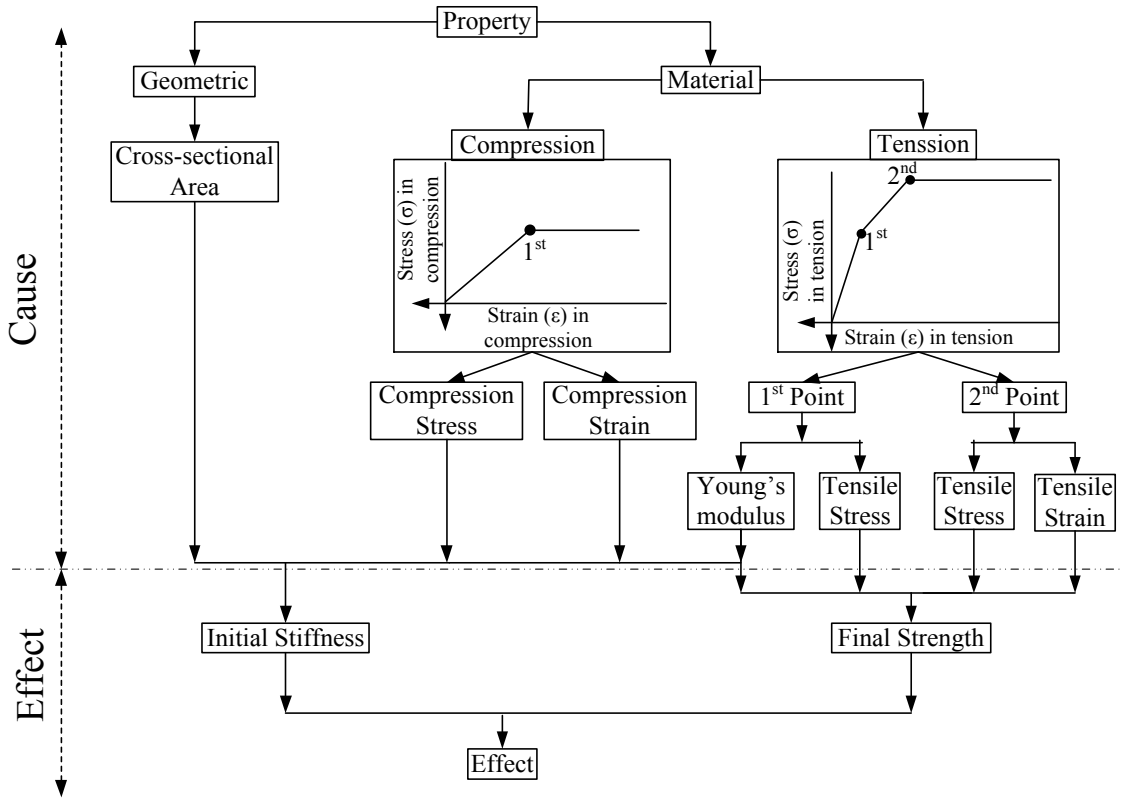

Figure 3.2: Property of truss braces to be adjusted to get desires effect from EQ.BF model

However, for very tall structures this assumption may have to be revisited and further study of the braced model accounting for the bending effect is required. Once the area of brace is established, material properties needs to be calibrated. The final strength of SPSW system depends greatly on material properties of infill plate. If the structure under consideration has more than one storey, than there may be some observable higher strength in infill plate for balance of storey forces. This storey effect can be used to revise the young's modulus for the braces. Since, young's modulus also affect the stiffness, the increased stiffness of infill plate due to bounding stories can thus be accounted. Yielding of braces is expected to start at same point as

in case of infill plate. To account for failure of infill plate in tension, at least one more stress strain point in tension for the material property of braces is considered. An analytical study with conservation of energy is used to calibrate the second point of the stress-strain curve in tension. Based on the force at which the plate buckles and its corresponding deformation, the compressive property of braces can be calibrated. For all these work repeated parametric study and a detailed statistical analysis are considered.

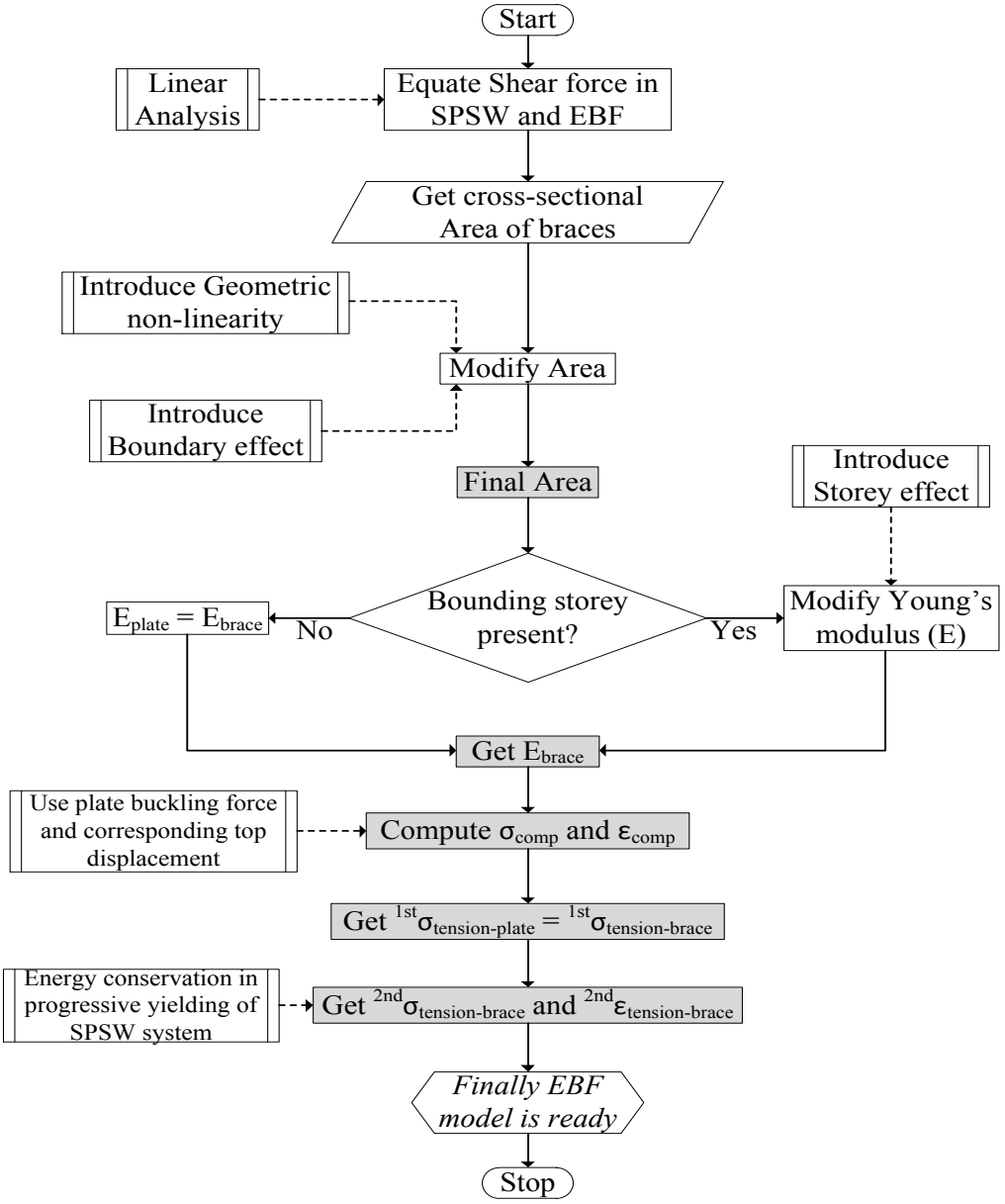

Figure 3.3: Flowchart representation of EQ.BF model development methodology

3.6 **Summary**

A step-by-step work sequence is outlined in this chapter. Based on the described methodology, a series of numerical study has to be carried out. As mentioned in the methodology, the numerical models must be validated against experimental results or results from any other established working models. Also, optimization may be required for the parametric study indicated to avoid make the braced model efficient. It is noticeable through this chapter that synchronization of different parts of work, like two dimensional models with three dimensional models during indirect validation, is a necessity. A significant amount of the deficiency in current research on the area of SPSW system is expected to be solved once the research work is complete.

Chapter 4. Development and Validation of FE model

4.1 Introduction

This chapter presents the development of the detailed finite element model. Selection of both material and geometric properties has been described in detail. Selection of element in detailed FE model analysis has also been justified. This chapter also describes the details of validation of the finite element model (FE model) by comparing the results from quasi-static experimental program with finite element analysis results. The developed detailed FE model is used to study several multi-storey steel plate shear wall structures. Static and dynamic results obtained from the detailed FE model are used for validation of simplified equivalent brace model in chapter 6.

4.2 Finite Element Modeling Technique

For detailed three-dimensional Finite Element Analysis (FEA), standard available commercial package Abaqus (Hibbitt, 2011) has been used. Abaqus is one of the most popular finite element modeling softwares where detailed modeling can be easily carried out using its pre-defined material models, element library and solver techniques. In the current scenario owing to buckling of thin plates, severe geometric non-linearity is expected. Also, material non-linearity is unavoidable to make this study complete. Thus, with so many complexities in non-linearity convergence problem is expected. Severe convergence problems have also been reported in published literatures (Mohammad et al., 2003). Abaqus has both the option of

carrying out Explicit or Implicit analysis. Abaqus/Explicit is at times used to escape the convergence problem. With proper control on kinetic energy, the explicit approach can be used for quasi-static loading analysis (Bhowmick et al., 2010). In Abaqus/Explicit instead of using iterative method, central difference method (which is conditionally stable) is used. However, the time increment needs to be extremely small to achieve reliable results (Bhowmick et al., 2010). Also, if stiffness damping is included then the situation worsens. So, finally Abaqus/Standard, in which the solver follows implicit formulation, with quasi-static loading was chosen for the analysis. The method uses the Hilber-Hughes-Taylor operator, which is an extension of the trapezoidal rule (Hilber et al., 1978). This operator is unconditionally stable, which is of great value when studying nonlinear structural systems. With implicit time integration, sometimes it is difficult to obtain a solution for a static analysis when the system is highly nonlinear. However, nonlinearities are usually more easily accounted for in dynamic analysis than in static analysis because the inertia terms provide mathematical stability to the system, making the method more robust. In the implicit dynamic analysis, to have reliable results, at every automatic time step increment the work done by the external forces were nearly equal to the internal energy of the system, whereas the kinetic energy remained bounded and small. A detailed description on each individual items of the modeling technique used for this study in Abaqus has been described through the set of subtopics. This three dimensional modeling is regarded as the detailed FE modeling which is highly accurate but at the price of excessive computational time consumption.

4.2.1 **Geometry and initial conditions**

Attempts have been made to construct FE models that can closely represent some available experimental studies. This has been done to validate the models and then use them for further studies. For validation, the geometric dimensions and the overall experimental environment have been maintained as close to real experimental setup as possible. The fish plate required in practical experimentation for connecting the thin plate with the boundary has not been considered since their influence in overall structural strength is almost insignificant. In practice it is almost impossible to have a perfect geometry. So, in the model some imperfection in geometry was required to be added. This initial imperfection for the FE model was introduced by the deformation due to the first buckling mode of the plate due to similar loading conditions. For multi-storey structures imperfection was assigned based on the buckling shape of the first mode of every plate i.e. instead of assigning a particular imperfection value to a plate set of imperfection was assigned for plates at every storey. The magnitude of initial imperfection in all cases is assumed to be two times the thickness of the plate being considered. Some other imperfections close to this value have been tested to have no significant impact on the output push-over curves. So, for all the models an initial imperfection of twice the thickness of infill plate is considered. Also, study with no imperfection assigned to plates showed slightly higher initial stiffness but a sudden fall of stiffness was observed when the plate suddenly starts to buckle under higher lateral loads. This study of initial stiffness without imperfection i.e. without any geometric non-linearity will be required for making a parametric study on SPSW systems.

4.2.2 **Element selection**

Abaqus provides a wide range of element selection options and user defined element if the standard element library does not have the element required. Since, the expected deformations of the plate can be best captured by shell element; general-purpose four node shell element (Abaqus element S4R) with reduced integration has been chosen from its library. Finite member stains and large rotations are accounted for by the shell element. It has six degrees of freedom defined in its global co-ordinates (three translations and three rotations defined along the x, y, z axes). To report the stress-strain component default local directions are used (Figure 3.1). These local directions rotate with average rotation of surface. The positive normal for these elements are usually given by right hand thumb rule. The top and bottom surface of the shell element is defined by the positive and negative direction of the normal respectively. This element has the capability to model both thin and thick shell behavior i.e. under given conditions it can handle both Kirchhoff's classical plate theory and Mindlin's shear flexible theory. The S4R element is based on an iso-parametric formulation which indicates that the same shape function is used for interpolation of displacement fields. It uses one integration point on its mid-surface to form the element internal force vector. The number of integration point along the thickness is chosen as five (Figure 4.1), which is also the default value for this element in Abaqus. With fine meshing the chance of local distortion of elements become negligible, so to have less number of iterations with accurate result reduced integration elements are used. This element has been used not just in developing the infill plate but also for the flanges and webs or boundary beam columns.

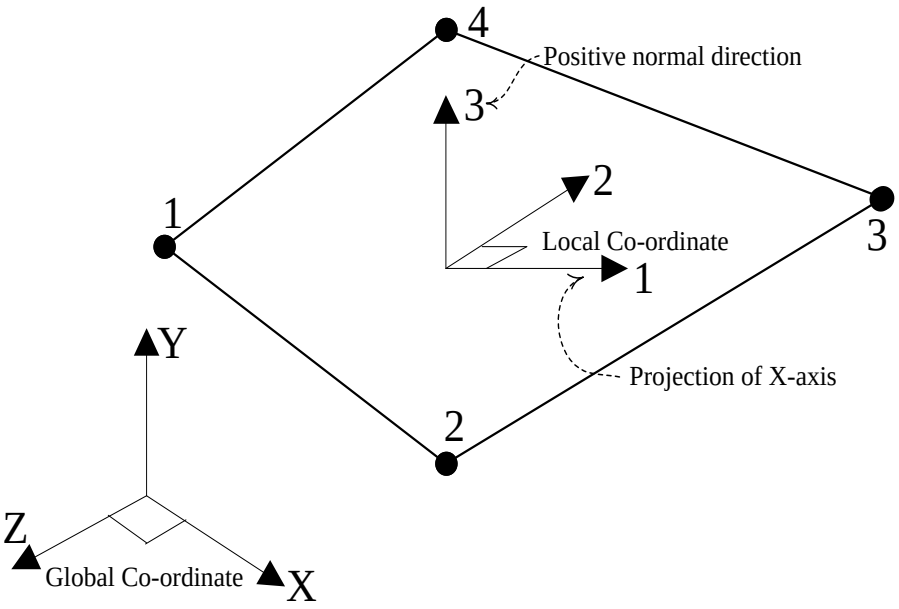

(a) Default local and global axis orientation in Shell elements

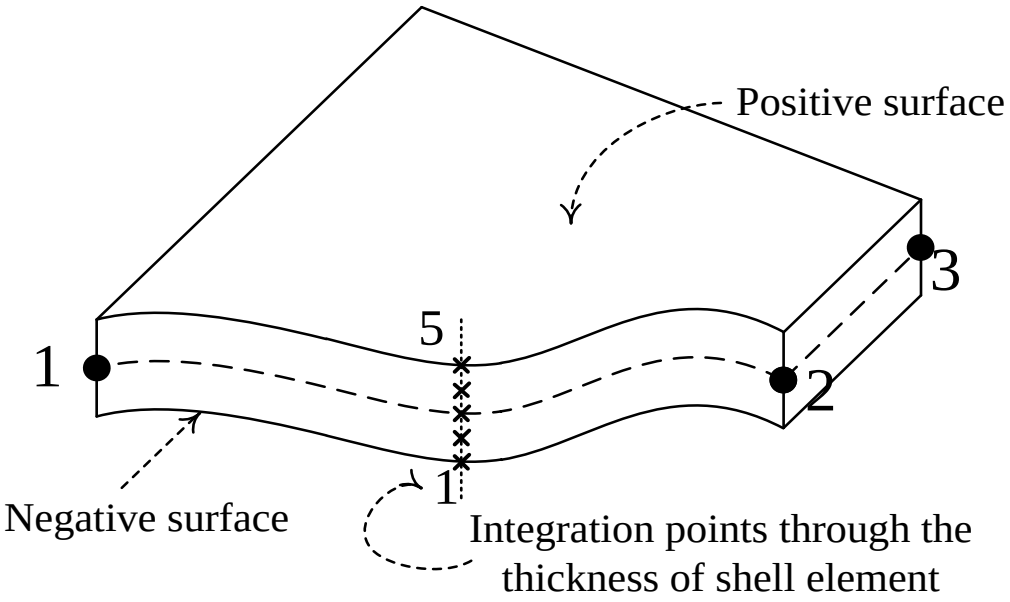

(b) Thickness integration points

Figure 4.1: Default local axis and integration points for shell element S4R

4.2.3 **Material properties**

Abaqus offers a wide range of options on the type of material to be defined. For validation of the test results, material properties used were as described by the tension coupon test results reported in the original research. For other analysis, a theoretical elasto-plastic stress versus strain curve was adopted. However, the stress and strain data reported for any experiment is usually engineering stress and engineering stain based on the initial cross section and initial gauge length of the coupon. Abaqus uses true stress or Cauchy stress and logarithmic strain for stress-strain formulation, regardless of the type of analysis being done. True stress (σ_{true}) and logarithmic plastic strain ($^{pl}\varepsilon_{ln}$) can be obtained by using the relations indicated in Equation 4.1 and Equation 4.2., respectively. The Von-Mises yield criterion with associated flow rule was used in the analysis. For the monotonic pushover analyses, a nonlinear isotropic hardening model was used. Additional to the defined materials, for dynamic analysis the density needs to be defined. Since, to account for the mass, additional masses are defined in dynamic analysis so, density of material was kept sufficiently low such that the final results are not affected by it.

$$\sigma_{true} = \sigma_{norm}\,(1 + \varepsilon_{norm}) \tag{4.1}$$

$$^{pl}\varepsilon_{ln} = ln\,(1 + \varepsilon_{norm}) - (\sigma_{true} / E) \tag{4.2}$$

where, E is the modulus of elasticity, σ_{norm} and ε_{norm} are the respective nominal stress and strain obtained experimentally.

4.2.4 **Analysis controls**

Displacement control solution strategy is usually preferred for static analysis of SPSW systems. For pushover analysis, where the objective is to find the stiffness and capacity of the shear wall, the desired displacement is applied in steps as boundary at the loading point. To make correct estimation of the capacity, the solution strategy should be able to trace response at and just more than the limit point. Since, load displacement is almost flat near the limit point so a very small change in load will result in large change in displacement. With a load control scheme, sometimes it is not possible to obtain the complete pushover curve including the descending branch. Thus a displacement control analysis scheme is adopted for all the pushover analysis. For cyclic analysis the total drift of the structure is increased by integer multiples of drift when first significant yielding is observed. With load control capturing the yield points and achieving the correct drift is almost impossible once the elastic limits are exceeded. Within elastic limit however, load control strategy would make analysis faster. Both cyclic and pushover analysis was carried out in Static-General module of Abaqus with defined smooth step amplitude for the displacement control point. Also, to avoid local effect at loading points the load was distributed to three adjacent nodes. This was done by connecting the loading nodes to an external reference point, located very close in the lateral direction, by rigid beam multi-point-constraint. Abaqus/Standard allows the application of acceleration as a boundary condition. Releasing the support condition in the direction of application of ground motion and applying the scaled acceleration data of selected ground motion would finally achieve the response time history for the concerned structure. Dynamic Implicit analysis was used for time history analysis.

Frequency analysis was carried out on multi-storey structures before a response spectrum analysis with hazard spectrum.

4.3 **Validation of detailed FE models**

The finite element model developed has been validated by comparing the results of the available tests. As, already reported in chapter 2, very few experimental tests have been performed with light-gauge steel plate shear wall. Neilson (2010), Kharrazi (2005) being two of those people who performed experiments with single storey light-gauge SPSW systems. Neilson's investigation was mainly concentrated on the development of welding technology for working with light-gauge SPSW systems. Kharrazi (2005) studied light-gauge SPSW systems using HSS sections for columns to avoid local failure. Both the tests conducted by Kharrazi (2005) and Neilson (2010) have been used for validating the detailed FE model. Pushover analysis has been carried out and the resulting curves are compared with the experimental ones already reported. These validated models have been used for further studies.

The specimen designed based on CAN/CSA S16 – 01 was tested by Neilson (2010). The objective of his work was to Neilson (2010) investigated the behavior under cyclic load displacements of a large scale steel plate shear wall with a thin infill plate welded to the boundary frame using fish plate. More stress was given on the development of suitable welding technology development. The size of beams and columns were so chosen that they were capable of developing the full tension field in the plate at the same time do not impart additional lateral stiffness to the system. The specimen tested by Neilson was modeled in Abaqus using the

detailed FE modeling technique already described. Material properties are chosen identical to the one reported by the tension coupon test in author's work like yield strength of boundary as 380Mpa and that of thin infill plate as 275MPa. However, the engineering stress and strain were converted to true stress strain as already described in chapter 3. Additionally, an imperfection of *2*b* (= 1.96), where *b* is the thickness of the infill plate, was used. As in the test, displacement loading has been applied through the center line of the top beam level. The displacement was increased to a maximum value of 70 mm as obtained from the envelope of hysteresis curve of physical test. The geometry of the test specimen was presented earlier in Chapter 2 (Fig. 2.10). Figure 4.2 presents the FE element mesh of the specimen tested by Neilson (2010). The measured (as obtained from physical experimentation) and predicted (from FEA) base shear values are plotted against the storey drifts in Figure 4.3. The figure indicates that the finite element model predicts the initial stiffness and post-yield response of the shear wall very well. The ultimate capacity of the specimen is over estimated by less than 2%.

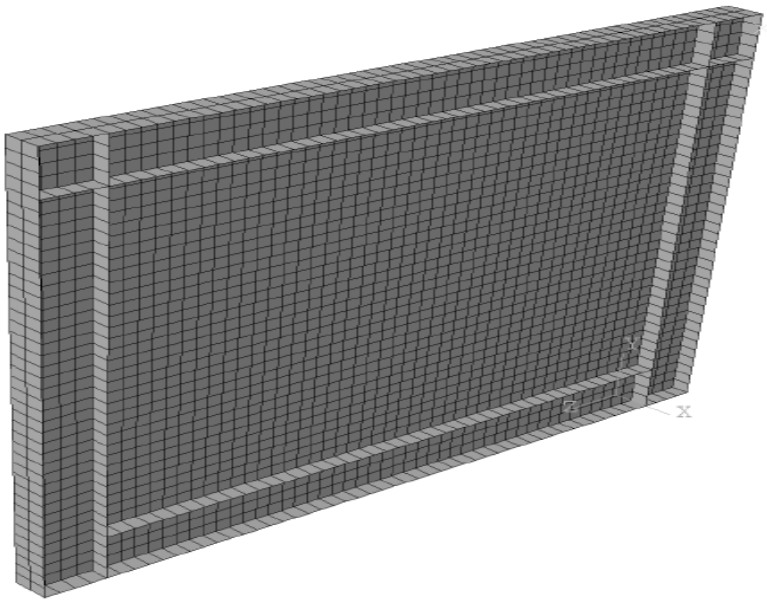

Figure 4.2: Meshed geometry of detailed FE model of Neilson's (2010) specimen

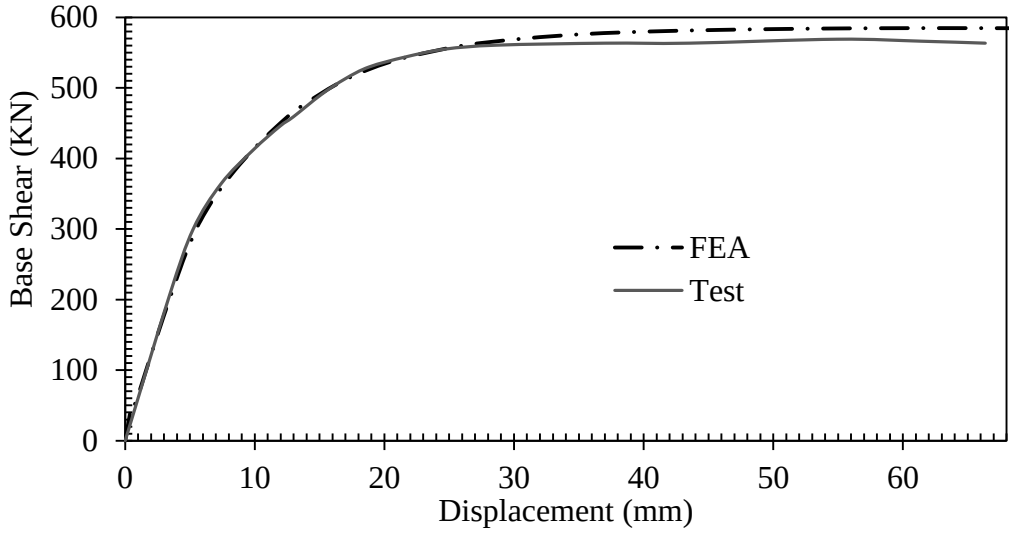

Figure 4.3: Validation of Push over curves for Neilson's (2010) test

Kharrazi (2005) tested two single storey SPSWs (designated as DSPW1 and DSPW2) with light-gauge infill plates as described in more details in chapter 2. Instead of using W-sections for their columns, Hollow Steel Sections (HSS) were used. The primary reason for this was to avoid local buckling. However, for beams W-section was used. A monotonic pushover analysis was conducted with a lateral load applied along the center-line of the top beam. As earlier, initial imperfection of *2*b* (*=1.4mm*) was used. For both specimens, tension coupon tests were conducted and the exact material properties were obtained. For DSPW-1 the yield strength of the thin plate was considered as 200 MPa and for DSPW-2, the yield strength was 150 MPa. The material properties obtained by physical experimentation have been used here for developing the FEA model. The displacement of a node at top level was monitored and the analysis was terminated when the maximum lateral deflection has reached 115mm for DSPW-1 and 95 mm for DSPW-2, obtained from the envelope of hysteresis curves of the physical test. No failure criterion for the model was defined. Figure 4.4 presents the pushover curves generated for

both DSPW1 and DSPW2. For both specimens (DSPW-1 and DSPW-2), the analysis results show excellent agreement for the initial stiffness. For DSPW-2, the ultimate capacity obtained from the experiment agrees well with the FEA model. However, in DSPW1, the FEA model underestimates the capacity by a maximum of 3.4%.

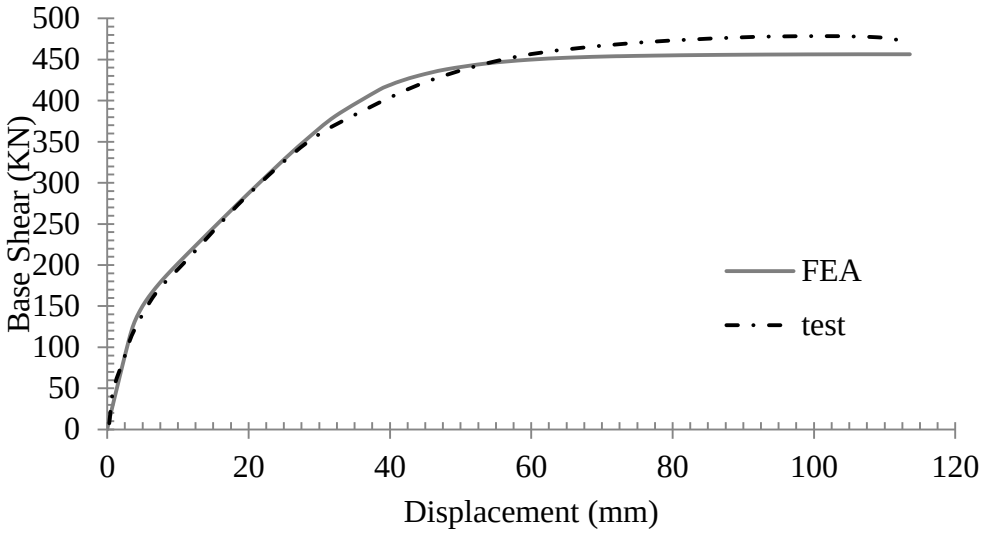

(a) DSPW-1

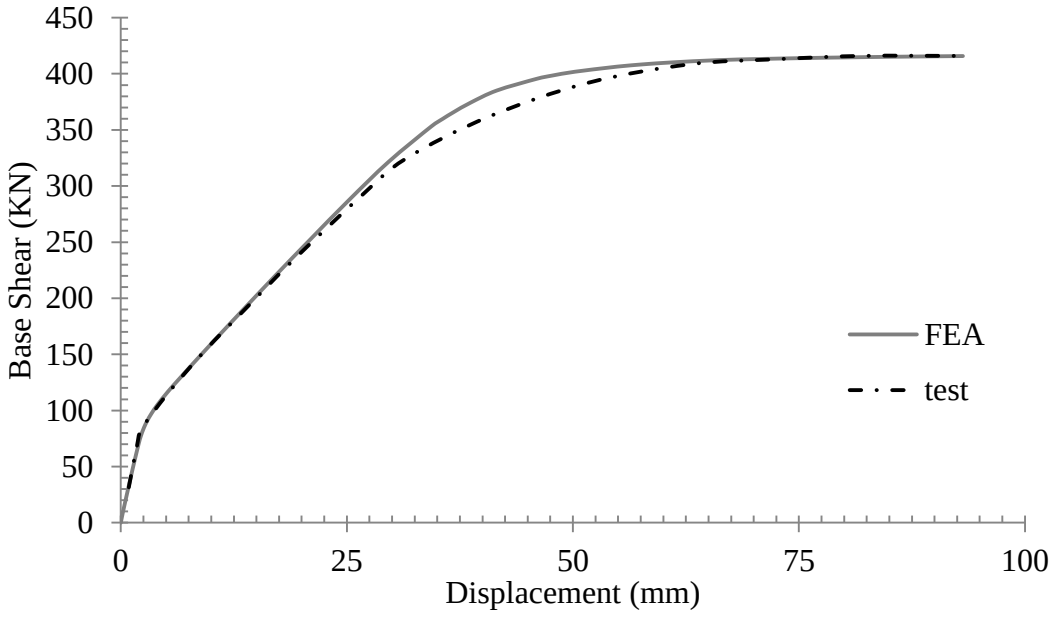

(b) DSPW-2

Figure 4.4: Validation of Push over curves from Kharrazi's work (2005)

4.4 **Design of multi-storey structures**

Four-storey, six-storey and ten-storey buildings are considered here to evaluate the performance of the proposed modeling technique for SPSW systems. All buildings have identical plan with a total plan area of 2014 m^2 and represent hypothetical office buildings which are assumed to be located in Vancouver. The plan of the building and location of gravity columns, beams and SPSWs are shown in Figure 4.5. The building has two identical shear walls to resist lateral forces in each direction and thus each shear wall will resist one half of the design seismic loads. For simplicity, torsion is neglected. Each shear wall panel is 7.6 m wide, measured from centre to centre of columns, and has an aspect ratio of 2.0 (i.e. storey height of 3.8 m). The building is assumed to be founded on soil of site class C according to NBCC 2010. A dead load of 4.26kPa is used for each floor and 1.12kPa for the roof. The live load on all floors is taken as 2.4kPa and no live load is assumed for the roof. The nominal yield strength and the modulus of elasticity of steel used in the beams and columns are assumed to be 350 MPa and 200000 MPa, respectively. Steel plates used here are assumed to be similar to the specimen tested by Neilson (2010), which has yield strength of 173 MPa and the modulus of elasticity of 210000 MPa. Test results have shown that welded shear walls have a very high ductility. Thus, a ductility-related force modification factor, R_d, of 5.0 and an over-strength force modification factor, R_o, of 1.6 are used in the design of the light-gauge shear walls. The equivalent static lateral loads due to the design seismic event have been computed using the seismic provision of NBCC 2010 (NRC 2010). The lateral forces determined for each 4-storey shear wall are 152.1 KN, 304.3 KN, 456.4 KN, and 212.8 KN at the 1^{st} storey, 2^{nd} storey, 3^{rd} storey and roof respectively. For the 6-storey SPSW, the lateral forces were determined as 105.1 KN, 210.2 KN, 315.4 KN, 420.5 KN, 525.6

KN, and 220.6 KN at the 1st storey, 2nd storey, 3rd storey, 4th storey, 5th storey, and roof respectively. For the 10-storey light-gauge SPSW, the lateral forces were determined as 46.5 KN, 93.1 KN, 139.6 KN, 186.1 KN, 232.6 KN, 279.2 KN, 325.7 KN, 372.2 KN, 418.7 KN and 162.7 KN at the 1st storey, 2nd storey, 3rd storey, 4th storey, 5th storey, 6th storey, 7th storey, 8th storey, 9th storey and roof respectively. Since there are no design guidelines for design of light-gauge steel shear walls, for this research, the light-gauge shear walls were designed according to the capacity design concepts used for conventional ductile SPSWs. Thus, boundary members are designed to develop full capacity of light-gauge infill plates. The probable shear resistance of the wall V_{re} is given by (CSA 2009):

$$V_{re} = 0.4\varphi F_y bL \sin 2\alpha \tag{4.3}$$

where b is the infill plate thickness; L is the bay width; α is the angle of the tension field developed in the infill plate and is obtained from CAN/CSA-S16-09.

Table 4.1: Details of structural elements for 4-storey, 6-storey and 10-storey SPSW systems

Storey	10-storey wall		6-storey wall		4-storey wall	
	Plate thickness (mm)	Column	Plate thickness (mm)	Column	Plate thickness (mm)	Column
1	5	W360x900	3	*W360x744*	2.75	*W360x634*
2	5	W360x900	3	*W360x744*	2.5	*W360x634*
3	5	W360x677	2.75	*W360x382*	2	*W360x382*
4	4.5	W360x677	2	*W360x382*	1	*W360x382*
5	4	W360x509	1.5	*W360x262*		
6	3.5	W360x509	1	*W360x262*		
7	3	W360x463				
8	2.5	W360x463				
9	1.5	W360x463				
10	1	W360x463				

The boundary members are designed according to CSA-S16-09 (CSA, 2009) to develop the full capacity of light-gauge infill plates. For 4-storey and 6-storey shear walls (Figure 4.6), a beam size of W610x372 has been selected at the base of the walls to anchor the forces developed due to the yielding of the bottom storey infill plates and for all other storeys, the beam section of W460x158 has been utilized. For the 10-storey structure the base beam is selected as W690x419. From first to sixth storey the beams are W610x372 and the top four storeys have W460x286 beams. CAN/CSA-S16-09 (CSA, 2009) also has provisions for the stiffness of the columns to ensure the development of an essentially uniform tension field in the infill plate. Table 4.1 presents the final columns sections and plate thicknesses for the four, six and ten storey light-gauge SPSWs.

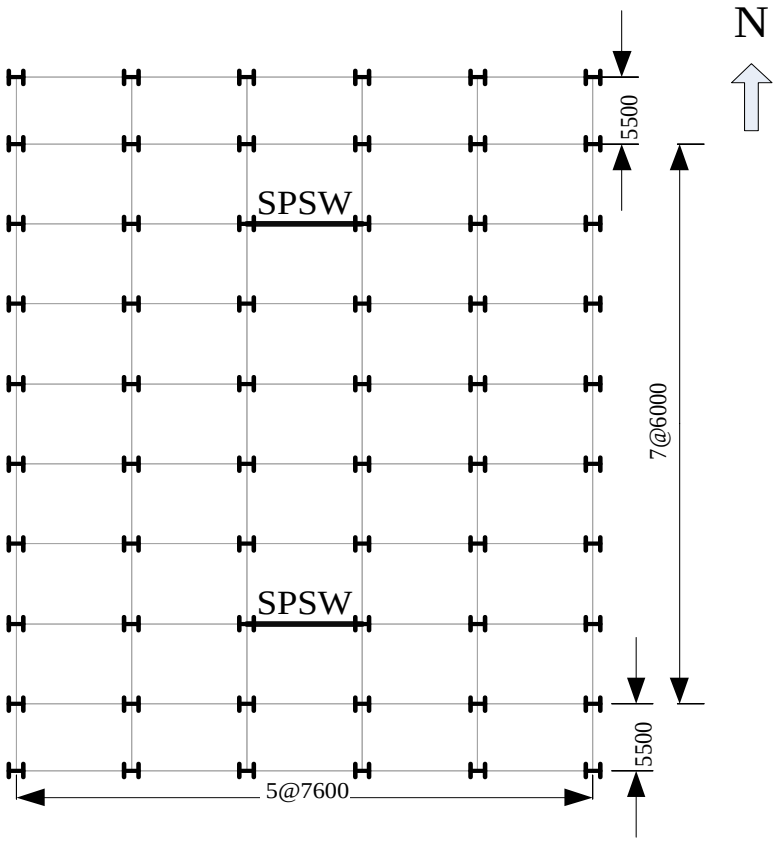

Figure 4.5: Plan of 4, 6 and 10-storey SPSWs

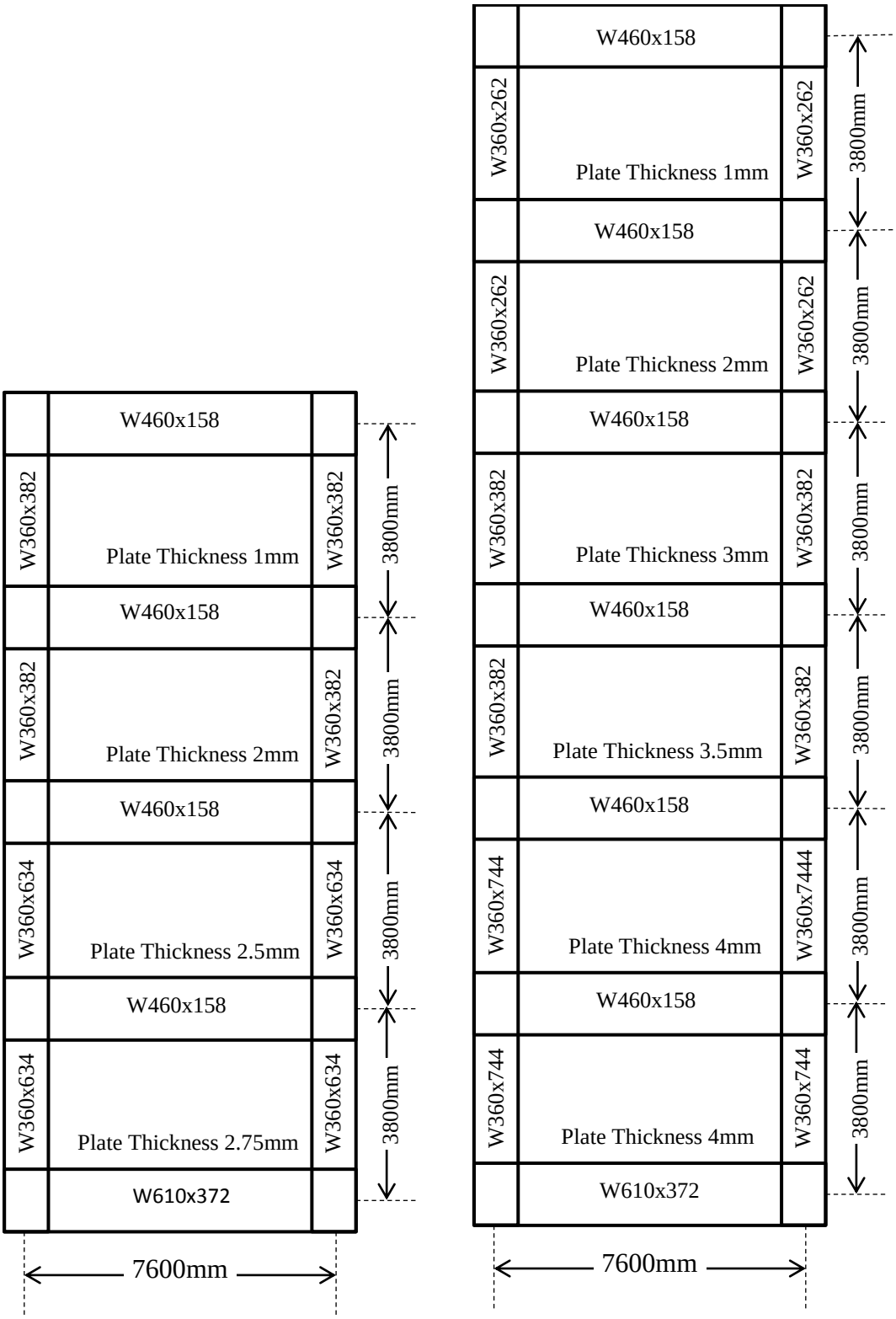

Figure 4.6: Schematic diagrams for the 4-storey and 6-storey light gauge SPSWs

4.5 **Selection of ground motion**

The hypothetical buildings have been assumed to be located in the region of Vancouver, Canada. To carry out time history and response spectrum analysis, the hazard spectrum for that region provided in NBCC 2010 has to be considered. Also, the set of ground motions selected should be compatible with the defined hazard spectrum. Ground Motions Records (GMR) has been selected from the database of real earthquake records available at the Canadian Association for Earthquake Engineering (Naumoski, 2008). NBCC 2010 and FEMA356 recommend a set of minimum seven ground motions to be considered for analysis if the average value of each response parameter is used in design or three different records are enough if the maximum response is selected. So, eight historical crustal ground motion records are selected (Table 4.2) with all having magnitude in between 6.4 to 7.6. For the selected ground motions, the ratio A/V (A, peak acceleration in scale of g and V, peak velocity in m/s, where g is acceleration due to gravity in m/s^2) are within range of 0.8 to 1.2 which is close to the A/V ratio expected for an earthquake in Vancouver (Naumoski et al., 2004). Other than ground motion record number#2, #3 and #6, which are ground motions on rock, all others correspond to soil type C (according to the shear wave range specified by NBCC 2010). Since, a total of eight ground motions, which are more than required , have been used in this study, no modifications has been done to ground motions on rock type of soil. Also, their shear wave velocities are in close proximity to the shear wave velocity for soil type Class C. The selected GMRs are scaled to match the uniform hazard spectrum of Vancouver (Figure 4.7) over a period of 0.2T to 1.5T (where T is the fundamental time period of the structure). During inelastic behavior, stiffness of the structure degrades and the period of the building may extend and thus the upper limit of the hazard spectrum is increased up

to 1.5T. For scaling the response spectrum of each GMR, the SeismoMatch (Abrahamson et al., 2006) software has been used. Further details on the selected ground motion characteristics are given in Appendix I.

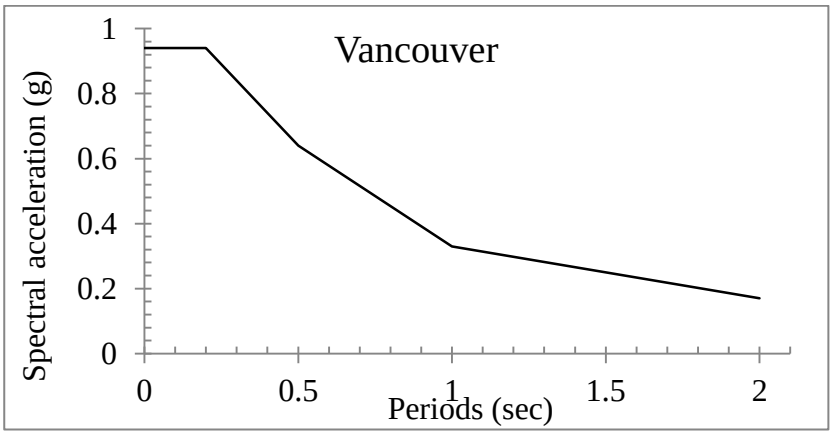

Figure 4.7: Uniform Hazard Spectrum for Vancouver (NBCC 2010)

Table 4.2: Description and peak ground motion parameters for selected ground motions

Rec. No	Earthquake	Date	Mag^n	Site	Max. Acc. A(g)	Max. Vel. V(m/s)	A/V
1	Imperial Valley California	May-18, 1940	6.6	El Centro	0.348	0.334	1.04
2	Kern County California	Jul-21, 1952	7.6	Taft Lincoln School Tunnel	0.179	0.177	1.01
3	Kern County California	Jul-21, 1952	7.6	Taft Lincoln School Tunnel	0.156	0.157	0.99
4	Borrego Mtn. California	Apr-08, 1968	6.5	San Onofre SCE Power Plant	0.046	0.042	1.1
5	Borrego Mtn. California	Apr-08, 1968	6.5	San Onofre SCE Power Plant	0.041	0.037	1.11
6	San Fernando California	Feb. 9, 1971	6.4	3838 Lankershim Blvd., L.A.	0.15	0.149	1.01
7	San Fernando California	Feb. 9, 1971	6.4	Hollywood Storage P.E. Lot, L.A.	0.211	0.211	1
8	San Fernando California	Feb. 9, 1971	6.4	3407 6th Street, L.A.	0.165	0.166	0.99

4.6 **Time History analysis with detailed FE model**

The designed four-storey and the six-storey have been subjected to time history analysis with detailed FE model with shell element in Abaqus. Detailed analysis on the performance of the ductile SPSW structures is discussed in chapter 7. It is worth mentioning that with an average efficient computer and coarse mesh takes few days or at times weeks to complete the time history analysis with a set of eight selected and scaled ground motions. So, analysis of the ten-storey was intentionally avoided with this detailed FE model. A simplified model developed in next chapter is used to analyze the ten-storey light-gauge SPSW. The time history graphs (Figure 4.8 to Figure 4.23) obtained from the detailed analysis will not only be used to test the performance of the light gauge SPSW systems but also to validate the simplified braced model.

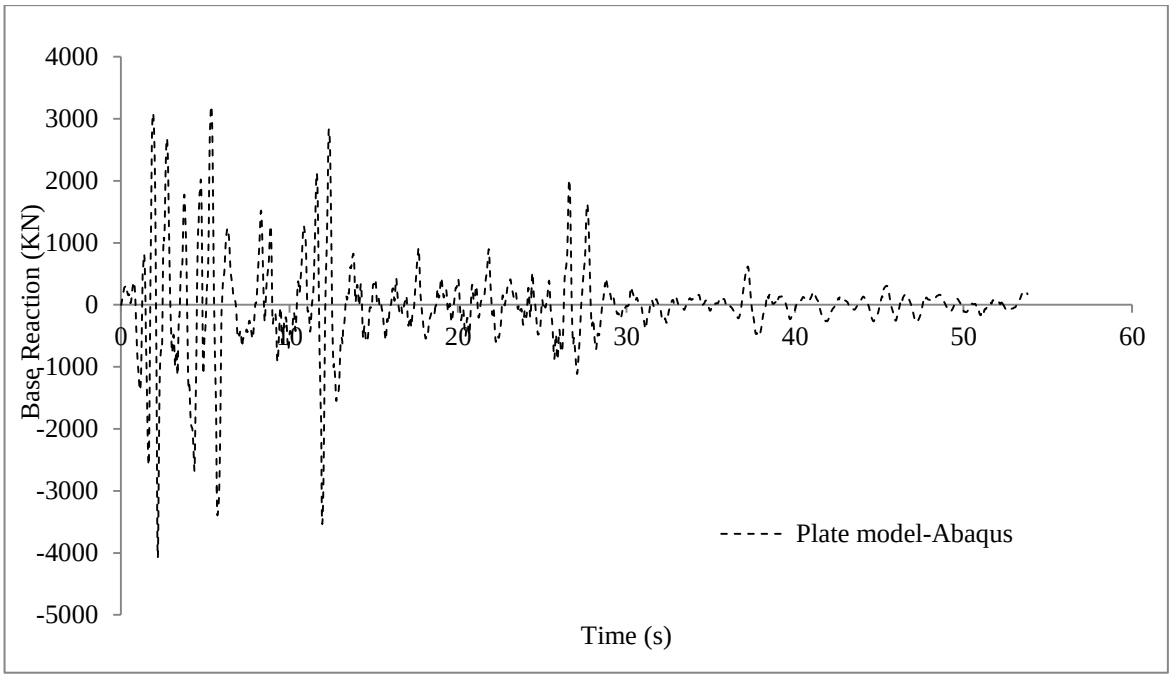

(a) Base Reaction

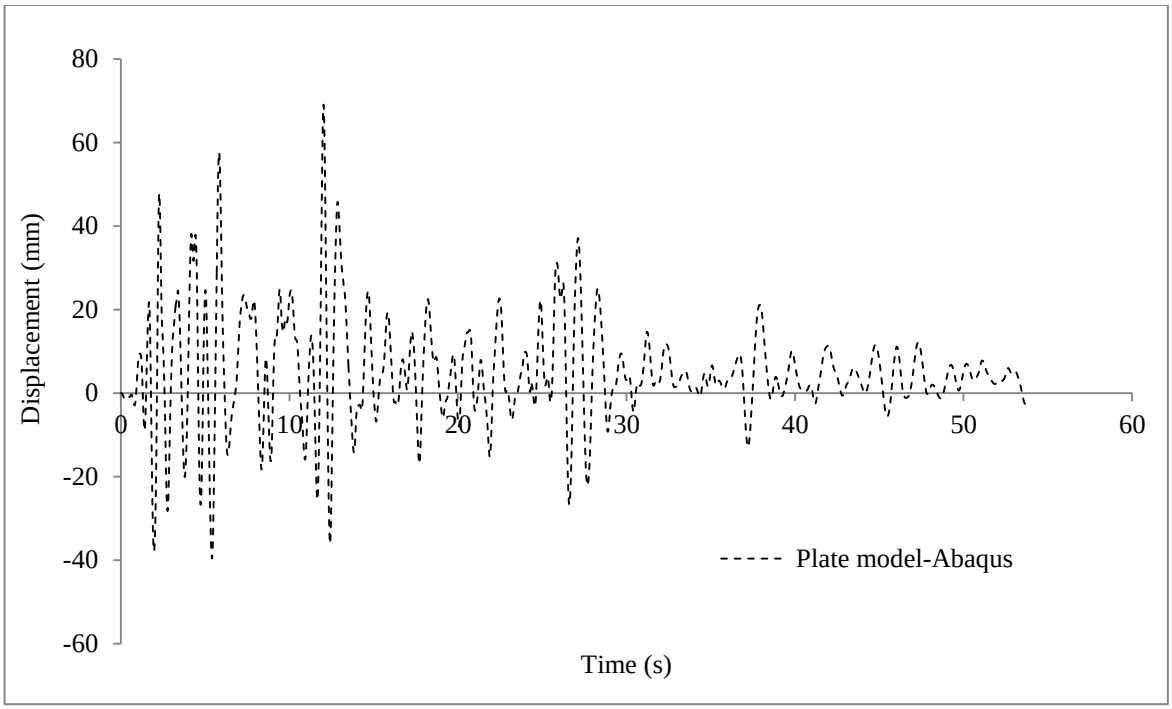

(b) Top Displacement

Figure 4.8: Response of 4-storey structure from Abaqus for Earthquake Record#1

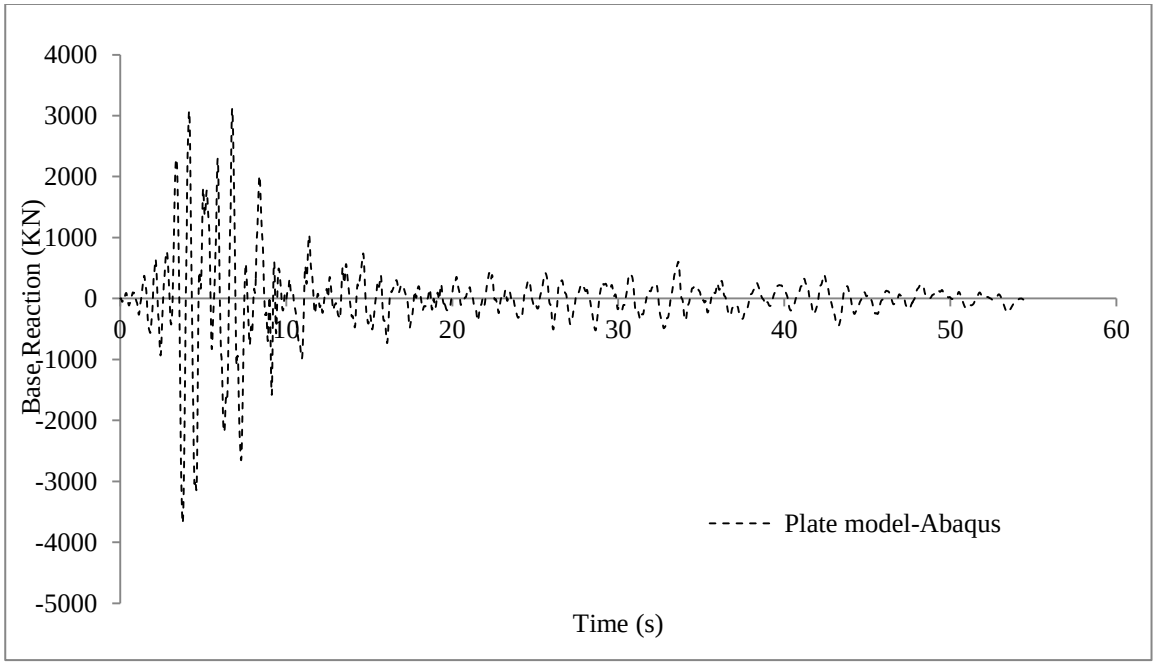

(a) Base Reaction

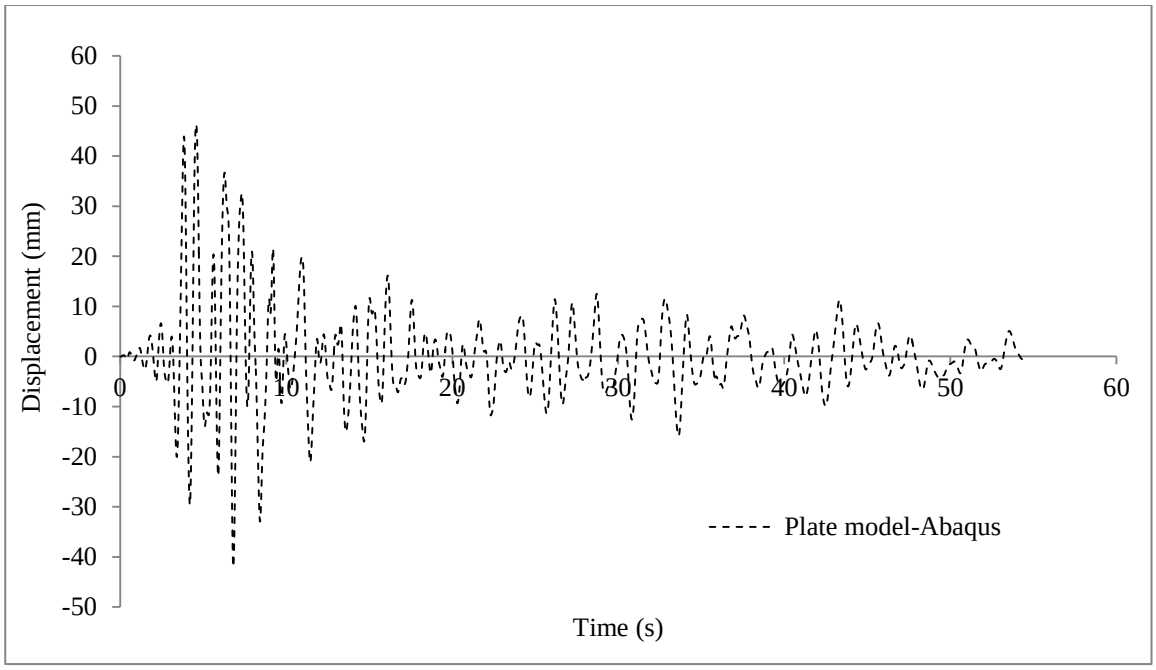

(b) Top Displacement

Figure 4.9: Response of 4-storey structure from Abaqus for Earthquake Record#2

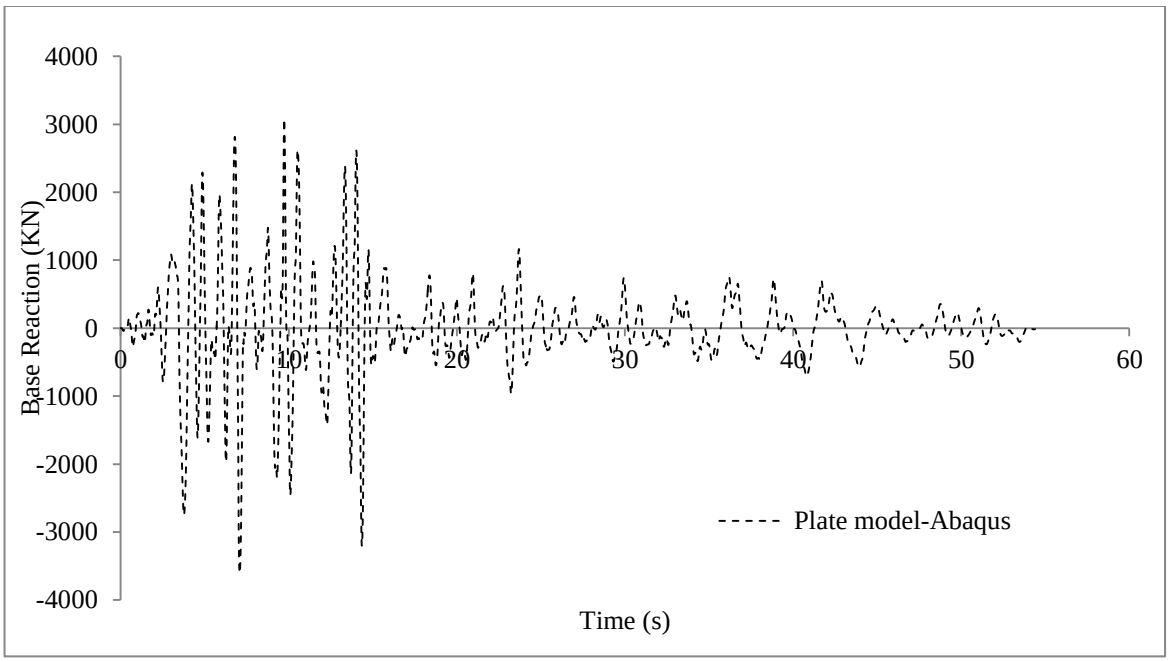

(a) Base Reaction

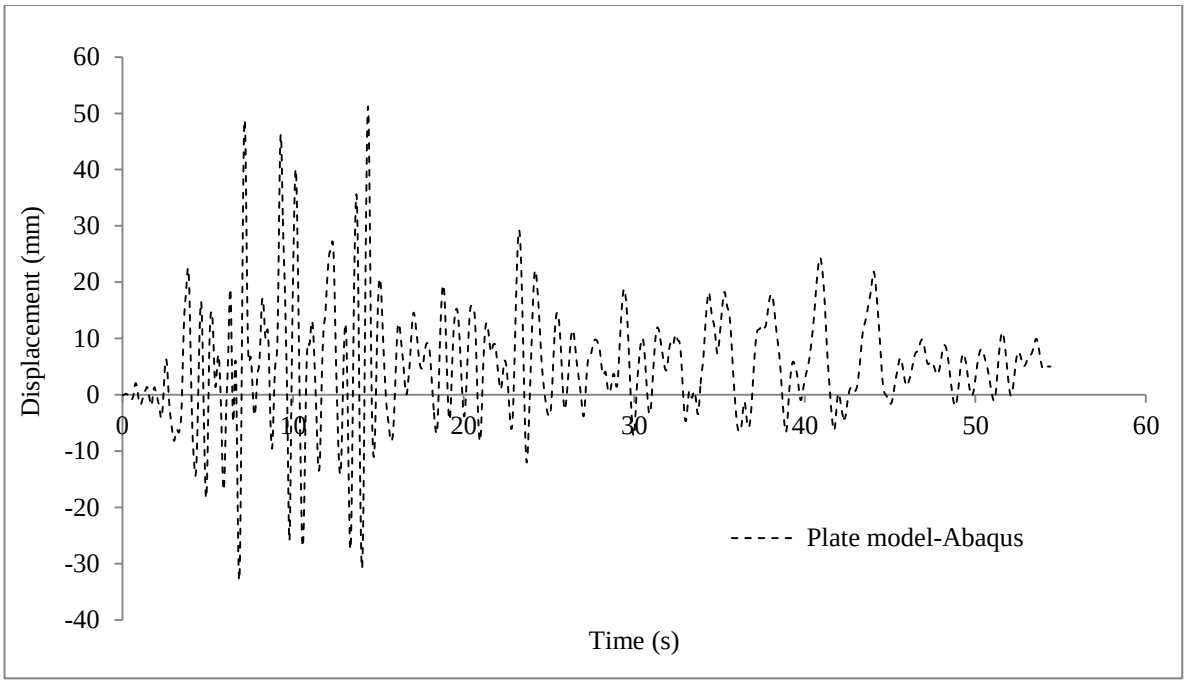

(b) Top Displacement

Figure 4.10: Response of 4-storey structure from Abaqus for Earthquake Record#3

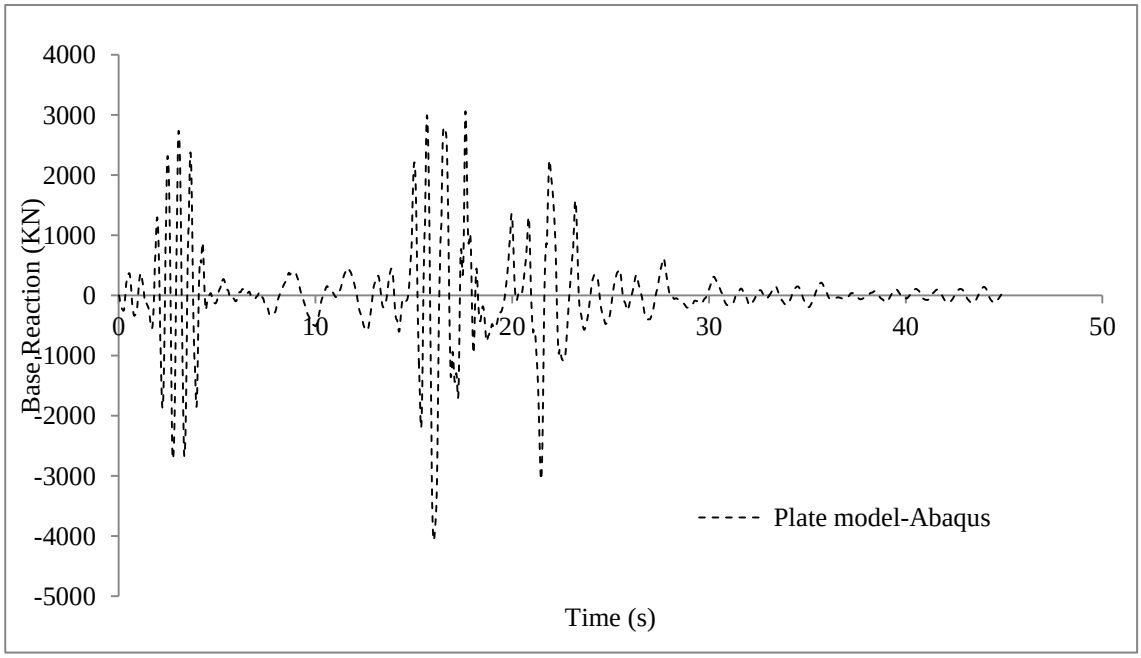

(a) Base Reaction

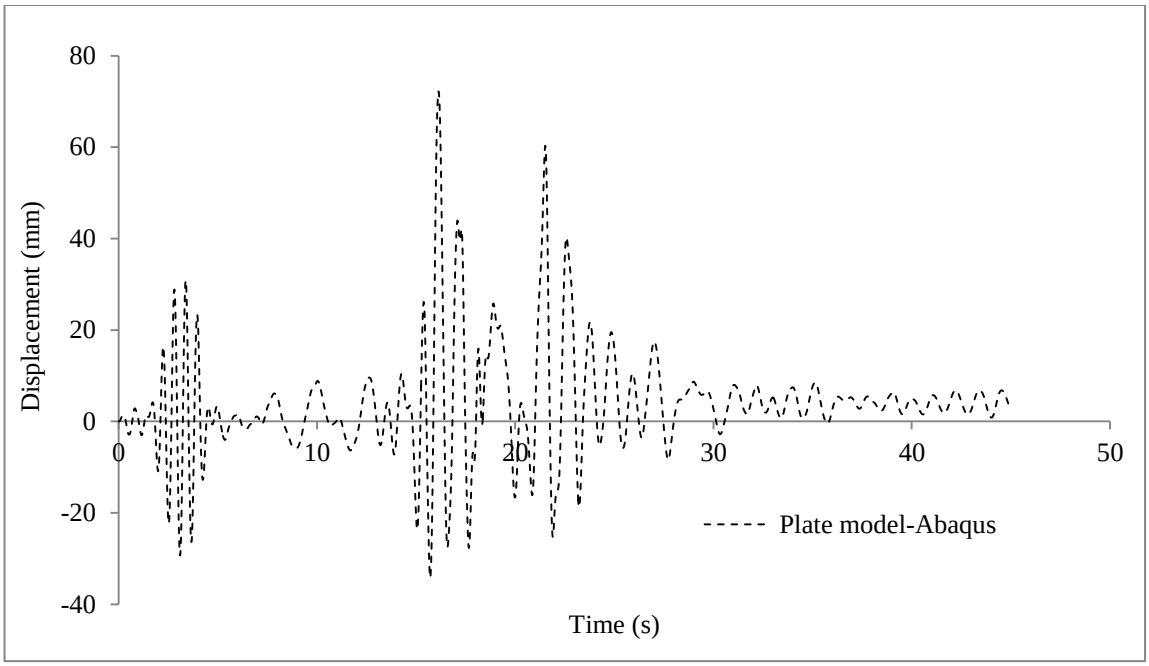

(b) Top Displacement

Figure 4.11: Response of 4-storey structure from Abaqus for Earthquake Record#4

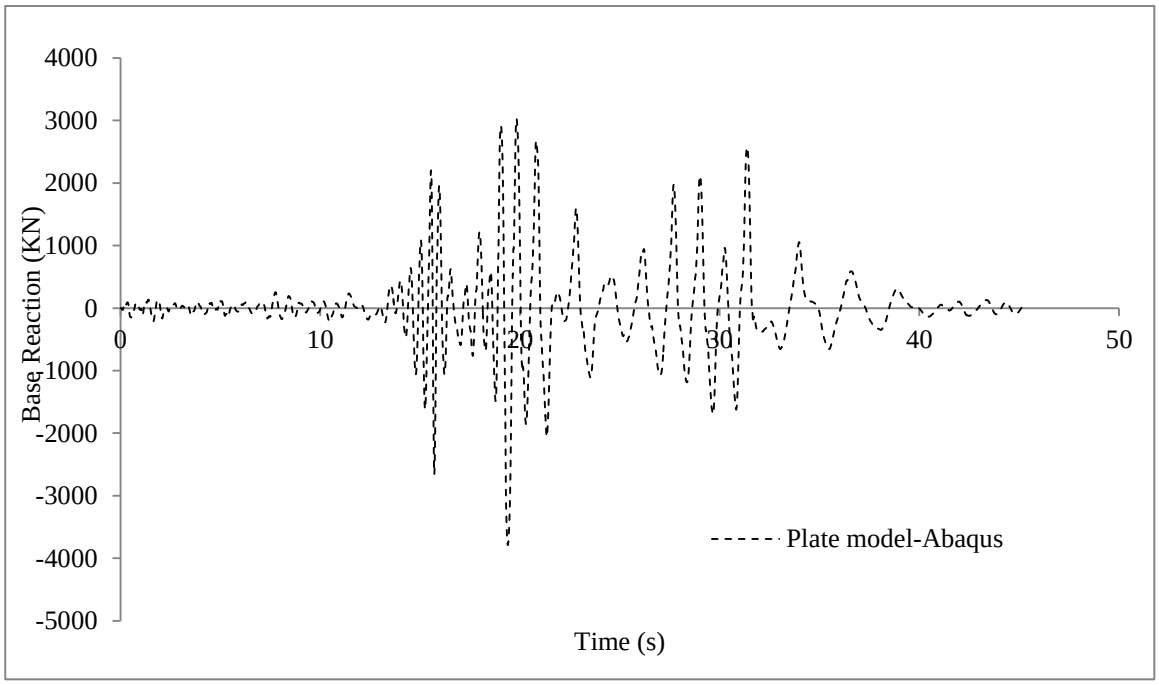

(a) Base Reaction

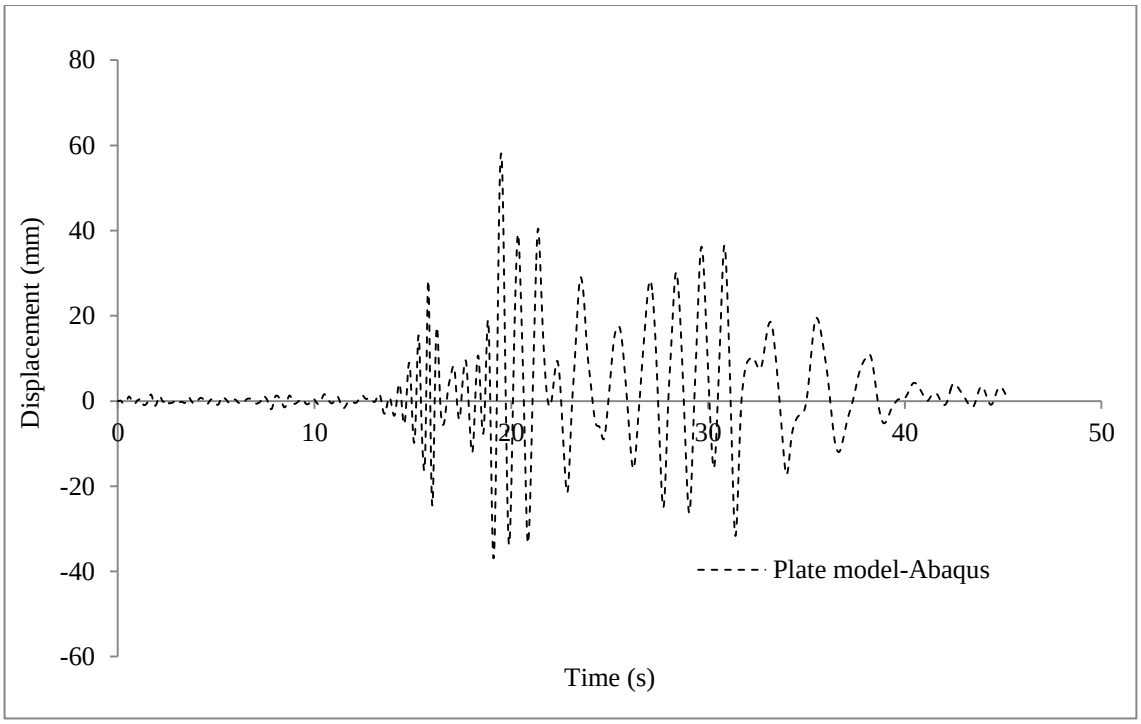

(b) Top Displacement

Figure 4.12: Response of 4-storey structure from Abaqus for Earthquake Record#5

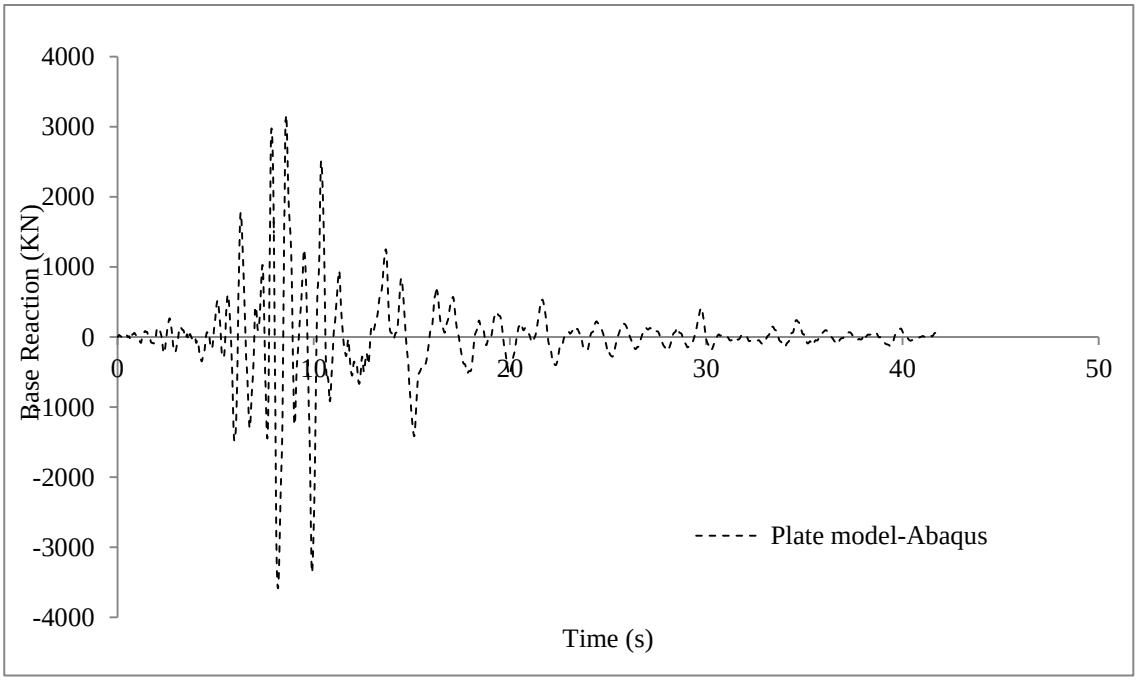

(a) Base Reaction

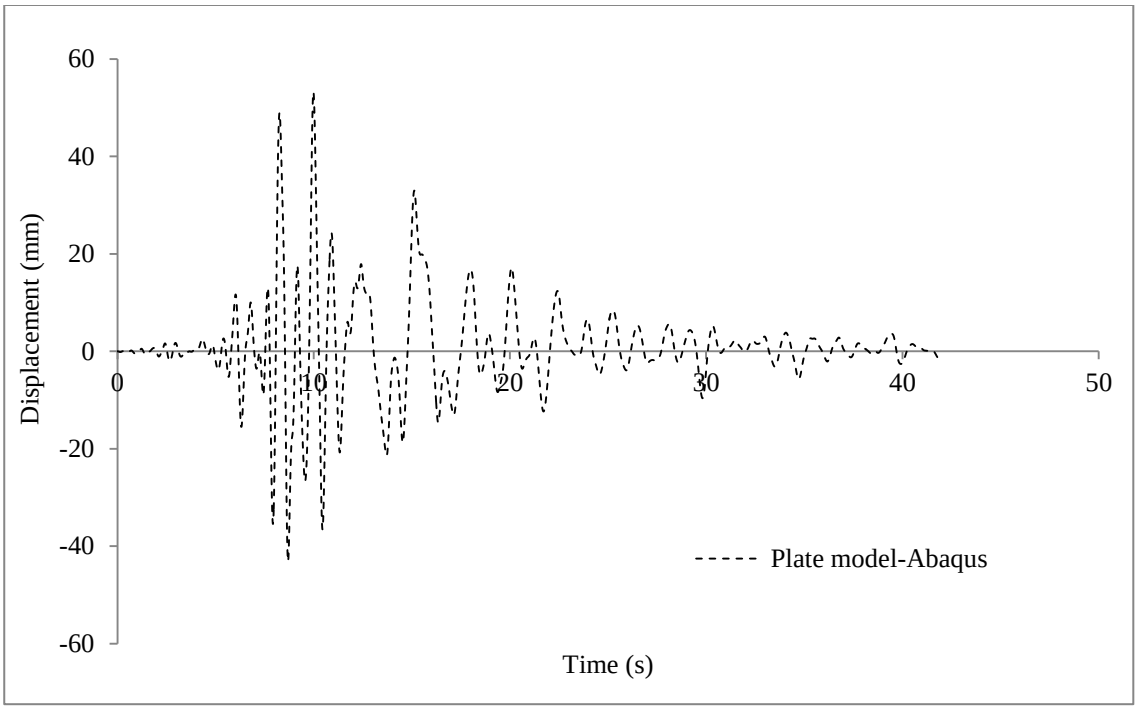

(b) Top Displacement

Figure 4.13: Response of 4-storey structure from Abaqus for Earthquake Record#6

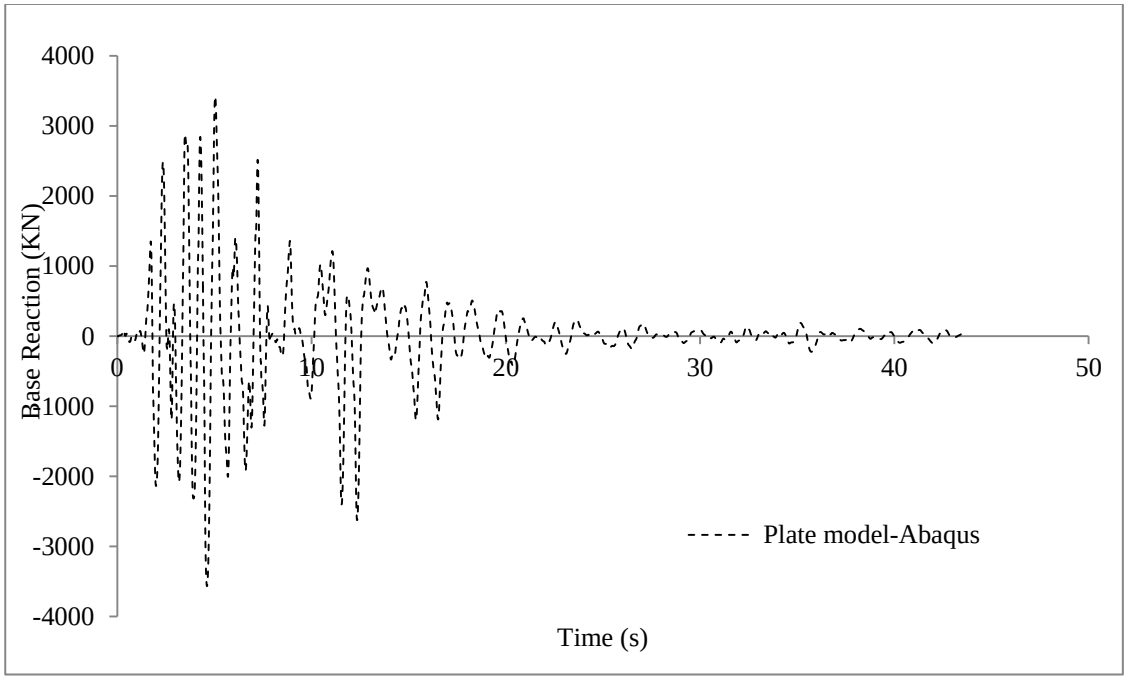

(a) Base Reaction

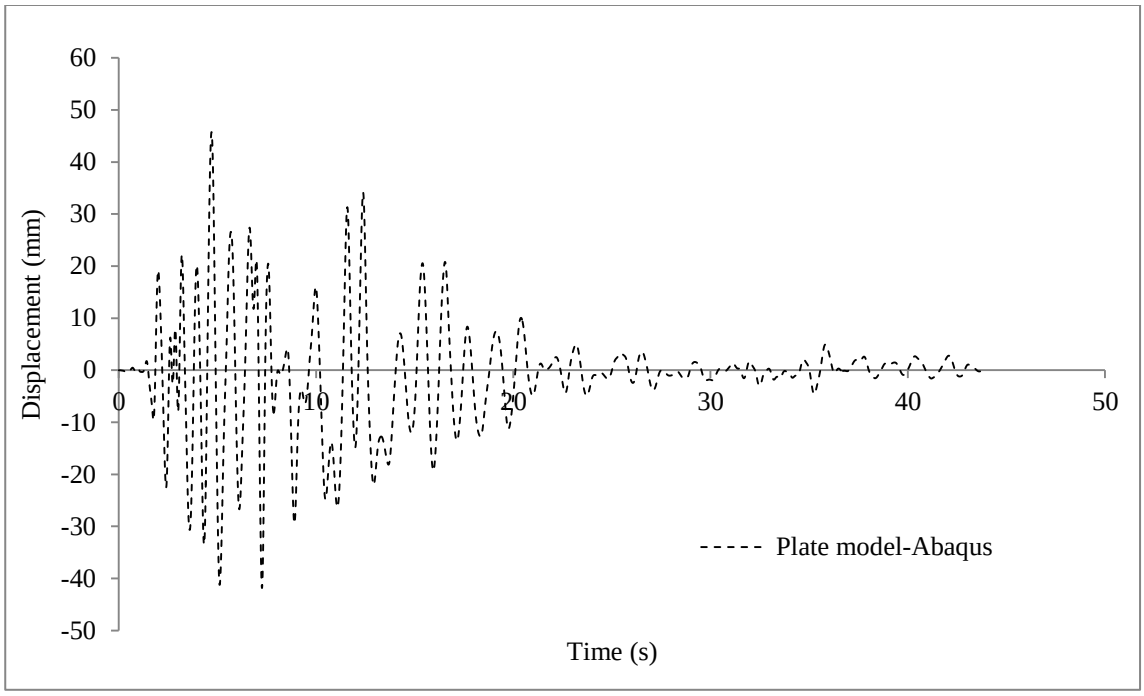

(b) Top Displacement

Figure 4.14: Response of 4-storey structure from Abaqus for Earthquake Record#7

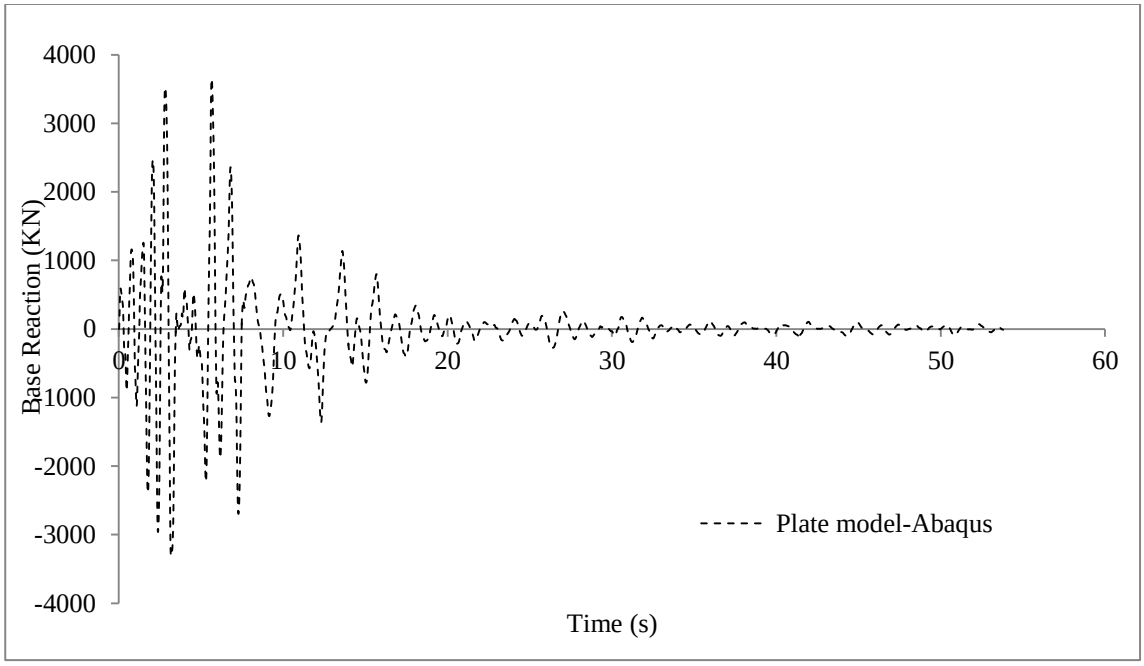

(a) Base Reaction

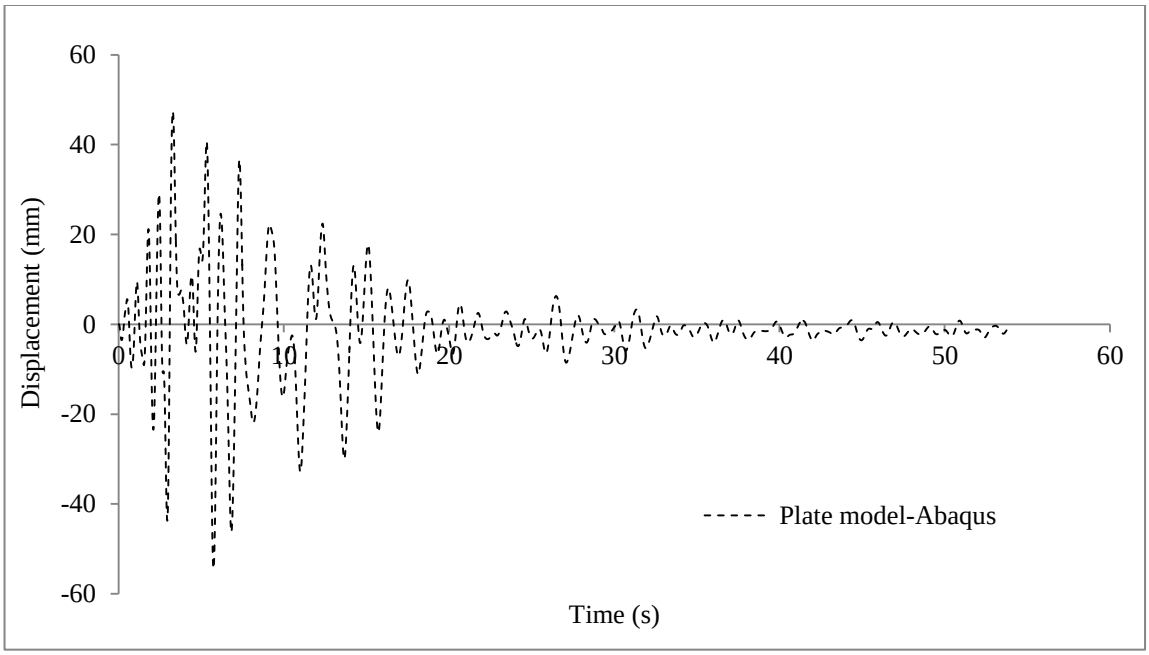

(b) Top Displacement

Figure 4.15: Response of 4-storey structure from Abaqus for Earthquake Record#8

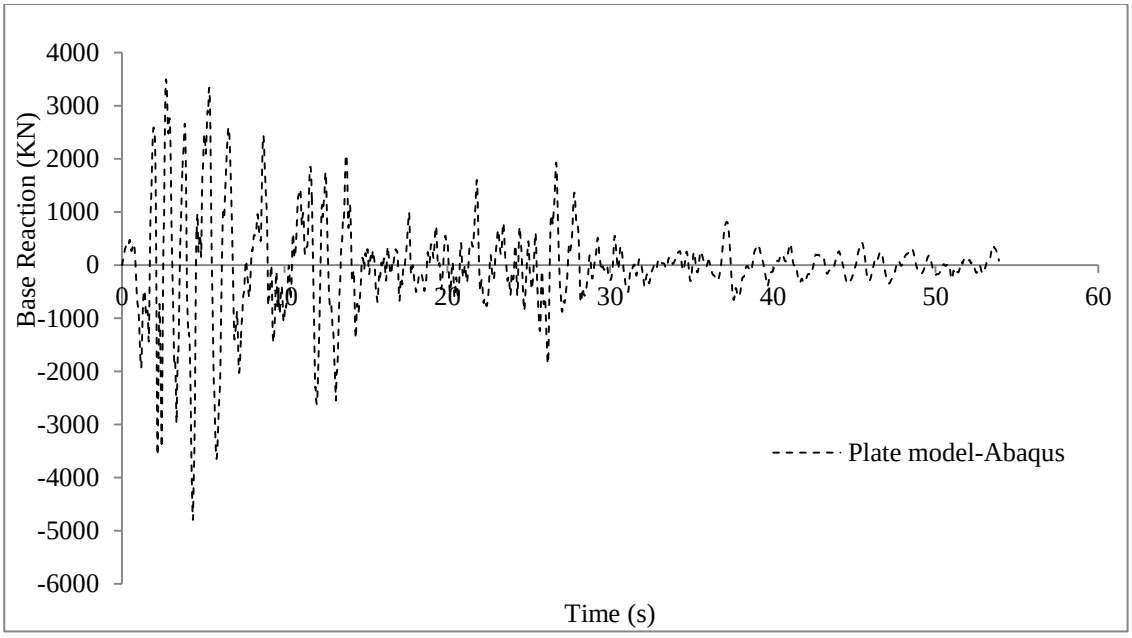

(a) Base Reaction

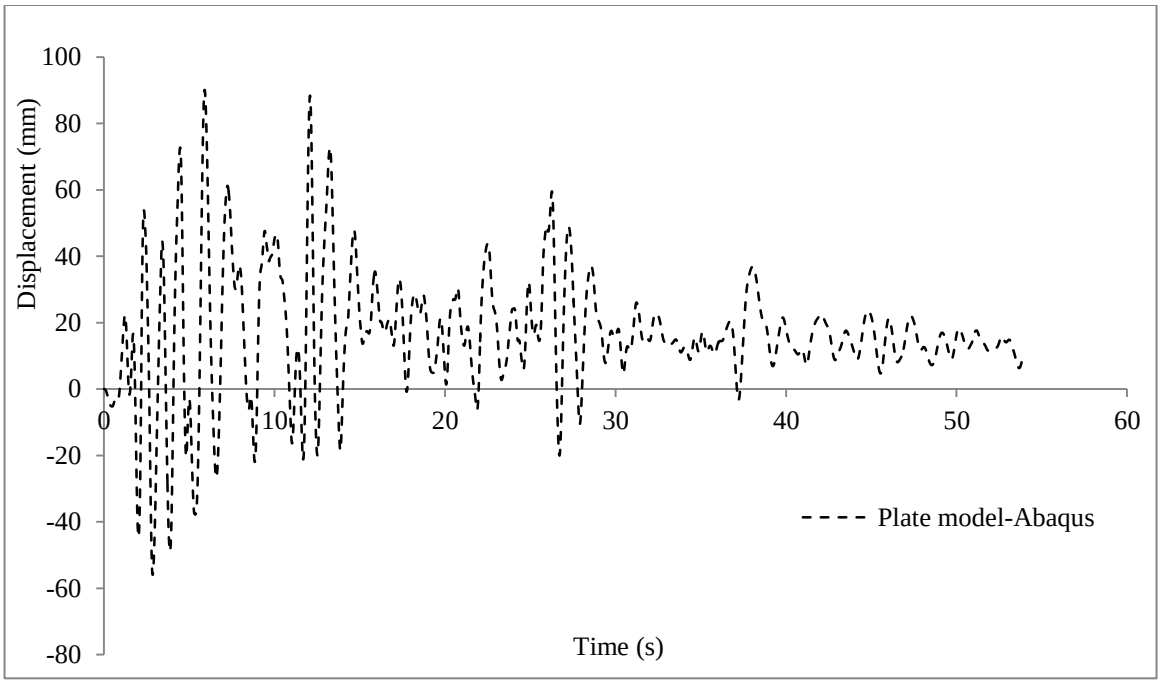

(b) Top Displacement

Figure 4.16: Response of 6-storey structure from Abaqus for Earthquake Record#1

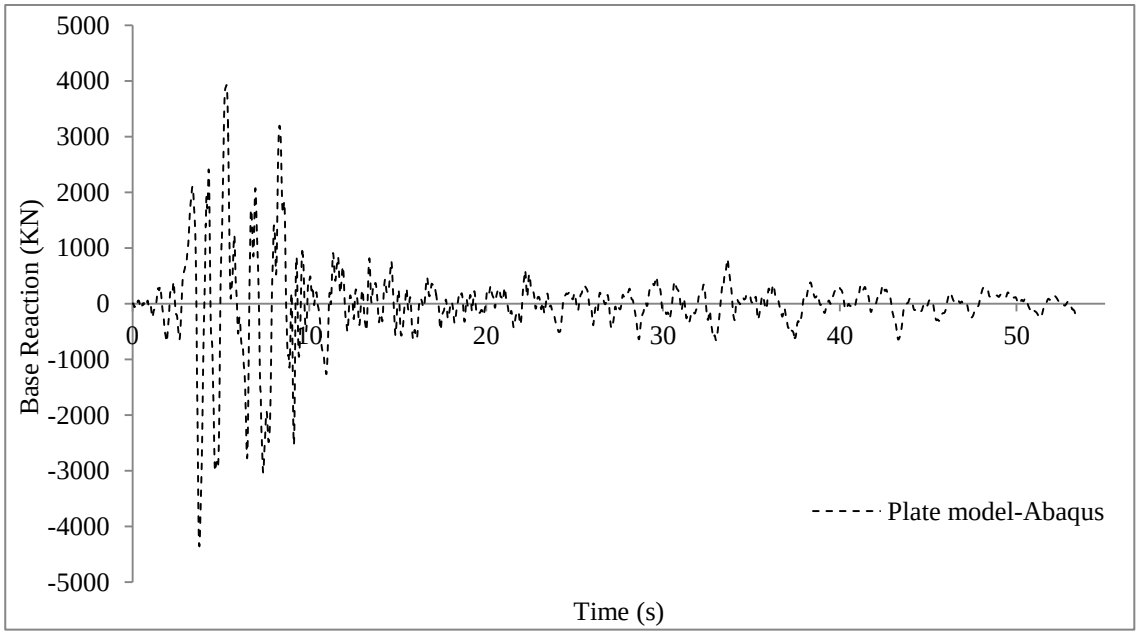

(a) Base Reaction

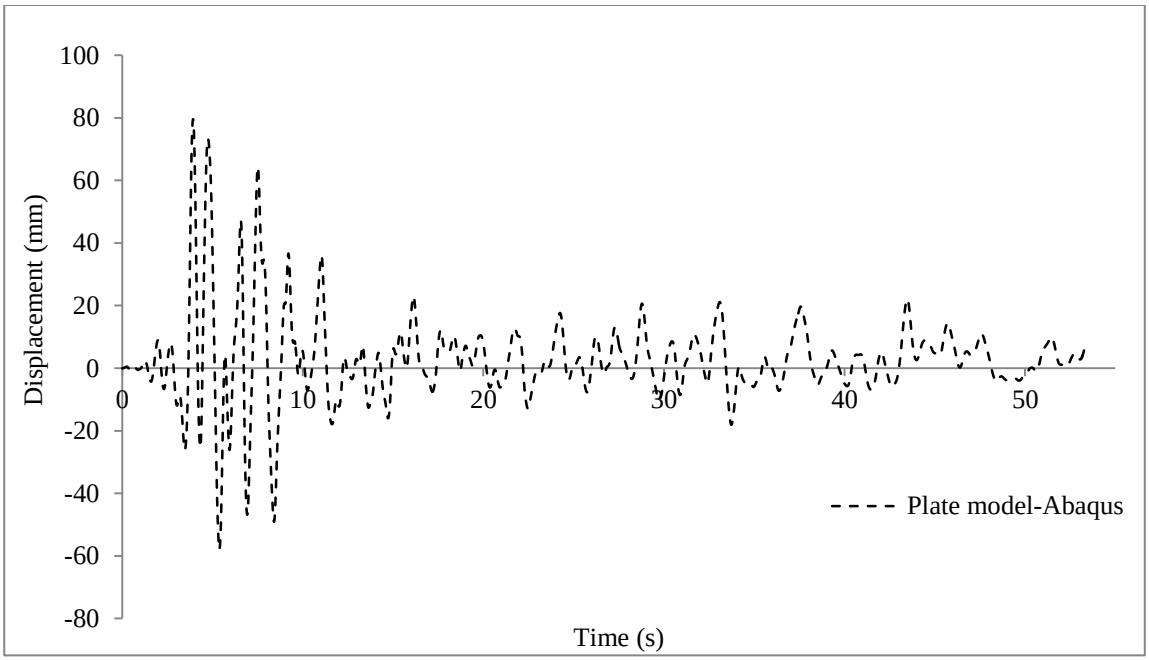

(b) Top Displacement

Figure 4.17: Response of 6-storey structure from Abaqus for Earthquake Record#2

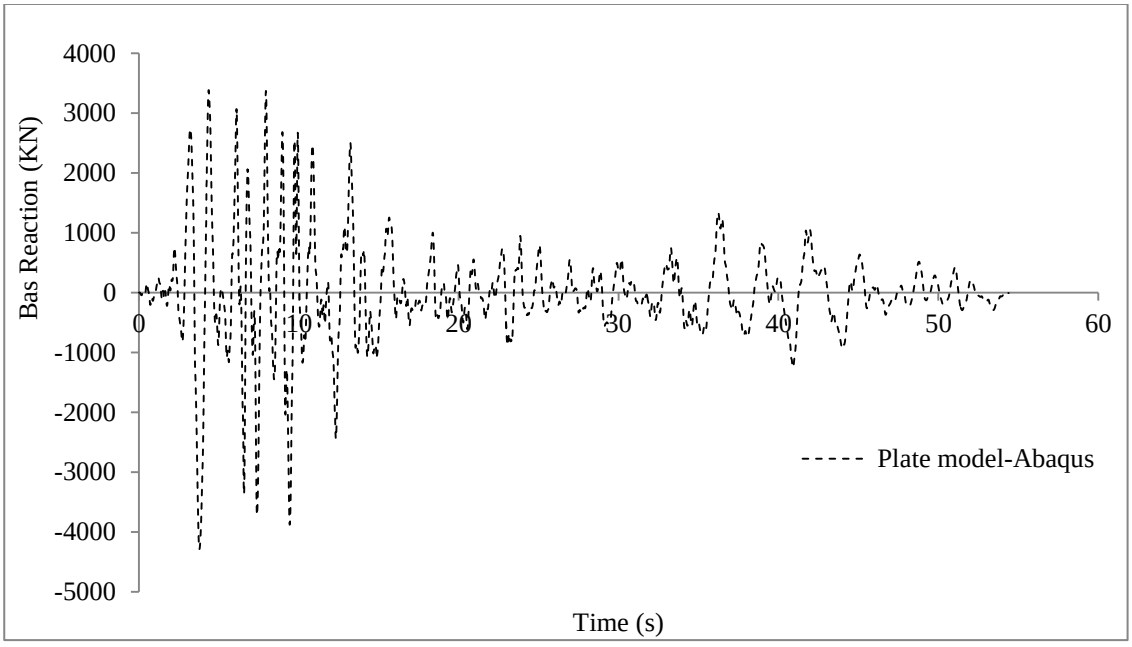

(a) Base Reaction

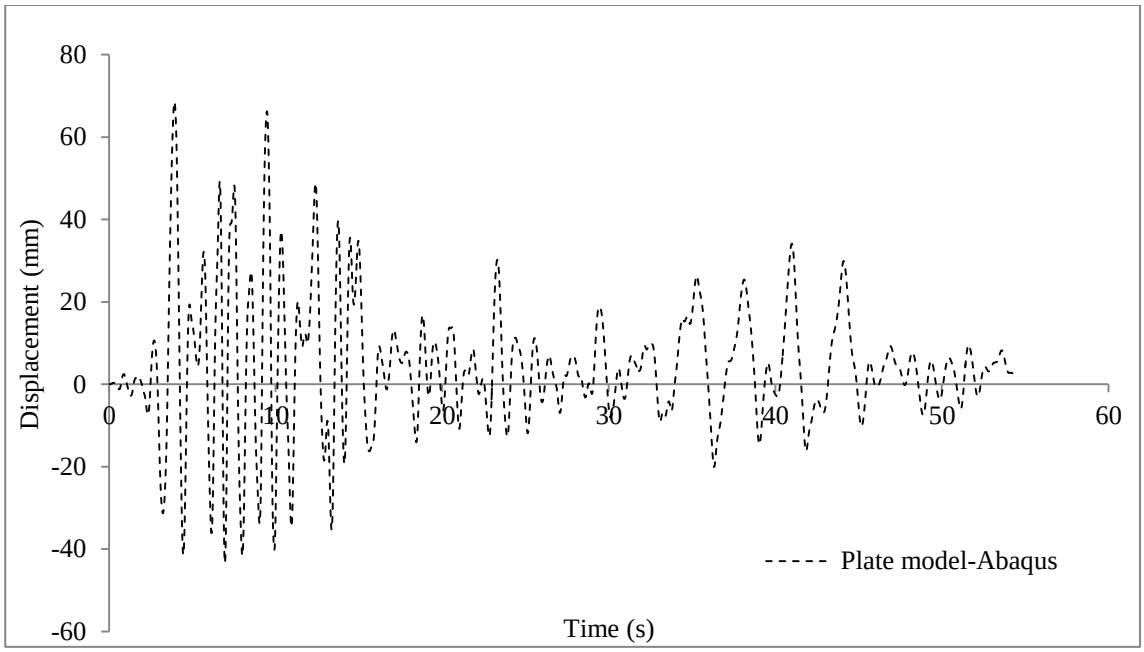

(b) Top Displacement

Figure 4.18: Response of 6-storey structure from Abaqus for Earthquake Record#3

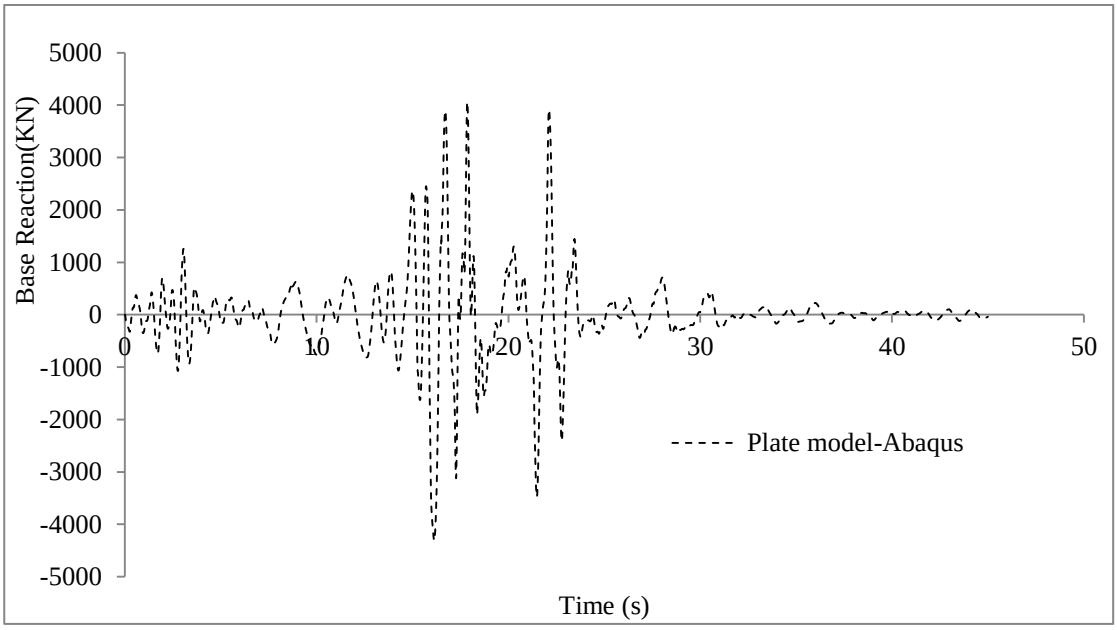

(a) Base Reaction

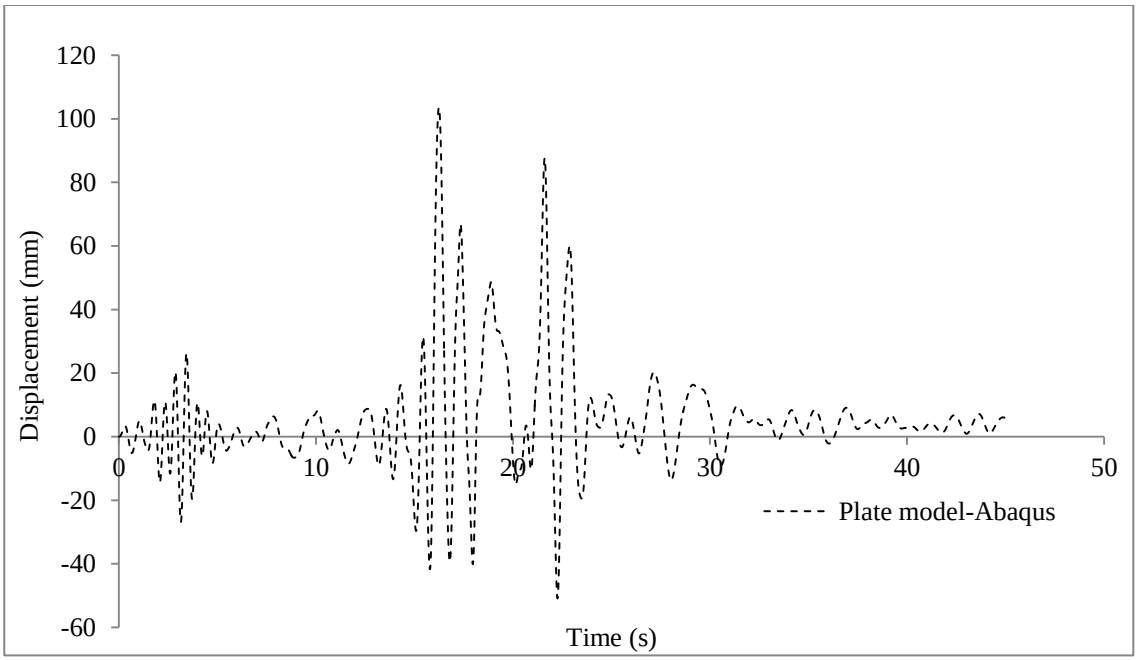

(b) Top Displacement

Figure 4.19: Response of 6-storey structure from Abaqus for Earthquake Record#4

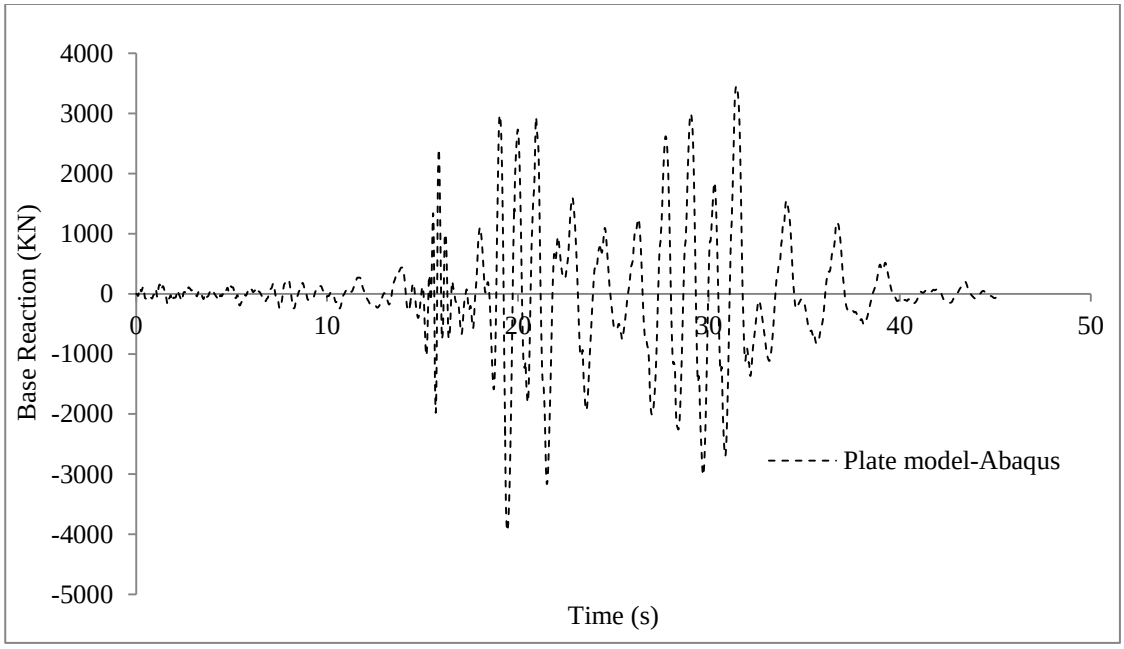

(a) Base Reaction

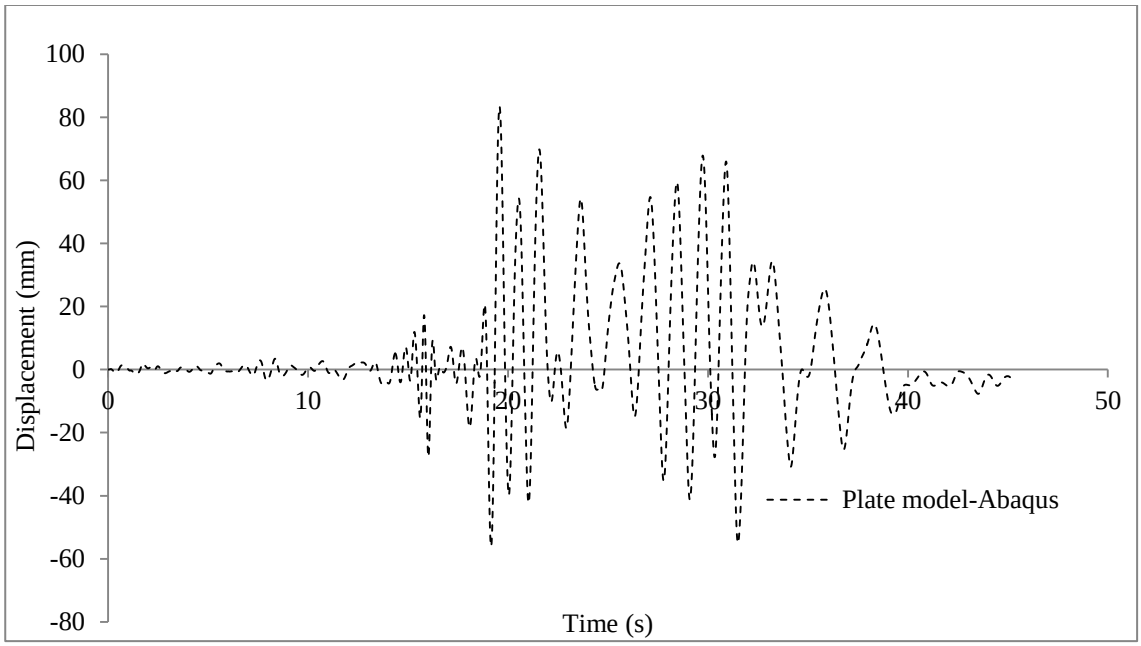

(b) Top Displacement

Figure 4.20: Response of 6-storey structure from Abaqus for Earthquake Record#5

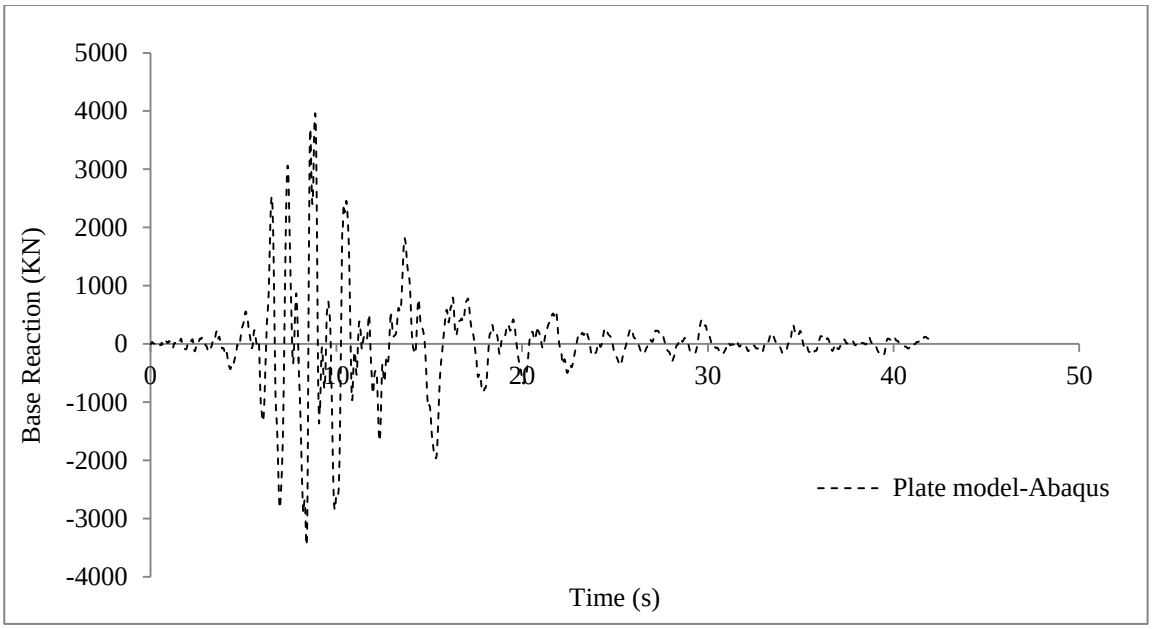

(a) Base Reaction

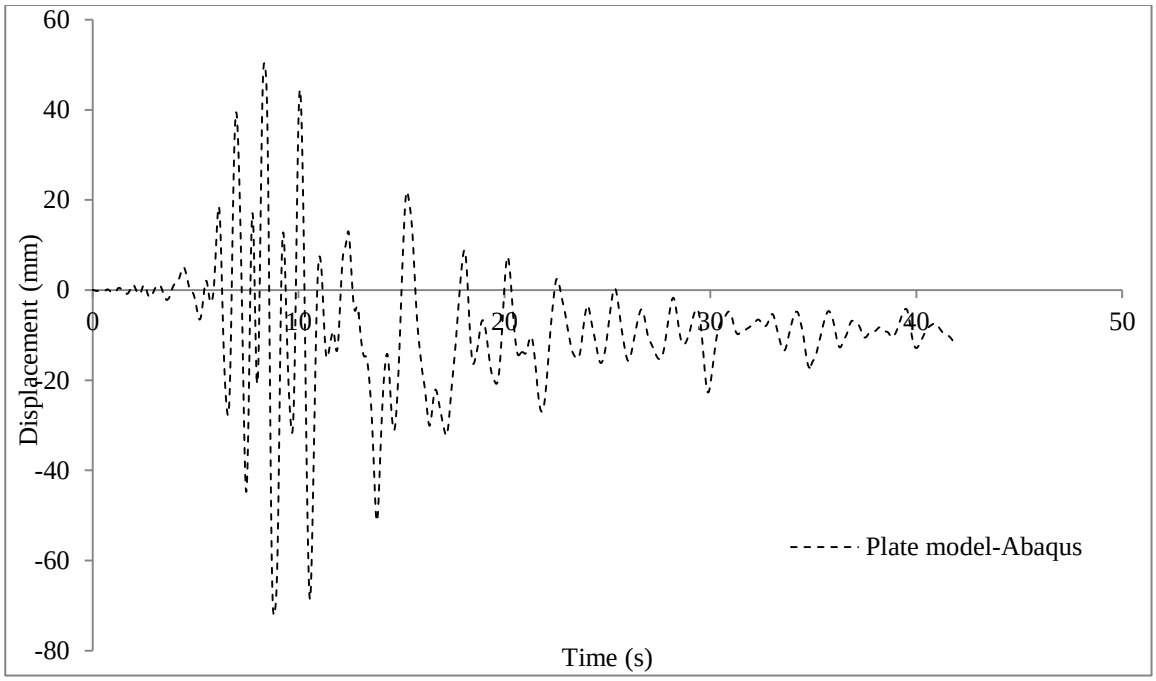

(b) Top Displacement

Figure 4.21: Response of 6-storey structure from Abaqus for Earthquake Record#6

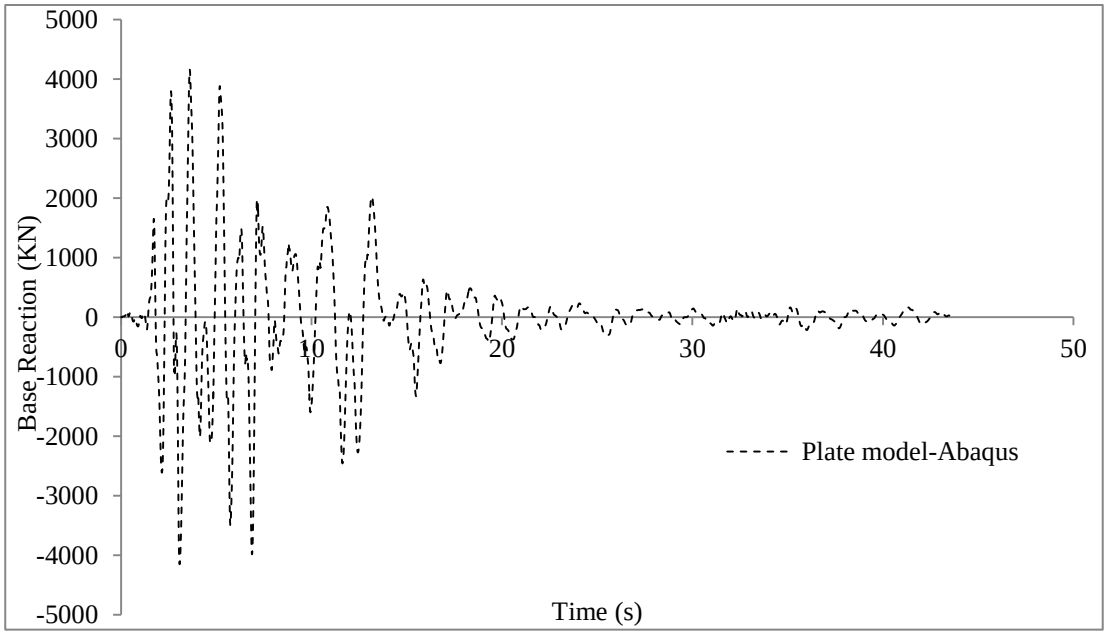

(a) Base Reaction

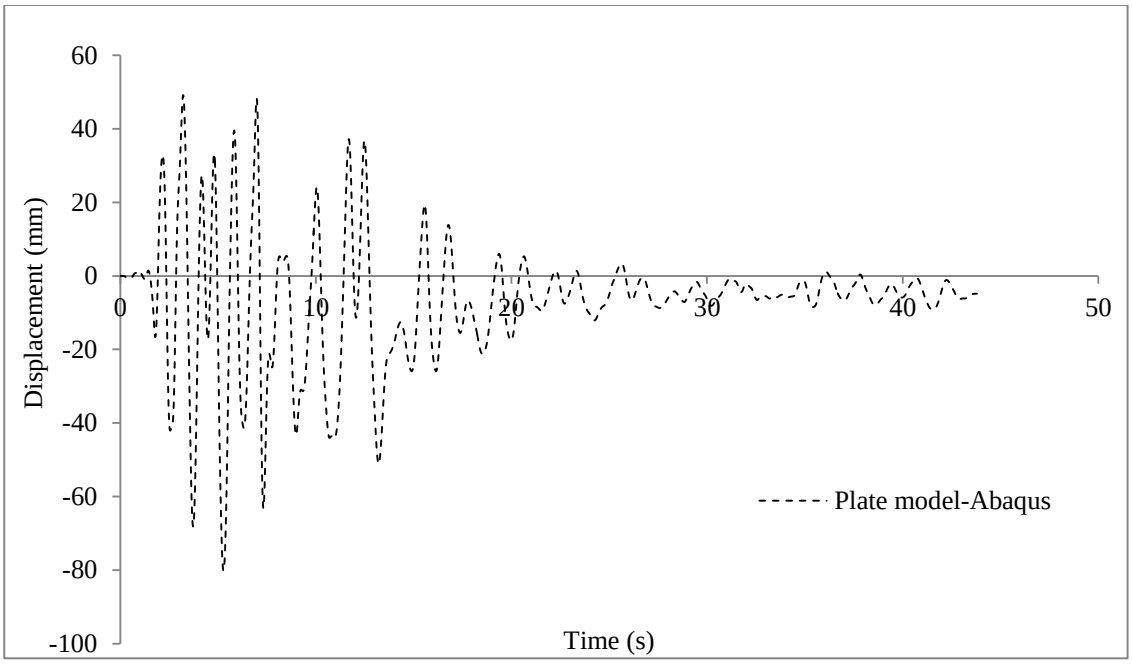

(b) Top Displacement

Figure 4.22: Response of 6-storey structure from Abaqus for Earthquake Record#7

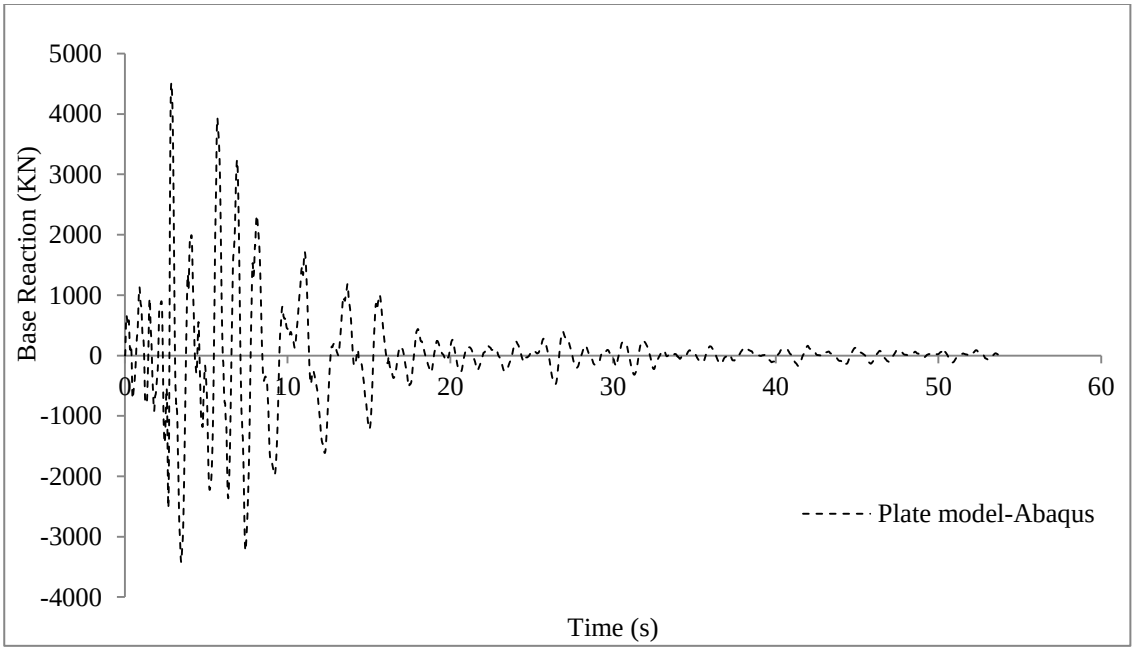

(a) Base Reaction

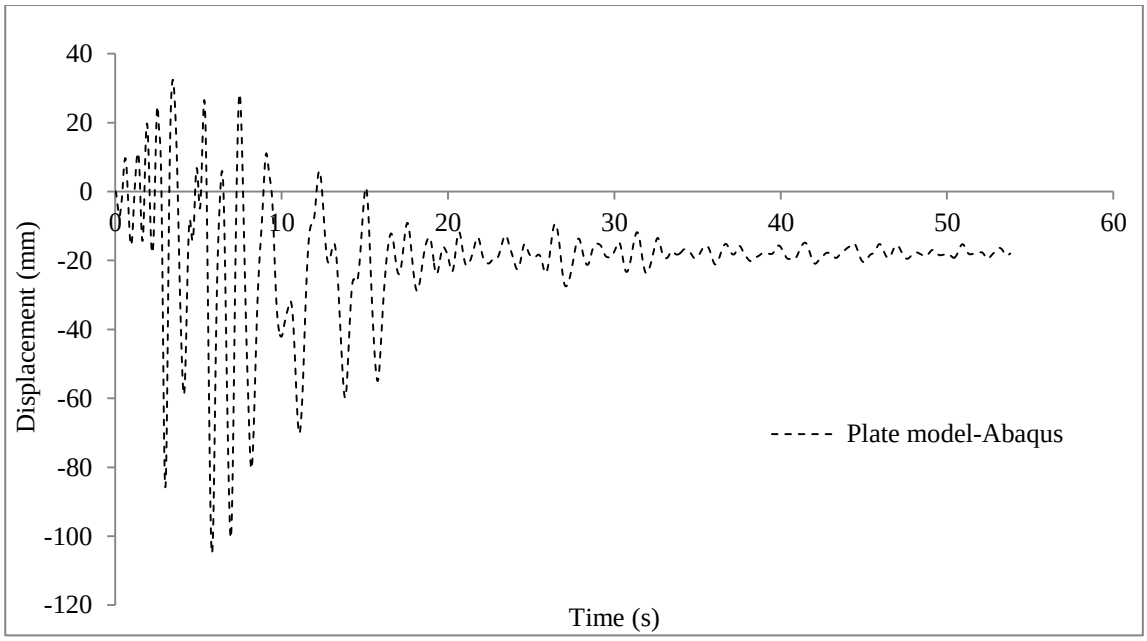

(b) Top Displacement

Figure 4.23: Response of 6-storey structure from Abaqus for Earthquake Record#8

4.7 **Summary**

In this chapter, the detailed FE model has been developed and validated with experimental results. Also, the detailed model has been used for time history analysis of two multi-storey (4-storey and 6-storey) light-gauge SPSWSs with a set of eight selected ground motions. Results from detailed FE model have been used to develop and validate the simplified model. Though the detailed model is very accurate, it is usually not popular among design engineers because of its complexity and longer analysis time. That is where the need to develop simplified model lies. The details of the development of the simplified braced model will be discussed in the next chapter.

Chapter 5. Development of Equivalent Braced Frame Model

5.1 Introduction

Based on the methodology presented in Chapter 2, an equivalent braced frame (EQ.BF) model of steel plate shear wall (SPSW) system has been developed here. This chapter presents the details of the EQ.BF model. However, before going into EQ.BF model, a short study on the existing strut and tie models that represents SPSW systems has been reviewed. The short study highlights in more details the need for a new equivalent braced frame model. Detailed parametric study on SPSW systems has been carried out to observe the significant parameters that independently affect the structural behavior. To represent SPSW behavior in an equivalent braced frame model, some of those independent parameters has statistically related to basic section properties. The statistical relations are developed on the basis of repeated analysis using detailed FE model and some analytical observations. With those equations, the sectional properties of EQ.BF model can be calculated. The EQ.BF model developed here will be subjected to some validation tests in the next chapter.

5.2 Comparison of 2-D Opensees model with 3-D Abaqus model

Three dimensional models with shell-plate element in Abaqus have shown to give acceptably accurate estimate on the behavior of SPSW systems. However, to make time efficient analysis and develop simplified modeling techniques, the three dimensional analysis must be

reduced to two dimensional simplified models. As already discussed, a two dimensional braced frame system with modified properties of braces can represent a complicated three dimensional SYSW system in term of global behavior. So, first the modeling technique in two dimensional frame work, as already discussed in previous chapter, needs to be verified. The easiest way of carrying out this verification is construct some bare frame models both in Abaqus (three dimensional models) and in Opensees (two dimensional models). Modeling in Abaqus can be considered reliable since already validations with some experimental results have been performed. If a test of pushover curve in either of these two models match then it can be inferred that the two dimensional modeling program has no error and can be used for further studies. This indirect validation is particularly useful in eliminating chances of human errors.

A four-storey and a six-storey bare frame structure have been considered for this study. Both these four-storey and six-storey have been designed as SPSW system. The details of the design and selected member sections are given in the next chapter. For the sake of this part of analysis, the infill plate is deleted and only the bare frame model has been used. Figure 5.1 shows that the pushovers are in good agreement. Thus, safely the two-dimensional modeling technique in Opensees can be used for further study.

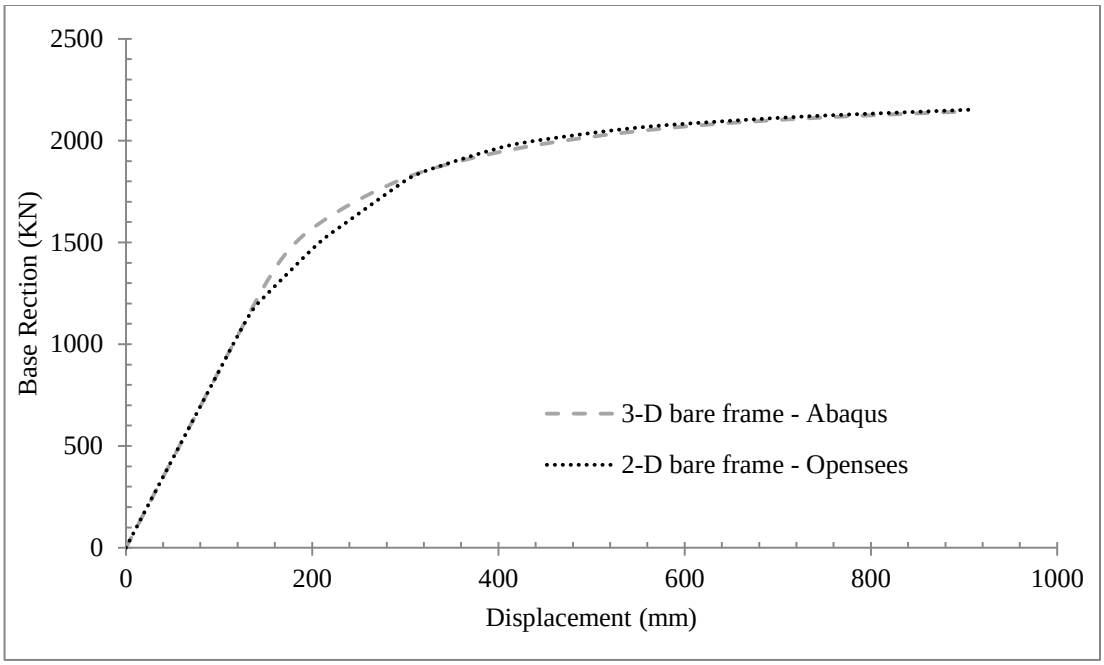

(a) 4-storey

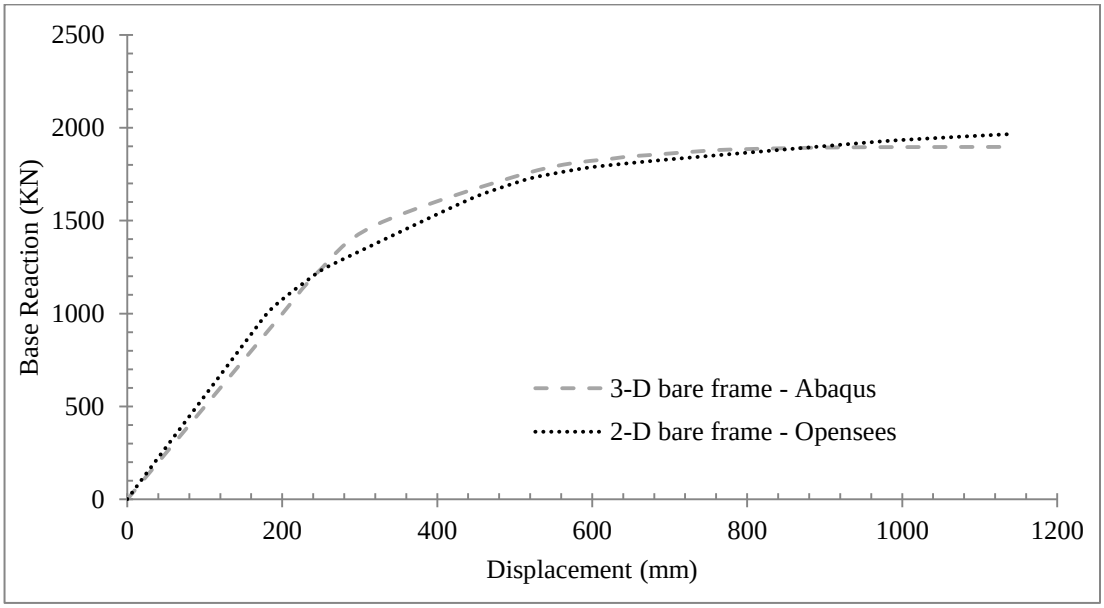

(b) 6-storey

Figure 5.1: Validation of Opensees bare-frame two-dimensional models with that of Abaqus three-dimensional models for 4-storey and 6-storey structures

5.3 Test of existing braced models

A set of just three single-storey models have been used to test the workability of the existing equivalent braced models. As already indicated in Chapter 2, there are basically two available equivalent braced models. The first one was established by Thorburn et al. (1983) where the formulation was mainly based on geometric configurations and the principle of least work. The second model was established by Topkaya and Atasoy (2009) where along with the computation of cross-sectional area for the braces, a change in properties of the boundary sections was recommended. Three sample single storey SPSW systems are selected here based on strength boundary members to study the above models and develop the new EQ.BF model. Two of the samples correspond to experimental works reported earlier (Lubell et al., 2000 and Neilson, 2010) and the third sample was produced here which was designed in accordance with NBCC2010. All these samples have also been subjected to test with detailed FE models to make sure their behaviors are reliability represented. The three specimens (the single-storey specimen designed presently, Lubell et al., 2000 specimen (SPSW-2) and Neilson, 2010 specimen) are have been used to test other established models to assess their reliability. Specimen tested by Lubell et al. (2000) had the lightest boundary sections comprising of S75x8 (Figure 2.3 (a)) and the newly designed specimen had the heaviest sections amongst the chosen set of three specimens. The aspect ratio of Lubell's specimen was 1:1, whereas that of the newly designed specimen was 2:1. The details on the experimental specimens of Lubell (specimen SPSW-2) and Neilson (Figure 2.10) have already been described in Chapter 2. A summary of all three specimens are presented in Table 5.1.

Table 5.1: Details for the selected single-storey SPSW specimen

Specimen	Boundary		Plate		
	Beam	Column	Thickness	E(MPa)	σ_y(MPa)
Newly designed	W530x272	W360x509	3 mm	200,000	385
Lubell et al. (2000)	S75x8	S75x8	1.5mm	200,000	320
Neilson (2010)	W200x31	W200x31	0.98mm	210,000	275

Based on the equations proposed by Thorburn et al. (1983) and Topkaya et al. (2009) two sets of equivalent strut and tie models are created. Along with the strut and tie model analysis in Opensees a detailed FE model has also been studied in Abaqus. The results from Abaqus agree well with the experimental results indicating the reliability of the FE models, and the percentage error in the initial stiffness and the final strength are found to be negligible. For the single storey newly designed sample of SPSW, the results from Abaqus is considered as the reference results and the results from the braced model are compared against them.

In the analytically developed braced model by Thorburn et al. (1983), only the cross sectional area of braces are computed according to Equation 2.3. The remaining geometry and material properties remain identical to the original SPSW system. In that model, the major part of analytical work was on the geometric distribution of the tension field. This method of formulation is not necessarily always correct and based on the stiffness of the boundary members, the final strength and initial stiffness predicted by the model can be overestimated or underestimated. Thus, the strength indicated by this braced model, as observed from pushover analysis, is overestimated in case of the newly designed specimen (Figure 5.3) where the stiffness of the boundary elements is high, and underestimated in case of Lubell's specimen

(Figure 5.4) where the boundary elements are lighter. However, for Neilson's specimen the estimate is better (Figure 5.2) as compared to the other two.

For the strut and tie model developed by Topkaya and Atasoy (2009), calculating the cross sectional area of braces according to Equation 2.4 is not enough. The arrea of the vertical member also needs to be determined according to Equation 2.5. Their formulation was based on a combination of analytical and numerical study. The analytical work had some similarity with the deep beam theory. Also, their study was within linear elastic limit and a major concern was to estimate the initial stiffness correctly. For all the three specimens under consideration, this model could estimate the initial stiffness with relatively low percentage of error (Figure 5.2 to Figure 5.4). However, the final strength after the beginning of column yielding showed significant error. Particularly, for Neilson's specimen the percentage error in estimation of the final strength is significantly high (Figure5.2). Also, since the strength of the boundary members are significantly increased in this model, the strength is almost always overestimated. Thus, the above two models are found to be inadequate for capturing the behavior of the laterally loaded SPSW systems with different stiffness characteristics of the boundary elements. There is a need for either a modification of the existing models or the development of a new model. The latter is attempted herein.

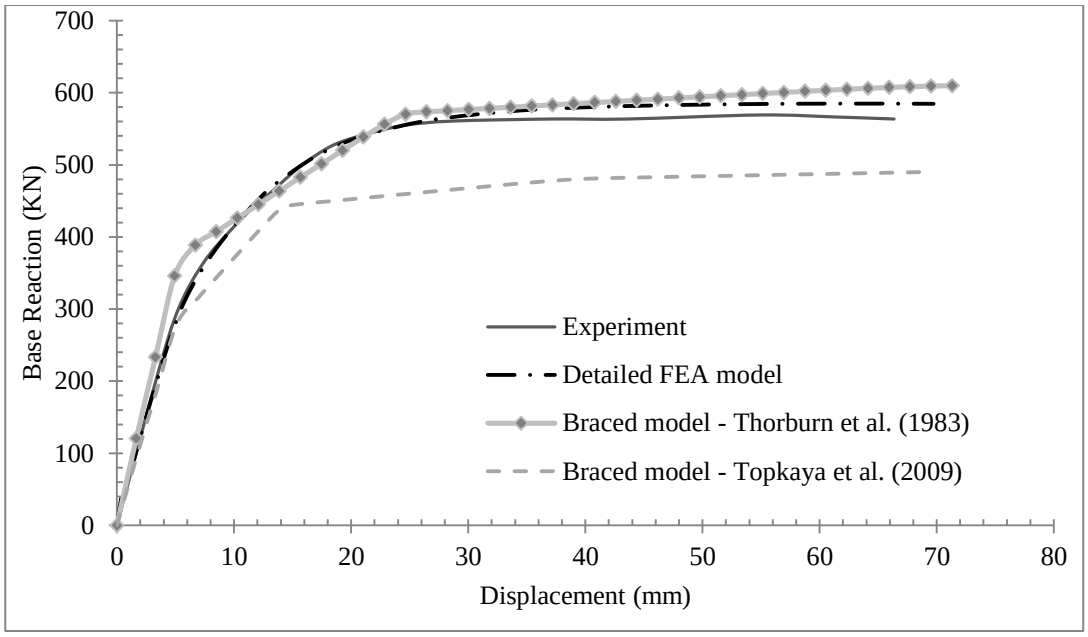

Figure 5.2: Test of available braced models and FE model on Neilson's (2010) specimen

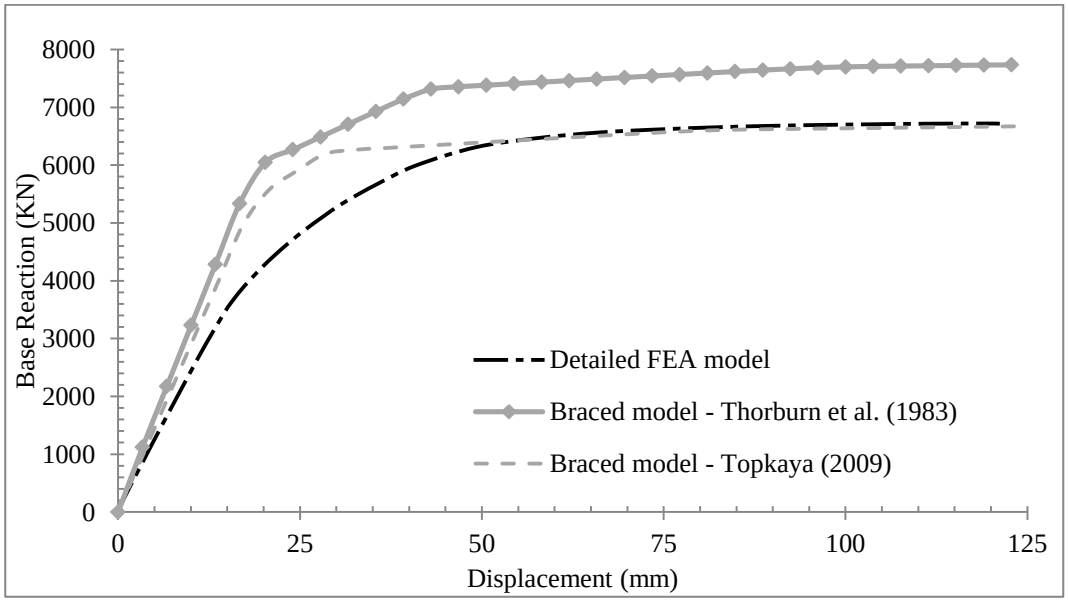

Figure 5.3: Test of available braced models and FE model on the newly designed single-storey specimen

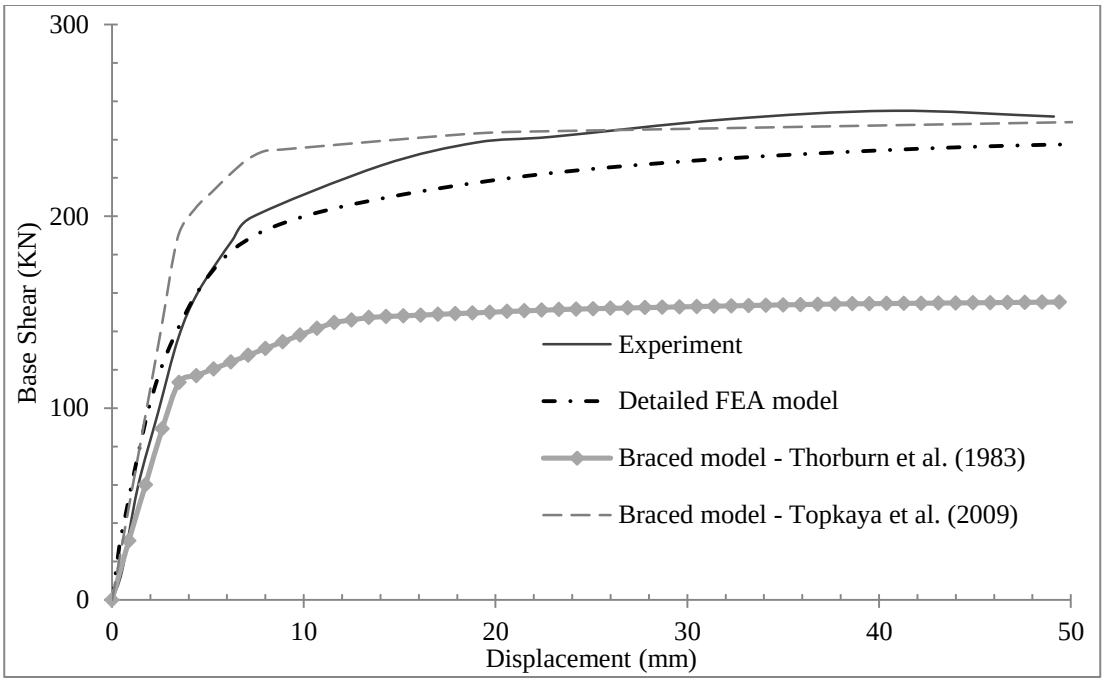

Figure 5.4: Test of available braced models and FE model on Lubell et al. (2000 specimen

5.4 Evolution of EQ.BF model

To model the behavior of steel plate in a steel plate shear wall system by equivalent truss bracing, a linear relation between their stiffness is first established. From the established relations, the required cross-sectional area of the truss bracing is found. An equivalent linear model is created by parametric study to establish the geometric non-linear behavior of the steel plate to equivalent bracing. Several parameters have been introduced to simulate the non-linear behavior of the plate in the equivalent behavior in the brace element. Stiffness of the brace element can be adjusted by multiplying the brace area with appropriate parameters obtained by linear equations to simulate the non-linear brace stiffness. Also, to capture the ultimate strength of a SPSW system in EQ.BF model, the material properties of the bracing system need to be parametrically modified.

5.4.1 **Stiffness reduction due to buckling of the plates**

As introduced by Topkaya and Atasoy (2009), a parameter αs which is the ratio of the post-buckled stiffness of the plate to the pre-buckled original stiffness is important to represent the reduction of the stiffness of the plate due to buckling. It is a parameter which can capture geometric non-linearity of plates in SPSW system. Through a trial and error analysis, it has been observed that the two main dimensionless parameters responsible for the geometric non-linear behavior of steel plate are the thickness to panel size (the size of a plate panel expressed as the length of diagonal) ratio of the plate and aspect ratio of infill plate. The parameters can be mathematically expressed as, b/L ($=\beta_1$) and l/h ($=\beta_2$), which are similar to the relevant parameters used by Topkaya and Atasoy (2009). However, their attempt in establishing a proper relation of α_s with the primary variable remained incomplete.

Since, the concern here is the geometric non-linearity only and no material non-linearity, all analysis for parameterizing α_s is kept within the elastic limit. Also, no bounding beam column is considered since the study is related only to the panel plate. The parametric study is carried out using detailed FEA models in Abaqus. In that case, the modeling technique is kept close to the one used for the validation study, as far as possible. Shell elements (S4R from Abaqus element directory) have been used to model the plate. The two bottom corners of the plate are assumed to be hinged to formulate the support condition. All four edges are restrained against lateral rotation and translation out of the plane. Due to the presence of heavy boundary members in steel plate shear wall, the out-of-plane rotation of the plate elements at the edges is practically negligible. Quasi-static load was applied along the plane of the plate along the top edge, to represent the

shear from an imaginary axially rigid beam. To compare the stiffness of the perfect geometry (linear behavior) with that of the buckled plate (geometric non-linear behavior), the same model was analyzed once without imperfection and then with imperfection (Figure 5.5). The model without imperfection shows a much higher strength than the one with imperfection. Figure 5.6 shows a sample example of the stiffness reduction with and without imperfection for plate with $\beta_2 = 0.7$ and $\beta_1 = 3\sqrt{2}$. It should be noted that no attempt was made to reach the plastic limit of the plate and introduce material non-linearity. After a certain limit of the lateral load (sufficiently large for the plate) the perfect geometry suddenly fails and an abrupt change in the load-displacement curve is observed. The stiffness below that limit is constant and is the one considered. As mentioned earlier, with and imperfection, the load-displacement curve is not linear even within the elastic limit. However, an approximate straight line, representing an equivalent linear relation the strength and displacement can be assumed in that case. For all the cases considered here the approximate linearization of the force-deformation curve result in $R^2 > 0.8$.

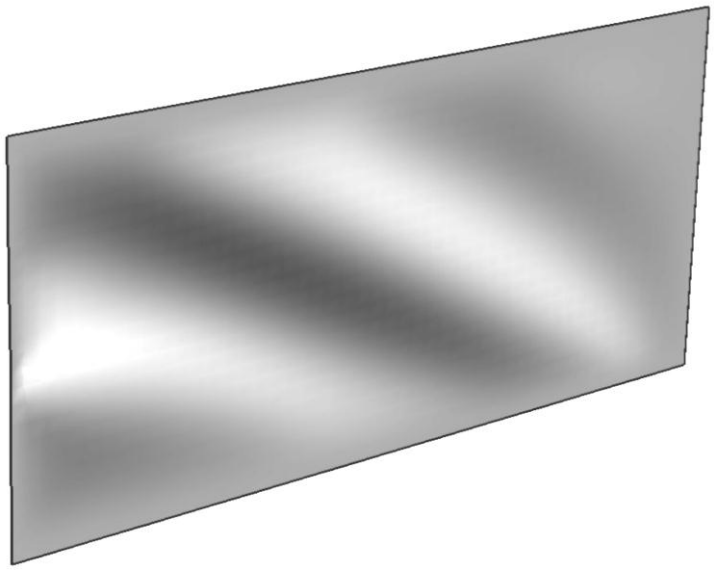

Figure 5.5: Sample image of a buckled plate (i.e. geometric non-linearity for buckling)

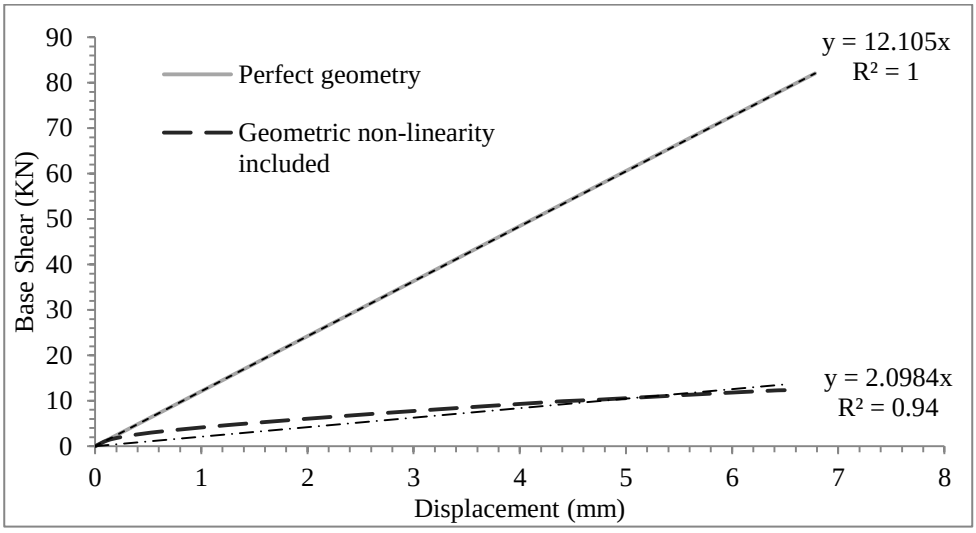

Figure 5.6: Sample example of shear stiffness reduction for geometric non-linearity (achieved with imperfection) in plates

Parameter α_s is found to be linearly related to β_1 (Figure 5.7), but depending on the aspect ratio (β_2), the slope of the line may change. It is also observed that α_s is almost constant when β_1=0, irrespective of different values of β_2. Thus, fitting a linear equation (Equation 5.1) with varying slope (slope given by *m*) of the line yielded an $R^2 > 0.99$. The variation of *'m'* with β_2 is then represented through a polynomial fit (Figure 5.8). The relation is established in Equation 5.2 with an error of $R^2 = 0.99$.

$$\alpha_s = m * \beta_1 + 0.06 \tag{5.1}$$

$$m = -0.2102(\beta_2)^3 + 1.1062(\beta_2)^2 - 1.5923(\beta_2) + 1.0862 \tag{5.2}$$

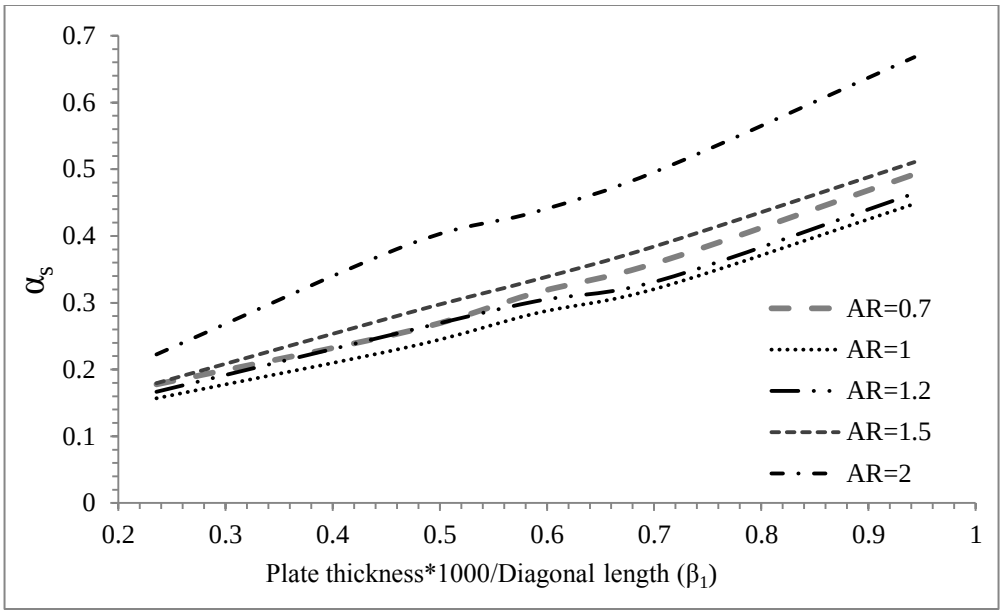

Figure 5.7: Variation of α_s in relation to β_1

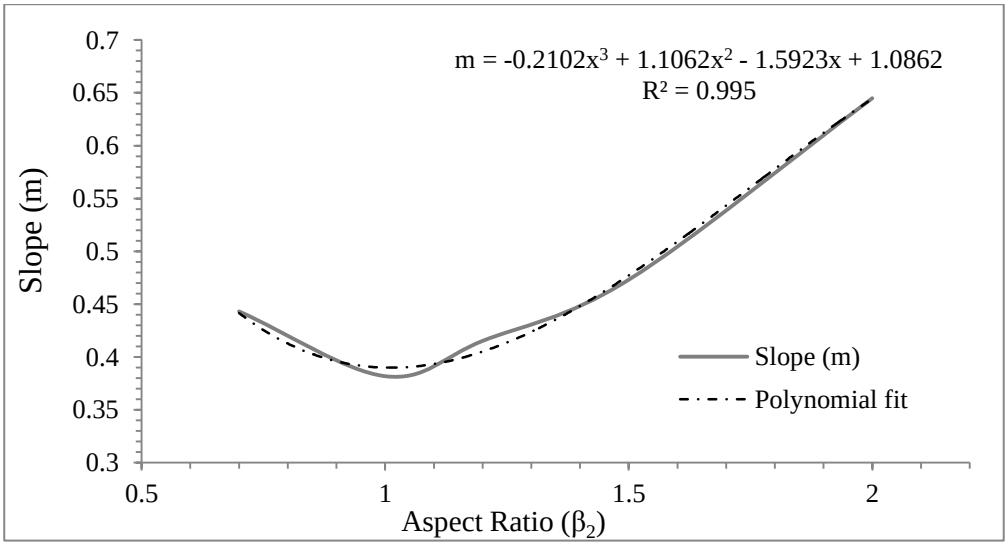

Figure 5.8: Variation of '*m*' with aspect ratio

5.4.2 **Linear stiffness relation of SPSW system and EQ.BF model**

The stiffness of SPSW system and EQ.BF model are equated under linear conditions to obtain the cross sectional area of the cross braces. In SPSW system the significant force is in the

form of shear. Bending effect becomes significant only when the aspect ratio is very low, which are is not common. So, for this study it is assumed that the bending effect on the plate is negligible. Thus, the stiffness of the plate can be established by shear rigidity alone. The symbols used through this derivation are introduced as below (Figure 5.9 and Figure 5.10).

Diagonal length of brace = $L = \sqrt{l^2 + h^2}$

b = Thickness of plate

μ = Poisson's Ratio

I = Moment of Inertia of transverse section = $\frac{b*l^3}{12}$

$$Q = \bar{y}' * A' = \left(\frac{l}{4}\right) * \left(\frac{l*b}{2}\right) \tag{5.3}$$

V = Applied shear force on plate

G = Shear modulus = $\frac{\tau}{\theta}$

Since the shear stress, $\tau = \frac{VQ}{Ib}$

$$\Rightarrow V = \left(\frac{Ib}{Q}G\right) * \theta$$

$$\Rightarrow V = \left(\frac{Ib}{Q} * \frac{G}{l}\right) * (\Delta l)$$

$$\Rightarrow V = K_{plate-linear} * \Delta l \tag{5.4}$$

α_s is the ratio of stiffness of the buckled plate to that of the plate with perfect geometry (linear), as already discussed;

So,

$$\alpha_s = \frac{K_{plate-buckled}}{K_{plate-linear}}$$

For bracing,

$$K_{brace} = \left(\frac{A_d E}{L}\right) * cos^2\varphi \tag{5.5}$$

where, φ is the brace angle, L is the length of the brace, A_d is the equivalent cross-sectional area for bracing and E is Young's modulus.

Thus,

$$\alpha_s * K_{plate-buckled} = K_{brace} \tag{5.6}$$

or, $$\alpha_s * \left(\frac{Ib}{Ql}\right) G = \left(\frac{A_d E}{L}\right) * cos^2\varphi \tag{5.7}$$

The modulus of elasticity E is related to the shear modulus G and the Poisson's Ratio μ, as follows: $E = 2G(1+\mu)$.

Therefore,

$$A_d = \frac{\alpha_s \left(\frac{Ib}{Ql}\right)}{2(1+\mu)\frac{cos^2\varphi}{L}} \tag{5.8}$$

The above expression for A_d is derived by assuming the absence of boundary members. A noticeable strength increase is observed in the presence of strong boundary members. Unless the boundary members are strong enough, tension field in the plate remains incomplete (Mohammad et al. (2003)). Thus, to estimate the increase in the capacity or strength of the plate due to presence of boundary members another parameter (α_m) is used.

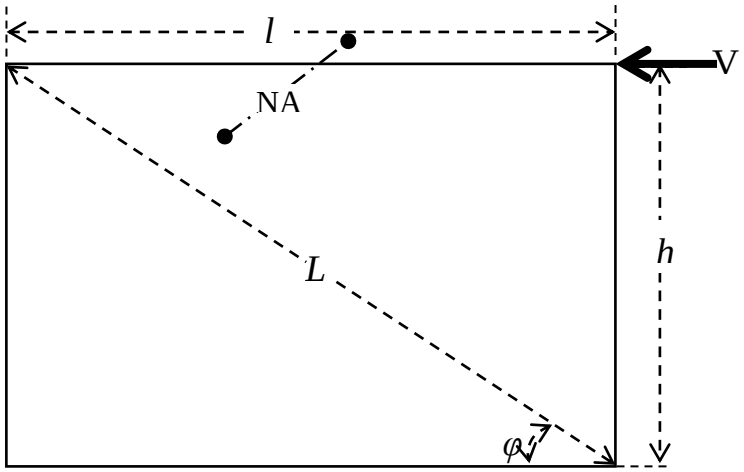

Figure 5.9: Shear load on infill plate

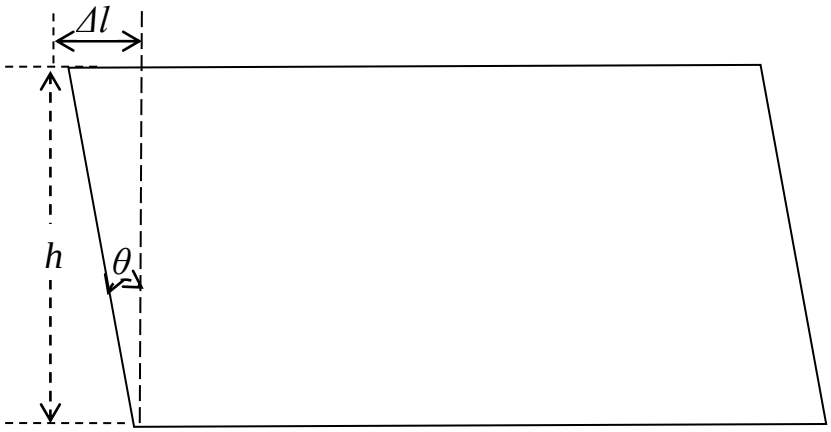

Figure 5.10: Shear deformation of plate frame under linear conditions

5.4.3 **Enhanced stiffness due to the boundary frame**

Stiffness reduction considered for buckling of plate (α_s) has been computed in the absence of boundary frame. With inclusion of the boundary frame, tension fields start to develop in the plate and for optimizing the use of plate i.e. for complete development of tension field boundary members should be strong enough. So, a parameter α_m is introduced which accounts for this increase of stiffness of the plate in presence of boundary frame, and thus the area of equivalent braces is increased. The physical entities responsible for parameter α_m are the overall non-linear strength of the plate and the boundary frame. Size, thickness and aspect ratio of a plate are the primary geometric parameters that determine the strength of steel plate within the elastic limit. Thus, it can be safely assumed that α_s is responsible for the variation in α_m. However, standardizing the strength of the boundary members is a formidable task. Wrangler (1931) introduced a flange flexibility parameter w_h to study the behavior of tension fields in W-sections. Owing to the behavioral similarity between SPSW and web girders, standard S16 of the Canadian Standards Association (CSA 2009) and the AISC Specification (AISC 2005) accepted this flexibility parameter as a measure for the strength of the boundary members in SPSW systems. Kuhn et al. (1952) simplified this parameter as given in Equation 5.9. The same parameter was as found to have an effect on the overall capacity of the plate by Mohammad et al. (2003). Dastfan and Driver (2008) modified the parameter as w_L (Equation 5.10) for the end panels (top and bottom). Thus, α_m is studied by varying the flexibility of the boundary elements, β_3 which is equal to w_h for an intermediate storey and w_L for the top storey. All other independent dimensionless parameters responsible for change in strength of SPSW as identified by Mohammad et al. (2003) are kept constant.

$$w_h = 0.7h * \sqrt[4]{\frac{b}{2LI_c}} \tag{5.9}$$

where, w_h is column flexibility for intermediate storey

$$w_L = 0.7 * \sqrt[4]{\left(\frac{h^4}{I_c} + \frac{L^4}{I_b}\right)\frac{b}{4L}} \tag{5.10}$$

where, w_L is column flexibility for top storey

For this parametric study similar plate model was created as for the study of α_s. The bounding members were considered as beam elements (B31 in Abaqus elements library) for simplicity. The change in column flexibility was brought about by changing the cross sectional area of the column profile. As the study is done for a single storey structure, the effect of beam is indirectly accounted for by considering the change in column flexibility corresponding to the top storey (i.e., by using w_L instead of w_h). The cross-sectional area of the beam was never changed. Also, the ratio of the moment of Inertia to area of a column was kept constant throughout the computation as that ratio is supposed to be an independent parameter affecting the behaviour of SPSW system (Mohammad et al. (2003)). Rigid connection between boundary and plate was been assumed. The boundary members were restrained against lateral rotation and out of plane translation. Hinge support was provided at the column base. Assuming the beam to be axially rigid, a quasi-static shear force was applied on the top beam (as in the case of the analysis of the plate alone while computing α_s). Imperfection was introduced in the plate such that the plate buckles with the application of load and the geometric non-linear behaviour is taken into

account. With the variation of β_3 and α_s, the variation in the stiffness is estimated from the load displacement curves. The slope of the load-displacement curve is obtained by linear fitting of the curve (with co-efficient of determination, $R^2 > 0.9$). As an example, a sample load-deflection curve for a single-storey SPSW system with the aspect ratio of *1.0* and the plate thickness of *2mm* is shown in Figure 5.10. An exactly similar analysis was carried out with the bare frame model (where the plate is absent, but all other parameters remain the same) and using the same process as above, the stiffness was estimated (with accuracy of $R^2 > 0.99$). The difference between the stiffness of the full SPSW system and that of the corresponding bare frame gives the portion on the stiffness contributed by the plate in the SPSW system. This stiffness of the plate when analyzed with the frame as above is significantly higher than that of a very similar plate analyzed alone without the boundary members. This is primarily because of the interaction between the structural members (one supporting the other collectively). The ratio of the stiffness of the plate in presence of boundary members to that of without boundary members is expressed as α_m (Equation 5.11).

$$\alpha_m = \frac{K_{plate|boundary}}{K_{plate|only}} \tag{5.11}$$

The relation between β_3 and α_m as shown in Figure 5.12 can be best represented by a quadratic function as given by Equation 5.12. The values of R^2 for all samples are found to be more than 0.99, indicating a close fit. The coefficients of Equation 5.12 can be further used to establish a relation with α_s (Figure 5.13). The independent co-efficient, *'C_1'* is always found to 1.0. The variation of the other two coefficients (*'A_1'* and *'B_1'*) with α_s, is given by Equations 5.13 and 5.14.

$$\alpha_m = A_1 * \beta_3^2 + B_1 * \beta_3 + C_1 \quad (5.12)$$

$$A_1 = -4.497 * \ln(\alpha_s) - 0.6184 \quad (5.13)$$

$$B_1 = -7.5789 * \alpha_s^2 + 2.2279 * \alpha_s - 0.6997 \quad (5.14)$$

This parameter (α_m), being responsible for strength increase in plate, is used as a multiplier to the area of the equivalent brace. Thus, the new non-concentric brace area can be represented by Equation 5.15. This area is computed based on parametric study as presented above on the single storey structure within elastic limit of the plate. The parameters to account for the material nonlinearity and multi storey effect are used to develop a suitable material property for the equivalent bracing system as presented later in this chapter.

$$A = \frac{\alpha_m \alpha_s \left(\frac{Ib}{Ql}\right)}{2(1+\mu)\frac{cos^2\varphi}{L}} \quad (5.15)$$

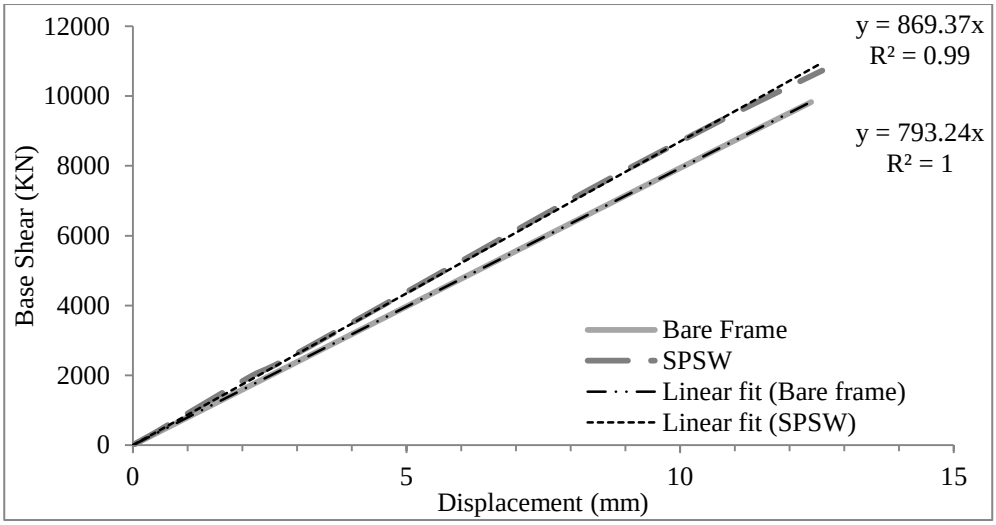

Figure 5.11: Sample stiffness comparison of bare frame and SPSW

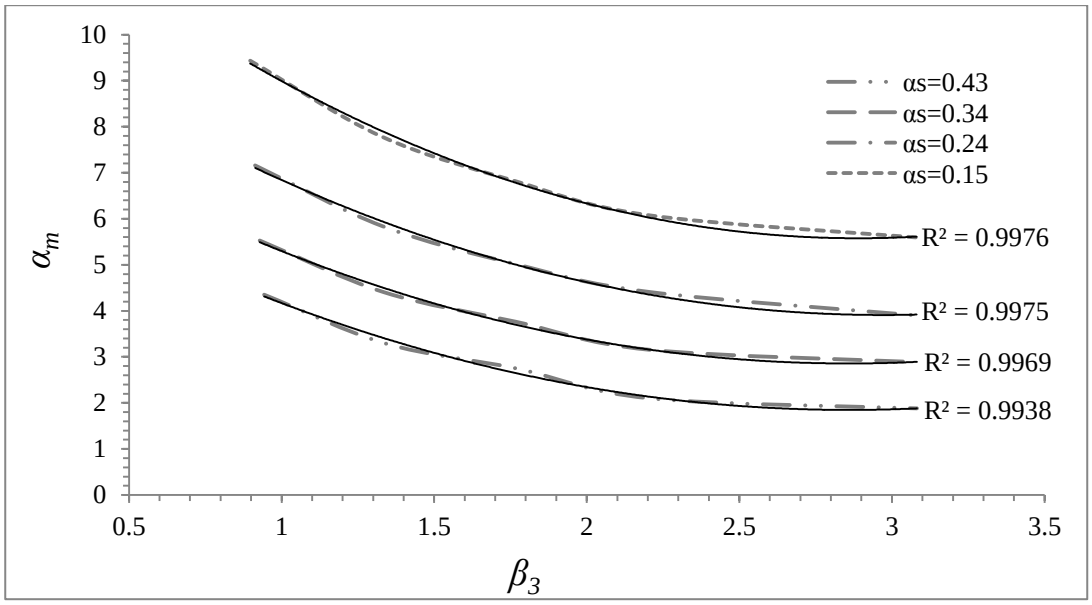

Figure 5.12: Relation between β_3 and α_m

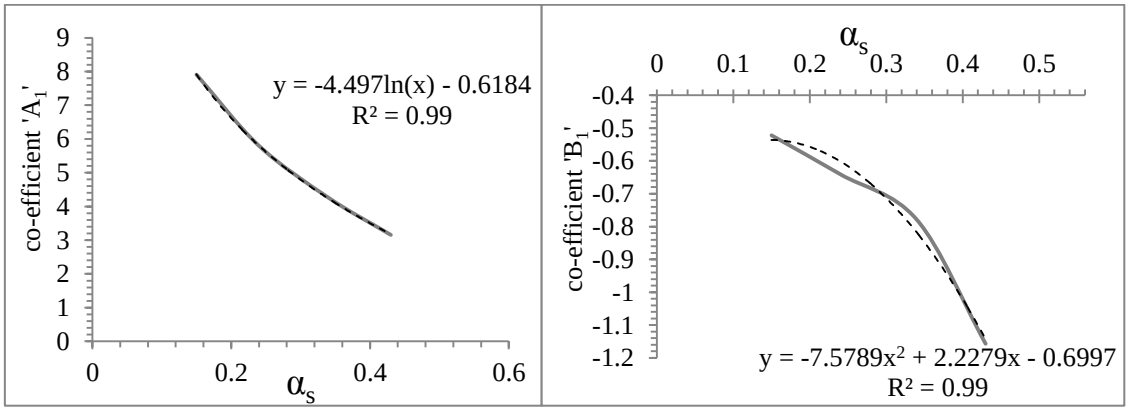

Figure 5.13: Variation of co-efficient A_1 and B_1 with α_s

5.4.4 **Compression strut in EQ.BF model**

Once the area of the bracing is determined, the behaviour of a compression strut needs to be characterized. Under a cyclic lateral loads, the plate in a SPSW system may alternately develop tension fields and buckling of the plate due to compression along its diagonals. When

the plate is modelled using the equivalent diagonal braced, they will also undergo tension or compression, depending on the direction of the lateral load. Though a brace as s compression strut does not have a very significant influence in the overall behaviour of a SPSW system, it is an important component of the EQ.BF model. When the plate was studied without the boundary members, it was found that only up to a small magnitude of the lateral force, the stiffness of the plate with and without any imperfection are close to each other. With a higher level of the lateral force, the stiffness of the plate with imperfection reduces significantly because of the buckling of the plate along the compression diagonal. A sample example of pushover curves indicating the limit of the compression force in the plate at which buckling occurs, is given in Figure 5.14, where the palte has an aspect ratio of 1.0 and thickness of 2 mm. This limiting force, up to which the behaviour of the plate is linear, is observed to depend on the aspect ratio and the thickness of the plate. The buckling force to thickness relation can be established by a quadratic equation (Equation 5.16, Figure 5.15) with $R^2 > 0.98$. The co-efficients X_1, X_2 and X_3 can be related to aspect ratio as given by Equation 5.17, Equation 5.18 and Equation 5.19 respectively (Figure 5.16).

$$F_{buckle} = X_1 b^2 + X_2 b + X_3 \tag{5.16}$$

where, X_1, X_2 and X_3 are constants depending on the aspect ratio of plates

$$X_1 = 7.2945(\beta_2)^2 + 5.6749(\beta_2) \tag{5.17}$$

$$X_2 = 11.265(\beta_2)^2 + 14.785(\beta_2) \tag{5.18}$$

$$X_3 = 16.325(\beta_2)^{1.4848} \tag{5.19}$$

Once F_{buckle} is known, taking its component along the brace and dividing by the area of the brace ('A_d'), the compression yield strength (i.e., buckling strength) of the brace can be

calculated. This parameter does not have a very significant effect on the final behavior of the model except a slight increase in the initial stiffness. At the onset of buckling, the top displacement of the plate without the boundary elements can be approximately related to the thickness of the plate by Equation 5.20. On application of the lateral force corresponding to F_{buckle} (which is a very small force), the change in top displacement (Δ_{buckle}) is negligibly small for different aspect ratios. However, Δ_{buckle} will change appreciably if a significant variation of the overall stiffness of the system is observed. But that is not a concern in regard to this parametric study. Therefore, for all aspect ratios under consideration, the average displacement is taken and is related to the plate thickness (Figure 5.17) by Equation 5.20. Thus, for a SPSW represented using bracing, the modulus of elasticity for the compression strut does not remain the same as that of the brace in tension.

$$\Delta_{buckle} = 0.0934b^2 - 0.0335b + 0.2178 \tag{5.20}$$

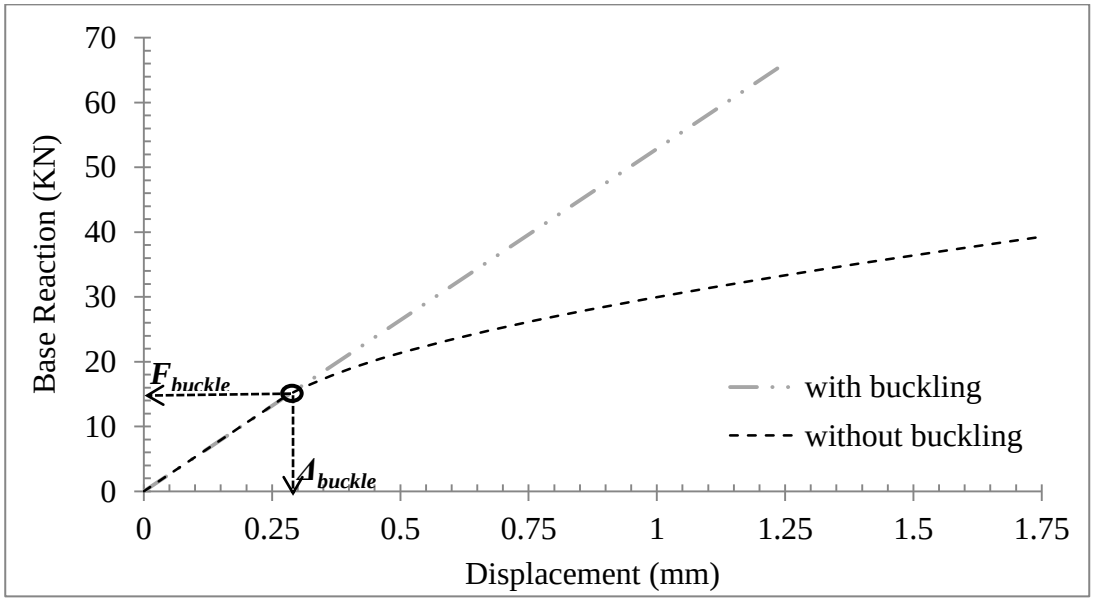

Figure 5.14: Sample comparison of plate pushover with and without imperfection

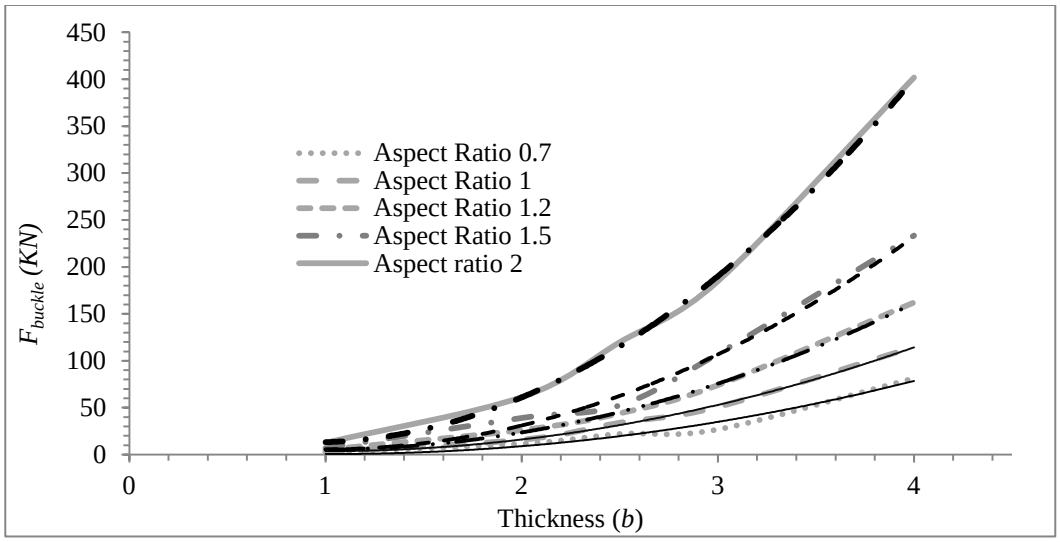

Figure 5.15: Relation between buckling force and thickness of plate

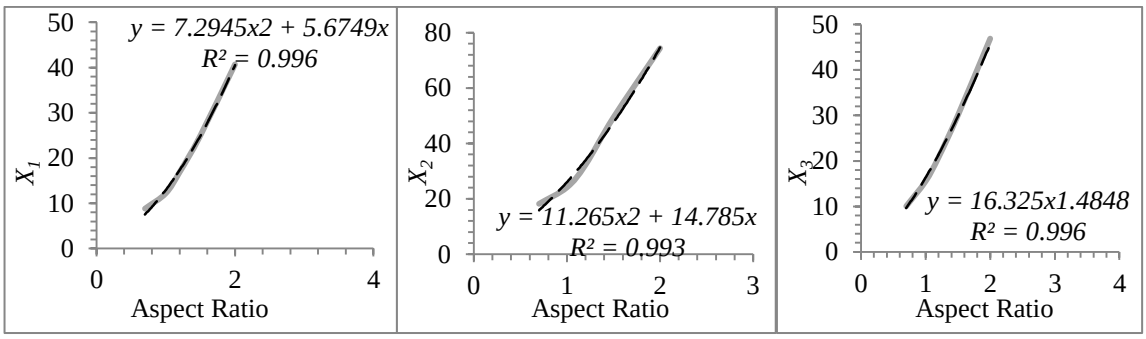

Figure 5.16: Relation between co-efficients X_1, X_2 and X_3 with aspect ratio

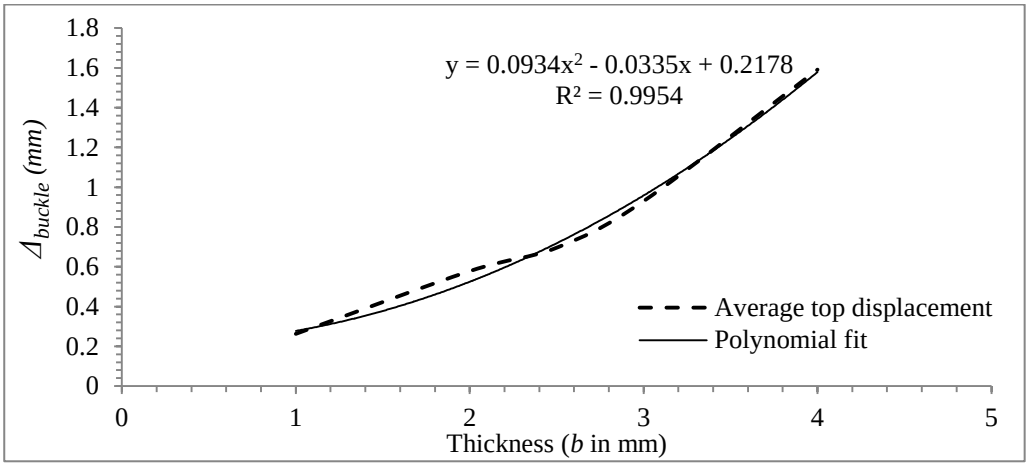

Figure 5.17: Variation of average top displacement with thickness for lateral force F_{buckle}

5.4.5 **Tension strut in EQ.BF model**

In a multi-storey steel plate shear wall, the presence of plates above and below causes a neutralizing effect on yield forces in the plates. Since, the plate is distributed throughout the width of the bay, as compared to a bracing system connected only at the corners, the vertical forces during plate yielding is higher than that of the vertical component of force from the brace. The vertical yield force from the plate can be taken as ($\sigma_y bl/2$), where it is assumed that only half the width of the bay is responsible for tension yielding of the plate; in this case, σ_y is the yield stress of the plate. This assumption arises from the fact that if the equivalent area of the brace is divided by the thickness of the plate, the observed length is very close to half the width of the bay. At yielding the vertical component of the force from the equivalent brace in tension is $\sigma_y * A_d * cos(\gamma)$, where γ is the angle of inclination of the brace with vertical column. The tensile force in the braces of the two consecutive stories also has a neutralizing effect at the corresponding beam column joints. The ratio of these balancing forces on a SPSW and equivalent brace is represented as α_{bal} as given by (Equation 5.21).

$$\alpha_{bal|storey-i} = \frac{Lower\ of\ \left\{\left(0.5lb\sigma_y\right)_{storey-i}\ ,\ \left(0.5lb\sigma_y\right)_{storey-i+1}\right\}}{Lower\ of\ \left\{\left(A_d\sigma_y cos\theta\right)_{storey-i}\ ,\ \left(A_d\sigma_y cos\theta\right)_{storey-i+1}\right\}} \tag{5.21}$$

The direct effect of this balancing of the storey forces is observable in the increased stiffness in case of multi-storey structures as compared to the single storey ones. To account for such increase in the stiffness in the corresponding braced model, the modulus of elasticity of a brace in tension is increased by α_{bal} (Equation 5.21). Instead of increasing the modulus of

elasticity, increasing the cross sectional area of the brace was considered in other models (like Thorburn et al., 1983; Topkaya and Atasoy, 2009). However, such strategy will make the model more complicated, as iterative techniques are needed to be introduced so that the behavior of the brace is represented correctly both in tension and in compression. For single-storey structures there is no need to increase the stiffness of the braces as there is no internal force balance as observed in the muti-storey systems. However, it is observed that if the beam web thickness is more than nearly fifteen times the thickness of the plate, a similar equilibrium of forces between the beam and the plate should be considered. In those cases, even though the external semi-supports from the upper and lower stories are absent, for its high stiffness as compared to plate, the beam acts as a rigid member. For an intermediate storey in multi-storey structure, α_{bal} is the sum of both upper and lower storey ratio as both have an increasing effect on the stiffness of the plate at that storey level.

$$E_{brace} = \alpha_{bal} * E \tag{5.22}$$

where, E represents the young's modulus of plate in SPSW systems and E_{brace} is the modulus of elasticity of the equivalent brace.

In the EQ.BF model, with perfectly elastic-plastic material property, the tensile yield stress indicates the stress beyond which the tension brace will stop taking further load. However, in case of a plate with the same perfectly elastic-plastic material property, the behavior is more like a bunch of parallel connected strips (with collective area same as that of brace). In that case, even though the yield stress is reached in some areas of the plate, other areas of the plate still continue taking further load (Figure 5.18). Elgaaly (1998) reported somewhat similar increase of

strength by indicating that the yield strain distribution in diagonal tension field is parabolic. So, a progressive failure curve of the material model needs to be defined in case of EQ.BF model. For a given tensile load, let the elongation of bracing element is Δh_b, and for the same load, the maximum elongation in a parallel strip is Δh_p (Figure 5.18). Thus, the volumetric change in the brace (with area *'A_d'*) is $A_d * \Delta h_b$ and that of parallel-strips is $\alpha_k * A * \Delta h_p$; where α_k is a factor which depends on the shape of the yield area formed by the nodes of the parallel strips (Figure 5.18). If the energy dissipated by both SPSW and EQ.BF systems are equated, the relationship between Δh_b and Δh_p can be established (Equation 5.23).

$$(\Delta h_b / \Delta h_p) = \alpha_k \tag{5.23}$$

To achieve the same level of the final deformation in the EQ.BF model, as in the corresponding SPSW system, the original yield stress needs to be multiplied by factor α_k. In this case, the enhanced material properties for the bracing are represented bys a tri-linear stress-strain curve as shown Figure 5.18. Since the stress, $\alpha_k * \sigma_y$ represents the point of final yielding point beyond which the stress-strain curve is perfectly plastic, a larger value of strain ($\varepsilon_1 > \varepsilon_y$) corresponding to that stress is assumed. Through a repeated study with varying parameters, it has been observed that α_k depends upon the ratio of the web thickness of the beam ($t_{web|beam}$) to the sum of the thickness of the connecting plates (Equation 5.24).

$$\beta_4^{\,i} = t_{web|beam} / (b_i + b_{i+1}) \tag{5.24}$$

where, i represents the i^{th} storey in a multi-storey system. For single storey structures $b_{i+1}=0$.

The relation between α_k and β_4 is established by carrying out parametric study with both plate frame model and equivalent braced model. In the braced model, the yield strength of braces in tension is enhanced experimentally so that both the plate model and the equivalent braced model have similar pushover curves. A sample pushover curve for a SPSW system with square beams (80 mm x 80 mm), square columns (200 mm x 200 mm) and plate thickness of 3 mm is shown in Figure 5.20. Since, thickness of beam to that of plate in the sample pushover study (Figure 5.21) is very large, an increased initial stiffness is observed in plate model as compared to equivalent bracing model. However, that can be neglected for this part of the study where the only concern is the representation of the yield strength. In this case, α_k is obtained by dividing the enhanced stress with that of the original yield stress of plate. The relation between α_k and β_4 as shown in Figure 5.21 can be expressed by a power curve fitted with Equation 5.25, where R^2 = 0.996.

$$\alpha_k = (\beta_4)^{0.12} \tag{5.25}$$

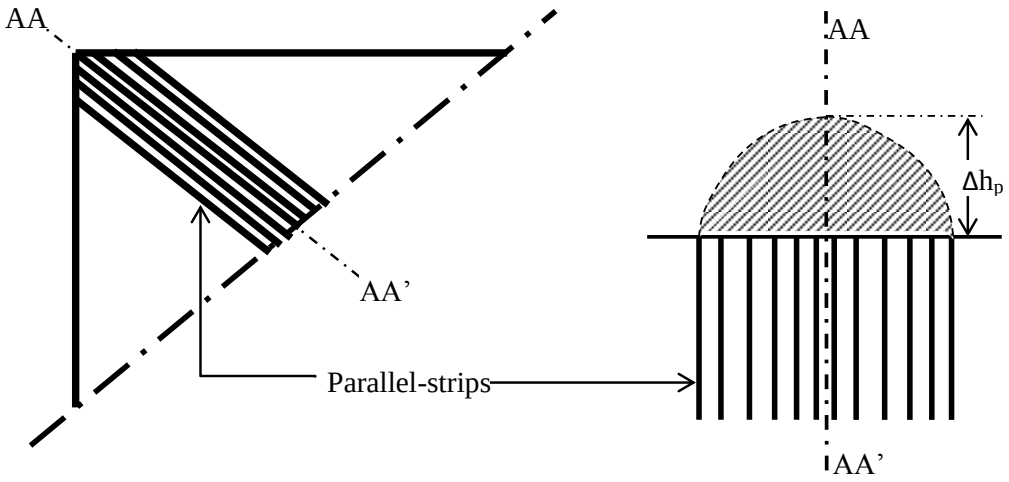

Figure 5.18: Arrangement of parallel strips to represent plates in SPSW system and yielding area covered

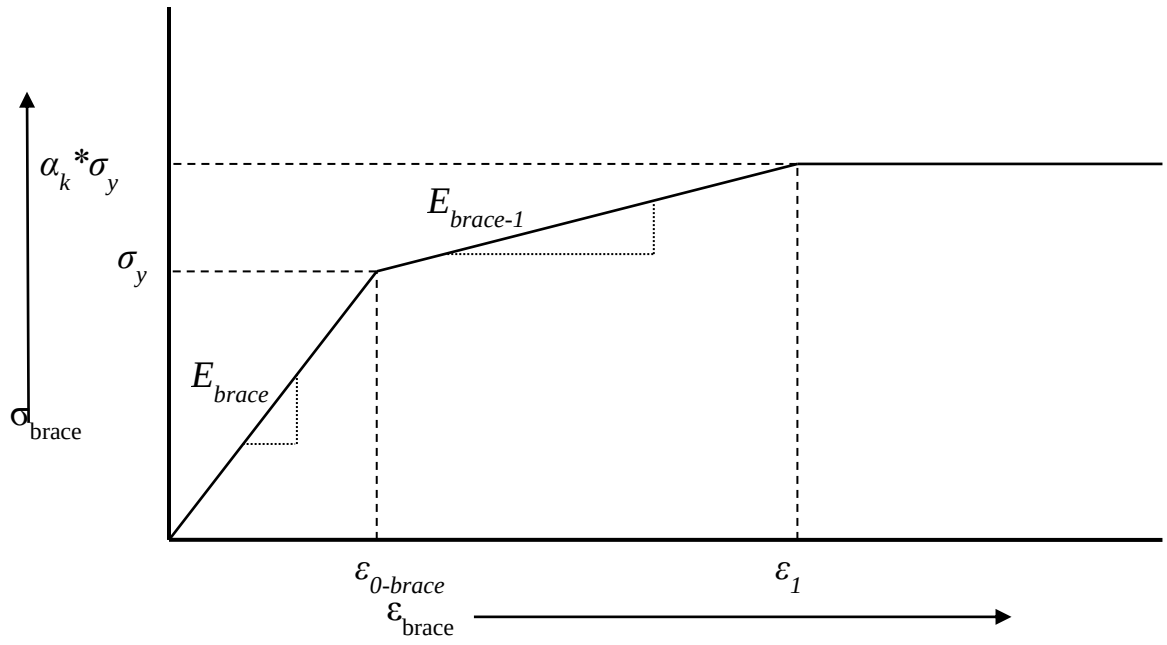

Figure 5.19: Material properties in tension of truss braces in EBM, where σ_y and ε_0 are yield stress and strain of plate in SPSW system.

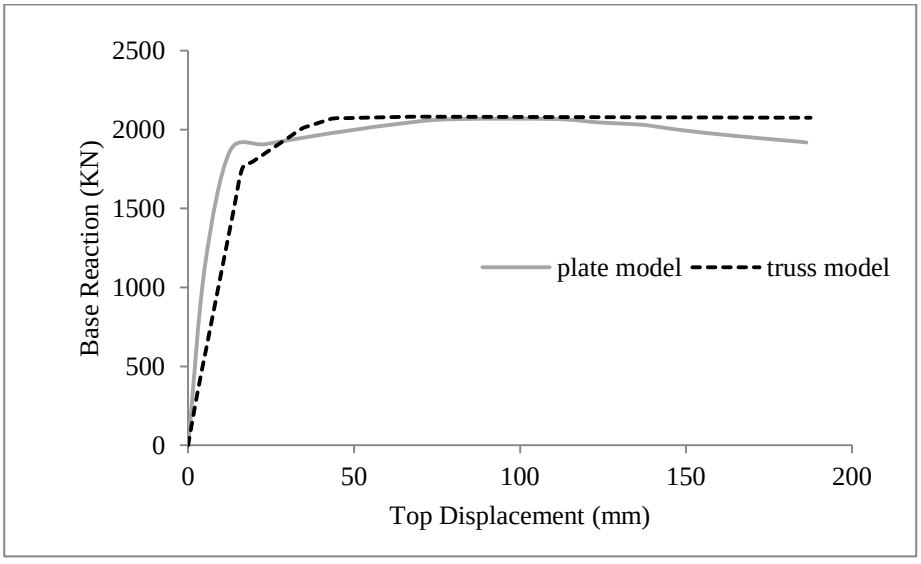

Figure 5.20: Sample pushover curve with enhanced material properties in EQ.BF model to match the SPSW system

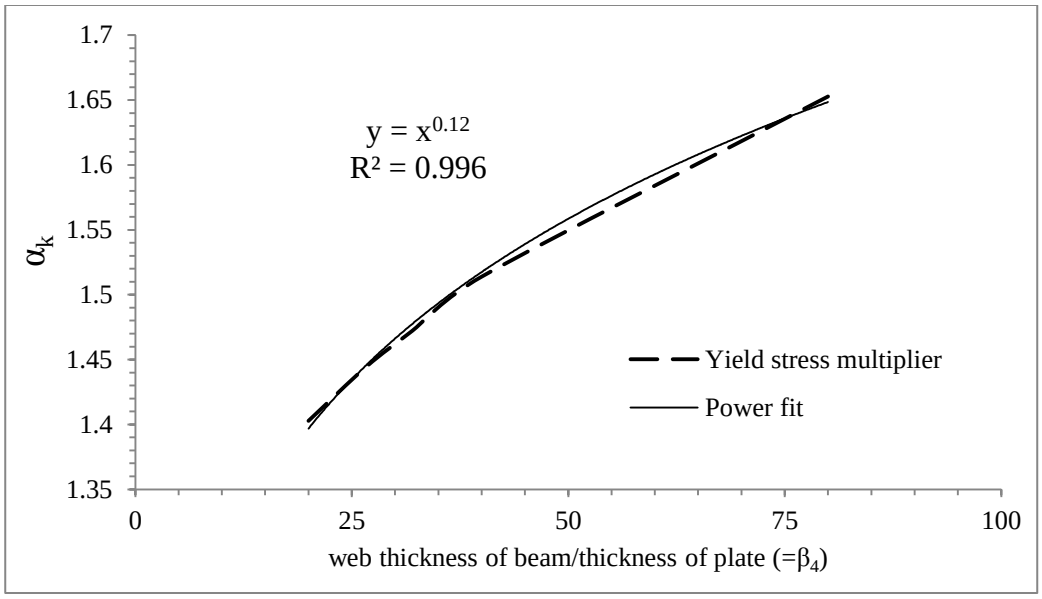

Figure 5.21: Relation between α_k and β_4

5.5 Summary

A detailed FE model has been used for the parametric study to develop the EQ.BF model of a SPSW system. A numerical study has been presented to show the limitations of the existing braced frame models. Finally, an EQ.BF model has been developed based on a detailed parametric study. Both material and geometric properties of the braces in EQ.BF can be calculated based on the statistical relations developed in this chapter. In EQ.BF model only the infill plate of SPSW is replaced by braces thus no change of boundary property is required to be made. In the next chapter the EQ.BF model will be validated both in static and in dynamic scenarios. Finally, the equivalent braced frame model and the detailed FE model will be used to test performance of multi-storey ductile steel plate shear walled structures.

Chapter 6. Validation of Equivalent Braced Frame Model Using Static and Dynamic Analyses

6.1 Introduction

The Equivalent Braced Frame (EQ.BF) model has been developed based on a detailed parametric study as discussed in the previous chapter. Acceptability of a model depends greatly on accuracy in validation with experimental or other established numerical results. For the proposed EQ.BF model, validation tests based on both static and dynamic responses have been carried out. A set of light-gauge SPSW systems are designed in accordance with NBCC 2010 following the capacity design requirements, with the purpose of testing the EQ.BF model as well as for determining applicability of the existing design procedure developed for the ductile SPSW systems to the light-gauge SPSW systems. For dynamic tests, the buildings are assumed to be located in the Vancouver region of Canada. Previously, for detailed FE model only the pushover curves from experiment have been used for validation. However, in case of an EQ.BF model both pushover and cyclic curves has been validated with some selected experimental results or results from a detailed FE model. An EQ.BF model was further used to validate some dynamic time history results derived from detailed FE model. Particular attention was given to the computation time of the EQ.BF model in Opensees as compared to the shell-plate model in Abaqus.

6.2 **Static validation of EQ.BF model**

Static loads include both monotonic pushover loading and cyclic loading on SPSW systems. A series of pushover curves are generated from EQ.BF model and results are compared to available results from experiments or output from detailed FE model. Exactly similar comparison has then been done for cyclic loading. The pushover validation test of the developed EQ.BF model is carried out in three steps. First, the experimental models are validated by comparing the pushover curves from EQ.BF models and reported experimental results. Then, the designed single storey model's push-over curve (generated in Abaqus) was compared to that of the pushover curve obtained from the EQ.BF model. Finally, the pushover curves for a set of multi-storey structures' designed for this study are obtained using detailed FE models by Abaqus and compared with those obtained using the corresponding EQ.BF models. In case of multi-storey SPSW structures special importance was given to individual storey drift so that the overall deflected shape of both Abaqus model with shell element matches with that of EQ.BF model with non-concentric truss braces.

The main advantage of the proposed simplified modeling technique (i.e., the EQ.BF model) is that it allows for repeated analysis in a very short time. When repeated loading scenario comes like cyclic loading or time history analysis with ground motion data, this model is expected to be very efficient. Thus, to ascertain that the EQ.BF model is a correct approximation of the full scale FE model (i.e., with shell elements representing plate) in a three dimensional environment, a set of cyclic tests have been performed. For testing the model under cyclic loads, a single storey specimen has been developed in Abaqus. Other than that, three

separate experimental multi-storey specimens whose hysteresis curves are available in the literature (Tromposch et al. (1987), Driver et al. (1997), Mohammed et al. (2003)) have been used for validation. All four cyclic curve tests indicated the acceptability of the EQ.BF model.

6.2.1 Validation of EQ.BF model with single-storey experimental results

The same two models which were used to validate the finite element modeling technique are used again to validate the EQ.BF model (Lubell et al., (2000) and Neilson, (2010)). Identical modeling parameters were maintained as reported for experiment. Parameters α_s and α_m are computed based on the set of relations developed for EQ.BF. Then equivalent areas for the braces are computed as 1115mm^2 and 642.3 mm^2 for models of Lubell and Neilson, respectively. The material properties for non-concentric braces of EQ.BF model are also computed based on the available set of equations. Finally, EQ.BF model was created in Opensees following the same modeling technique as was done for the bare frame model. The truss element representing a brace was chosen as uniaxial element with Material Hysteretic properties where uniaxial material property both in tension and compression can be defined. Since, each member (beam or column or brace) represented one element, a total of only six elements were required for the model. This made the analysis much more simple and robust in terms of the effort need for constructing a model and the time of computation. Results obtained from both the models are shown in Figure 6.1 and Figure 6.2. For both the models the initial stiffness is correctly estimated by the EQ.BF model. For Neilson's specimen (Figure 6.2) the ultimate strength and the sequence of yielding match almost perfectly with shell-plate model and with EQ.BF model. The amount of error estimated with EQ.BF model for experimental validation is less than 2% in term of the ultimate

strength. The results from the EQ.BF model are in excellent agreement with those from the detailed three dimensional FE model. With the specimen tested by Lubell et al. (Figure 6.1), the agreement of three dimensional FE model with EQ.BF model is satisfactory with approximately 6% error in ultimate strength. However, the initial stiffness is correctly estimated. The sequence of yielding is predicted correctly (as observed from the push-over curves) by both the models. However, the experimental pushover curve shows a slightly higher degree of strain hardening than those produced by the numerical models (both FEA and EQ.BF models).

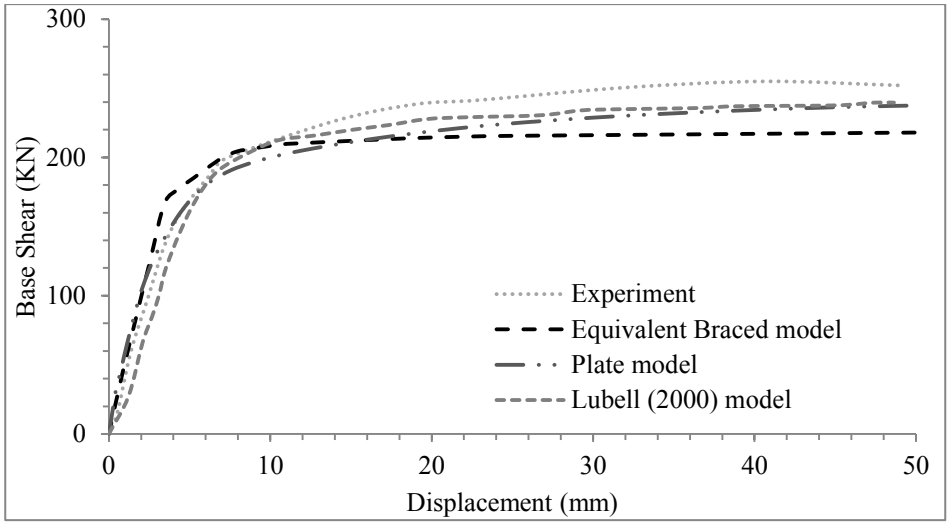

Figure 6.1: Push-overs curves from different models based on Lubell's (2000) specimen

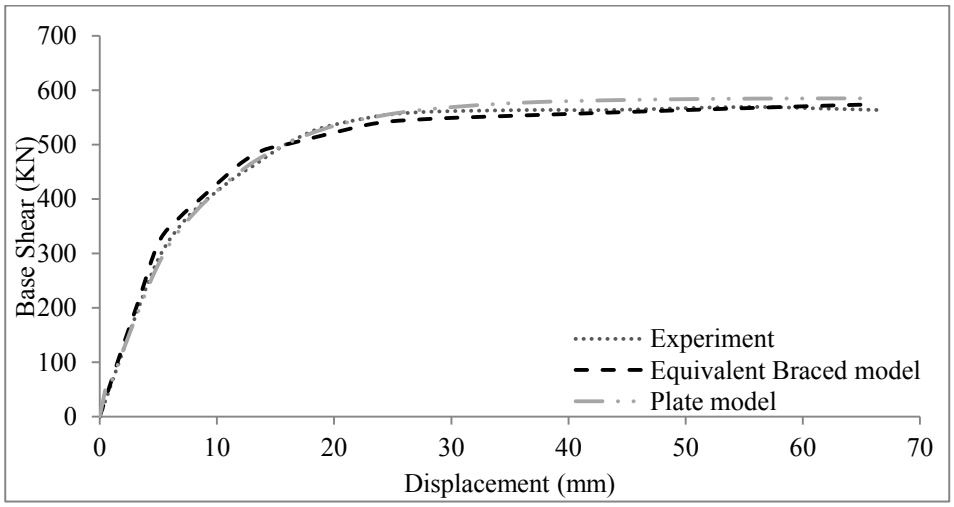

Figure 6.2: Push-overs curves from different models based on Neilson's (2010) specimen

6.2.2 Validation of EQ.BF model with single-storey detailed FE model

A single storey SPSW system was designed considering standard heavy sections which are of much use practically. An infill plate of thickness 3 mm and other beam-column dimensions along with material property chosen are indicated in Table 6.1. Following the same process as used for the previous validation example, the EQ.BF model parameters were computed. The cross-sectional area of the braces and modified material properties were computed (Table 6.2). Like the previous single-storey model, the newly designed SPSW does not have a storey above or the beam is not strong enough to be considered as rigid (i.e., ratio of beam web thickness to plate web thickness is less than fifteen). Therefore, no increase in Young's modulus is required for the braces of EQ.BF model. Comparing the pushover curves obtained from the two models (Figure 6.3), it can be said that with EQ.BF model reproduces the pushover curve accurately until the first yielding, and the ultimate strength is estimated with less than 2% error. The zone between first yielding and the yield plateau, the stiffness is over estimated by nearly 8%. Since, the EQ.BF model is an approximate model, a perfect agreement with the detailed FE model may not entirely achievable. However, the performance of the EQ.BF model in reproducing the pushover curve is adequate for assessing the overall behavior of a SPSW system.

Table 6.1: Details for the sample single-storey SPSW

Beam			Column			Plate		
Section	E (MPa)	σ_y(MPa)	Section	E(MPa)	σ_y(MPa)	Thickness	E(MPa)	σ_y(MPa)
W530x272	200,000	350	W360x509	200,000	350	3 mm	200,000	385

Table 6.2: Details of EQ.BF model parameters for designed single storey SPSW validation

α_s	0.31	Compression		Tenssion			
α_m	3.82	Stress	-16.2	σ_y (MPa)	385	$\alpha_k\sigma_y$	486.5
Area of brace	7982.3	Strain	0.00016	ε_0 (mm/mm)	0.00193	$\alpha_k\varepsilon_0$	0.00243

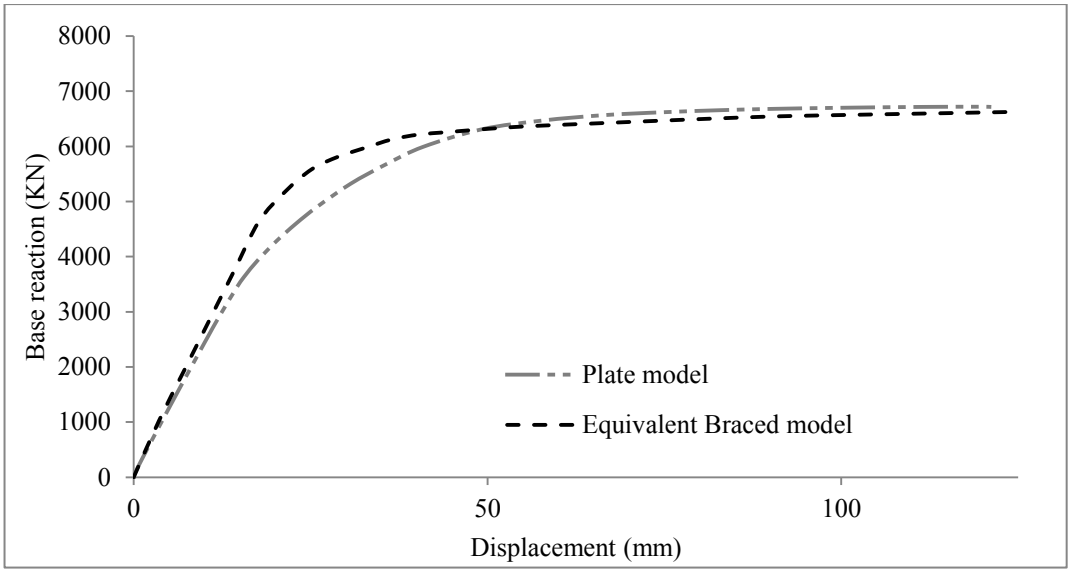

Figure 6.3: Pushover curves from different numerical models for single-storey specimen

6.2.3 **Validation on EQ.BF model of multi-storey structures**

The EQ.BF model was developed for all three multi-storey structures designed. Calculated model parameters for the 4-storey, 6-storey and 10-storey are indicated in Table 6.3, Table 6.4 and Table 6.5, respectively. Pushover curves based on top storey displacement and base reaction were constructed. For validating some of these models, detailed FE models with shell-plate elements were developed in Abaqus, for the four and six storey buildings. It's worth mentioning that the time required for developing and analyzing the EQ.BF models is significantly less as compared to the detailed FE models. The time difference is more noticeable

for 10-storey as compared to a single storey structure. For all the three multi-storey structures, the pushover curves (Figure 6.4, Figure 6.5 and Figure 6.6) obtained by the two types of models are in excellent agreement. The initial stiffness is very accurately estimated by the EQ.BF model. Also, there is no mentionable error in the ultimate strength indicated by the model. The sequence of hinge development in columns and the progress of material non-linearity induced in the members also have a reasonable match. Thus, it can be concluded that EQ.BF model is reasonably accurate and advantageous in terms of the modeling ease and analysis speed to study the overall behavior SPSW systems.

Just matching the pushover curves with the top displacement of a building leaves the work incomplete unless the displacement pattern of each storey and the inter-storey drift are also validated. Thus, from the same analysis, the storey wise displacements were plotted against the base reaction for each storey. For all the three multi-storey structures, the storey-wise pushover curves are in good agreement. However, the level of deference between the storey-wise pushover curves generated using the EQ.BF and the corresponding detailed FEM models were found to decrease with the increase of the height of the structure. For the 10-storey structure, the storey wise pushover curves are given in Figure 6.7. For all the stories, the initial stiffness approximation is reasonably accurate. Other than the first storey, the displacements in other storeys are accurately estimated, and the ultimate strength of a storey is estimated with a maximum of 2% error. For the first storey, the error is little less than 10% when the ultimate strength is concerned. The strength at which the plastic hinges start to form in columns is also approximated with reasonable accuracy. Though, there is some noticeable difference in the pushover curves for the first storey but for an approximate model, developed to estimate the

global behavior, this difference can be considered acceptable. This error may be because of the assumption in creating an EQ.BF model that there is no moment interaction involved, and only shear deformation of SPSW system is significant. For a more accurate result from the EQ.BF model, the model needs to be modified such to account for the contribution of flexure, which may be small.

Table 6.3: Calculated EQ.BF model properties for 4-storey

Storey	1	2	3	4
α_s	0.31	0.28	0.23	0.15
α_m	5.21	5.63	6.05	6.10
A	10860.07	9827.15	7145.84	2264.92
σ_{comp}	16.19	12.98	9.44	5.75
ε_{comp}	0.000106	9.13E-05	6.62E-05	3.51E-05
$\alpha_k\sigma_y$	196.23	199.89	209.86	239.43
$\alpha_k\varepsilon_0$	0.000436	0.000209	0.000159	0.000265

Table 6.4: Calculated EQ.BF model properties for 6-storey

Storey	1	2	3	4	5	6
α_s	0.42	0.41	0.37	0.32	0.23	0.15
α_m	3.68	3.70	3.72	4.39	5.72	6.08
A	15206.16	15172.03	11991.05	10667.15	6771.65	2262.47
σ_{comp}	30.86	29.34	26.93	20.12	10.04	5.79
ε_{comp}	0.000202	0.000201	0.000157	0.000121	6.6E-05	3.5E-05
$\alpha_k\sigma_y$	186.55	188.01	191.26	197.38	209.86	239.43
$\alpha_k\varepsilon_0$	0.000402	0.000191	0.000185	0.000187	0.000154	0.000262

Table 6.5: Calculated EQ.BF model properties for 10-storey

Storey	1	2	3	4	5	6	7	8	9	10
α_s	0.52	0.52	0.52	0.47	0.43	0.38	0.33	0.28	0.19	0.15
α_m	2.84	2.84	2.57	3.04	3.32	3.93	4.53	5.32	7.36	6.58
A	17927.19	17883.80	16246.59	15748.90	13856.25	12782.86	11082.31	9327.71	5311.29	2440.73
σ_{comp}	48.48	47.56	52.99	42.32	36.24	27.92	20.56	14.13	5.49	5.42
ε_{comp}	0.000309	0.000309	0.000307	0.000252	0.000202	0.000159	0.000122	9.11E-05	4.79E-05	3.52E-05
$\alpha_k\sigma_y$	181.63	181.63	182.75	185.20	188.01	191.26	195.13	202.74	214.50	239.43
$\alpha_k\varepsilon_0$	0.00035	0.00017	0.00017	0.00017	0.00018	0.00019	0.00020	0.00020	0.00017	0.00029

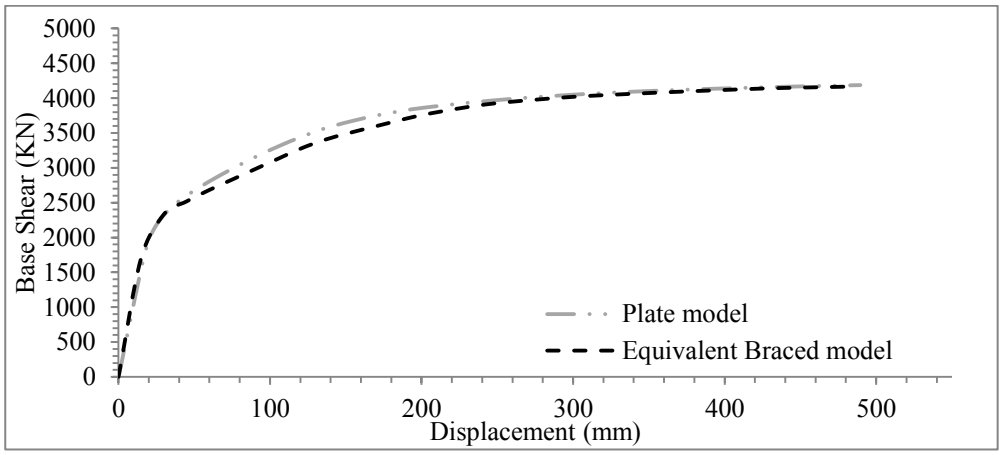

Figure 6.4: Pushover curves from different models for 4-storey SPSW system.

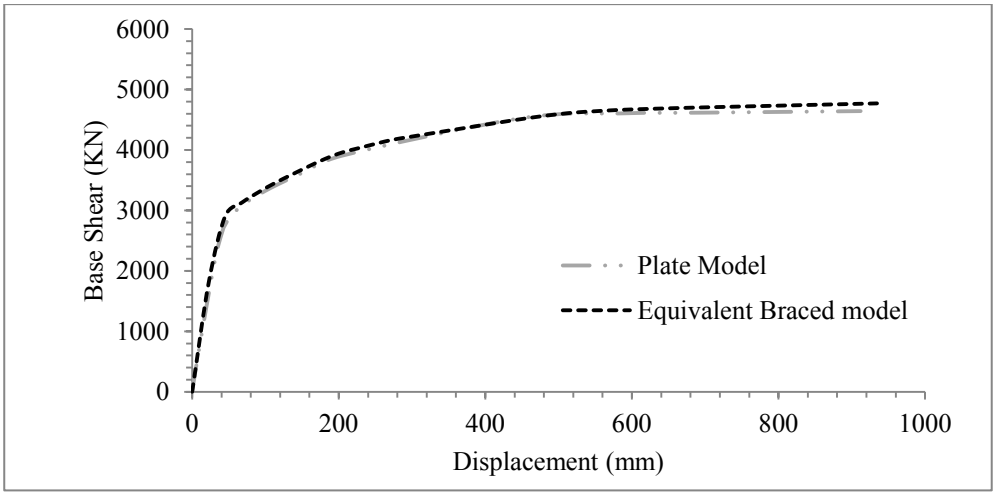

Figure 6.5: Pushover curves from different models for 6-storey SPSW system.

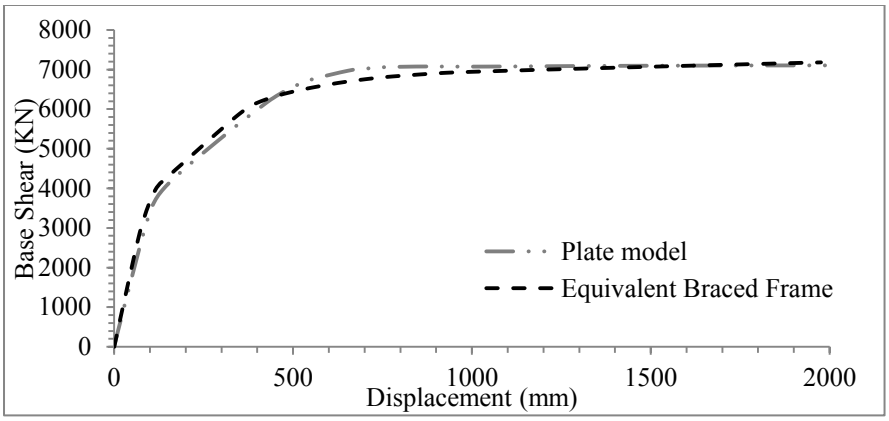

Figure 6.6: Pushover curves from different models for 10-storey SPSW system.

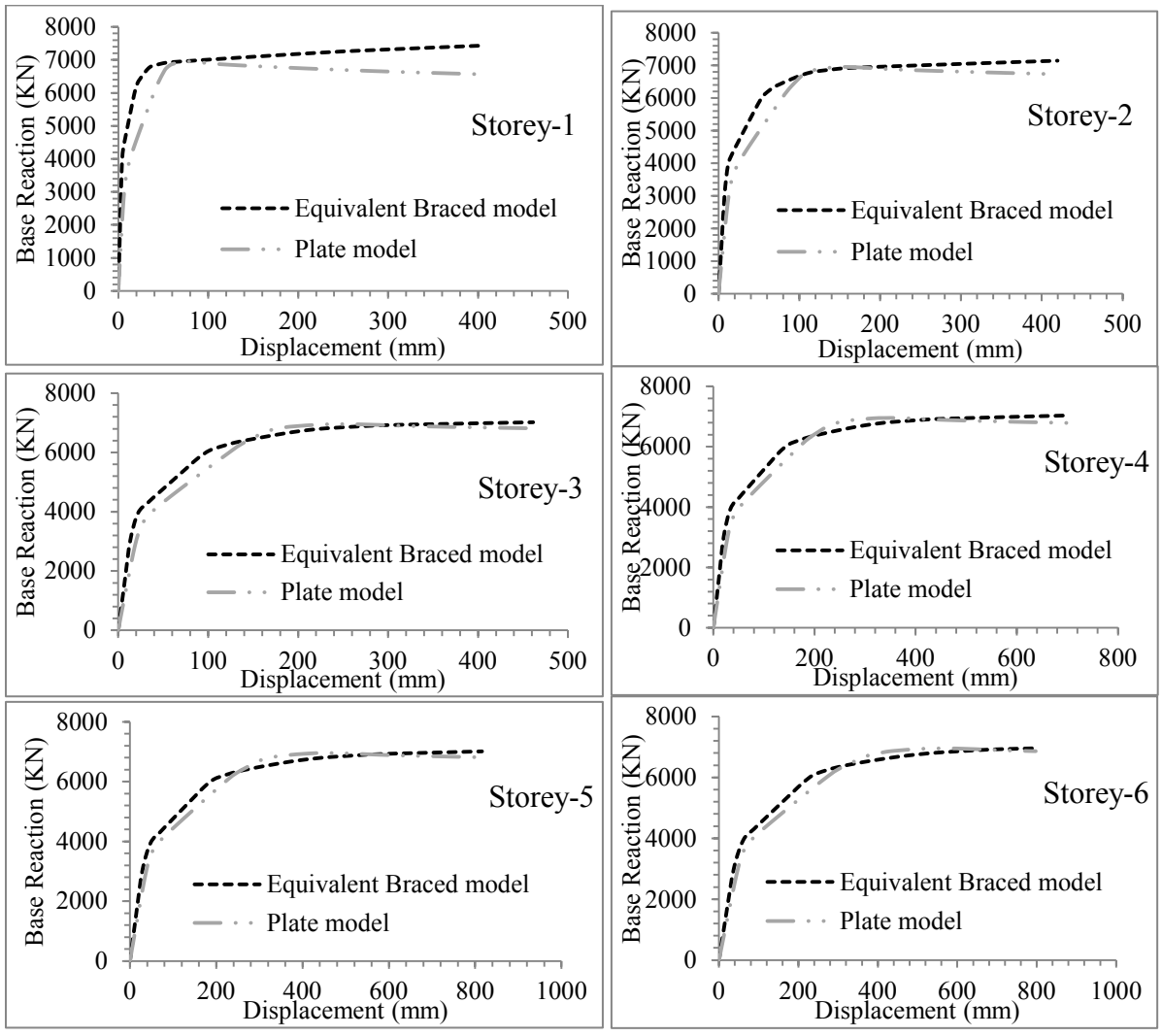

Figure 6.7: Comparison pushover curves of every storey height for 10-storey specimen (for Storey 1-6).

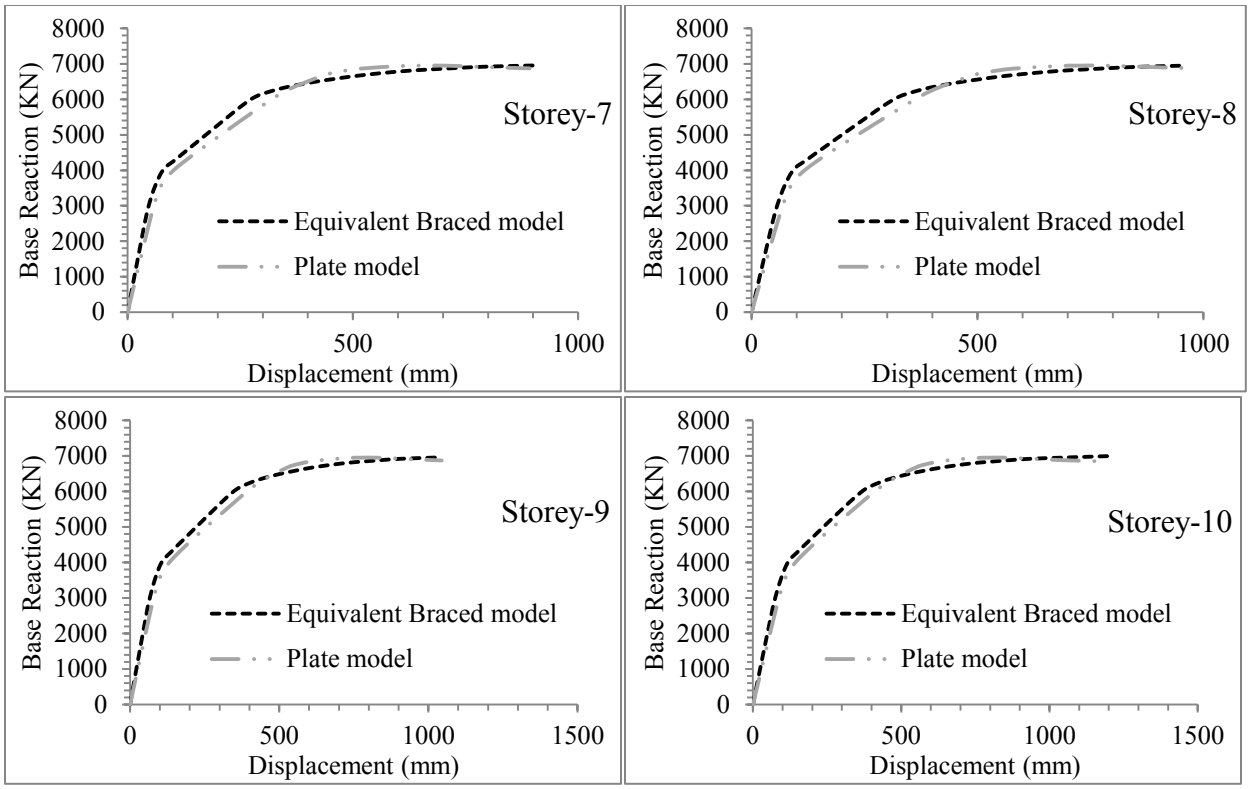

Figure 6.8: Comparison pushover curves of every storey height for 10-storey specimen (for Storey 6-10).

6.2.4 **Cyclic load validation test for Single-storey specimen**

A single storey sample SPSW model with columns W360x509 and beams W460x158 was developed in Abaqus. Infill plate of 1 mm thickness was made with shell elements. The center line dimension of the model is assumed 3000 x 3000 mm. A cyclic test displacement, with a maximum displacement of 60 mm, was applied on the model, the same way as in case of pushover analysis. Only this time, the applied load had amplitude oscillating from positive and negative (Figure 6.9). Two cycles of each displacement was applied to ensure the stability of the model. Using the relevant properties, EQ.BF model was also developed and a very similar

loading or displacement was applied. The hysteretic curve relating the base reaction and top displacement (Figure 6.10) obtained in both the models is compared and a good match is observed. Also, the analysis time with EQ.BF model is found to be less than a minute as compared to few hours required by the detailed FE model.

The Abaqus model showed a significant pinching effect, which has already been reported in many studies relating to SPSW system (Tromposch et al. (1987)). They also inferred from their study that an unstiffened SPSW system shows more pinching as compared to the one stiffened with additional members. Since, the material chosen for EQ.BF model is hysteric; it is not easy to incorporate the pinching effect into the model. Though, strictly speaking the pinching effect is a function of stiffness of the infill plate in the presence of the boundary members, the range of variation of pinching effect observed through the set of studies performed is not found to be very significant. So, for an approximate modeling technique such as EQ.BF, a constant pinching effect may be assumed for all possible models. From Figure 6.10, it can be said that the positive and negative displacements derived from the cyclic test show an excellent agreement between the two models.

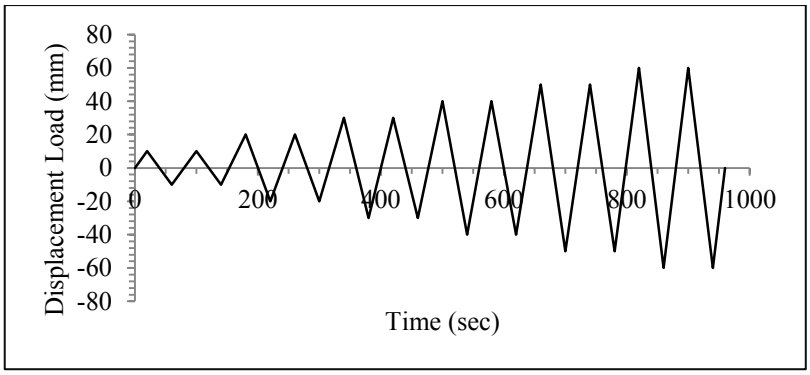

Figure 6.9: Cyclic load applied to the sample specimen prepared using shell elements

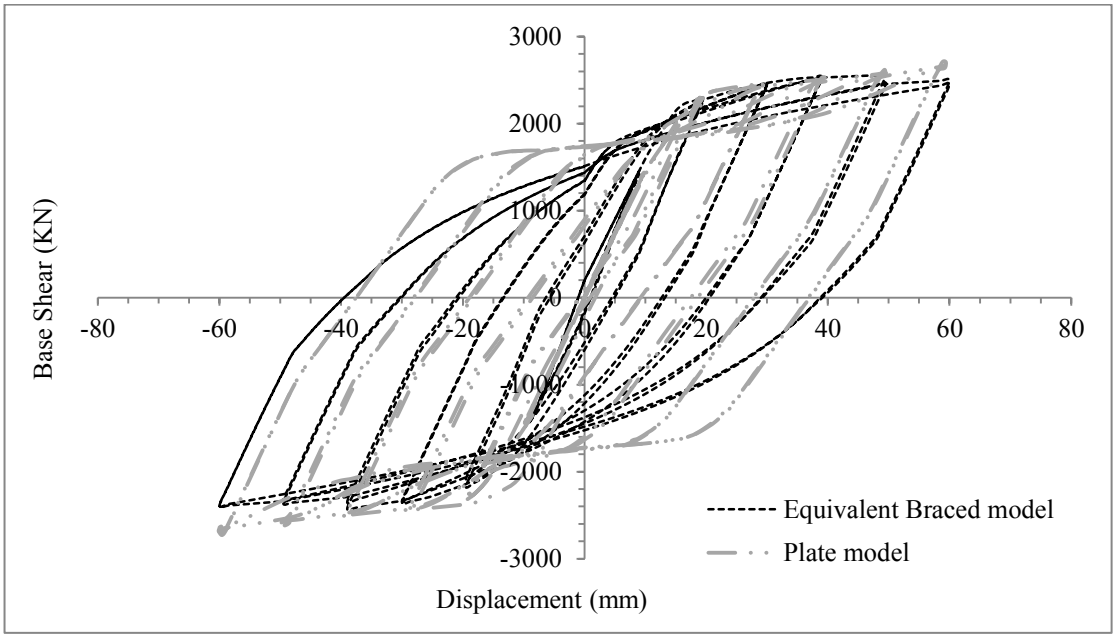

Figure 6.10: Hysteretic curve validation with single-storey model developed in Abaqus.

6.2.5 **Cyclic load test on Multi-storey specimens**

Three experimental multi-storey models were tested. A two storey model experimented by Tromposch et al. (1987), a three storey model experimented by Mohammad et al. (2003) and a four storey model tested by Driver et al. (1997). All these models had rigid member connections which is a necessary requirement for the developed model. Mohammed's specimen had the load control point at second storey level and Driver's specimen had it at the first storey level. For Tromposch's specimen, the vertical structure was placed horizontally and the central beam was pushed down. The reactions at the two support ends were noted along with the central deflection. Identical displacement loading scenario was maintained in EQ.BF model as compared to the experimental specimen. Full gravity load of 500KN for Tromposch's specimen and

540KN for Driver's specimen and Mohammad's specimen is carefully applied in the EQ.BF model. Material properties obtained from the tension coupon tests reported in the respective studies have been utilized in the current models. So, generating the model parameters based on the available material properties and section dimensions was a straight forward task as already done for so many cases tested earlier in this thesis. The section properties and material details used the experimental studies by Tromposch et al. (1987), Mohammad et al. (2003) and Driver et al. (1997) are summarized Tables 6.6, 6.7 and 6.8, respectively.

Figure 6.11 indicates Tromposch's specimen had more pinching in the hysteretic curve as compared to that of the EQ.BF model. Although there is a scope of improvement, for an approximate model predicting the overall behavior this level of error is acceptable. The agreement of initial stiffness and ultimate strength both in positive and negative side is in good agreement. The overall match with Driver's specimen is excellent (Figure 6.12). Not only the initial stiffness and ultimate strength, but also the pinching effect is captured to a good extent. The sequence of formation of hinges is in excellent agreement for both push and pull. Hysteric curves developed for Mohammad's specimen had an overall excellent agreement (Figure 6.13). In push loading scenario the positive pushover matches almost perfectly, estimating the initial stiffness and ultimate strength very accurately. But for compression, the EQ.BF seems to be a bit stiffer probably because the constant pinching effect assumed in this model which is perhaps more than what it should be. However, the ultimate strength in compression side has no significant error. Also, the cycles after which the positive side pushover curve starts to go down i.e. in experimental model fails, a numerical instability was observed. This numeric instability is not a limitation with the model; it is rather a limitation with the method of finite element analysis

used in Opensees. However, with the developed modeling technique, the pushover curve is never expected to show failure points, since no such material properties are defined. With some modification on the material properties of braces even that can be achieved.

Table 6.6: Material and section details for specimen tested by Tromposch et al. (1987)

Storey	Column	Beam	Plate Thickness (mm)	Height of floor (mm)	Width of bay (mm)	Yield Stress (MPa)	Young's modulus (MPa)
1	W310x129	W610x241	3	2200	2750	242.5	207590
2	W310x129	W610x241	3	2200	2750	242.5	207590
		W610x241					

Table 6.7: Material and section details for specimen tested by Mohammad et al. (2003)

Storey	Column	Beam	Plate Thickness (mm)	Height of floor (mm)	Width of bay (mm)	Yield Stress (MPa)	Young's modulus (MPa)
1	W360x634	W460x158	4.8	1830	3050	341	208800
2	W360x382	W460x158	3.4	1830	3050	257	210900
3	W360x382	W460x158	3.4	1837	3050	262	203100
		W460x158					

Table 6.8: Material and section details for specimen tested by Driver et al. (1997)

Storey	Column	Beam	Plate Thickness (mm)	Height of floor (mm)	Width of bay (mm)	Yield Stress (MPa)	Young's modulus (MPa)
1	W360x634	W610x372	4.54	1927	3050	341	208800
2	W360x634	W460x158	4.65	1830	3050	341	208800
3	W360x382	W460x158	3.35	1830	3050	257	210900
4	W360x382	W460x158	3.4	1837	3050	262	203100

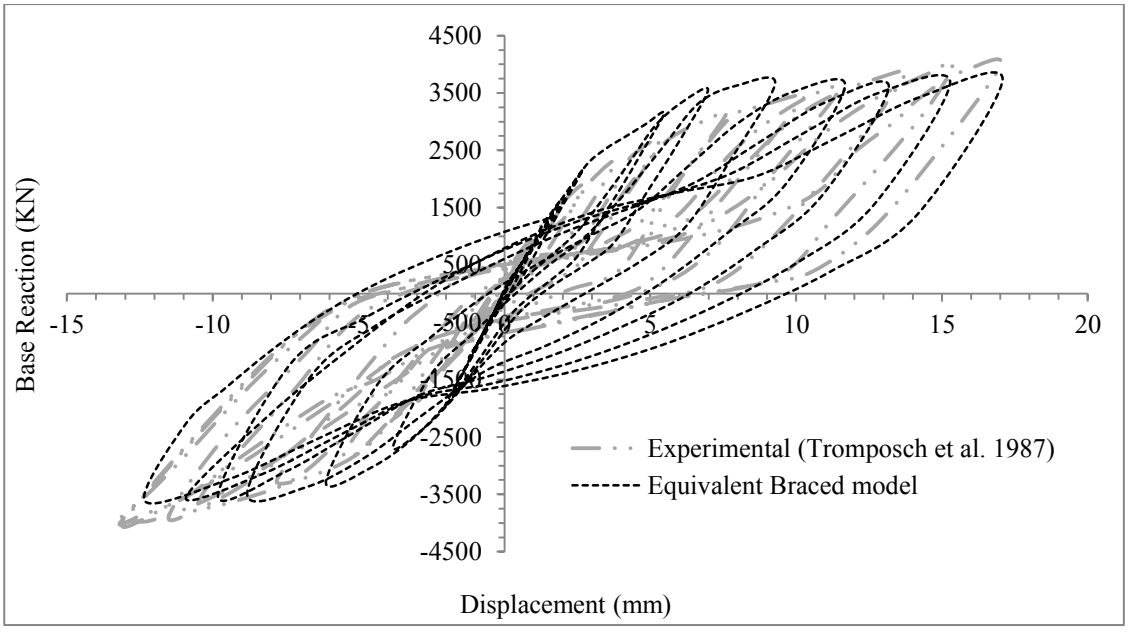

Figure 6.11: Validation of hysteretic curve result for Tromposch et al. 1987 specimen

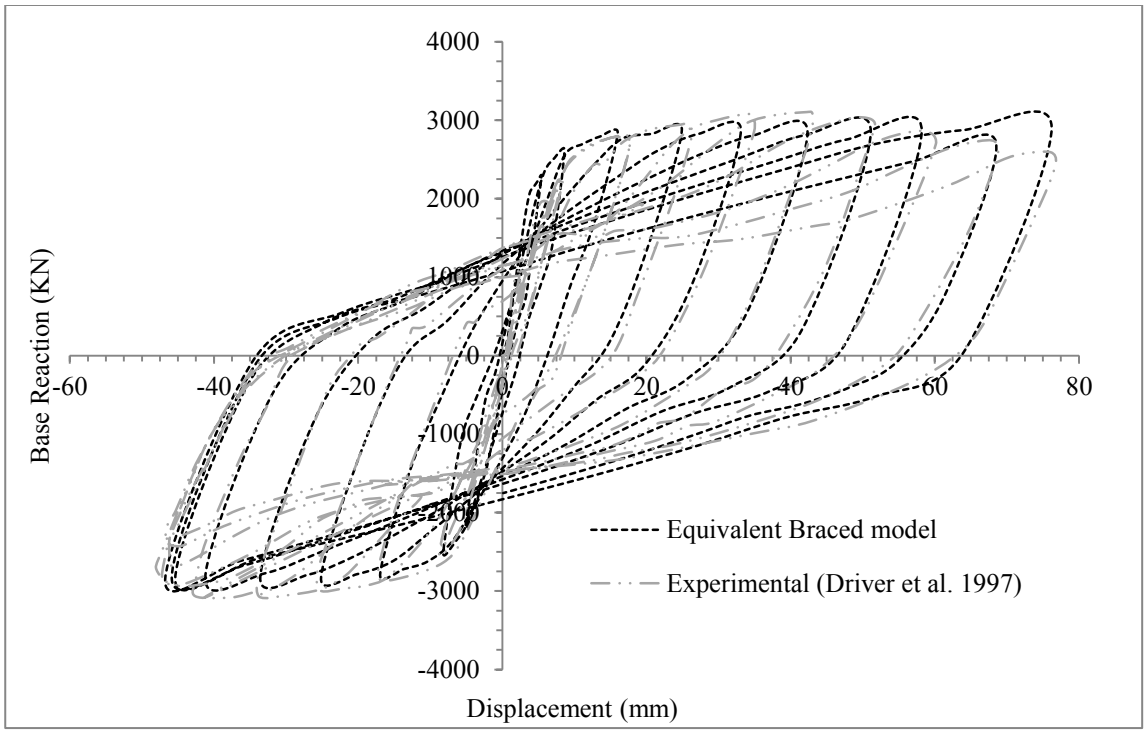

Figure 6.12: Validation of hysteretic curve result for Driver et al. 1997 specimen

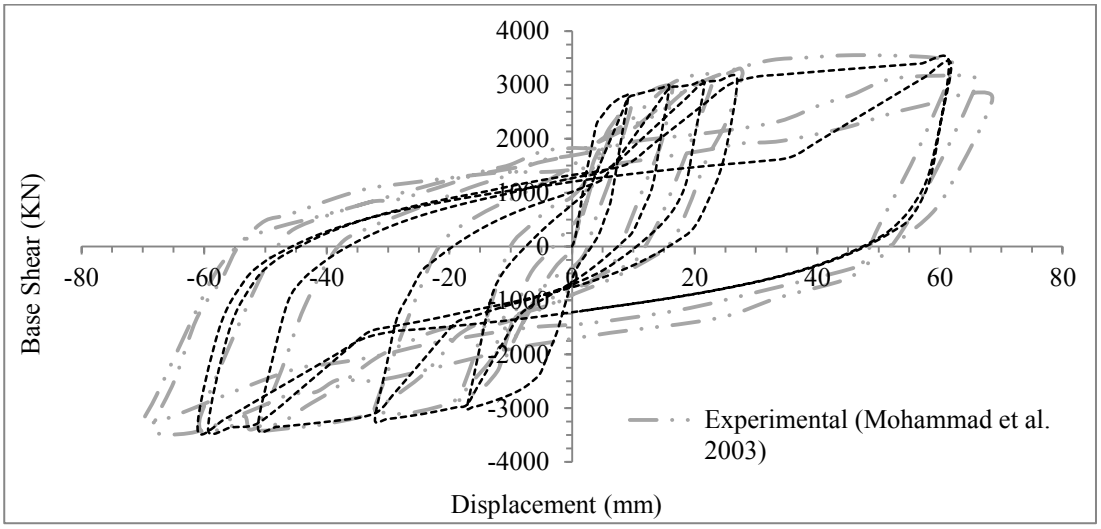

Figure 6.13: Validation of hysteretic curve result for Mohammad et al. 2003 specimen

6.3 Validation of EQ.BF models for dynamic response

The following two typed of analyses have been performed to study the dynamic behavior of SPSW systems: the frequency analysis, and then the time history analysis. Frequency analysis is carried out using both detailed FE modeling technique and the developed EQ.BF model. Since the structural stiffness estimated using the pushover analysis is reasonably accurate, with the same mass distribution, the EQ.BF model of a SPSW structure should give identical mode shapes and very close natural frequencies as obtained using the detailed FE model. All three multi-storey structures i.e. four-storey, six-storey and ten-storey will be subjected to this test. Further, the time history analysis with selected scaled ground motions will be conducted for above the three specimens. As the multi-storey structures are assumed to be located in Vancouver region, Canada, a set of ground motions are selected to be compatible with the seismicity of that region. The selected ground motion records are scaled to match the hazard spectrum of Vancouver. Further details on the ground motion selection and scaling is given in Appendix II. Based on the frequency of a structure and 5% critical damping, the parameters have been computed. These damping parameters are used in both the detailed FE model and in the EQ.BF model. Also, in the EQ.BF model, the time integration steps has been assumed to be smaller than time step for ground motion for a better accuracy.

6.3.1 Validation using frequency analysis

Frequency analysis for the detailed FE and the EQ.BF models was carried out in Abaqus and Opensees software systems, respectively. The model developed in Abaqus had additional

leaning column carrying the floor masses and gravity loads, which are not directly applied to the SPSW frame under consideration. Since, the EQ.BF model is a simplified version of the detailed model, the use of the leaning columns was purposefully avoided. All the mass and gravity loads are applied directly on the column nodes itself. A summary of the masses applied to the three structures are given in Table 6.9, Table 6.10 and Table 6.11.

Table 6.9: Summary of designed masses applied on 4-storey SPSW structure

Storey	H (m)	W	F (KN)	M (KNm)	Mass/column (ton)	Mass/leaning column (ton)
1	3.8	8579.6	152.1	11328.7	43.4	392.4
2	7.6	8579.6	304.3	10750.6	43.5	393.3
3	11.4	8579.6	456.4	8438.2	43.7	395.4
4	15.2	3000.9	212.8	3235.2	13.9	125.2
Total		**28739.8**	**1125.6**	**33752.7**	**144.5**	**1306.4**

Table 6.10: Summary of designed masses applied on 6-storey SPSW structure

Storey	H (m)	W	F (KN)	M(KNm)	Mass/column (ton)	Mass/leaning column
1	3.8	8579.6	105.1	26999.3	43.3	391.5
2	7.6	8579.6	210.2	26599.8	43.3	391.9
3	11.4	8579.6	315.4	25002.0	43.4	392.4
4	15.2	8579.6	420.5	21407.0	43.5	393.3
5	19	8579.6	525.6	15015.9	43.7	395.4
6	22.8	3000.9	220.6	5029.7	13.9	125.2
Total		**45899.1**	**1797.4**	**120053.7**	**231.1**	**2089.7**

Table 6.11: Summary of designed masses applied on 10-storey SPSW structure

Storey	H (m)	W	F (KN)	M(KNm)	Mass/column (ton)	Mass/leaning column
1	3.8	8579.6	46.5	50915.5	21.6	390.7
2	7.6	8579.6	93.1	50756.4	21.6	390.8
3	11.4	8579.6	139.6	50119.9	21.6	391.0
4	15.2	8579.6	186.1	48687.8	21.6	391.2
5	19	8579.6	232.6	46141.8	21.6	391.5
6	22.8	8579.6	279.2	42163.8	21.7	391.9
7	26.6	8579.6	325.7	36435.3	21.7	392.4
8	30.4	8579.6	372.2	28638.3	21.8	393.3
9	34.2	8579.6	418.7	18454.5	21.9	395.4
10	38	3000.9	162.7	5565.6	6.9	125.2
Total		**80217.6**	**2256.5**	**377878.8**	**202.0**	**3653.4**

First two mode shapes for all the three multi-storey structures showed excellent agreement as in indicated in Figure 6.14 to Figure 6.19. It should be mentioned that some initial modes of the detailed SPSW models had to be neglected as they showed local behavior i.e. buckling shapes of the infill plates. The effective mass involved in those modes were very less. Also, in Abaqus if the density is not assigned to the structure for frequency analysis, it generates warnings. So to avoid any such confusion, a very small density was assigned before the analysis for all the SPSW systems. Table 6.12 indicates a comparative estimate of the error observed in the frequency analysis with EQ.BF model. The first frequency computed according to NBCC 2010, is observed to be very conservation. Also, the maximum percentage error in the first two significant modal frequencies is approximately 5.7%. In the next stage, the validation of the EQ.BF models is extended to time history analysis with scaled real time ground motion records.

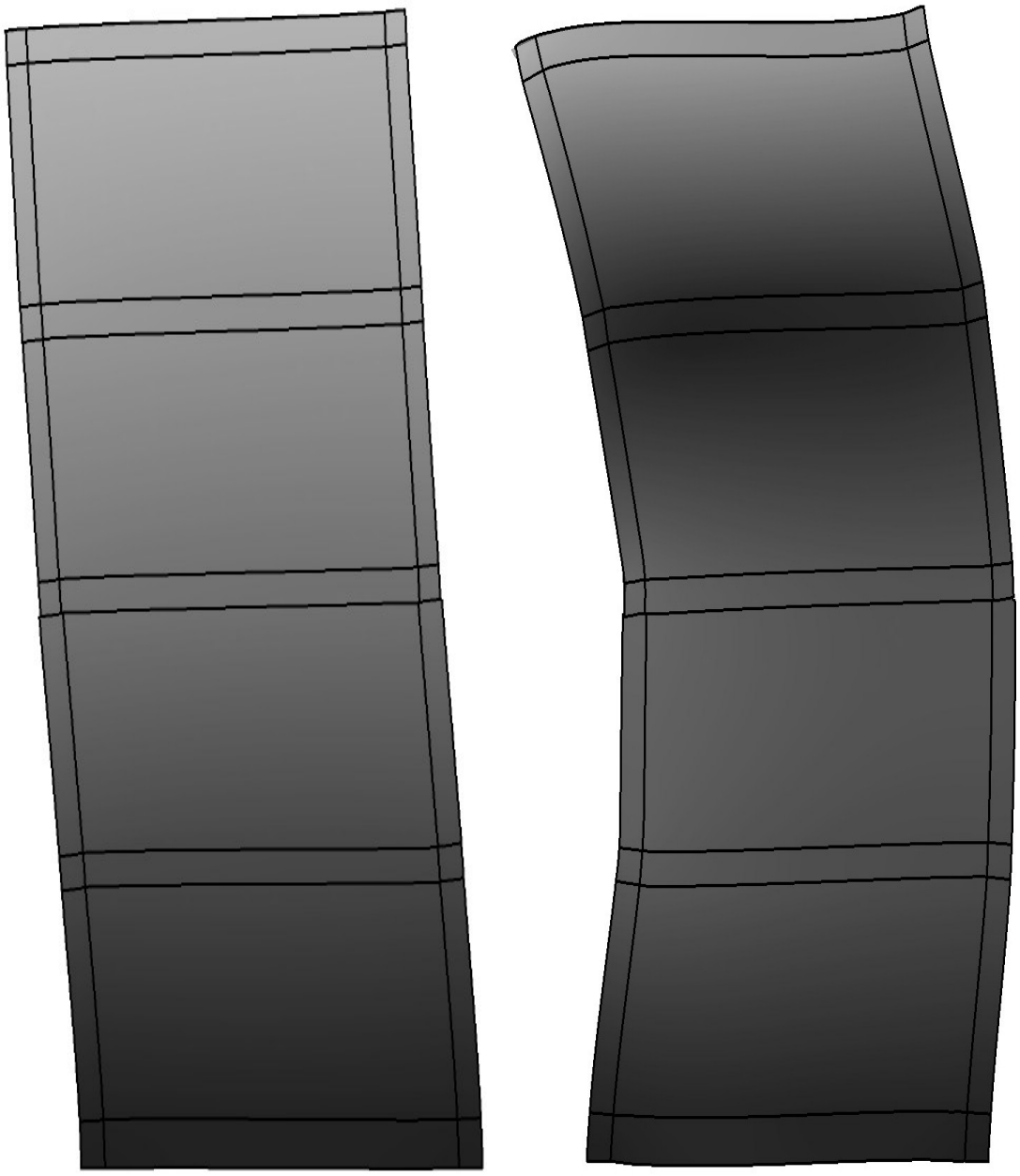

(a) 1st significant mode for 4-storey (b) 2nd significant mode for 4-storey

Figure 6.14: First two significant mode shapes of 4-storey structure from Abaqus

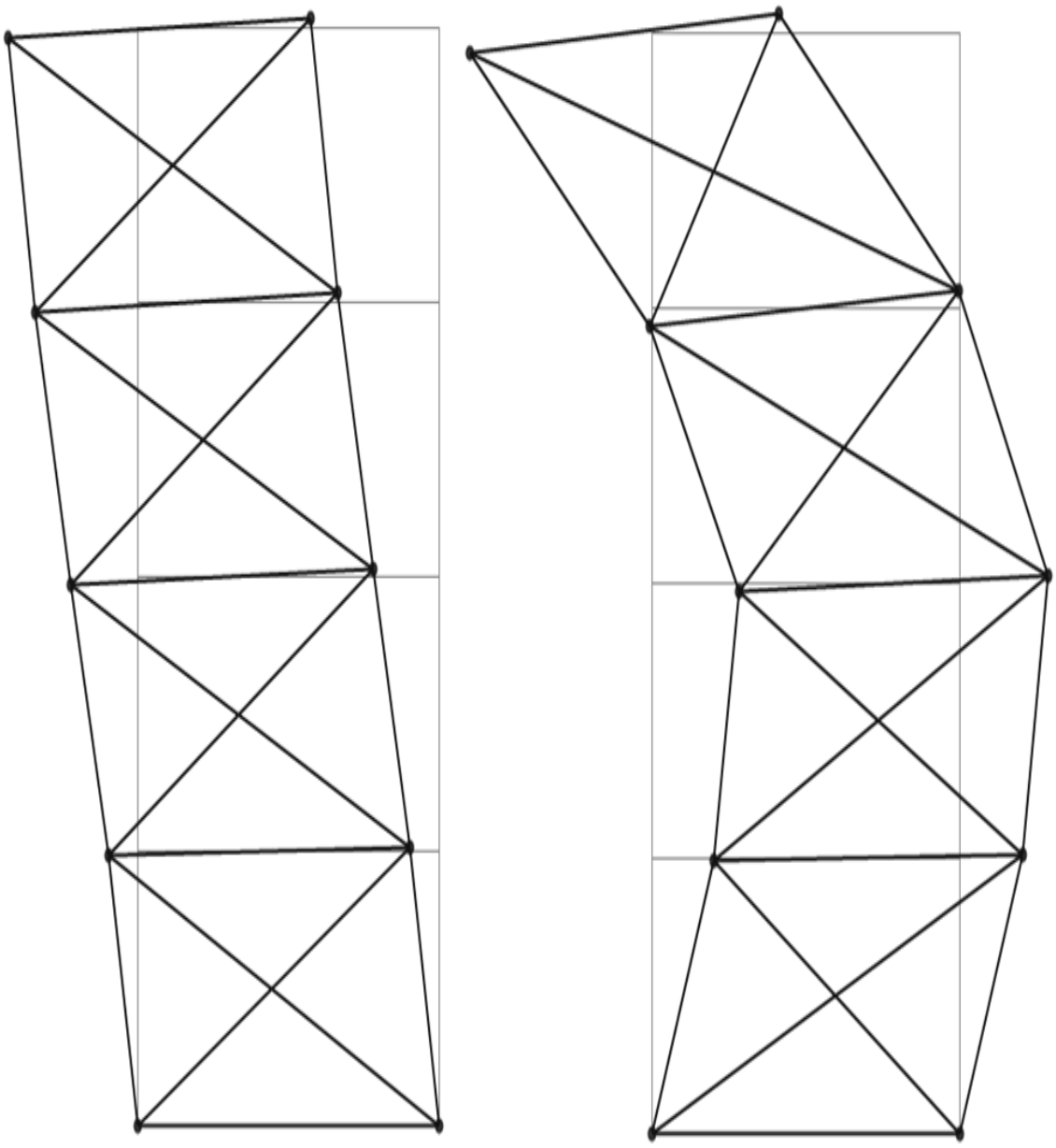

(a) 1st significant mode for 4-storey (b) 2nd significant mode for 4-storey

Figure 6.15: First two significant mode shapes of 4-storey structure from Opensees.

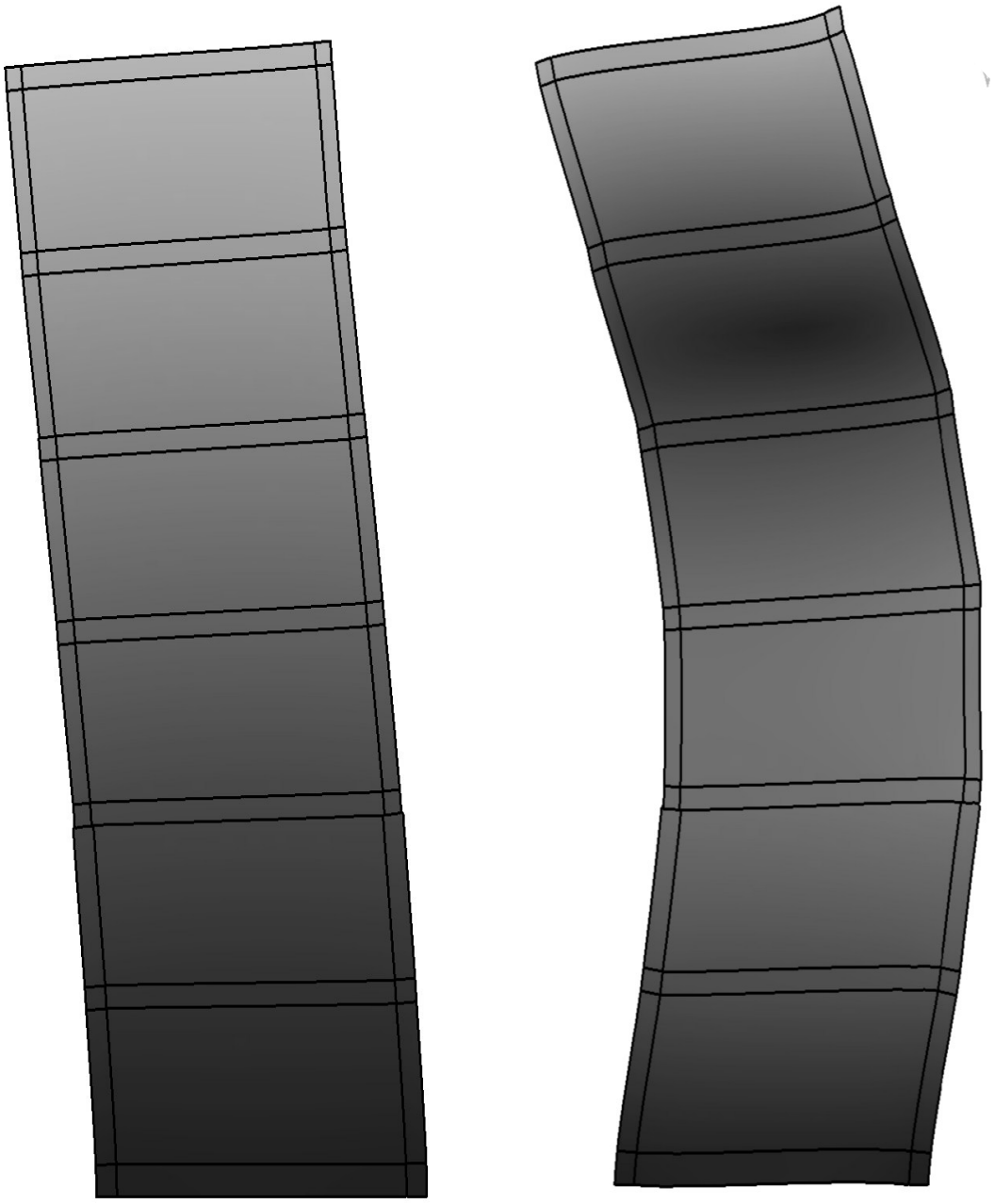

(a) 1st significant mode for 6-storey (b) 2nd significant mode for 6-storey

Figure 6.16: First two significant mode shapes of 6-storey structure from Abaqus

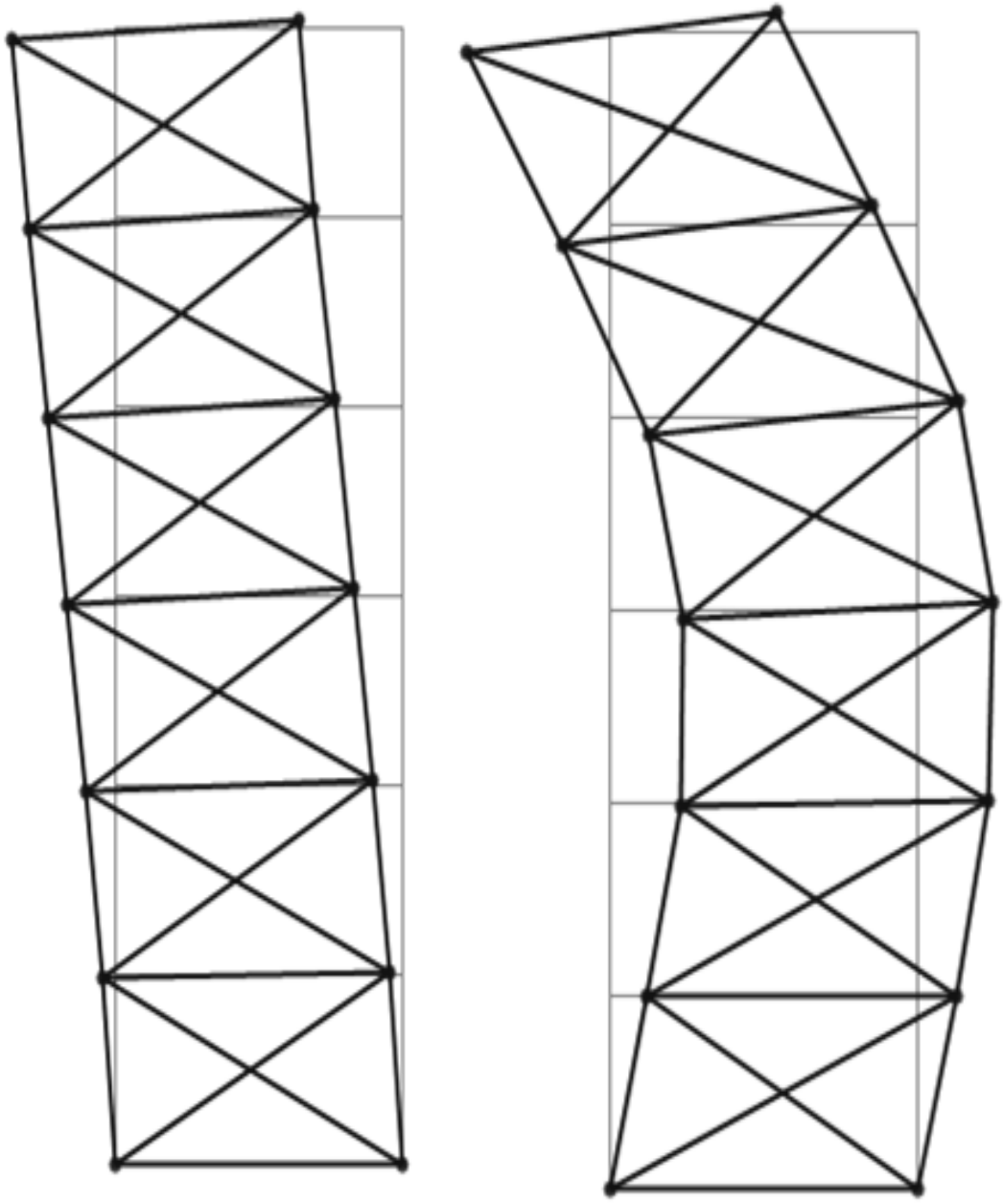

(a) 1st significant mode for 6-storey (b) 2nd significant mode for 6-storey

Figure 6.17: First two significant mode shapes of 6-storey structure from Opensees.

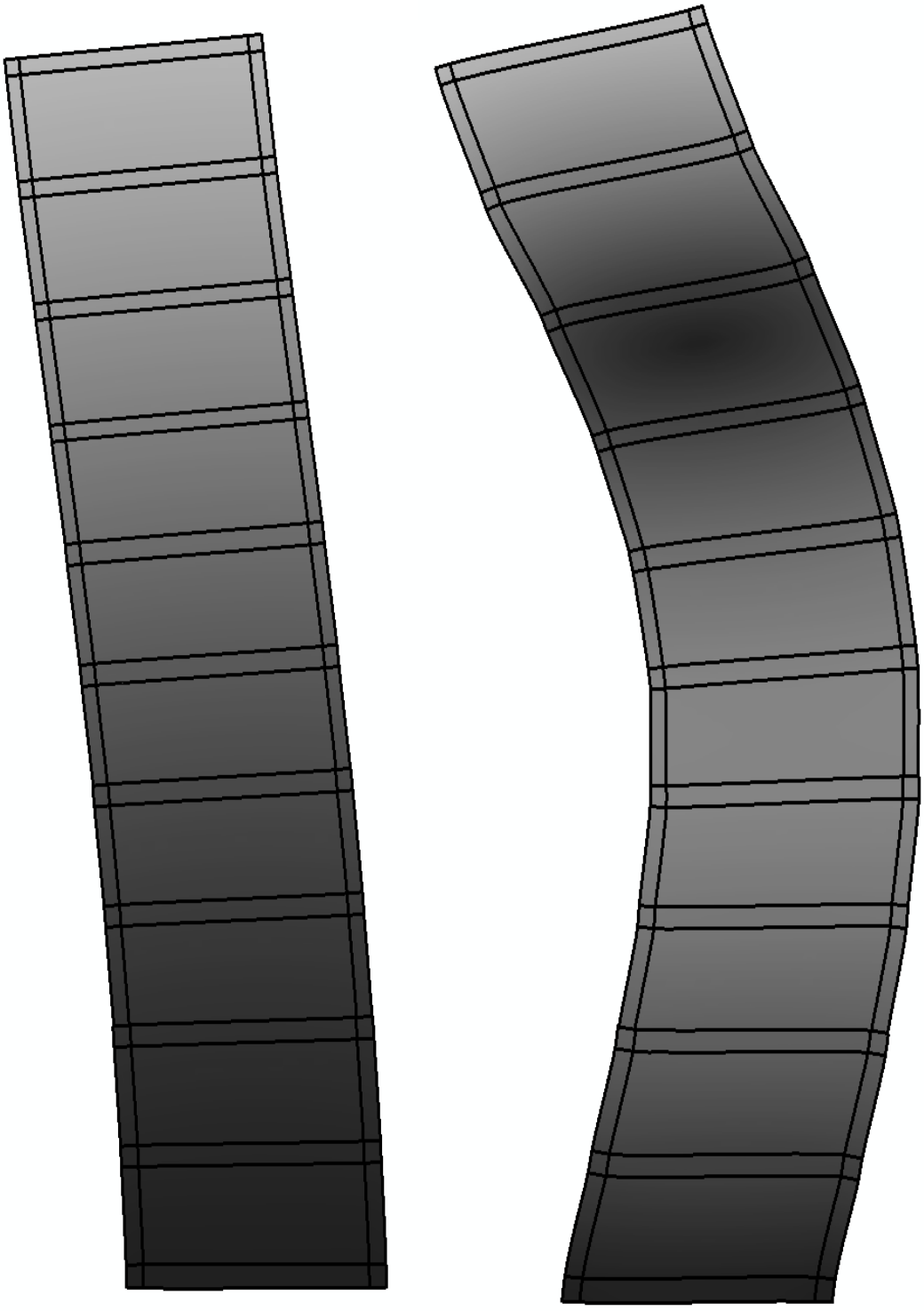

(a) 1st significant mode for 10-storey (b) 2nd significant mode for 10-storey

Figure 6.18: First two significant mode shapes of 10-storey from Abaqus

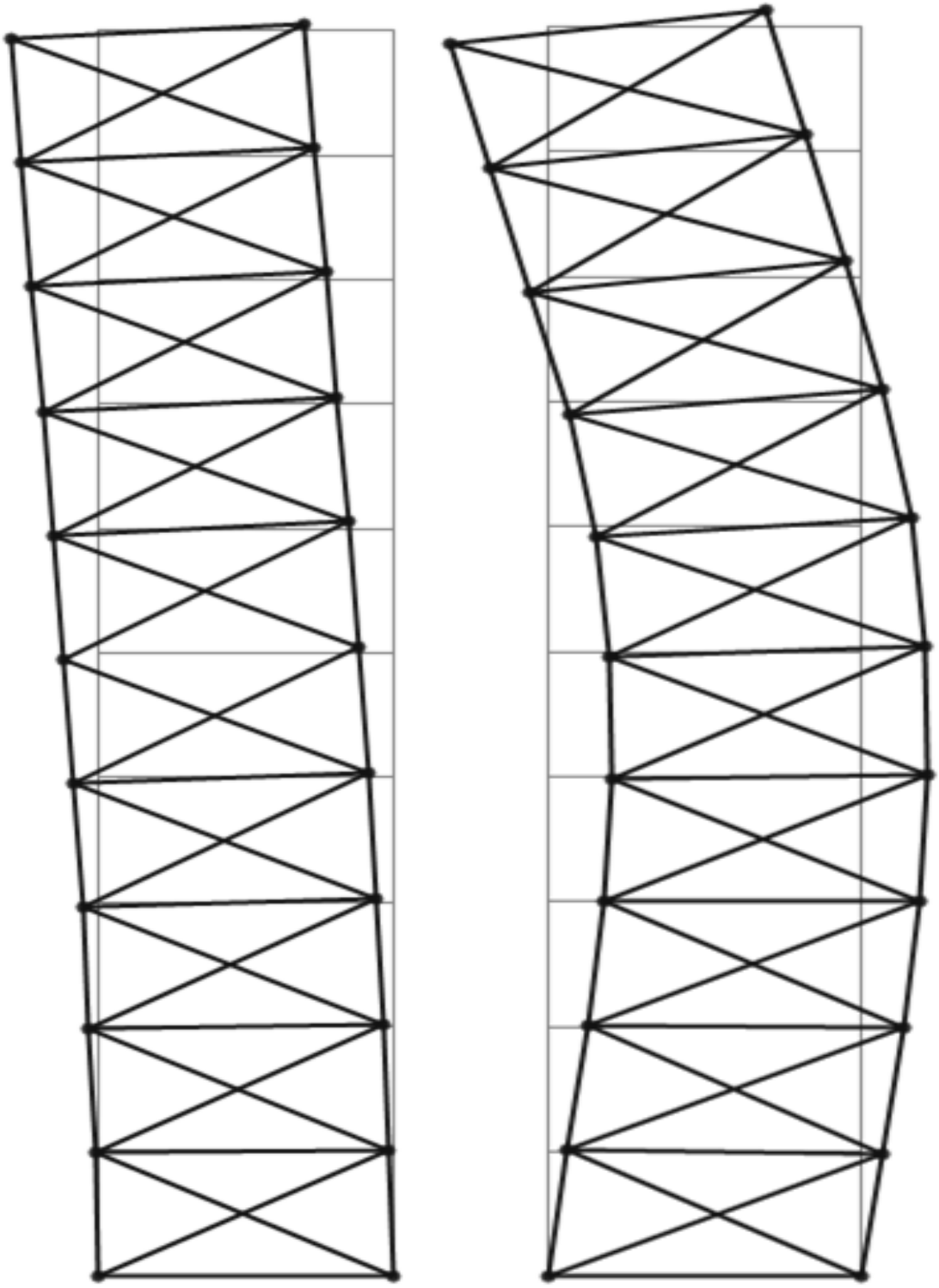

(a) 1st significant mode for 10-storey (b) 2nd significant mode for 10-storey

Figure 6.19: First two significant mode shapes of 10-storey structure from Opensees

Table 6.12: Comparison of frequency analysis for multi-storey specimen

SPSW Structure	Design Frequency	Mode	Frequency (Hz)		Percentage error
			Abaqus	Opensees	
10-storey	1.31Hz	1st	0.7	0.69	1.4
		2nd	2.3	2.43	5.7
6-storey	1.92Hz	1st	1.33	1.37	3.0
		2nd	3.634	3.83	5.4
4-storey	2.6Hz	1st	2.082	2.05	1.5
		2nd	5.164	5.25	1.7

6.3.2 Validation of the EQ.BF models for time history analysis

For the detailed FE model in Abaqus, the dynamic implicit analysis is performed with scaled ground motions. In the modeling cases (i.e., the Abaqus FE model and the EQ.BF model in Opensees), the gravity load and the floor masses have been applied the same way as in the frequency analysis. Only the 4-storey and 6-storey SPSW structures have been used for this validation as the detailed FE models take very long time to complete the analysis. A set of eight suitable ground motion records have been selected and scaled based on the design spectrum of Vancouver. The details on the selection and scaling of the earthquake records are given in the previous chapters. The main purpose of this study was to check whether the pattern of time history response and peak displacement response obtained using the detailed FE model and the Opensees model are reasonably close. Two sets of the selected time history analysis defining the full range within which the variation of the base reaction and the top displacement for time

history analysis of 4-storey and 6-storey structures is given in Figure 6.20 to Figure 6.23. It has been observed from the time history response that the EQ.BF model of a SPSW structure can produce the results very close to those obtained using the corresponding detailed FE model. However, for some ground motion records, the peak values of the top displacement and the base reaction are observed to be slightly more (almost 5%) in EQ.BF model as compared to the detailed FE model. The range of error in all ground motions are however acceptable. Inter-storey drifts are also measured for all eight ground motions which are found to match with reasonable accuracy. Sample inter-storey displacements for the 4-storey and 6-storey SPSW structures are given in Appendix II.

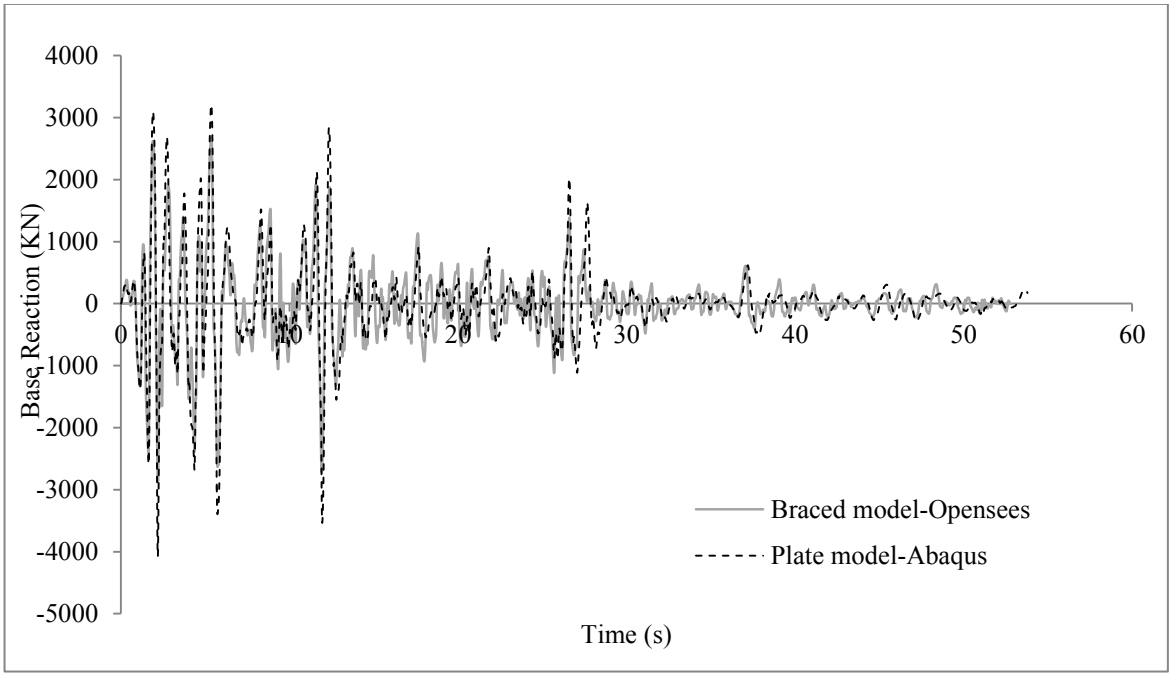

(a) Base Reaction

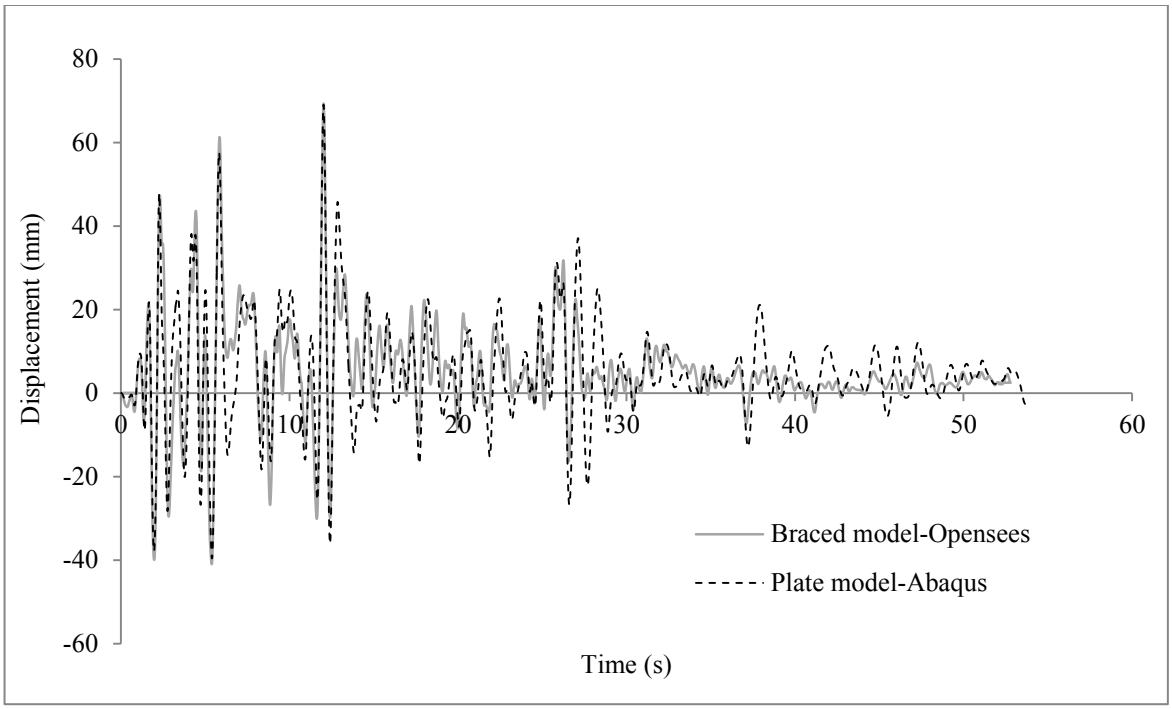

(b) Top Displacement

Figure 6.20: Response of 4-storey structure from Abaqus and Opensees for Earthquake Record#1

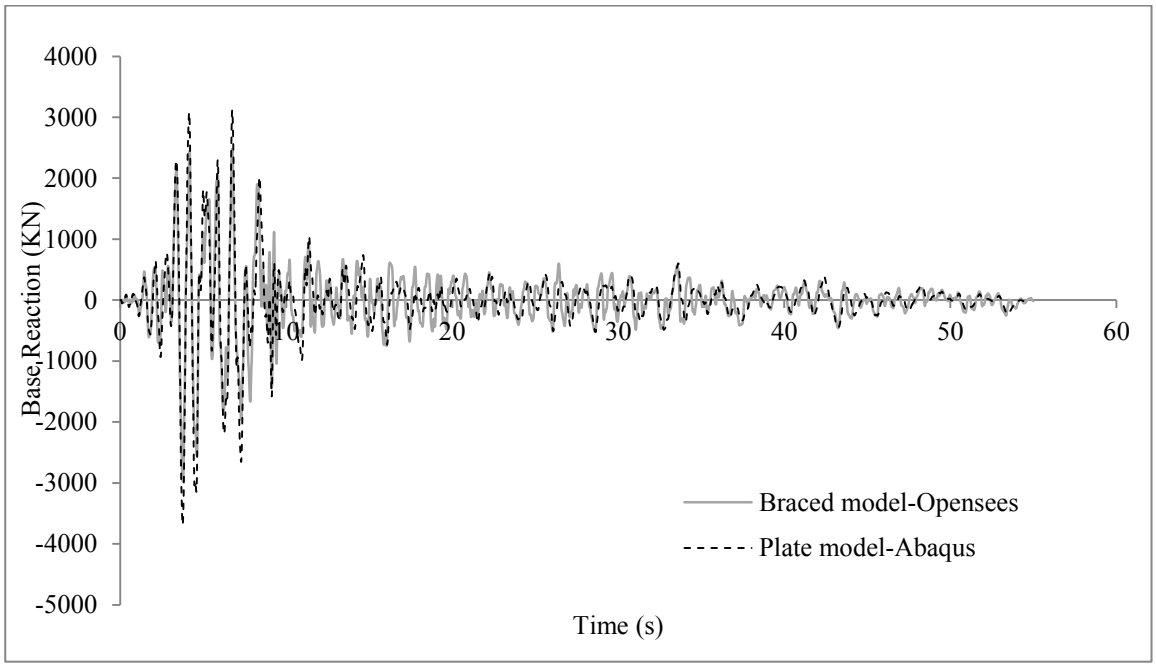

(a) Base Reaction

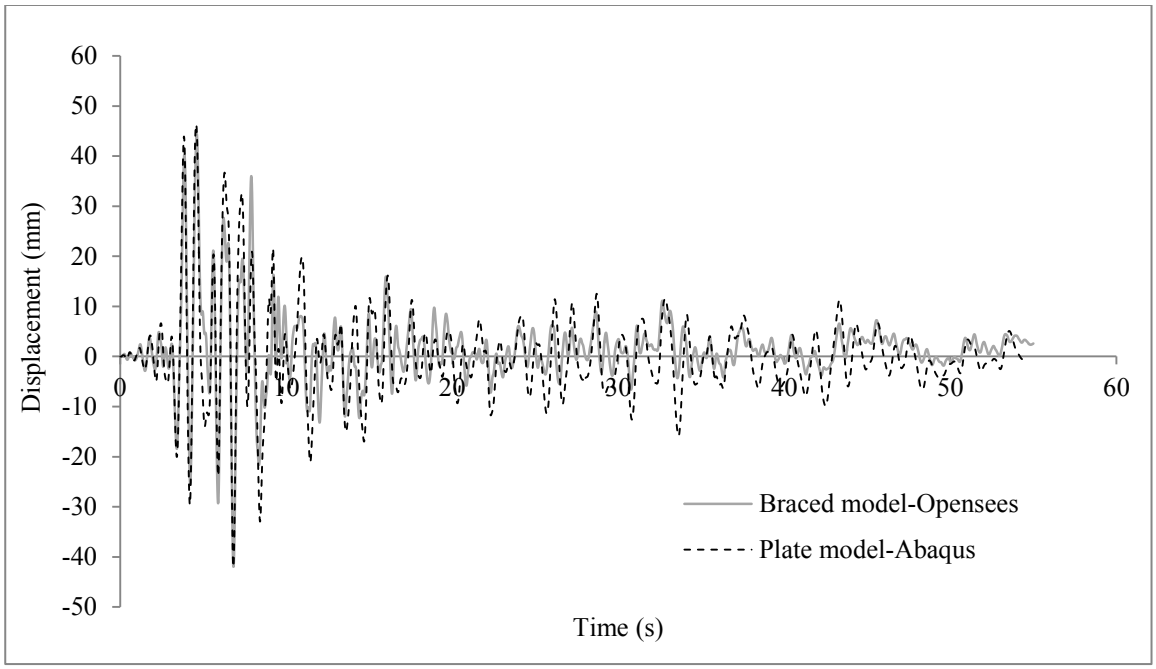

(b) Top Displacement

Figure 6.21: Response of 4-storey structure from Abaqus and Opensees for Earthquake Record#2

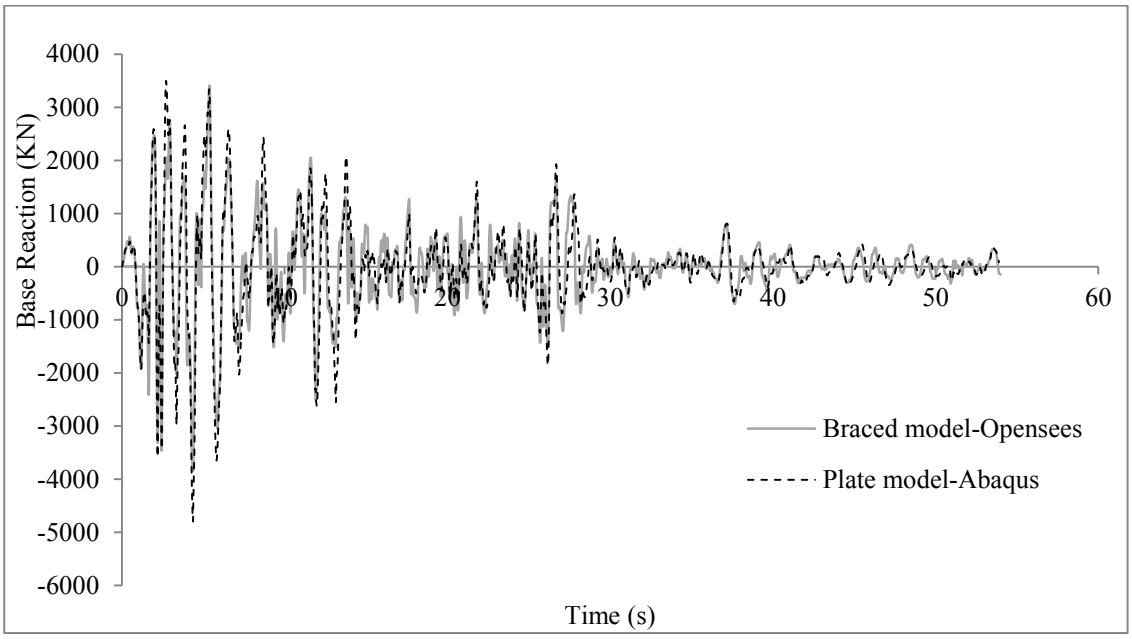

(a) Base Reaction

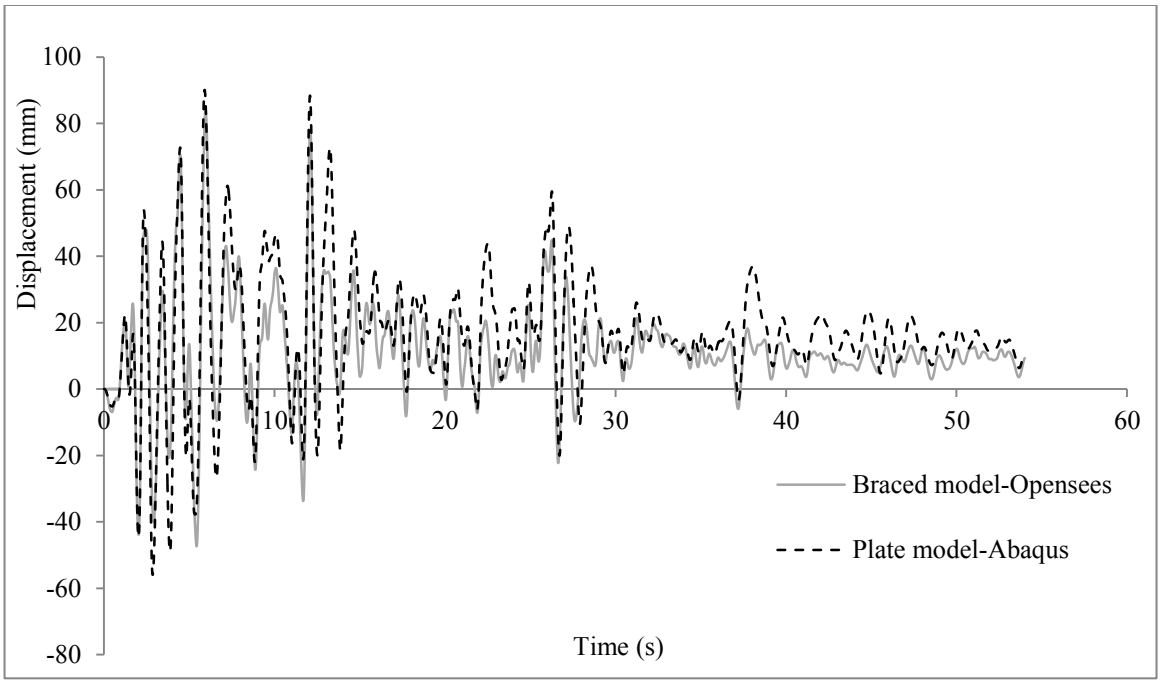

(b) Top Displacement

Figure 6.22: Response of 6-storey structure from Abaqus and Opensees for Earthquake Record#1

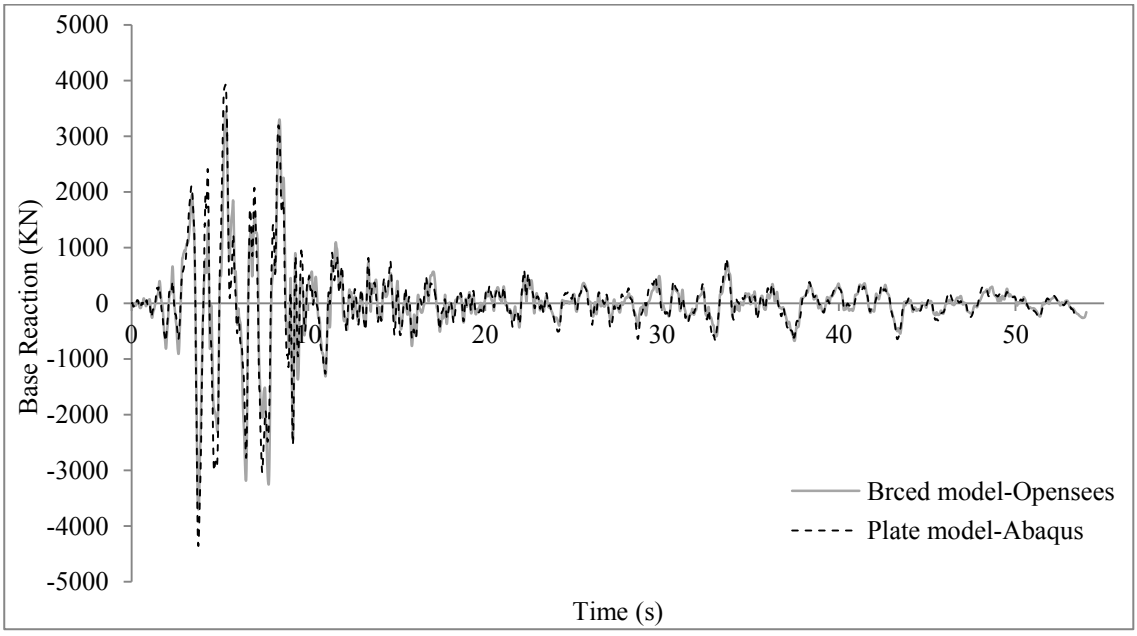

(a) Base Reaction

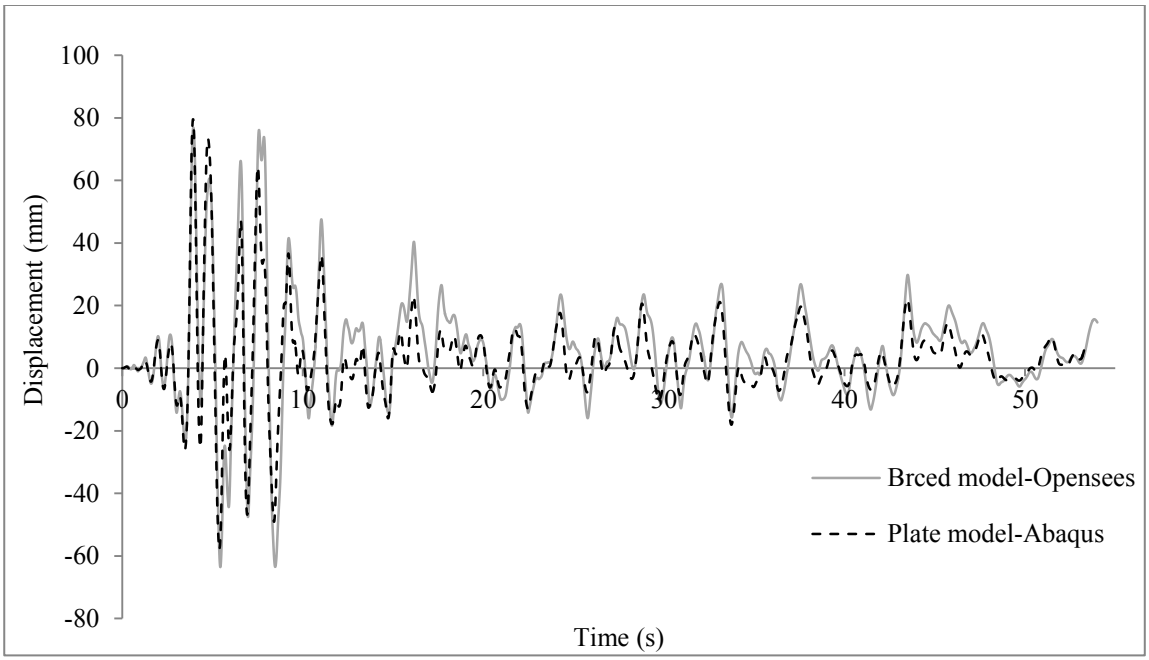

(b) Top Displacement

Figure 6.23: Response of 6-storey structure from Abaqus and Opensees for Earthquake Record#2

6.4 **Summary**

In this chapter, the static and dynamic analysis results of the EQ.BF models on a set of multi-storey SPSW structures have been validated against the corresponding results from the detailed FE models on those structures. The results of the static pushover and cyclic load analysis using the EQ.BF models have been validated with the available experimental and other numerical models. The validation of the EQ.BF models for dynamic analysis involving the modal (frequency) and time history analyses has been carried out for a set of multi-storey SPSW structures. The static, pseudo-static (cyclic) and dynamic analysis results from the EQ.BF models are found to be reliable and acceptable. The EQ.BF models are highly efficient in terms of the

effort in constructing a model and the computation time as compared to the corresponding detailed FE model. In the next chapter this model has been used to evaluate the seismic response of a 10-storey SPSW structure subjected to a suite of ground motions. The modeling and computational efficiency of the EQ.BF model as compared to the detailed FE model has been discussed in detail in the following chapter.

Chapter 7. Seismic Response Evaluation of Light-Gauge SPSW Systems

7.1 Introduction

As stated earlier, the primary objectives of this thesis are to determine whether current design method for ductile SPSW systems is equally applicable to light-gauge SPSW systems and finally, develop a simplified modeling technique to perform static and dynamic analysis of the SPSW systems. Through some already reported single-storey tests it can be concluded that no further modification is required in the existing design technique for it to use for design of cold rolled steel SPSWs. To justify this conclusion, further work has been done. A set of three multi-storey structures of four, six and the ten storey heights designed earlier (as reported in Chapter 4) have been utilized to study the static and dynamic behavior of these SPSW systems with light gauge infill plates. The results from the non-linear numerical analysis have been interpreted against the guidelines specified of NBCC 2010 on the acceptable seismic performance of light-gauge SPSW structures. The time history analysis of a multi-storey SPSW structure with a detailed FE model is not only time consuming, but also prone to modeling errors due to the complexity associated with such models. To avoid such complexity and reduce the computational time, the simplified equivalent braced frame (EQ.BF) model proposed described and validated in the earlier chapters will be used. The pushover and time-history analysis of four-storey and six-storey structures has already been performed using the detailed FE model for the purpose of validation of the EQ.BF model, and the validation study presented in Chapter 6 clearly demonstrates the correctness and efficiency of the EQ.BF models in computing the static and dynamic responses of SPSW systems. Therefore, the ten-storey structure will be analyzed

using the EQ.BF model only. The selection and scaling of a suite of eight ground motion records have been discussed in Chapter 4. The seismic response of these structures will be discussed in this chapter in detail, and the final conclusion on light gauge SPSW will be made based on all these study.

7.2 Static performance of 4-storey and 6-storey with detailed FE model

Nonlinear static pushover tests were already carried out both for four-storey (Figure 6.4) and six-storey (Figure 6.5) structures for the purpose of validation of EQ.BF model with detailed FE model. Base on the pushover analysis using the detained FE models, the nonlinear static response and the yielding sequence of both four-storey and six-storey structures have been studied and discussed here. The analysis showed that the concerned SPSW structures have excellent overall strength and very high ductility. Figure 7.1 presents the pushover curve for the 4-storey and 6-storey light-gauge SPSW with some additional details which has not been discussed in previous chapters. For the 4-storey shear wall, it is observed that yielding occurs in all the infill plates. Plastic hinges also formed in the first, second, and third storey beams. Also, some yielding has been observed in the beam at the base. As observed for the 4-storey SPSW structure, all the infill plates are found to have yielded in case of 6-storey light-gauge SPSW system. Plastic hinges are observed to be formed in the first, second, third, and fourth storey beams. No plastic hinging is found to occur in the two top storey beams. Partial yielding is observed in the beam at the base. For both 4-storey and 6-storey light-gauge SPSWs, no yielding has been observed in any intermediate column with the exception of some yielding on the outer flanges of the column base. The performance of the boundary columns thus satisfies the concepts

of the capacity design approach in each case. Figure 7.1 also shows the beginning of yielding of plate. Soon after the plate started to yield, the inter-storey drift was observed to have exceeded the code restrictions of 2.5% of storey height. It is at this point that the light-gauge SPSW structure can be considered as unstable. Just beyond the point of instability, drastic strength degradation has been observed with the beginning of yielding of columns indicating the failure of the structure.

It should be noted that the capacity of both 4-storey and 6-storey light-gauge SPSWs significantly exceed the design base shears as determined by the equivalent lateral force method of NBCC 2010. This is mainly because the infill plates have been designed to carry the total storey shear in every storey. Pushover analysis shows that a significant portion of the storey shear is taken by the boundary columns. Thus, the above design assumption results in over-strength in the light-gauge SPSW systems. The analysis shows that the columns at the base carry about 24% and 27% of the total storey shear in case of 4-storey and 6 storey light-gauge SPSW systems, respectively.

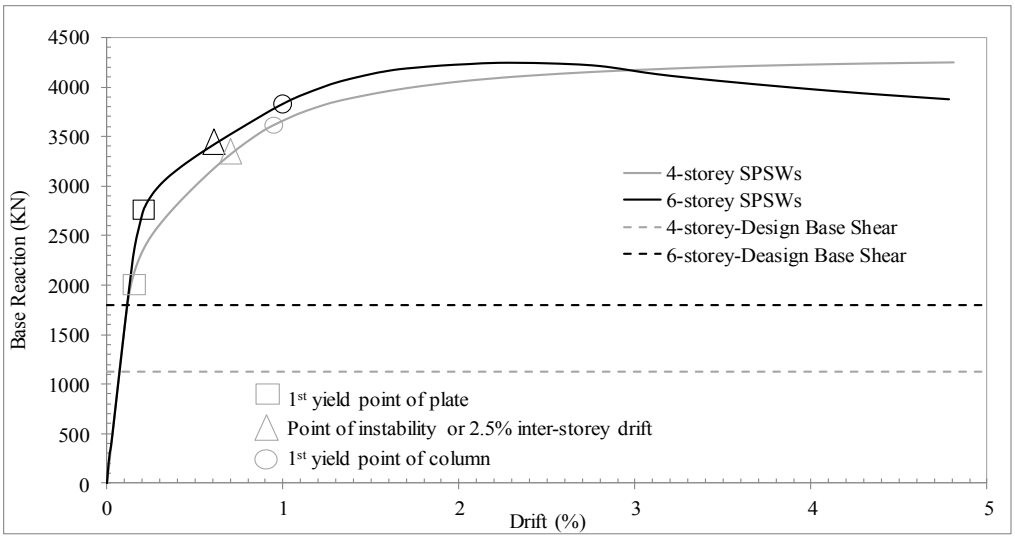

Figure 7.1: Nonlinear pushover curves for 4-storey and 6-storey light-gauge SPSWs

7.3 **Dynamic response of the 4 and 6 storey frames using detailed FE models**

Initially non-linear dynamic analysis was carried out with the detailed FE models of the four-storey and six-storey structures for the following two goals: (i) to understand the dynamic characteristics and seismic response of light gauge SPSW systems, and (ii) to validate the dynamic analysis results from the EQ.BF models of the structures with respect to the detailed FE models as they are deemed representative of the actual systems. While the dynamic analysis results from the detailed models and the validation study for the EQ.BF models have been presented earlier in Chapeters 5 and 6, respectively, the dynamic analysis results and seismic response characteristics of these structures are discussed here in detail. The efficacy of the EQ.BF model was adequately validated earlier and the model was proved to be much simpler and highly efficient. Therefore the seismic response analysis has been performed for the ten-storey SPSW structure using the EQ.BF model only. The results for the four and six storey analysis are already presented in Chapter 4 as they have also been used to validate the EQ.BF model. However, details on the inference from those analyses are discussed below. In addition to the modal analysis and time history analysis, the response spectrum analysis was also carried out for both four-storey and six-storey structures in Abaqus. Inference on sequence of yielding, and angle of formation of tension field are discussed here in details. One of the limitations with the EQ.BF model is that it can be used only to study the overall performance of a structure, not the local behavior of the plate or the frame. When local effect like local buckling or local yielding or angle of formation of tension field in the infill plates are to be studied, a detail FE model is required. The results from the detailed FE models in Abaqus have been used here to study the local effects on the plates and the members.

7.3.1 **Modal Analysis**

Frequency analysis has been performed for the 4-storey and the 6-storey SPSW structures to obtain the mode shapes and the corresponding fundamental frequencies. Starting with buckling of the thinnest infill plate on the top floor, the first few modes indicated buckling of the infill plates. As already discussed, the effective masses involved in these modes are insignificant compared to the full structural mass. So they are safely neglected as insignificant models, particularly when the response of the full SPSW structure is a concern. The first two significant modes in both 4-storey and 6-storey structures are shown in Figure 6.14 and Figure 6.16, respectively. The mode shapes indicate no abnormality or local effect in behavior of the structure in lateral direction. Fundamental frequency in 4-storey and 6-torey structures are observed to be 2.08Hz and 1.33Hz, respectively. Fundamental frequencies computed as per CSA-S16-09 design provisions are 2.6Hz and 1.92Hz for the 4-storey and 6-storey structures, respectively. Thus, the fundamental frequencies computed from the modal analysis are observed to close to that indicated by CSA-S-16 recommendations.

7.3.2 **Time History Analysis**

The time history analysis has been carried out to evaluate the dynamic response of the multi-storey light gauge SPSWs subjected to selected seismic ground motion. All eight ground motion records were used as base excitation to the SPSW structures. The Canadian steel code [CAN/CSA-S16-09] allows formation of plastic hinges on beams near beam-column joints. For

the 4-storey structure, other than earthquake record #4 (Table 7.1), no plastic hinging on beams is observed (Figure 7.2(a)). For the 6-storey frame earthquake record #4 and record #8 produce plastic hinges in beams. The regions of formation of plastic hinges are web and flanges close to the beam column joints of the first, second and third storey beams (Figure 7.2(b) & (c)). Sample of yielding pattern in plates corresponding to the Imperial Valley earthquake (record #1) is shown in Figure 7.3. The yielding of plate indicated that the first yield point of the pushover curve is exceeded (Figure 7.1) i.e. the structure has reached the non-linear zone. Since the point of instability in the pushover curves (Figure 7.1) was never reached through all eight ground motions, so it can be inferred that though there are some yielding being observed which do not have any structural strength degradation capability. But still it is strength beyond elastic limit is observed for the member parts. Thus, the concerned design is not just safe but economic as well.

Also, formation of hinges is allowed just above the base plate or just above the foundation beam. In case of the 4-storey structure, other than earthquake record #4, no plastic hinges in column is observed. For record #4, hinges are observed to be formed on the web of columns at base beam level (Figure 7.2(a)). In case of the 6-storey structure, with an exception of record #4 and #8, no plastic hinges are observed in the columns. For record #4 and record #8, hinges are observed on the flanges of a column at the base level beam (Figure 7.2(b) & (c)). Additionally, there is some partial local yielding observed on the webs of the higher storey columns, which do not have any effect on the overall behavior of light-gauge SPSWs. Thus, the selected light-gauge SPSWs showed excellent performance under the design level of seismic hazard. Also, with none of these scaled ground motions produce the level of displacement corresponding to the point of instability as indicated on the pushover curve Figure 7.1.

(a) 4-storey SPSW system for eq. Record no.# 4

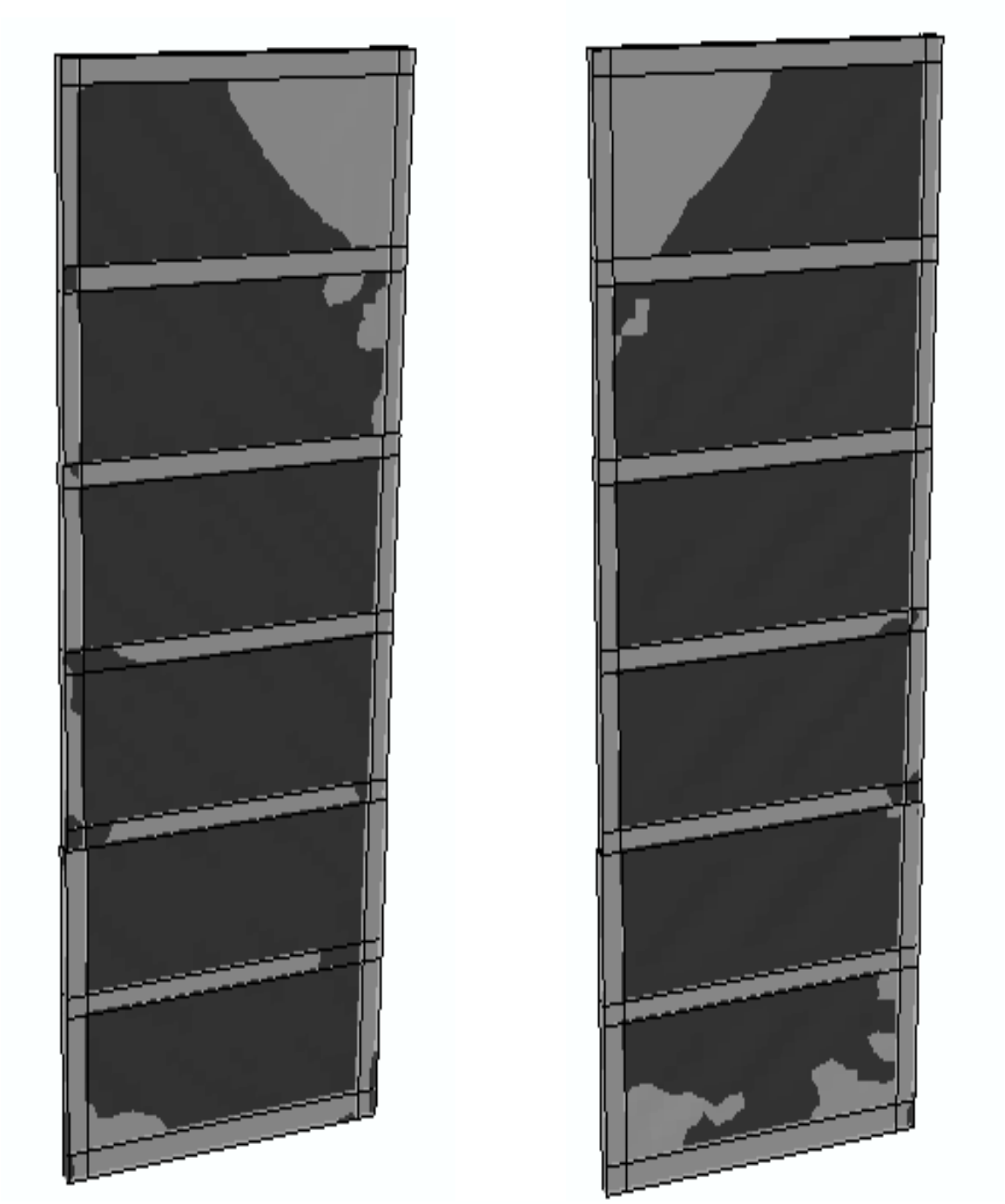

(b) 6-storey for eq. record no. 4 (c) 6-storey for eq. record no. 8

Figure 7.2: Partial yielding of beams columns and plates for earthquake Record no.#4 and Record no.#8.

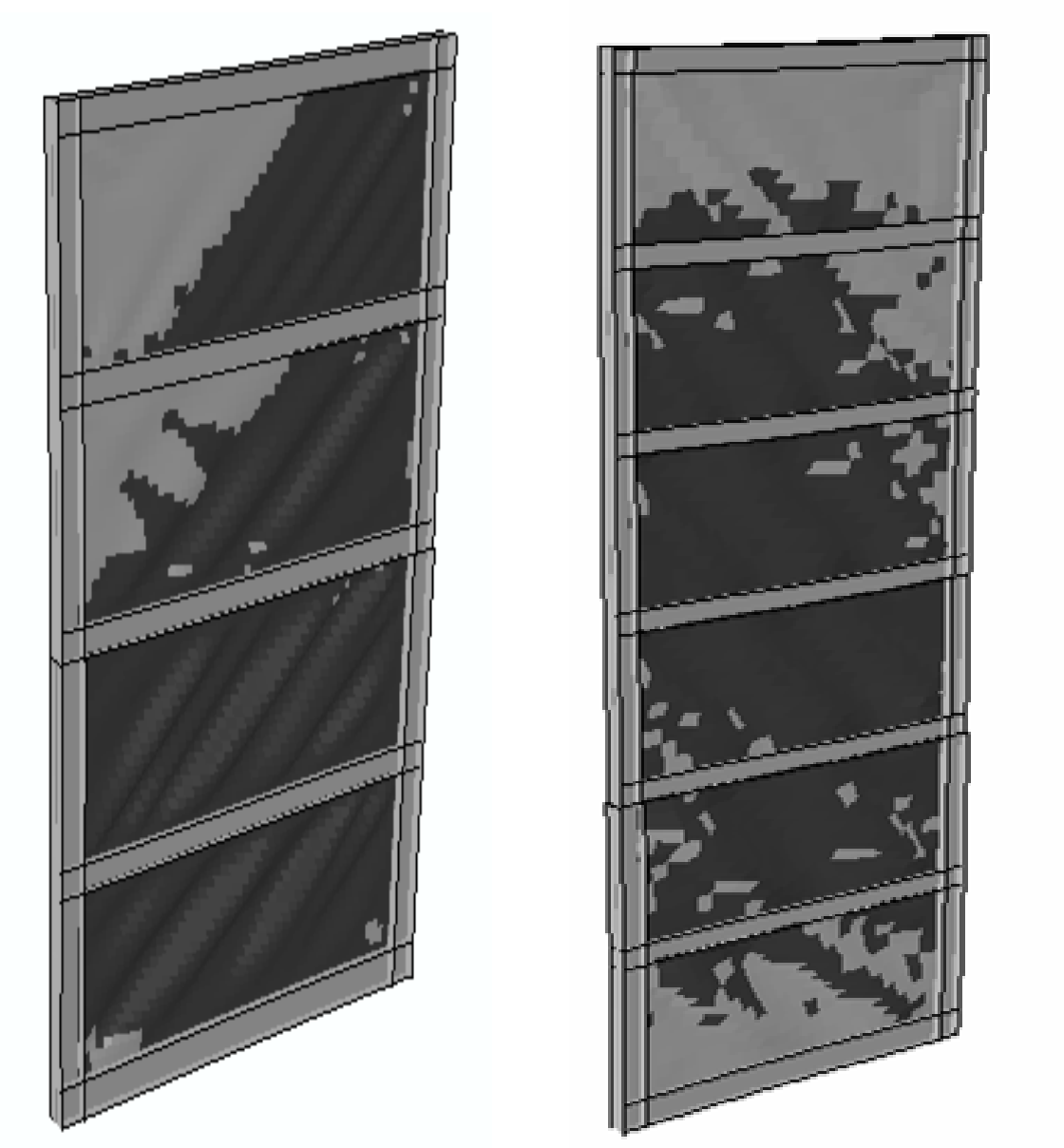

(a) 4-storey (b) 6-storey

Figure 7.3: Sample figure for yielding of plates for Imperial Valley earthquake (record no. 1) before any beam column yielding starts.

While designing the multi-storey structures the angle of tension field (α) has been computed at each floor level. Figure 7.4 shows a sample output indicating that the development of tension field is within 40^o to 50^o, which matches the range calculated while designing SPSWs.

This also indicated that though light gauge steel plates are being used, the structural behavior is approximately the same as that of SPSWs with hot rolled infill plates.

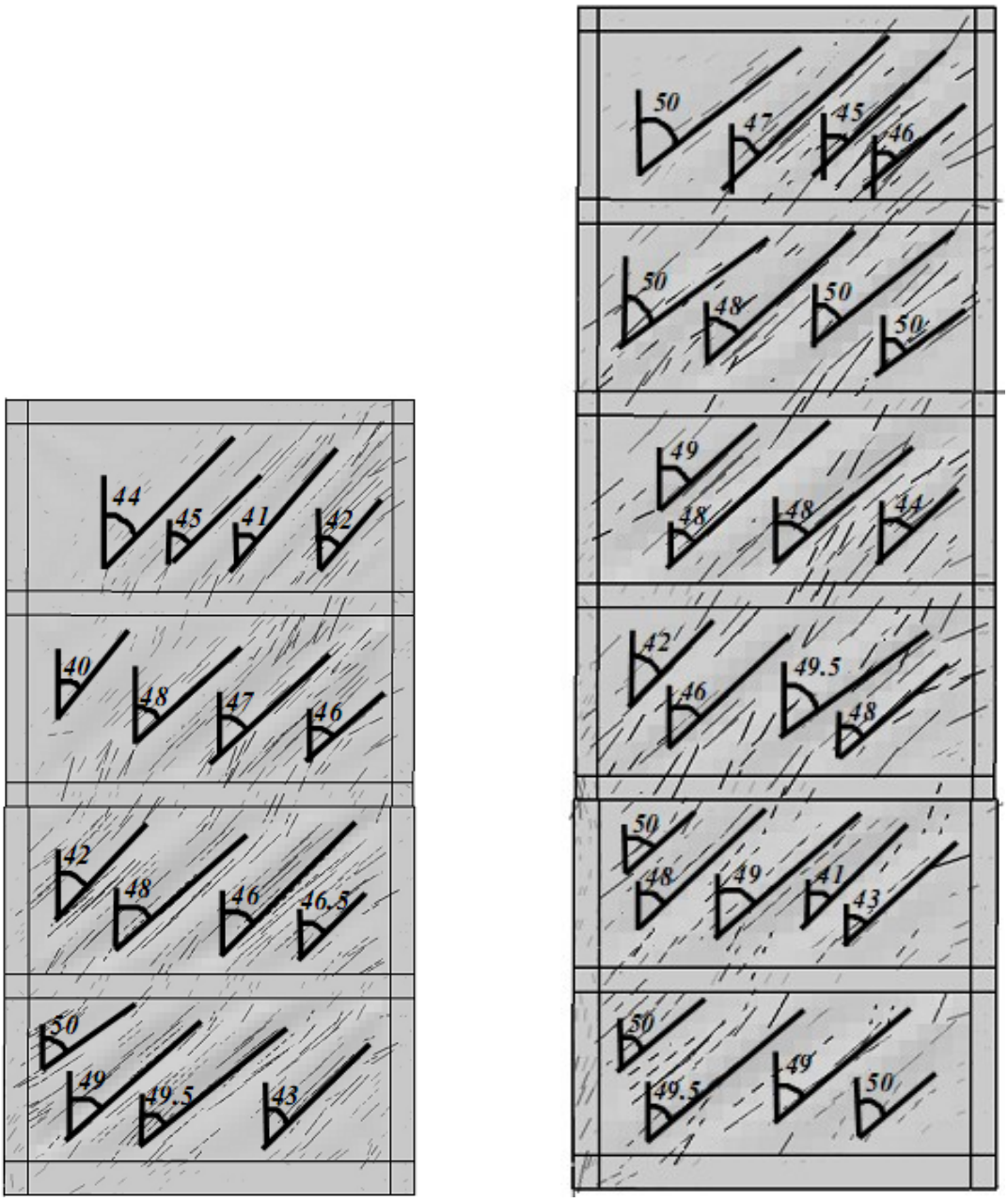

(a) 4-storey SPSW (b) 6-storey SPSW

Figure 7.4: Developed tension field angle with vertical on infill plates

The inter-storey drift limit specified by NBCC 2010 is 2.5% of h_s (where h_s is the storey height), which is 95 mm for the four storey and six storey building considered here. The maximum value of the inter-storey drift observed in 4-storey and 6-storey SPSW structures comparing all eight ground motions are found to be 0.75% (28.4 mm) (Table 7.1) and 0.62% (23.6 mm) (Table 7.2), respectively (Figure 7.5). Comparing these drifts with the pushover curves, it can be said that the structures are safe from any kind of instability. Figure 7.6 shows the relative displacements at different storey levels for the 4-storey and 6-storey light-gauge SPSWs. For all the eight ground motion records, it is observed that the inter-storey drift is the highest at the second storey level in case of 4-storey structure, and it is the highest at the third storey level in case of the 6-storey frame. This indicates a comparatively higher drift demand towards the mid-height of each shear wall. However, this is not a major concern in the design of the light-gauge shear wall as the drift is limited to the NBCC 2010 restrictions. The maximum total drift of the top storey relative to the ground is 72.2 mm and 103.6 mm in case of 4-storey and 6-storey structures, respectively (Figure 7.5). The top storey displacement (drift) in either shear wall is less than 1% of the total height of the building, which satisfies the serviceability requirement. Thus, the maximum drift demand remains well within permissible limits. The reported maximum base reaction of the 4-storey and the 6-storey structures are 4071.5 KN and 4796.9 KN, respectively (Table 7.3). Also, there is no observable soft-storey phenomenon in the shear walls leading to de stabilization of the structure.

Table 7.1: Inter storey displacement for 4-storey SPSW specimen

Ground Motion	Inter-storey displacements (mm) at			
	Level-4	Level-3	Level-2	Level-1
Rec. no#1	8.7	15.2	26.7	19.5
Rec. no#2	5.2	8.0	17.6	16.5
Rec. no#3	6.1	9.6	19.2	16.5
Rec. no#4	6.9	12.9	28.4	24.1
Rec. no#5	6.6	10.3	22.9	19.7
Rec. no#6	6.1	9.9	20.4	17.1
Rec. no#7	5.0	7.4	17.8	16.5
Rec. no#8	5.2	8.5	18.2	15.9
Average	**6.2**	**10.2**	**21.4**	**18.2**

Table 7.2: Inter storey displacement for 6-storey SPSW specimen

Ground Motion	Inter-storey displacements (mm) at					
	Level-6	Level-5	Level-4	Level-3	Level-2	Level-1
Rec. no#1	5.1	6.5	6.3	6.3	6.0	5.5
Rec. no#2	6.0	7.8	8.0	10.0	10.9	9.1
Rec. no#3	7.6	10.6	10.3	9.8	8.0	6.9
Rec. no#4	9.6	15.0	16.8	18.2	14.6	10.4
Rec. no#5	11.0	17.0	19.7	23.6	20.8	14.2
Rec. no#6	6.6	9.0	10.7	15.0	16.2	12.6
Rec. no#7	9.0	13.7	15.2	17.2	14.9	11.3
Rec. no#8	10.2	15.8	18.0	20.6	17.7	13.0
Average	8.1	11.9	13.1	15.1	13.6	10.4

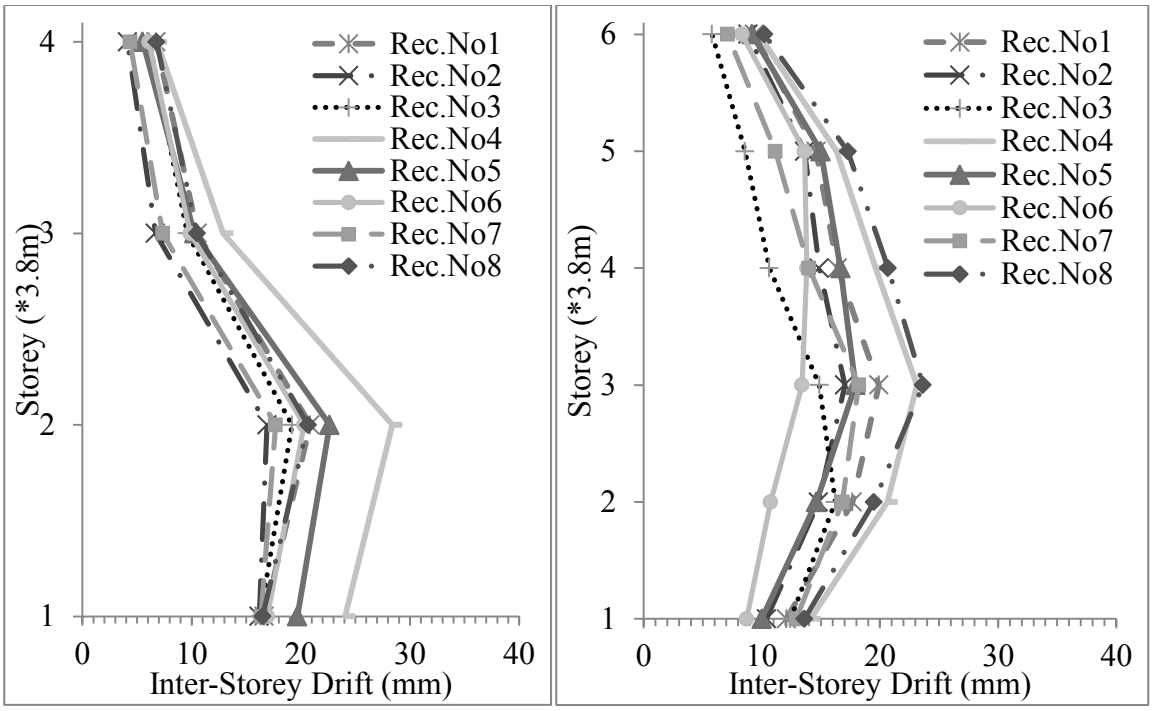

Figure 7.5: Inter-Storey Drift from time history analysis on (a) 4-storey (b) 6-storey

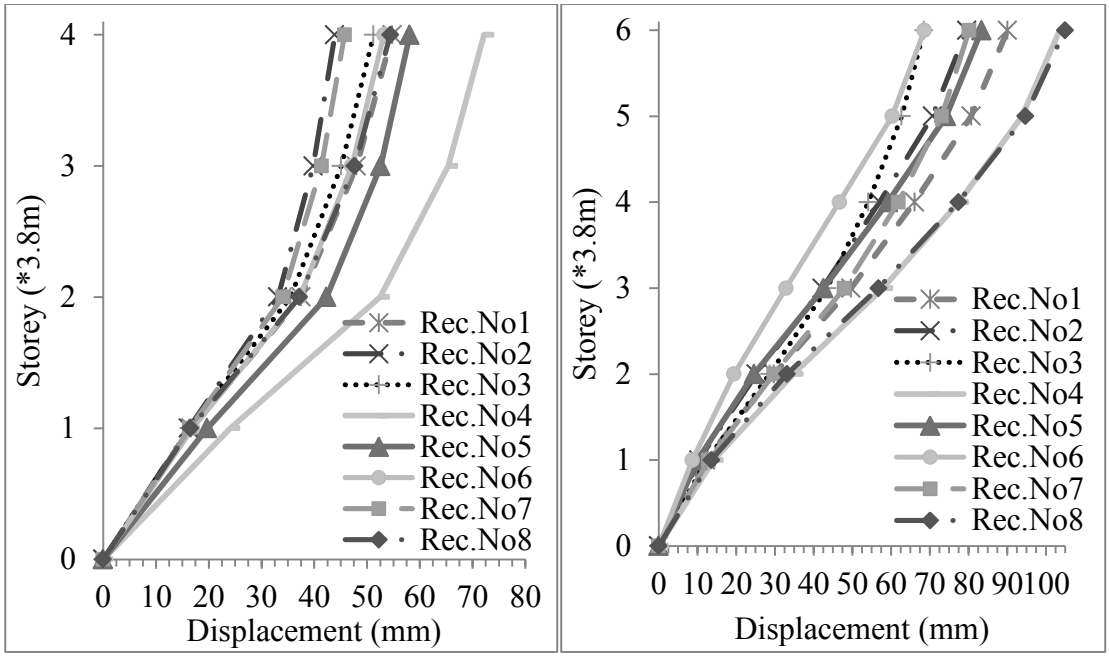

Figure 7.6: Relative displacement for time history analysis on (a) 4-storey (b) 6-storey

Table 7.3: Base shears and top displacements from time history analysis

	4-storey		6-storey	
Record no.	Peak Base Reaction (KN)	Top Disp (mm)	Peak Base Reaction (KN)	Top Disp (mm)
1	3648.8	54.8	4796.9	90.1
2	3688.1	43.9	4359.1	79.6
3	3604.5	51.2	4288.2	68.5
4	4071.5	72.2	4313.0	103.6
5	3788.4	58.1	3945.5	83.4
6	3584.9	53.2	3945.5	68.6
7	3568.0	45.8	4158.6	80.2
8	3649.9	54.4	4518.4	104.9
Average	**3700.5**	**54.2**	**4290.6**	**84.9**

7.3.3 **Response Spectrum analysis**

For the linear response spectrum analysis, the spectrum of each of the selected ground motion record and design hazard spectrum have been used. The mode combination technique used is Square Root Sum of Squares (SRSS). For the 4-storey and 6-storey specimens the highest inter-storey drift observed in the response spectrum analysis is nearly 4.06 mm at level two for ground motion record no #5and 12.05 mm at level 5 for ground motion record no #2. The highest response base reaction achieved for 4-storey and 6-storey is 2437 KN and 5698 KN, respectively (Table 7.4). The relative displacement with respect to ground movement of the structures is shown in Figure 7.7. These displacement responses also satisfy the safety and serviceability requirements.

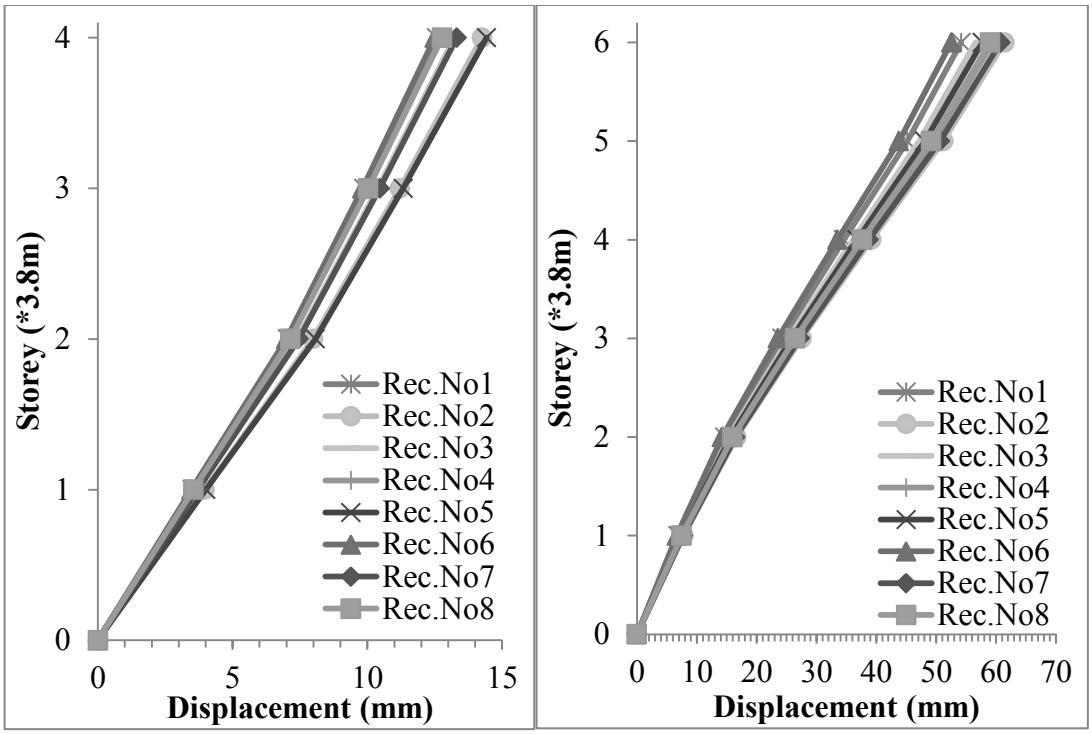

(a) 4-storey (b) 6-storey

Figure 7.7: Relative displacement from response spectrum analysis on SPSW structures

Table 7.4: Base shears and top displacements through response spectrum analysis

	4-storey		6-storey	
Record no.	Maximum Base Reaction (KN)	Top Disp (mm)	Maximum Base Reaction (KN)	Top Disp (mm)
1	2124.58	12.57	5023.08	54.19
2	2409.8	14.25	5697.8	61.41
3	2234.9	13.22	5245.97	56.599
4	2149.24	12.71	5509.29	59.47
5	2437.08	14.42	5347.77	57.71
6	2113.51	12.496	4874.12	52.52
7	2252.5	13.32	5631.79	60.77
8	2161.77	12.77	5475.95	58.996
Design Spectrum	2308.86	14.0536	4905.85	52.4079

7.4 Performance assessment of 10-storey SPSW system with EQ.BF model

To assess the performance of the ten-storey structure non-linear static pushover analysis followed by frequency and non-linear time history analysis are carried out. Although a detailed FE model of the ten-storey has been developed, it is expected to take very large amount of time both for the modeling and computation, as explained earlier. For example, the time history analysis of the four storey frame using the detailed FE model takes about a day of solution time in Abaqus for a single ground motion record. On the other hand the corresponding EQ.BF model takes and a few minutes to compute the dynamic response of the structure with sufficient accuracy in drift demand, top displacement and base reaction. For that reason, only the EQ.BF model implemented here in the Opensees software has been considered for the time history analysis of the ten-storey structure. The detailed model is used for only the pushover analysis. The graphical output in Abaqus for detailed FE model can be easily utilized to observe the sequence of significant yielding in members or any other local effect. This observation from EQ.BF model is also possible by introducing a display script to generate the desired graphics. However, based on the nodal displacements and stresses achieved at integration points of each member the same inference is possible to be made. But EQ.BF model being a simplified version of the detailed FE modeling technique; it will lack the capability to show local effects like details on yielding of flange or web of boundary members or tension field orientation. Points of the first and second hinge formation in this regard can be considered as those points where the slope of the pushover curve reduces abruptly. Figure 7.8 shows the pushover curve for ten-storey as obtained from EQ.BF model as well as Abaqus model.

It is observed from Figure 7.8 that the actual capacity of the SPSW structure is significantly higher the design base shears (2256.45KN) as determined using the equivalent lateral force method of NBCC 2010. This is mainly because, in pushover analysis a significant portion of the storey shear is taken by the boundary columns. Whereas, in the design it has been considered that the infill-plate alone should take the storey shear force. This leads to the over-strength problem for SPSW systems. The first significant hinge was observed at around 4100 KN resulting in a reduction in the stiffness of the SPSW system. This is the point where the infill-plate has reached its elastic limit. In case of the corresponding EQ.BF model, it is expected that the tension brace has reached its yield point. Both Abaqus and Opensees indicate almost the same point on the pushover curve where the first plastic hinge is formed. This also confirms that even the sequence of yielding of members in EQ.BF is as reliable as in the detailed FE model. As already discussed in case of the four-storey and six-storey structures, the point of instability can be considered as the point at which the inter-storey drift limit, as specified by NBCC 2010, of 2.5%h (95 mm for 10-storey SPSW with floor height of 3800 mm) is reached. For the detailed FE model in Abaqus, this structural instability is reached at the 7^{th} floor level, when the base-shear force of the SPSW structure is observed to be nearly 6743 KN. The EQ.BF model shows the same pattern and the base shear is estimated as 6571 KN. The EQ.BF model is found to estimate the maximum inter-storey drift to be very close to that by the detailed FE model (with the maximum difference of 3%). The second plastic hinge is found to form in the base of the columns. Beyond this point the SPSW structure stops taking further load and progressively fails. The second plastic yield point is observed at a base shear of 6969 KN in Abaqus and 6687 KN in Opensees (less than 4.3% difference from the EQ.BF model). Any strength beyond this is of no use from practical design point of view. The overall conclusion that can be drawn from the static

test on 10-storey SPSW structure is that the light-gauge infill panel works fine when the full structure is designed with the same provision of the code (i.e. CSA-S16) as recommended for the hot rolled SPSW systems. Since there are no provisions available in the code for cold-rolled SPSW system, the above observation provides as important basis for the design of such systems. Also, another obvious observation is that the final strength of this ten-storey SPSW structure is higher than that of previously discussed four-storey and six-storey SPSW structures.

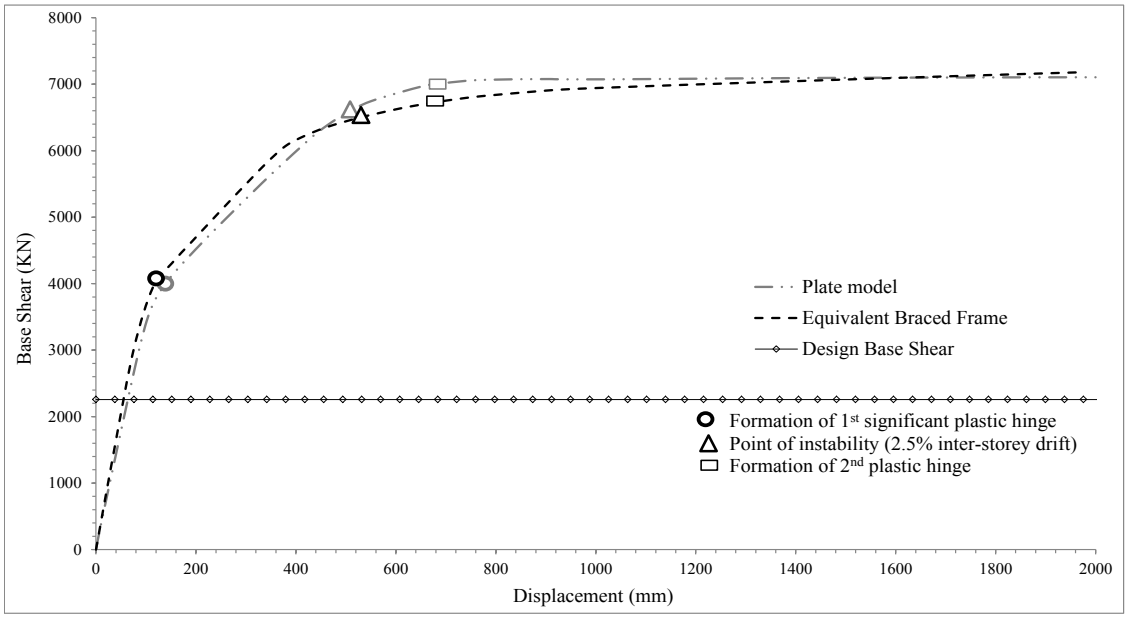

Figure 7.8: Pushover curve from Abaqus and Opensees for 10-storey SPSW system

From the frequency analysis of the ten-storey structure inference on its dynamic behavior can be made. The first two mode shapes indicated by both the detailed FE model analysis and the EQ.BF model analysis (Figure 6.17 and Figure 6.18) match the expected deformation for a multi-storey SPSW structure. No abnormal local deformation due to the presence of light-gauge infill plates has been observed. From the comparative results provided in Table 6.12, it can be

inferred that the computed first frequency (0.7Hz) is also less than that of the design frequency (1.3Hz) obtained according to the conservative approach from NBCC2010.

The seismic response of the ten-storey SPSW is then evaluated using the nonlinear time history analysis, and the same set of earthquake record which was used for the four-storey and six-storey structures have been used here. The time history analysis of the ten-storey structure has been carried out only in Opensees using the established EQ.BF model. Table 7.5 shows the peak inter-storey displacements for the structure. For ground motion record number #4, the peak inter-storey drift is found to be at the 9^{th} floor level. Also, the average peak inter-storey displacements considering all the eight ground motion records is calculated as 0.9% (34.3 mm). These values of the inter-storey drift indicate that the structure is well below the instability point or 2.5% drift as observed through the pushover curves (Figure 7.8). Thus according to NBCC 2010 recommendations, this ten-storey SPSW structure with light-gauge steel infill plate can be considered have an acceptable level of safety and deformation capacity. Table 7.6 shows the top storey displacements and the corresponding base reactions for all the eight selected ground motion records as considered here. For ground motion record no#3, the peak base reaction is observed to be 5314 KN which is higher than the design base shear (2256.45 KN) the ten-storey structure. Also, the peak displacement at the top storey is found to be 218.7 mm (0.58% of total height) which occurs when ground motion record no#8 is applied. Thus, even though the ground motion induces the base shear exceeding the design value, the drift demand and the member forces in the structure are found to be within the acceptable range. The average base reaction and the top displacement from all the eight ground motion records are calculated as 4719 KN and 173.1mm, respectively. Combining these results with the observation from the pushover

analysis, it can be inferred that on an average basis, the infill plates of the SPSW system have yielded. For the EQ.BF modeling technique, the braces which are expected to have yielded (to represent plate yielding). No sudden degradation of stiffness or strength due to local effect or fatigue or any other reason has been observed. Also, in regards to the overall performance, no soft storey phenomenon has been observed. As previously mentioned, one limitation with the EQ.BF model is its inability of capturing local behavior. On the other hand, the biggest advantage with this modeling technique is that it saves huge amount of time and complicated modeling. As mentioned earlier, the detailed FE model can take a few days to complete the time history analysis using all the ground motion records, while the EQ.BF model can be used to produce an equivalent set of results in a very short period of time. Through Figure 7.10 to Figure 7.17, the response time history of the structure has been studied in more details. The inter-storey drift and the storey level displacements represented in Figure 7.9 shows a stable behavior of the ten-storey SPSW structure. Also, from Figure 7.9(b) it can be observed that the inter-storey drift increases more rapidly for the top four stories. This doesn't have any significant structural effect as far as the drift is within the limits prescribed by NBCC 2010. Earthquake record no#4 can be considered as the most sever one for this structure as compared to other ground motions, since both the storey level displacements (Figure 7.9(a)) and inter-storey drift (Figure 7.9(b)) is the highest when the structure is subjected to this ground motion. Further details like the inter-storey drift response has also been computed and a sample of these are provided in Appendix II. Overall, the performance of the ten-storey structure can be considered to be safe from a designer's point of view achieving the "life-safe" performance as expected in the design.

Table 7.5: Maximum intre-storey displacements of 10-storey SPSW structure for 8 ground motions

GMR	Peak Inter-storey displacements (mm) at Level									
no.*	1	2	3	4	5	6	7	8	9	10
1	5.6	8.7	9.1	9.1	10.1	11.7	14.8	20.5	21.0	13.5
2	6.0	11.3	12.4	11.6	11.8	13.3	21.3	26.0	22.4	13.6
3	6.1	11.2	15.3	19.6	23.7	24.8	30.7	28.8	29.4	28.1
4	8.1	14.2	18.0	21.1	25.2	28.0	41.1	46.1	47.8	36.7
5	5.3	8.0	8.9	10.2	12.9	16.8	26.0	35.0	39.1	35.0
6	5.3	8.9	10.2	12.3	16.2	21.8	33.2	43.4	42.5	31.1
7	6.4	10.9	12.3	13.4	15.0	16.6	24.0	33.6	32.3	25.3
8	6.0	11.1	13.5	15.7	18.4	20.6	31.9	38.5	39.7	35.8
Average	**6.1**	**10.5**	**12.5**	**14.1**	**16.7**	**19.2**	**27.9**	**34.0**	**34.3**	**27.4**

*GMR is Ground Motion Record

Table 7.6: Maximum top displacement and corresponding Base Reaction of 10-storey structure

Ground motion Record no.	Top Displacement (mm)	Base Reaction (KN)
1	104.2	4594.5
2	124.2	4953.6
3	194.3	5314.0
4	179.6	3422.7
5	178.8	4835.0
6	215.0	5065.9
7	169.9	4814.5
8	218.7	4754.6
Average	**173.1**	**4719.3**

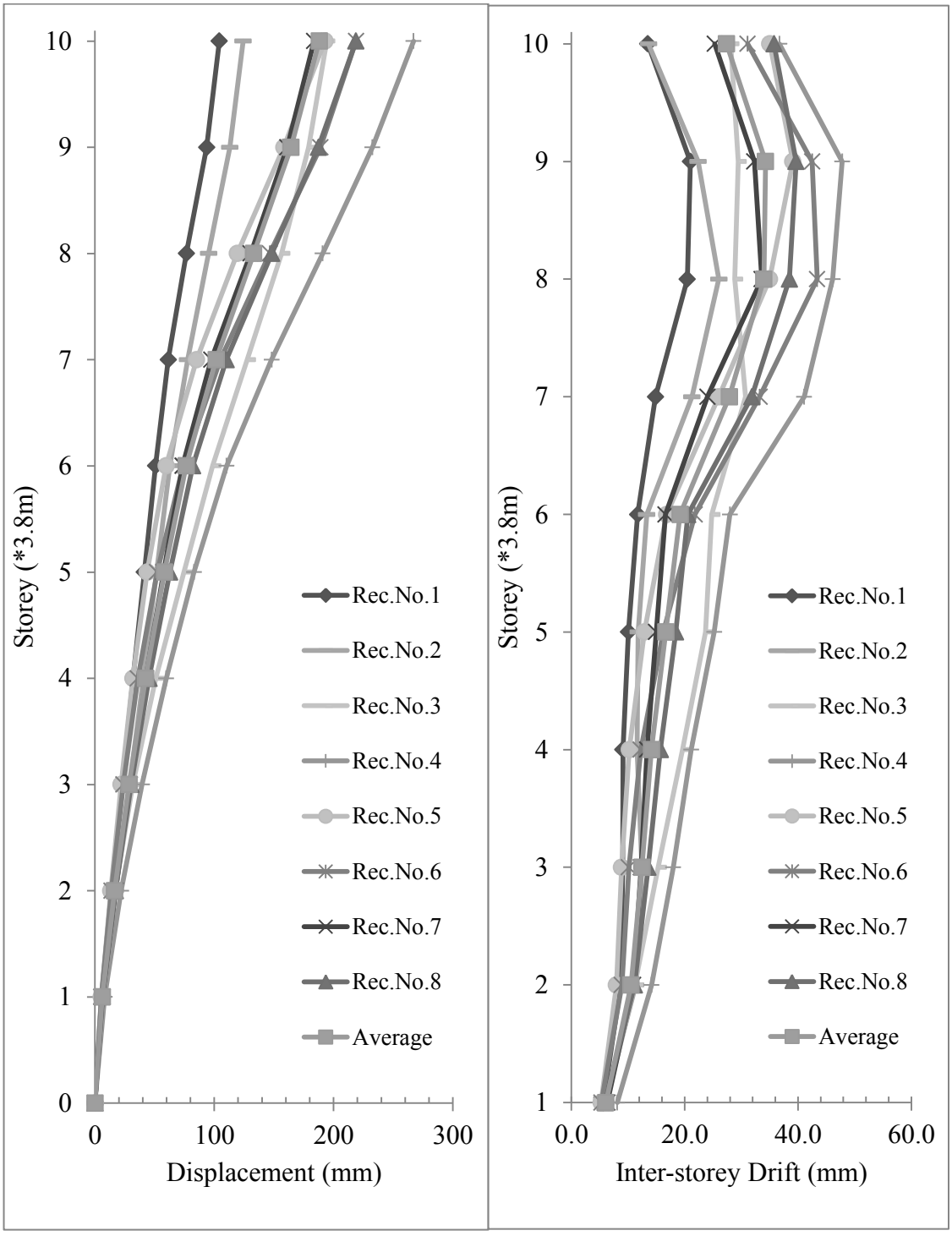

(a) Storey level displacement (b) Inter-storey drift

Figure 7.9: Response resulting from time history analysis of ten-storey structure

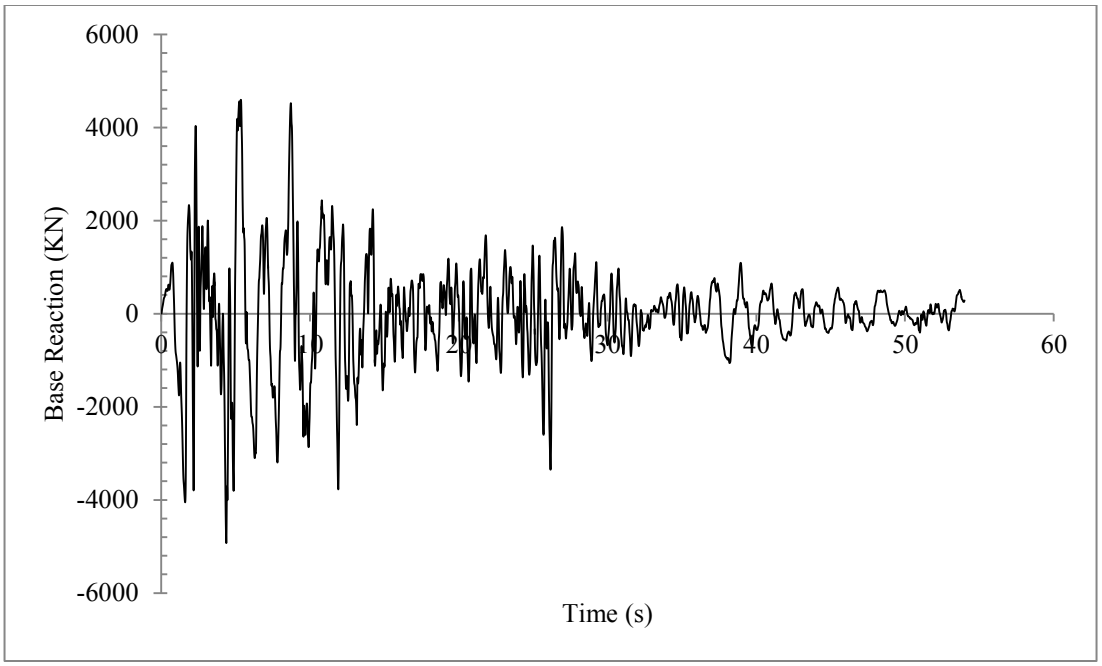

(a) Base Reaction

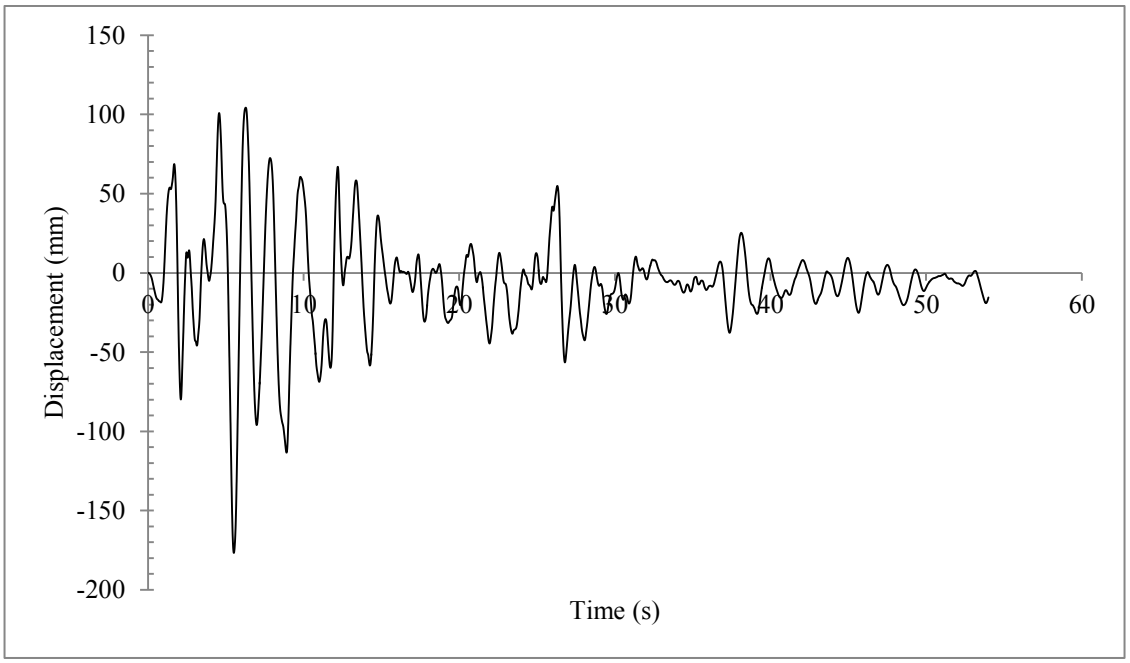

(b) Top Displacement

Figure 7.10: Response of 10-storey Equivalent Braced model in Opensees for Earthquake Record#1

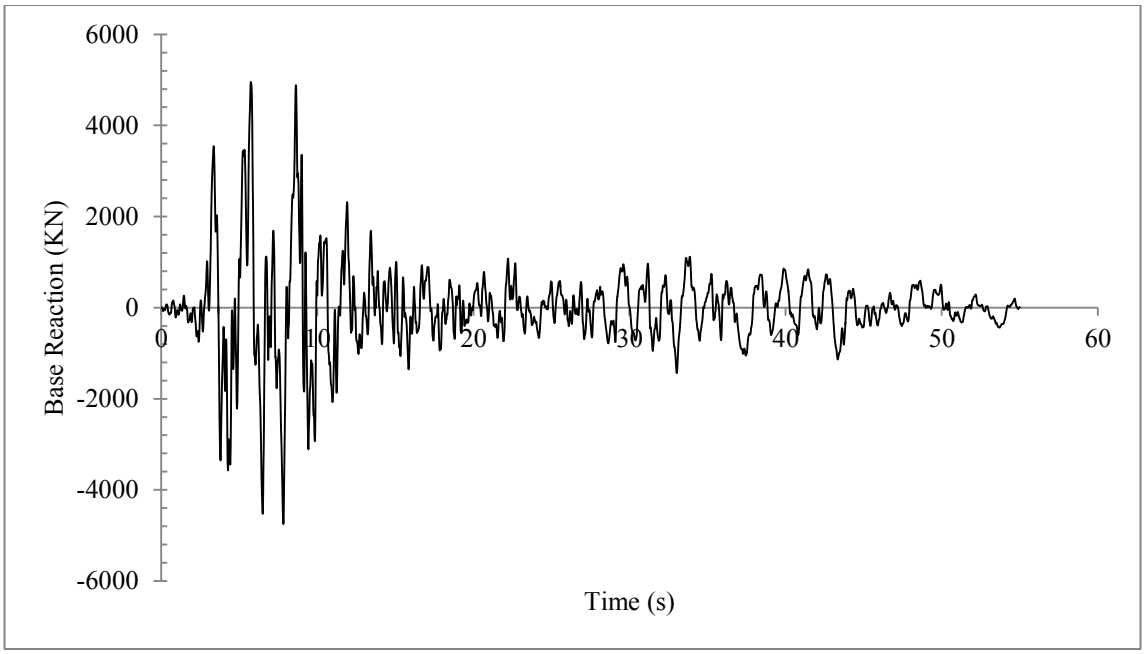

(a) Base Reaction

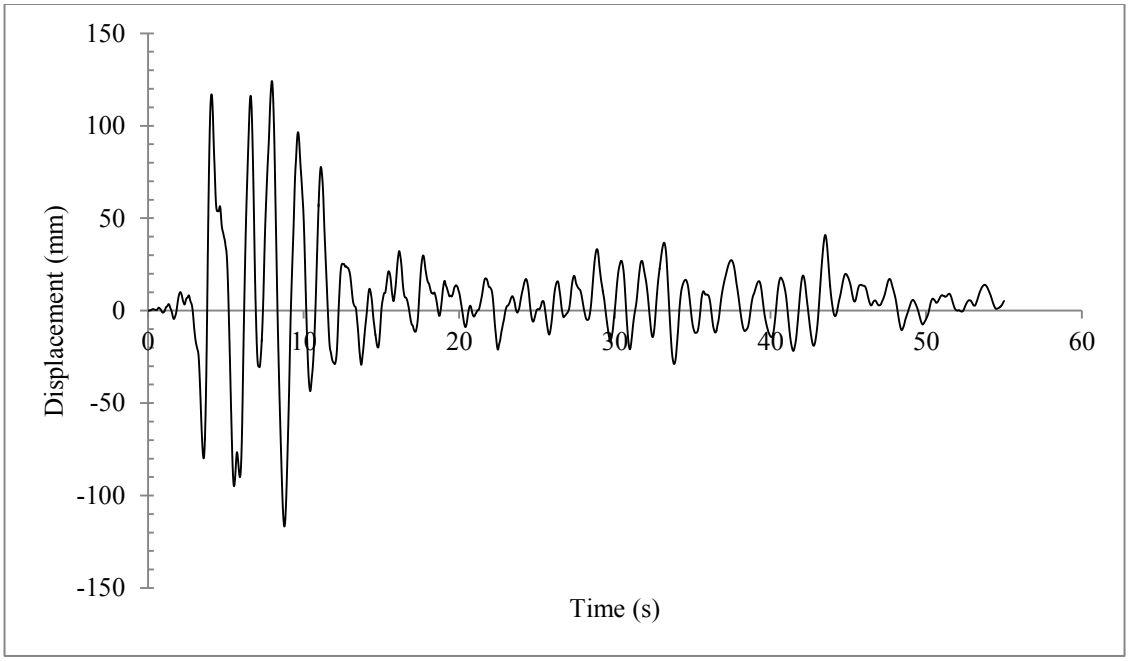

(b) Top Displacement

Figure 7.11: Response of 10-storey Equivalent Braced model in Opensees for Earthquake Record#2

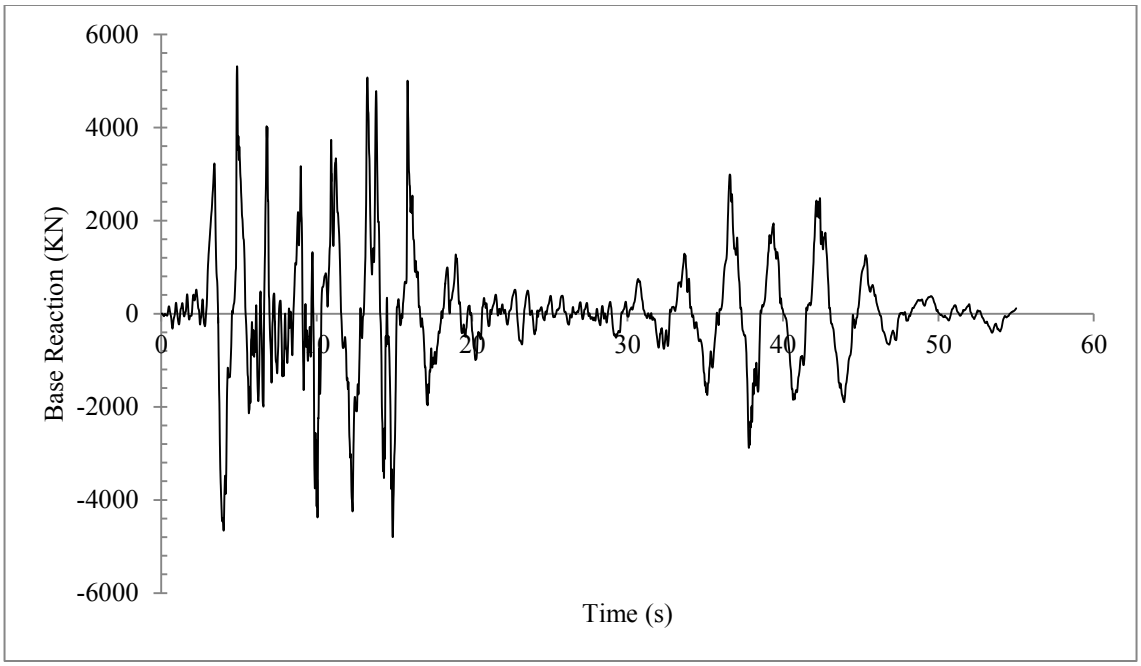

(a) Base Reaction

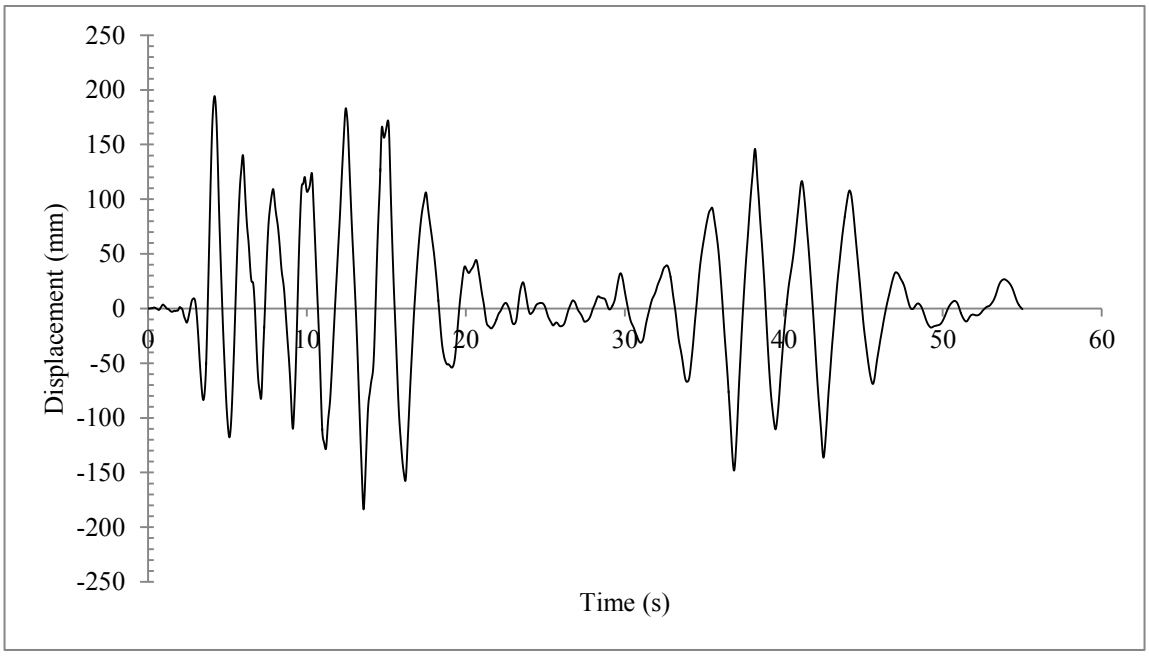

(b) Top Displacement

Figure 7.12: Response of 10-storey Equivalent Braced model in Opensees for Earthquake Record#3

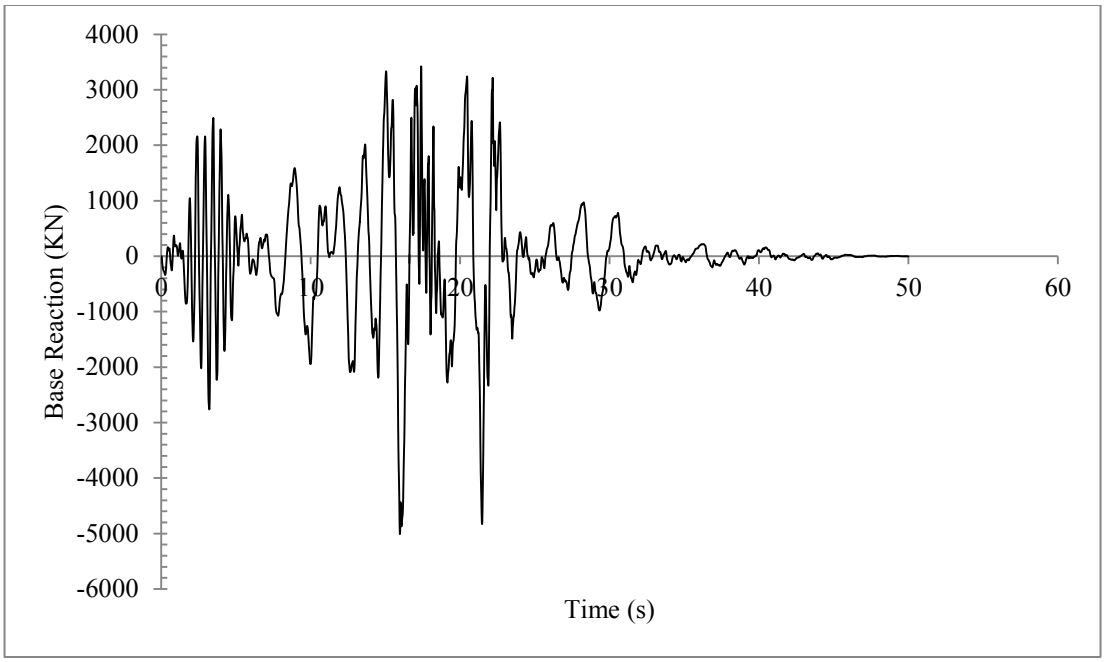

(a) Base Reaction

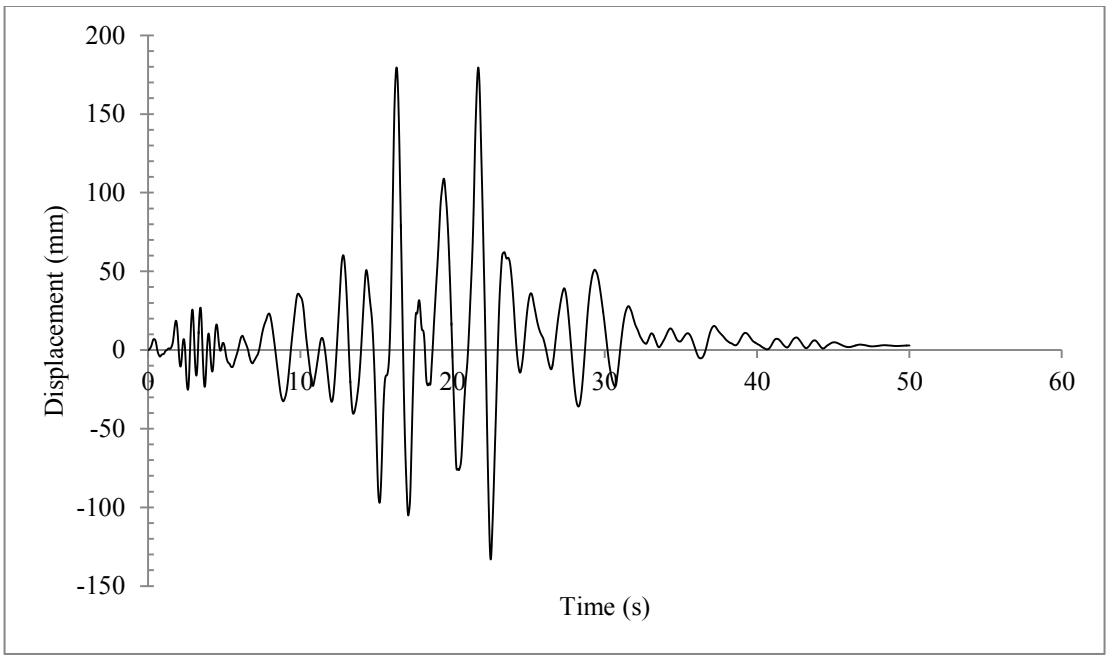

(b) Top Displacement

Figure 7.13: Response of 10-storey Equivalent Braced model in Opensees for Earthquake Record#4

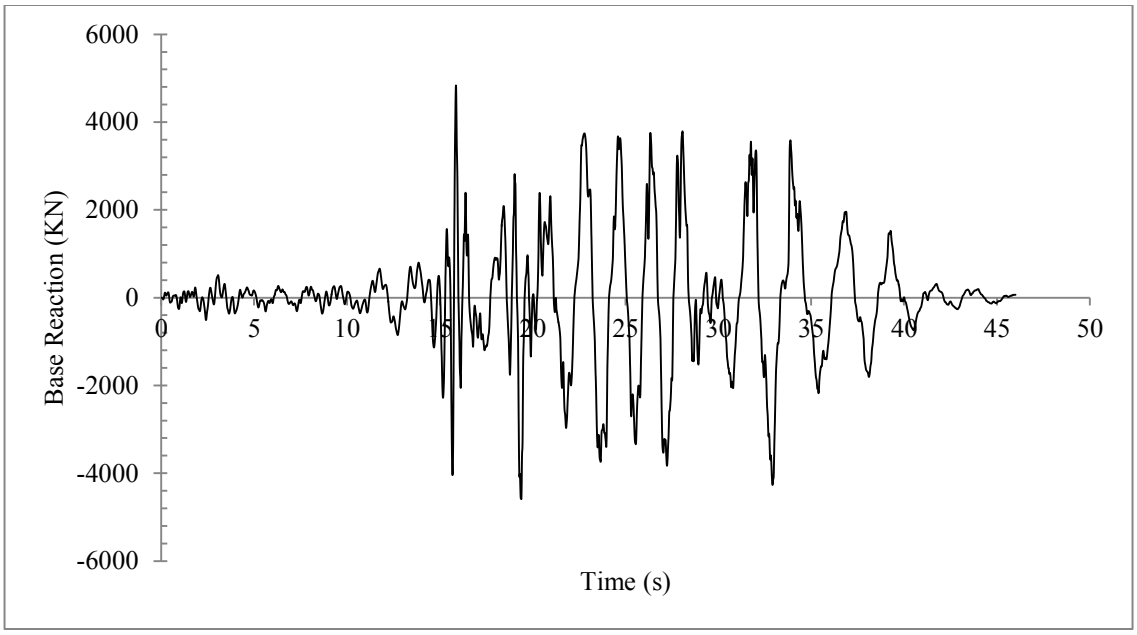

(a) Base Reaction

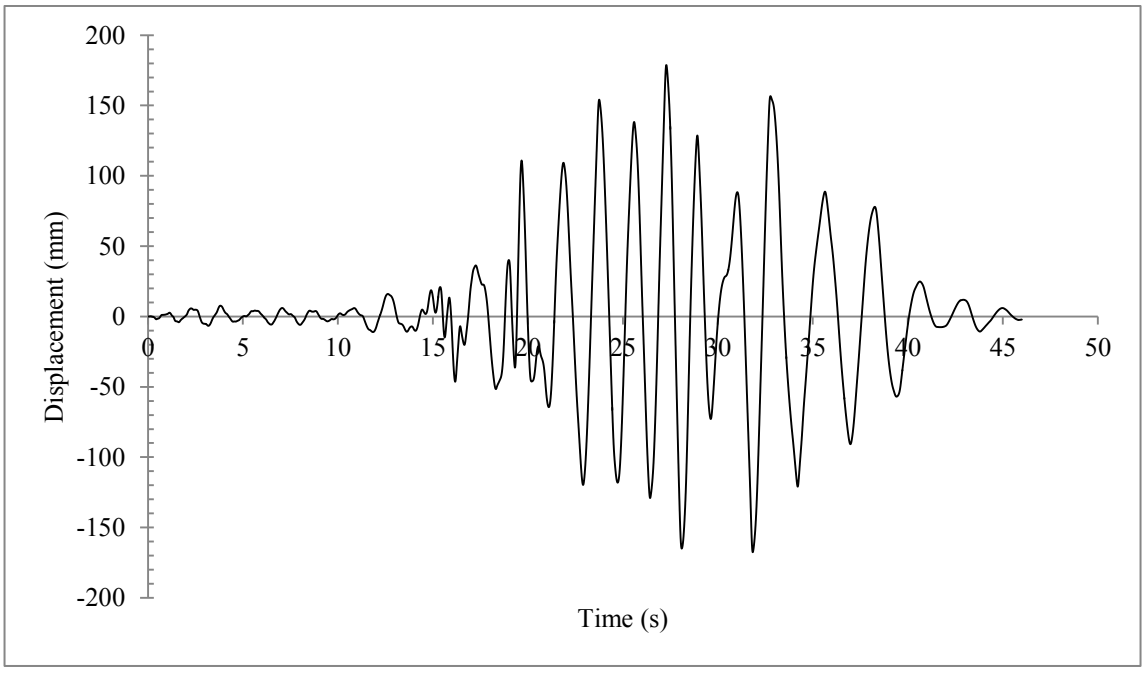

(b) Top Displacement

Figure 7.14: Response of 10-storey Equivalent Braced model in Opensees for Earthquake Record#5

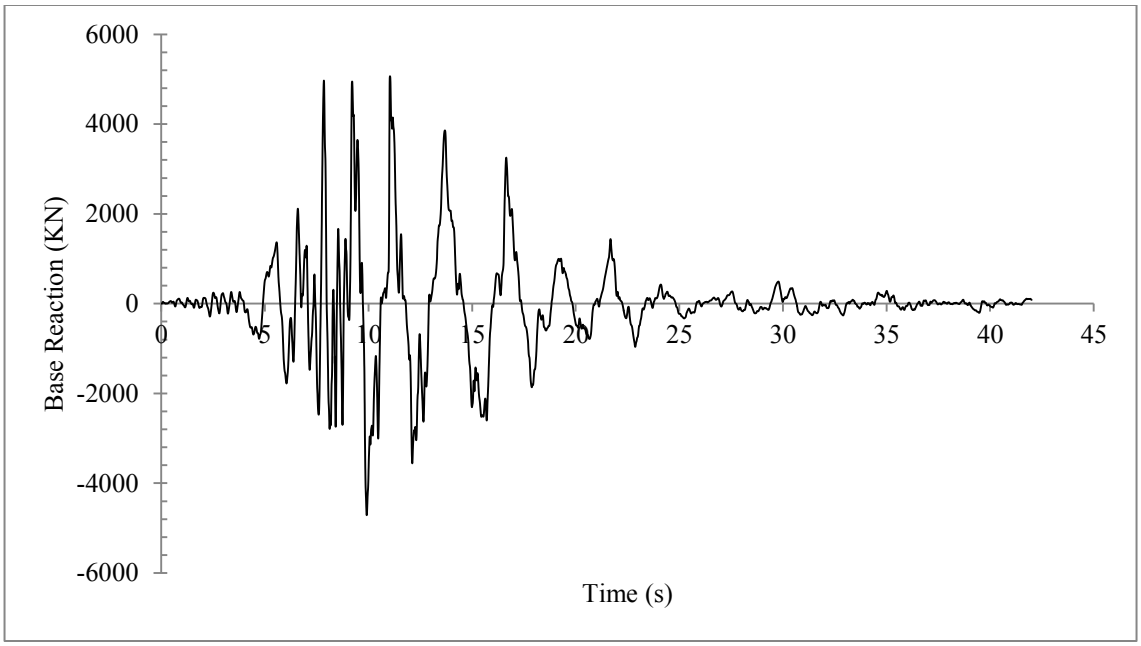

(a) Base Reaction

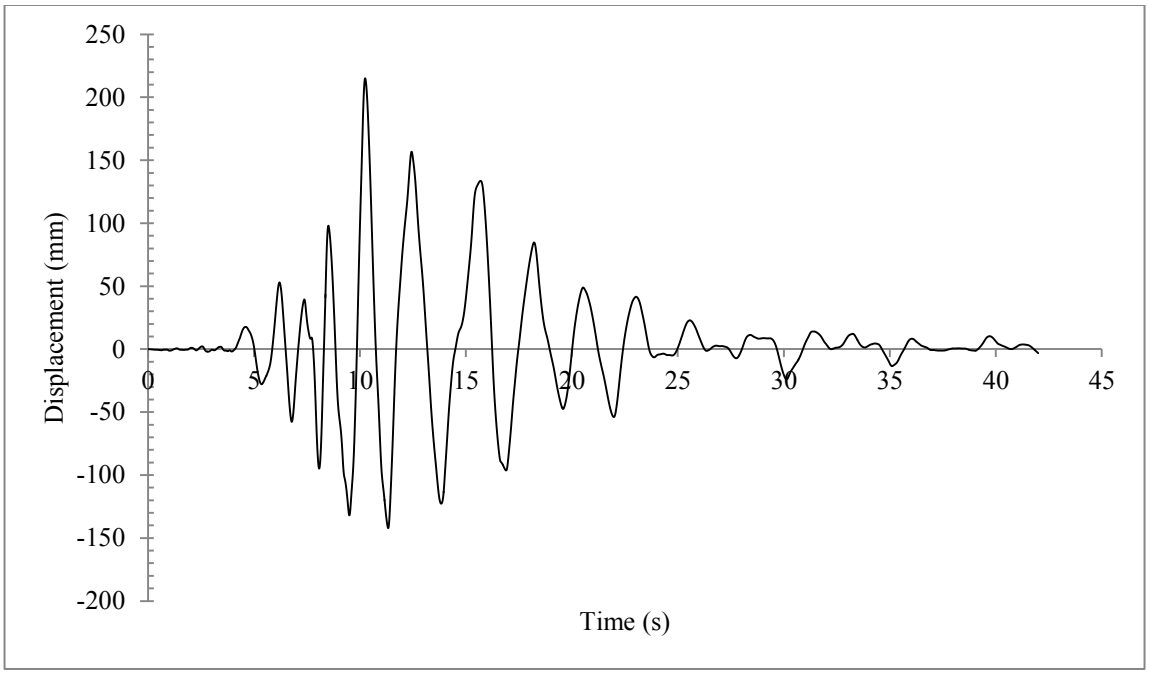

(b) Top Displacement

Figure 7.15: Response of 10-storey Equivalent Braced model in Opensees for Earthquake Record#6

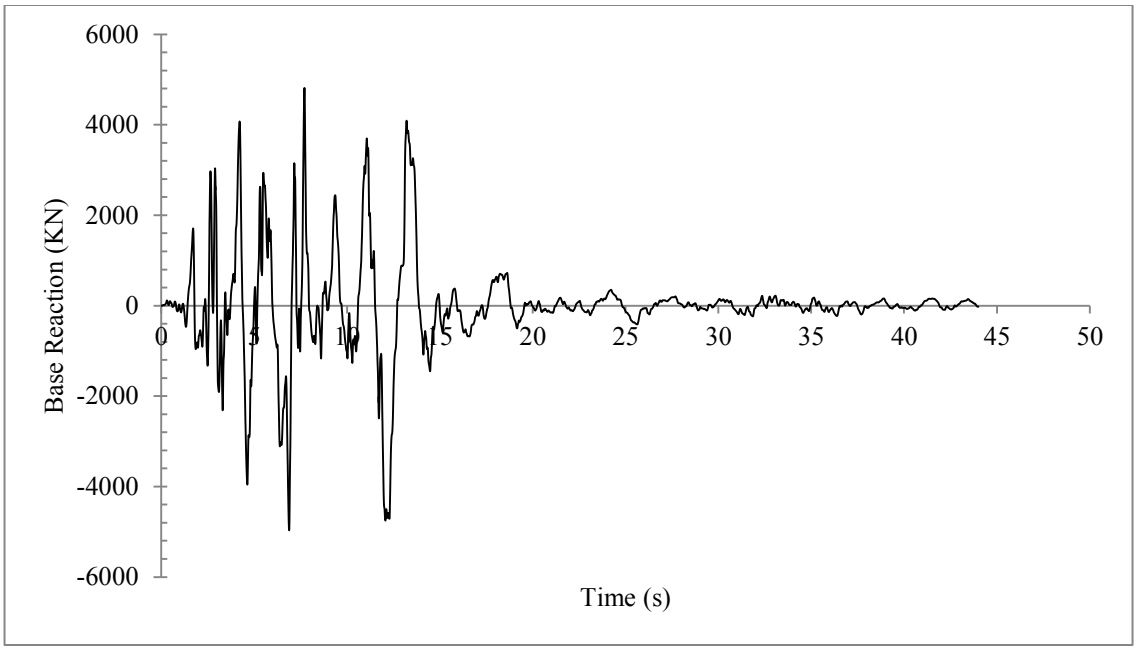

(a) Base Reaction

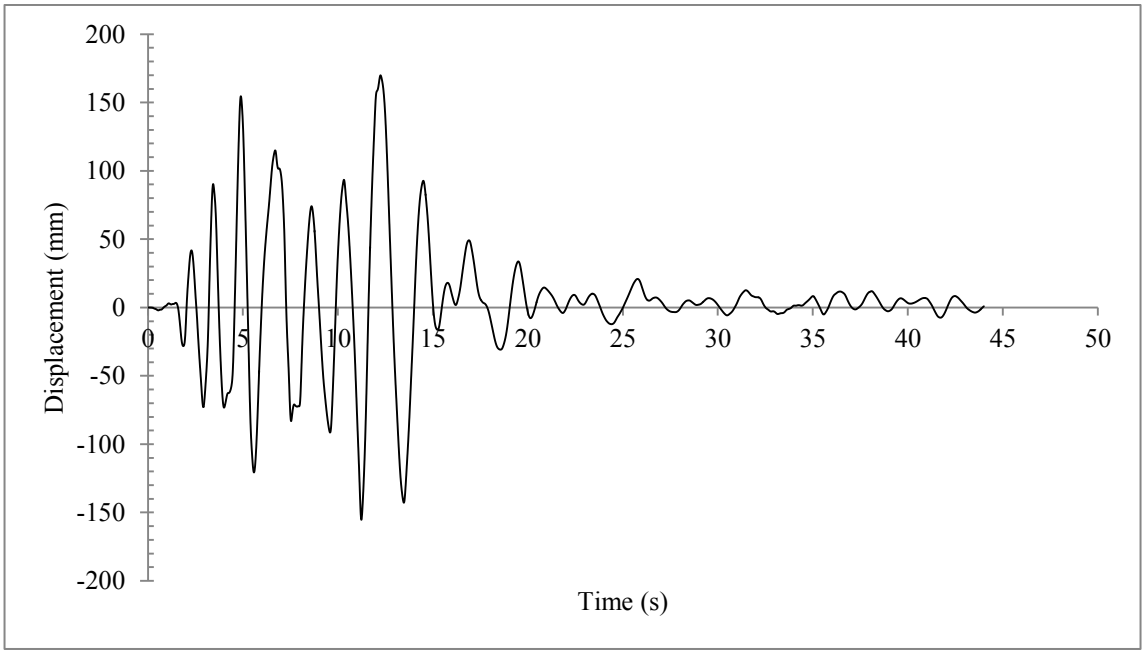

(b) Top Displacement

Figure 7.16: Response of 10-storey Equivalent Braced model in Opensees for Earthquake Record#7

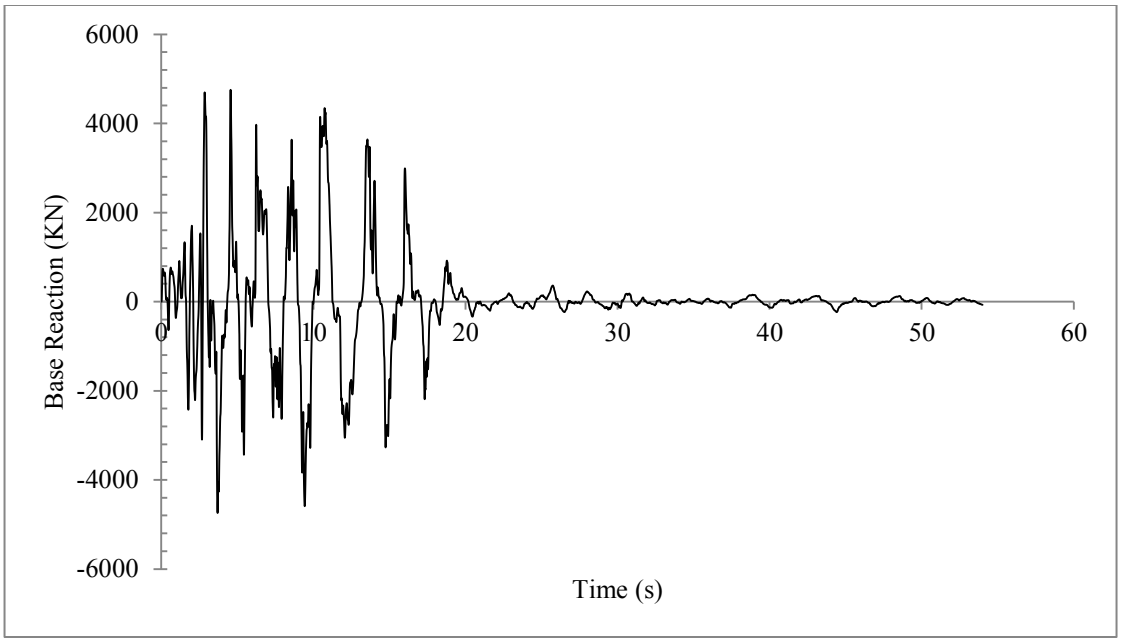

(a) Base Reaction

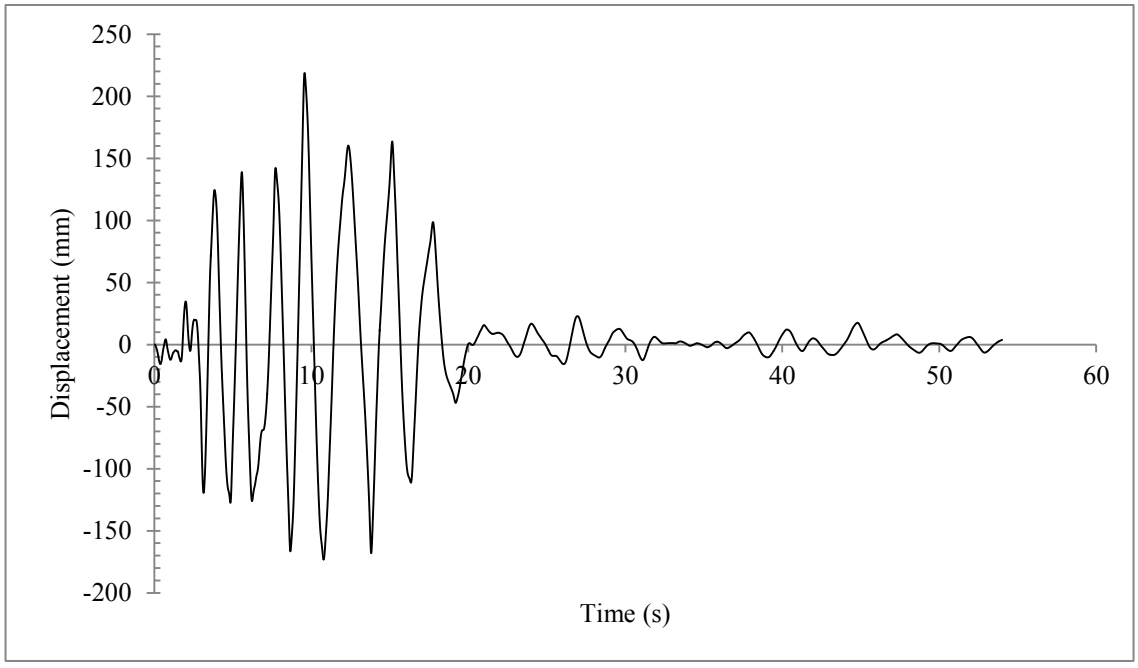

(b) Top Displacement

Figure 7.17: Response of 10-storey Equivalent Braced model in Opensees for Earthquake Record#8

7.5 **Summary**

In this chapter, the seismic response of three multi-storey SPSW structures designed with light gauge infill plates have evaluated and discussed. The detailed FE models have been used to analyze the four-storey and the six-storey structures. Static non-linear pushover analysis and dynamic nonlinear time history analysis has been carried out. Also, the modal analysis and response spectrum analysis were carried out. A set of eight suitably scaled ground motions were selected for the time history analysis and response spectrum analysis. The seismic provisions of NBCC 2010 were used for determine if the structures achieved an adequate level of seismic performance (i.e. "life-safety"). The EQ.BF model which has been developed and validated in the previous chapters has been used for evaluating the response of these structures. While the detailed FEM model has been used for the time history analysis of the 4 and 6 storey structures, only the EQ.BF model has been used for analyzing the 10 storey structure due to the computational efficiency of the model. With some limitation on the local behavior of the ten-storey SPSW structure, the EQ.BF model can give a detailed estimate on the overall performance of the structure in a very short time. This is particularly important for conducting a performance-based design of SPSW systems where repetitive analysis of the system is required. Based on the detailed analysis of three multi-storey structures, it is can be concluded that the design techniques provided for SPSW structures with hot rolled steel is conservative enough and can be safely used for shear walls with light-gauge steel infill plates.

Chapter 8. Conclusion and Future work

8.1 Summary and Conclusion

A simplified Equivalent Braced Model has been proposed in this research to study the seismic behavior of steel plate shear walls. A detailed step by step procedure for the development of the braced model has been presented. A series of static and dynamic nonlinear validations has been carried out to check the accuracy and efficiency of the equivalent braced frame (EQ.BF) model. The developed EQ.BF model has been used to study the performance of a series of light-gauge shear walls (4-storey, 6-storey, and 10-storey).

All available design recommendations for SPSW systems are based on research on hot rolled steel infill plate. Research has indicated that the thickness demand of infill plate for multi-storey structures are so small, especially for low-to-medium rise SPSW buildings, that it is almost impossible to achieve that thickness with hot rolled steel. Use of thin light-gauge steel plate instead of thicker hot rolled steel plate is a potential solution. Unfortunately, very limited research on light-gauge shear wall systems is currently available and to date no research has been done on seismic performance of light-gauge shear walls. Thus, a detailed study on light-gauge steel shear walls has been carried out. The main objective of this study is to check whether the code designed seismic design guidelines for ductile steel plate shear walls can equally be used for design of light-gauge shear walls or any modification on recommended design philosophy is required. A detailed FE model was developed to study the behavior of light-gauge steel shear walls. Three different multi storey (Four-storey, six-storey and ten-storey) light-gauge SPSWs

have been designed based on the current seismic design recommendations for Canada. Nonlinear static pushover, modal and nonlinear response history analyses were carried out to evaluate the performance of the light-gauge shear walls.

It has been observed that both the detailed FE model and the simplified braced model developed here are able to provide very good predictions for quasi-static pushover response of three light-gauge shear wall specimens with different geometry. The models captured all essential features of the test specimens analyzed: initial stiffness, peak load, and the post-peak behavior. The main findings of the non-linear static analysis and non-linear dynamic analysis using a set of eight ground motion records scaled to the seismic hazard corresponding to the building site (i.e., Vancouver) are summarized below.

- Light-gauge SPWs with moment-resisting beam-to-column connections provide excellent structural performance in terms of stiffness and ductility. Similar to the conventional ductile plate walls, light-gauge shear walls were observed to have excellent ductility. In any case, no yielding in either column in any intermediate floor has been observed. As expected, from capacity design approach, yielding occurs at the infill plates and plastic hinges are formed at the end of beams only.

- As has been widely discussed in the literature, the difficulty in optimizing the design of conventional ductile SPSWs due to the minimum practical infill plate thickness has been overcome by using the light-gauge infill plates where a thinner plate can be used. The angle of the tension filed developed in the plate ranges

from 40^0 to 50^0 which is compatible with the design assumption in that regard. Also, the tension field formed in the cold form steel plates is similar to that of hot rolled steel plates. This observation clearly indicates that the same design technique can be used when cold form steel is used as the plate material.

- From the study on fundamental time period for both 4-storey and 6-storey structures, it can be concluded that even with introduction of thinner infill plates the time period of vibration for full SPSWs is still within the conservative limit of design. Thus, no additional design guideline in regard to calculation of design fundamental time period is recommended for use of light-gauge steel plate shear walled structures.

- No significant strength degradation or local failure have been observed in the light-gauge steel plate shear walls subjected to the selected set of ground motions both in case of time history analysis. The maximum inter-storey drift demand is found to be well below the design limits specified by NBCC 2010. The structures meet the drift demand and yet safe against design ground motions.

In addition to the above mentioned conclusion, another set of advantages that is a direct outcome of this research is in the establishment of the EQ.BF model. This model is not just easy to construct and very fast in terms of analysis time, but also very efficient in estimating the correct overall behavior. Through several tests put forward in this research the accuracy of this model can be judges to be within acceptable engineering limits. For both static and dynamic non-

linear tests EQ.BF model could estimate the initial stiffness, final strength, sequence of yielding, frequency, inter-storey drift with an average error of less than 5%. Calculating the model parameters from the configuration of a given SPSW system is easy and not at all cumbersome. The main efficiency of the model lies in its time for analysis. A huge saving of time and human effort is possible by using EQ.BF model rather than detailed FE models. Particularly for industries dealing with performance based design, repeated analysis is required. So, this model can help speeding the design process since analysis is short and reliable. However, it must always be accounted that EQ.BF model is a simplified modeling technique shown to be an excellent approximation only for predicting the overall global performance of structure. Where detailed structural behavior is a concern, it is recommended that analysis with full scale detailed FE model is carried out. The parametric study for modeling involved through this study has also introduced a statistical method for modeling equivalent linear models when complex non-linearity is involved in structures. Development of simplified FE models that can estimate the complex behavior of SPSW systems in a global sense has been successfully achieved through this research.

8.2 **Scope for future work**

The present study establishes that the current design methods for ductile SPSW systems can be adapted to the design of Light Gauge SPSW systems. The Light Gauge SPSW systems are shown to exhibit ductile response under seismic excitation. Finite element modeling of systems is an approach for studying their static and dynamic behavior of such systems. However, detailed FE modeling is at times very complex and time consuming work. So, a simplified

equivalent braced frame modeling technique has been successfully established. Though, the modeling technique has shown to estimate the SPSW behavior significantly accurate but some limitations and scope for further development of the model are highlighted. Also, further scope on study of light-gauge steel plate shear wall systems has been mentioned.

- A limited number of light-gauge steel shear walls have been tested in this work. More SPSW systems with varying geometry need to be tested before final design recommendations can be made. More importantly, a series of experimental study on multi-storey light gauge SPSW structures needs to be independently performed.

- The limitations on EQ.BF model are actually areas where the model can be further improved. For cyclic validation with experimental results the percentage error observed was highest as compared to other validations, though amount of error was within engineering limits. A probable reason for this can be the pinching effect which has been assumed to be constant. Further study with parameters like pinching effect may be carried out to obtain even more accurate estimates of SPSW behavior from the EQ.BF model. If greater accuracy is demanded in cyclic test results, then a study on pinching effect of plates is required. Also, nothing on ultimate strength is discussed in the EQ.BF model, so, to study the failure of SPSW systems, some ultimate strength parameters may be introduced in the material properties. Some dynamic test with real time earthquake data and time history analysis might be useful for sketching out the dynamic parameters of

EQ.BF model. The EQ.BF model is just the first step and a wide field of development scope is open for further research.

- With this developed EQ.BF model, performance based design guidelines can now be developed for seismic design of SPSWs, since repeated analysis can be easily carried out within very less time and effort.

REFERENCE

Abaqus. Abaqus/Standard user's manual. Version 6.11. 2011. Pawtucket (RI): Hibbitt, Karlsson, & Sorensen, Inc., (HKS).

Abrahamson, N.A., Hancock , J., Watson-Lamprey J., Markatis, A., McCoy, E., Mendis, R., 2006. Program SeismoMatch v2 – software capable of adjusting earthquake accelerograms to match a specific design response spectrum, using the wavelets algorithm proposed by Abrahamson (1992) and Hancock et al. (2006). http://www.seismosoft.com/en/Seis moMatch.aspx (cited October 2005).

AISC. 2005. *Seismic Provisions for Structural Steel Buildings*, ANSI/AISC 341-05, Chicago, IL: American Institute of Steel Construction.

Applied Technology Council, 1992. *Guidelines for Cyclic Seismic Testing of Component of Steel Structures.* ATC-24, Redwood City, CA.

Berman J.W. and Bruneau M. 2005. *Experimental Investigation of Light-Gauge Steel Plate Shear*. Journal of Structural Enginering 131, no. 2 : 259–267.

Berman J.W. and Bruneau M. 2008. *Capacity Design of Vertical Boundary Elements in Steel Plate Shear Walls*. Engineering Journal. First Quarter.: 57–71.

Bhowmick A.K., Grondin G.Y. and Driver R.G. 2009. *Seismic analysis of steel plate shear walls considering strain rate and P-delta effects*. Journal of Constructional Steel Research, 65: 1149-1159.

Bhowmick A.K., Grondin G.Y. and Driver R.G. 2010. *Performance of Type D and Type LD steel plate*. Canadian Journal of Civil Engineering, 37: 88-98.

CSA. 2009. *Limit states design of steel structures*. CAN/CSA-S16-09, Canadian Standards Association, Toronto, ON.

Dastfan M. and Driver R.G. 2008. *Flexural Stiffness Limits for Frame Members of Steel Plate Shear Wall Systems*. Proceeding of Annual Stability Conference, Structural Stability Research Council, Nashville, TN.

Driver R.G., Kulak G.L.,Kennedy D.J.L. and Elwi A.E. 1997. *Seismic behaviour of steel plate shear walls.* Structural ngineering Report No. 215. Department of Civil and Environmental Engineering, University of Alberta, Canada.

Driver R.G., Kulak G.L.,Kennedy D.J.L. and Elwi A.E. 1998a. *Cyclic test of a Four-Storey Steel Plate Shear Wall.* ASCE Journal of Structural Engineering, Vol. 124, No. 2, 112-120.

Driver R.G., Kulak G.L.,Kennedy D.J.L. and Elwi A.E. 1998b. *FE and Simplified Models of Steel Plate Shear Wall*. ASCE Journal of Structural Engineering, Vol. 124, No. 2, 121-130.

Elgaaly M., Caccese V. and Du C. 1993. *Post-buckling behavior of steel-plate shear walls under cyclic loads*. Journal of Structural Engineering 119, no. 2: 588–605.

Elgaaly M. 1998. *Thin steel plate shear walls behavior and analysis*. Thin-Walled Structures, 32: 151–180.

Federal Emergency Mangament Agency. 2000. FEMA 356: *Pre-standard and commentary for the seismic rehabilitation of buildings*. Building Seismic Safety Council of the National Institute of Building Sciences; Washington, D.C.

Hilber H.M., Hughes T.J.R. and Taylor R.L. 1978. *Collocation, dissipation and 'overshoot' for time integration schemes in structural dynamics*. Earthquake Engineering & Structural Dynamics 6(1): 99-117.

Kharrazi M.H.K., Ventura C.E., Prion H.G.L. and Ghomi S.S. 2004. *Bending and shear analysis and design of ductile steel Plate walls*. 13th World Conference on Earthquake Engineering, Vancouver, B.C., Canada: Paper No **77**.

Kharrazi M.H.K. 2005. *Rational method for analysis and design of steel plate walls*. Ph.D. thesis, University of British Columbia, Canada.

Kuhn P., Peterson, J.P. and Levin L.R. 1952. *A Summary of Diagonal Tension, Part I: Methods of Analysis*. NACA technical note 2661, Washington, DC: National Advisory Committee for Aeronautics.

Lubell S., Prion H. G. L., Ventura C. E. and Rezai M. April, 2000. *Unstiffened steel-plate-shear wall performance under cyclic loading*. Journal of Structural Enginering 126(4): 453-460.

Mazzoni, S., McKenna, F., Scott, M.H. and Fenves, G.L. et al. 2007. *OpenSees command language manual*. Pacific Eathquake Engineering Research Center, University of California, Berkeley.

Mimura, H. and Akiyana, H., 1977. *Load-Deflection Relationship of Earthquke Resistant Steel Shear Walls with a Developed Diagonal Tension Field.* Transactions, Architectural Institute of Japan, 260, October, 109-114 (in Japanese).

Mohammad R.B., Grondin G.Y. and Elwi A.E. 2003. *Experimental and Numerical Investigation of Steel Plate Shear Wall*. Department of Civil and Environmental Engineering, University of Alberta, Edmonton, Alberta: Structural Engineering Report No. 254.

Montgomery, C.J., and Medhekar, M., 2001. *Discussion of Unstiffened Steel Plate Shear Wall Performane Under Cyclic Loading by Lubell, A.S. Prion, H.G.L., Ventura, C.E., and Rezai, M.* Journal of Structural Engineering, ASCE, Vol. 127, No. 8: August, 1973.

Naumoski, N., Saatcioglu, M., and Amiri-Hormozaki, K. 2004. *Effects of Scaling of earthquake excitations on the dynamic response of reinforced concrete frame buildings*. 13th World Conference on Earthquake Engineering, Paper # 2917: 15.

Neilson D.A.H. 2010. *Welding of light gauge infill panels for steel plate shear walls*. Department of Civil and Environmental Engineering, M.Sc. thesis, University of Alberta, Edmonton, Alberta.

Nove Naumoski [2008]. The Canadian Association for Earthquake Engineering. http://www.caee.uottawa.ca/Publications/Earthquake%20records/Earthquake%20Records.htm (Updated till 2008).

NRC. 2010. *National Building Code of Canada* (NBCC). Canadian Commission on Building and Fire Codes, National Research Council of Canada, Ottawa, Ontario, Canada.

Rezai, M., 1999. *Seismic Behaviour of Steel Plate Shear Walls by Shake Table Testing*. PhD Dissertation, Department of Civil Engineering, University of British Columbia, Vancouver, BC, Canada.

Thorburn L.J., Kulak G.L. and Montgomery C.J. 1983. *Analysis of Steel Plate Shear Walls.* Department of Civil Engineering, University of Alberta, Edmonton, Alberta: Structural Engineering Report No. 107.

Timler P.A., and Kulak G.L. 1983. *Experimental Study on Steel Plate Shear Walls.* Structural Engineering Report o. 114, Department of Civil Engineering, University of Alberta, Edmonton, Canada.

Timler, P.A., Ventura, C.E., Prion, H., and Anjam, R., 1998. *Experimental and Analytical Studies of Steel Plate Shear Wall as Applied to the Design of Tall Buildings*. Structural Design of Tall Buildings, Vol. 7: 233-249.

Topkaya C. and Atasoy M. 2009. *Lateral stiffness of steel plate shear wall systems.* Thin-Walled Structures, 47: 827–835.

Tromposch E.W. and Kulak G.L. 1987. *Cyclic and Static Behaviour of Thin Panel Steel Plate Shear Wall*. Department of Civil and Environmental Engineering, University of Alberta, Edmonton, Alberta: Structural Engineering Report No. 145.

Vian D., Bruneau M. 2005. *Steel plate shear walls for seismic design and retrofit of building structures.* Technical Report No. MCEER-05-0010, State University of New York at Buffalo, Buffalo, NY: Multidisciplinary Centre for Earthquake Engineering Research.

Wagner, H. 1931. *Flat Sheet Metal Girders with Very Thin Metal Web, Part III*. NACA technical note 605, Washington, DC: National Advisory Committee for Aeronautics.

Appendix I – Selected Ground Motions

In this appendix the characteristics of the selected ground motions mentioned in Table 4.2 are shown. The original and scaled time history acceleration and acceleration-spectra for each of eight selected earthquakes are plotted.

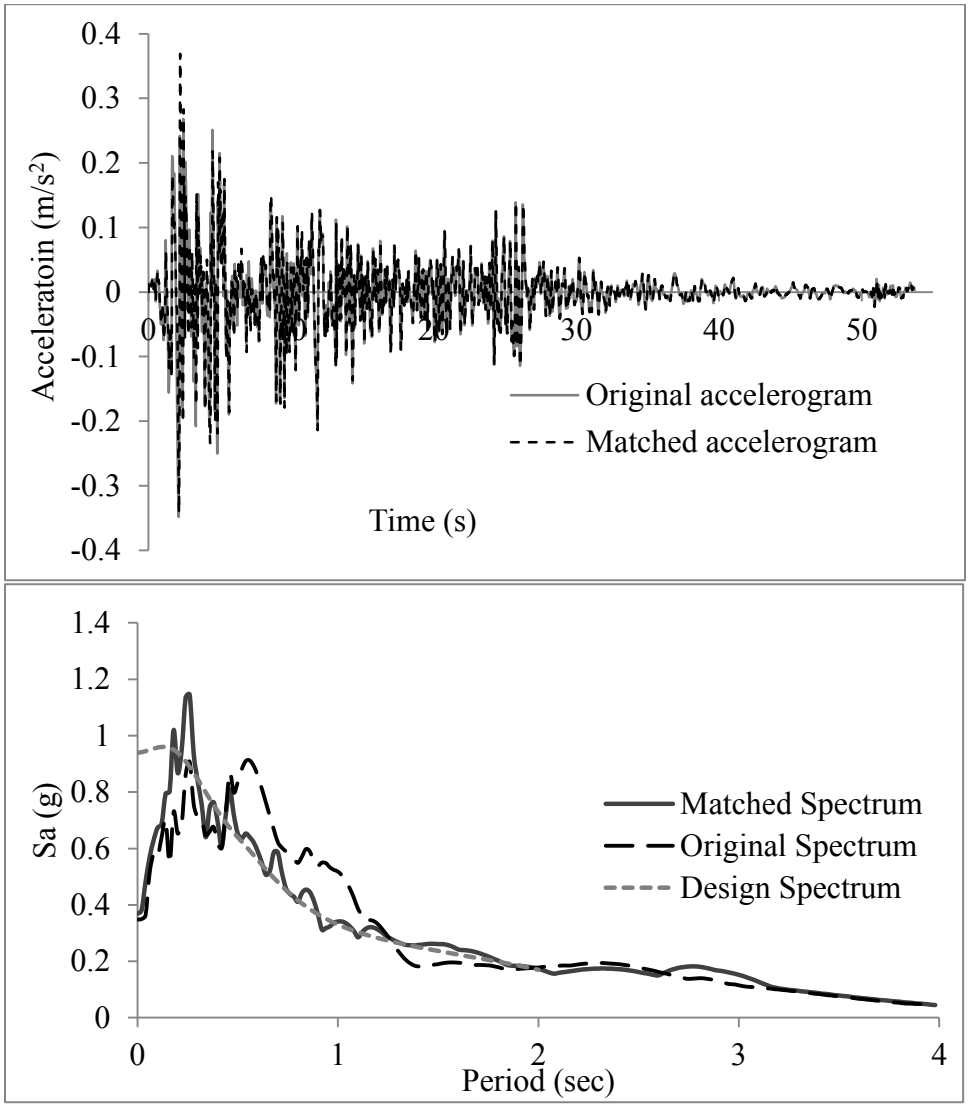

Figure I.1: Ground Motion Record No#1

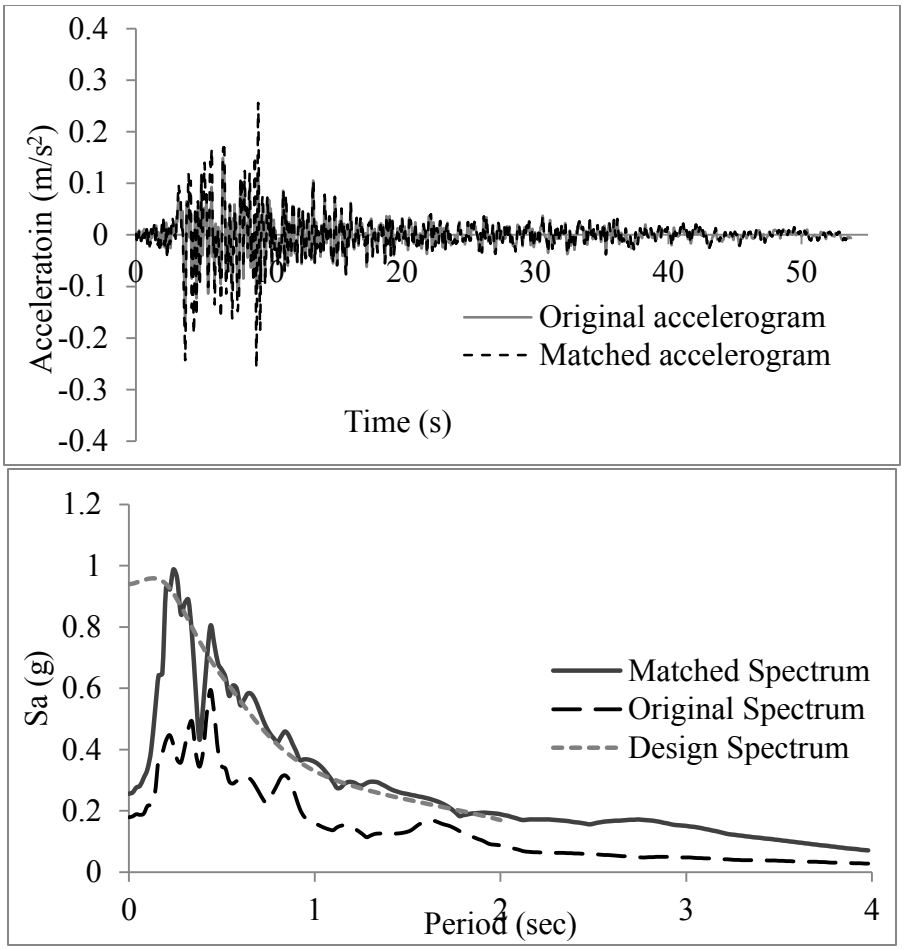

Figure I.2: Ground Motion Record No#2

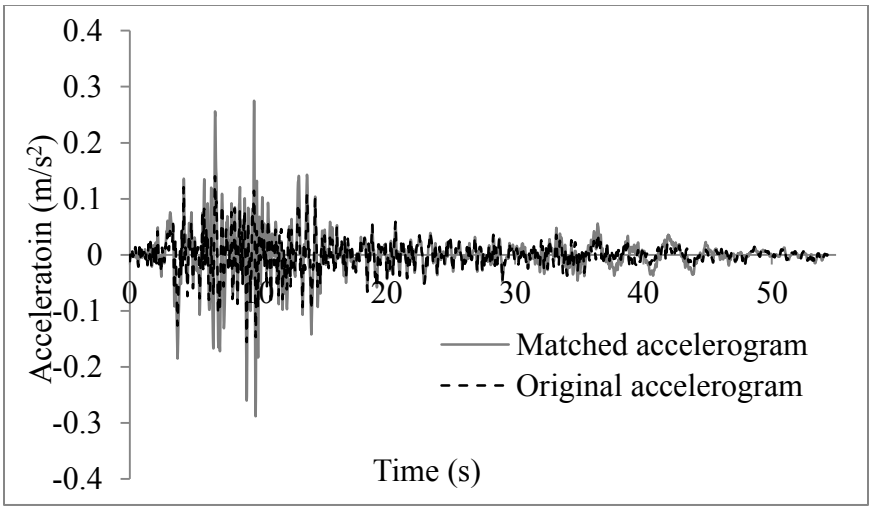

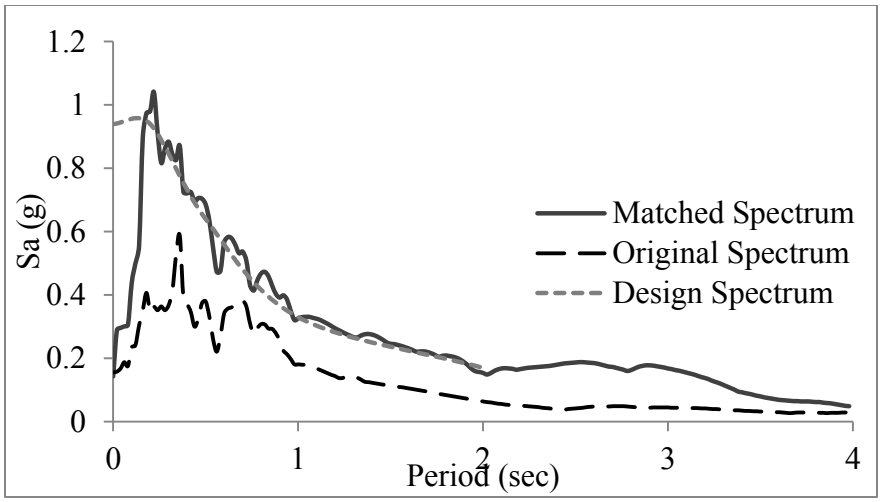

Figure I.3: Ground Motion Record No#3

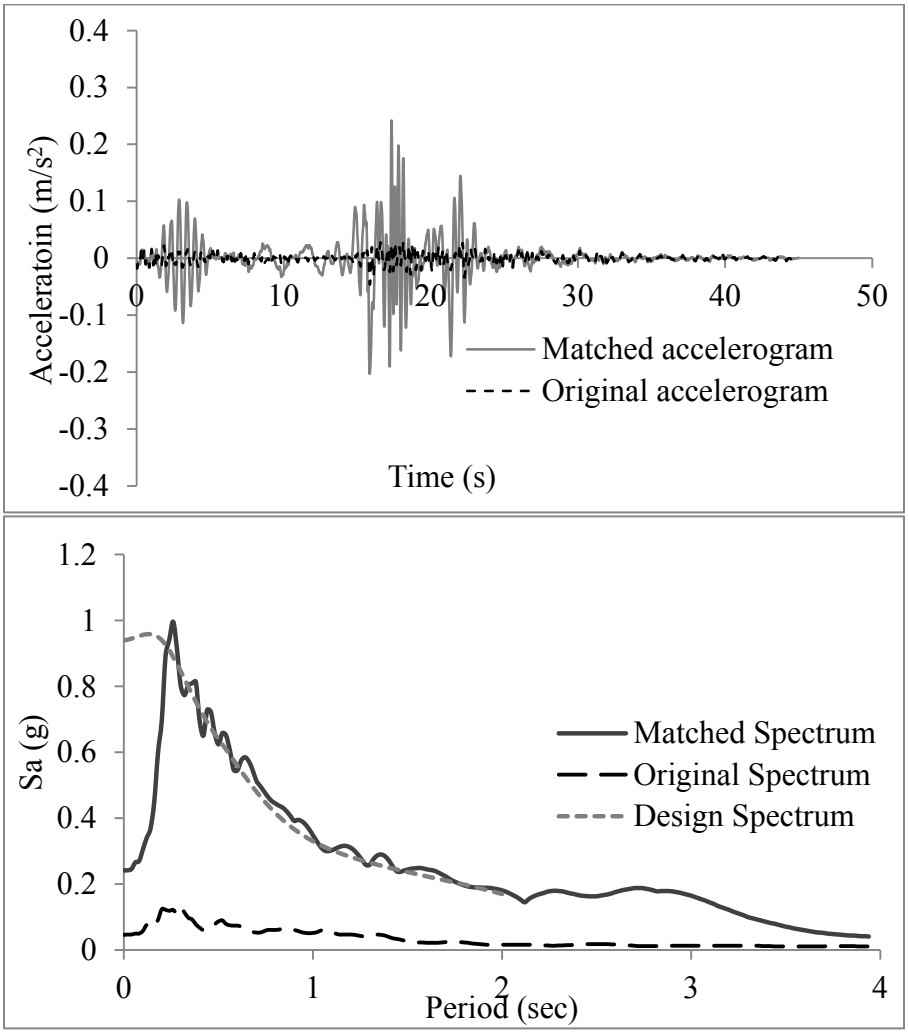

Figure I.4: Ground Motion Record No#4

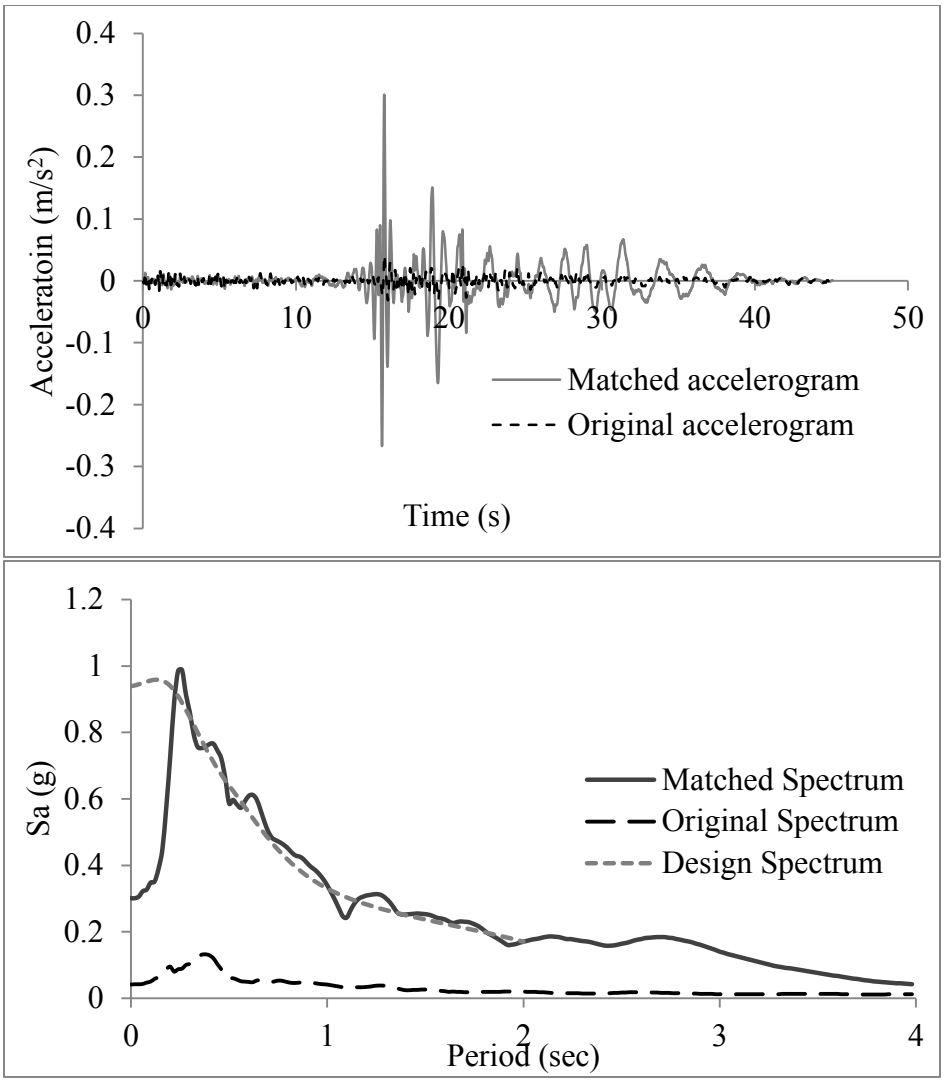

Figure I.5: Ground Motion Record No#5

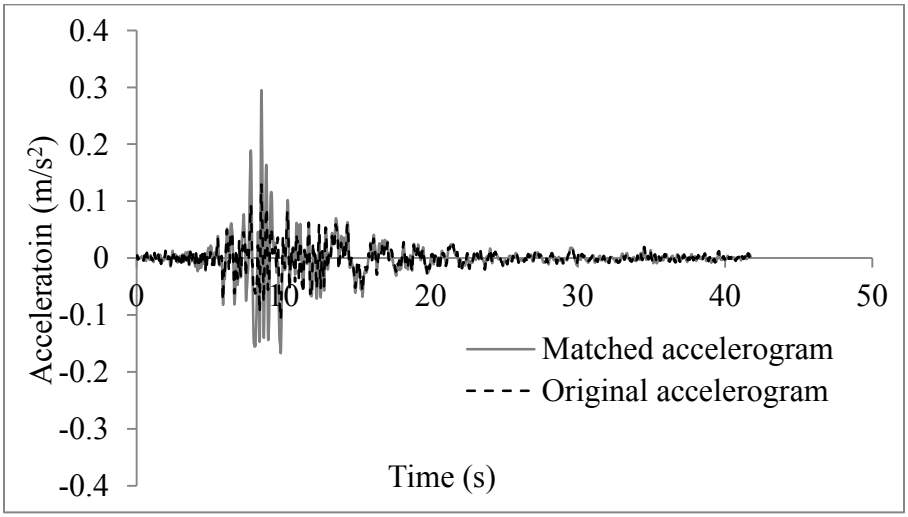

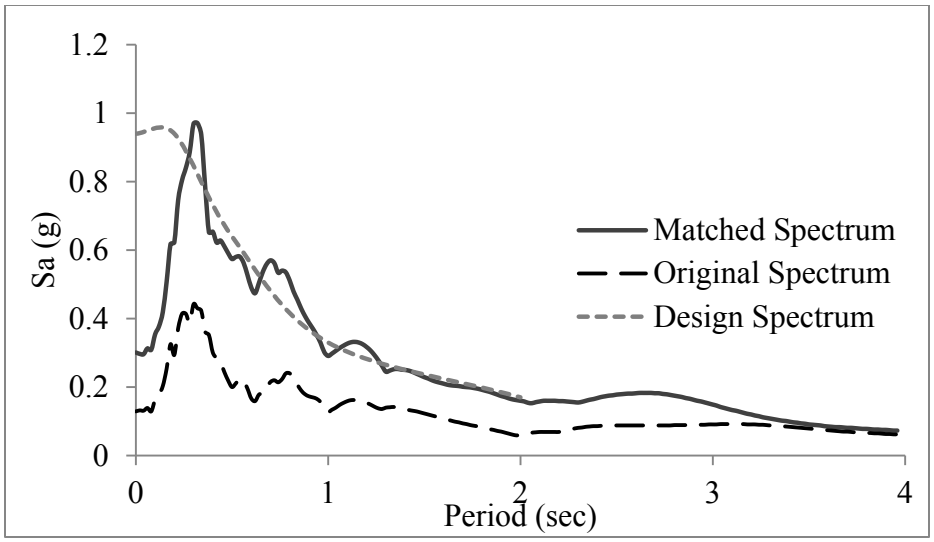

Figure I.6: Ground Motion Record No#6

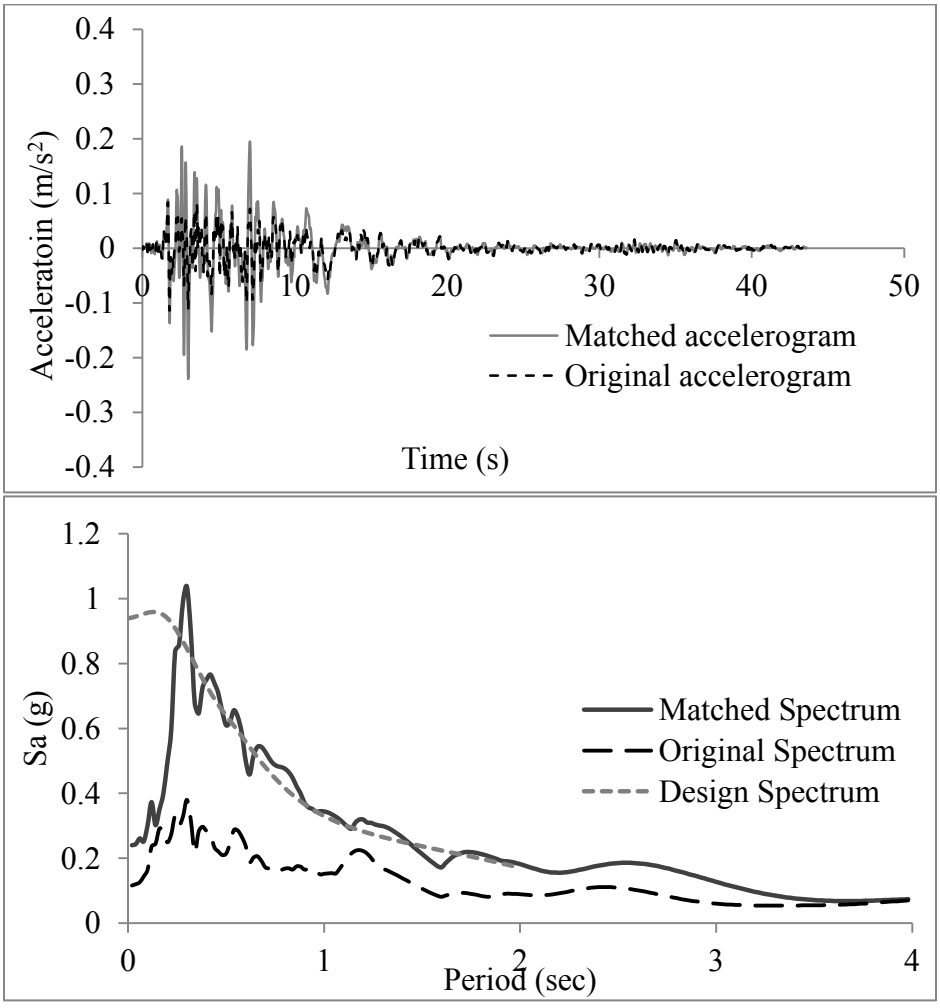

Figure I.7: Ground Motion Record No#7

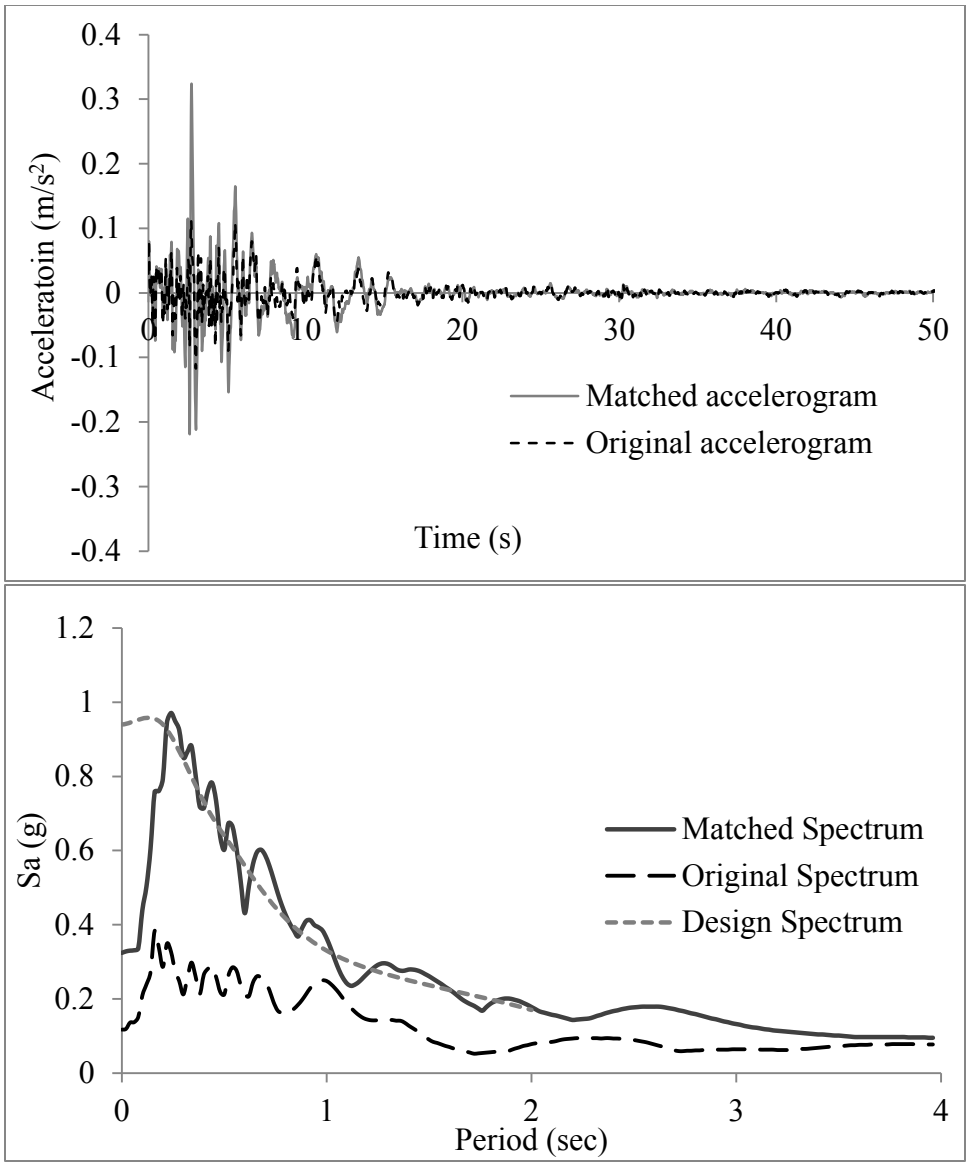

Figure I.8: Ground Motion Record No#8

Appendix II – Sample Inter-storey Displacements

Sample inter-storey displacements at every floor level for all the designed SPSW structures (four-storey, six-storey and ten-storey) are shown in this appendix. For the four-storey and six-storey SPSW structures, results from both detailed FE model in Abaqus and simplified EQ.BF model in Opensees are presented. However, for the ten-storey the time history response indicates the results from EQ.BF model alone.

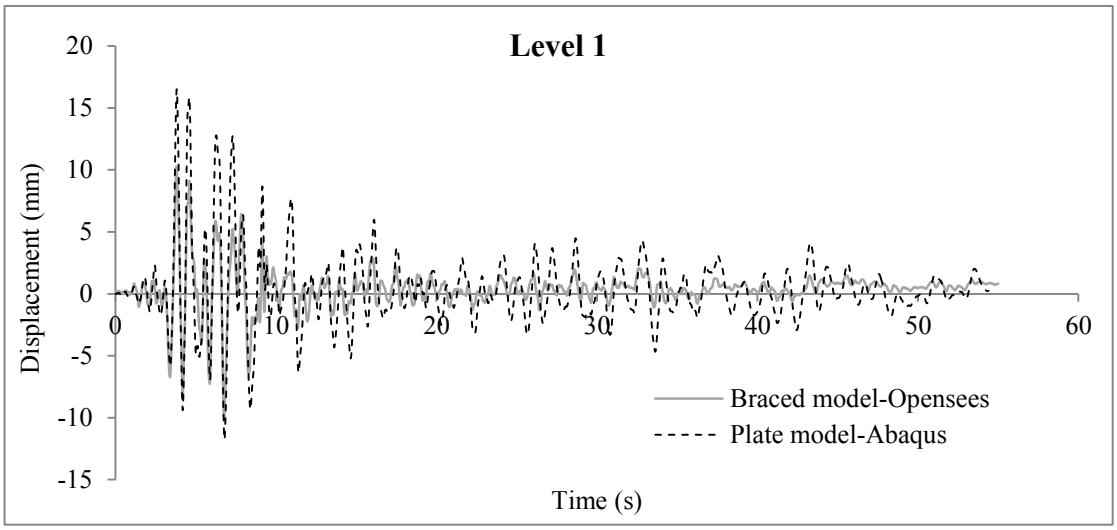

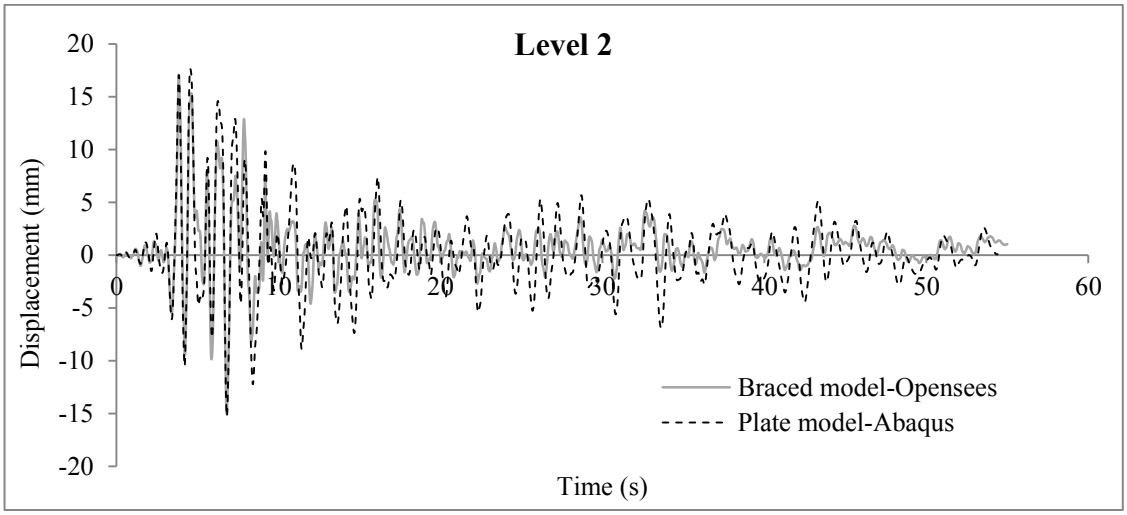

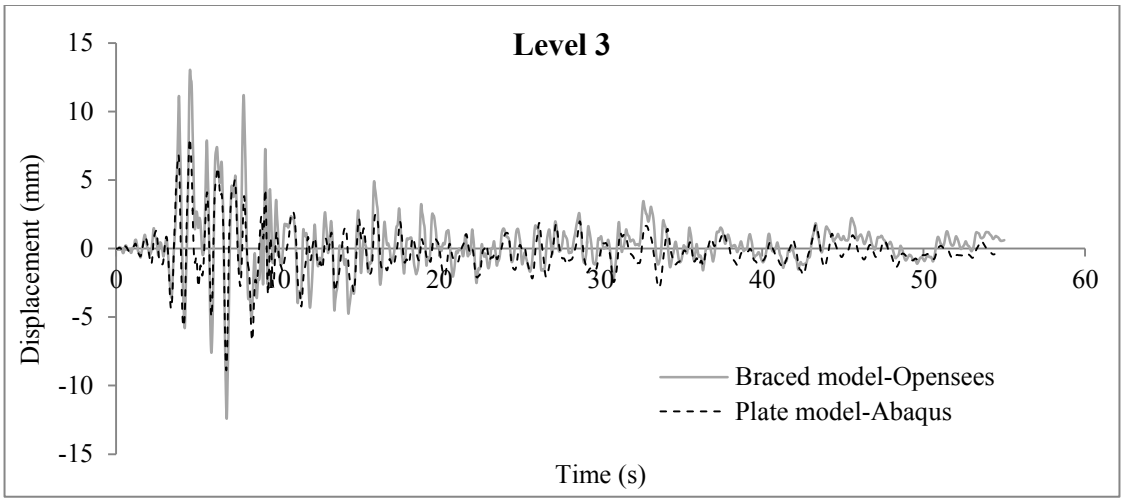

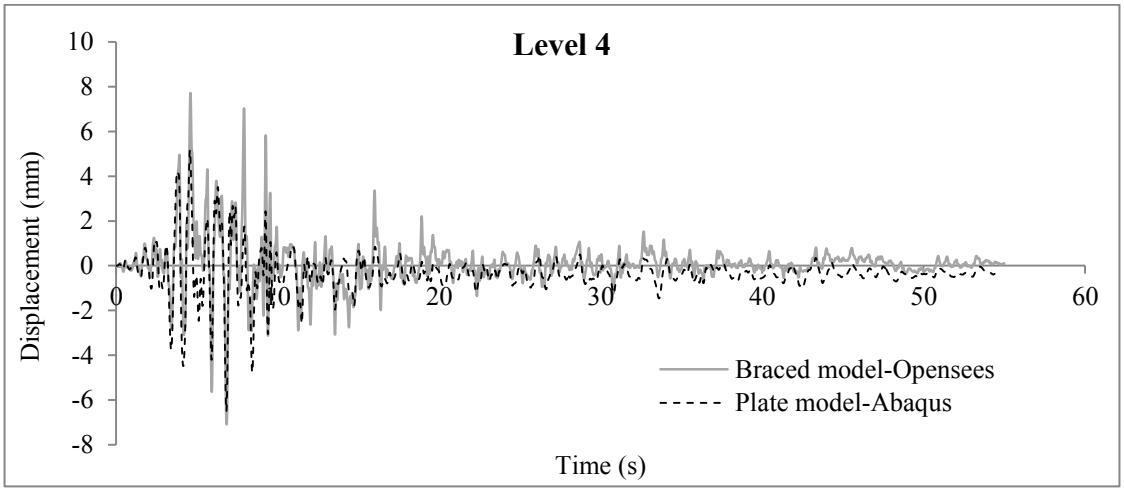

Figure II.1: Sample inter-storey drift for Earthquake Record No#2 at different storey levels as obtained from Abaqus and Opensees for 4-storey SPSW.

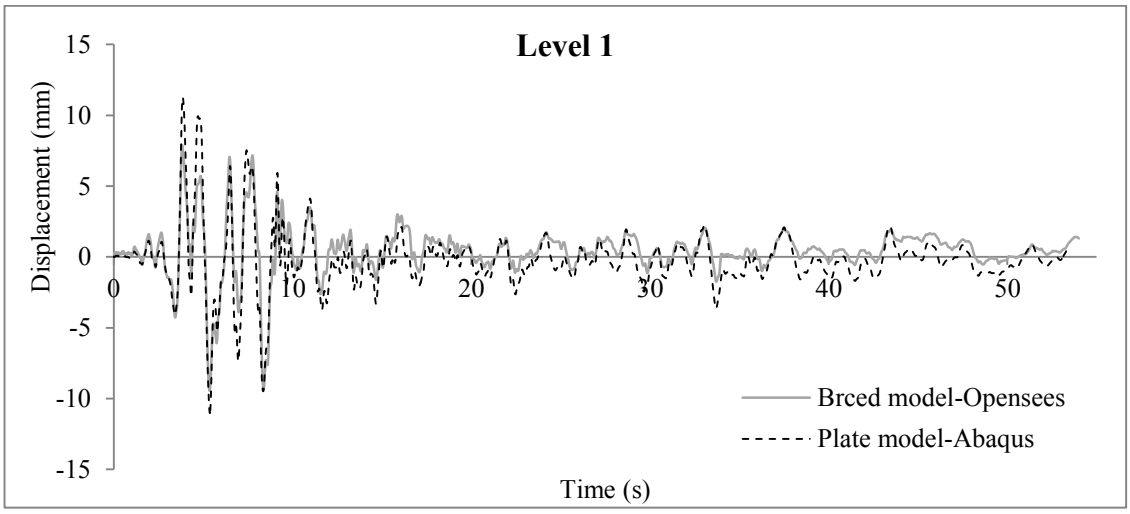

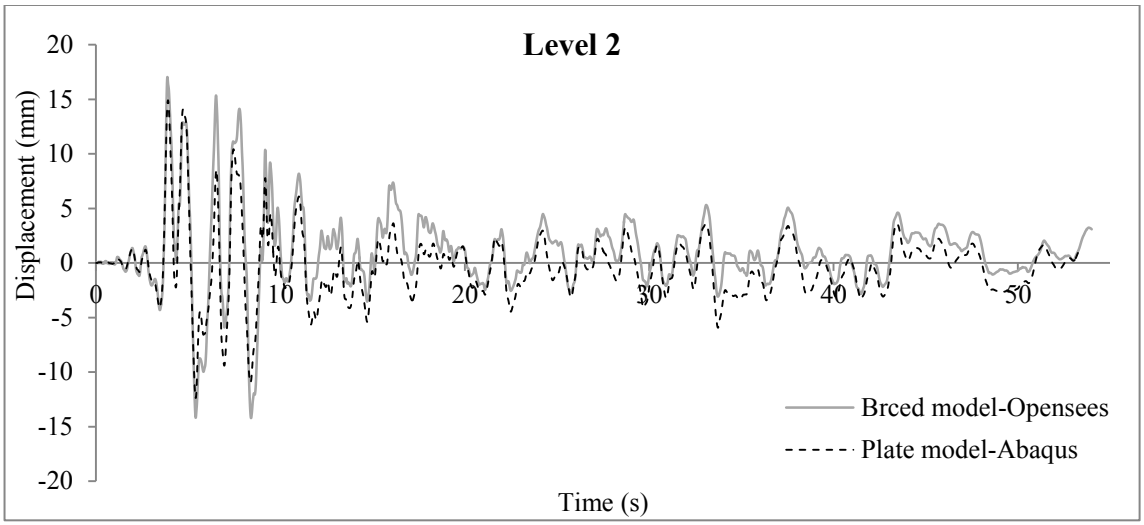
Level 2
Displacement (mm)
20
15
10
5
0
-5
-10
-15
-20
0
10
20
30
40
50
Brced model-Opensees
Plate model-Abaqus
Time (s)

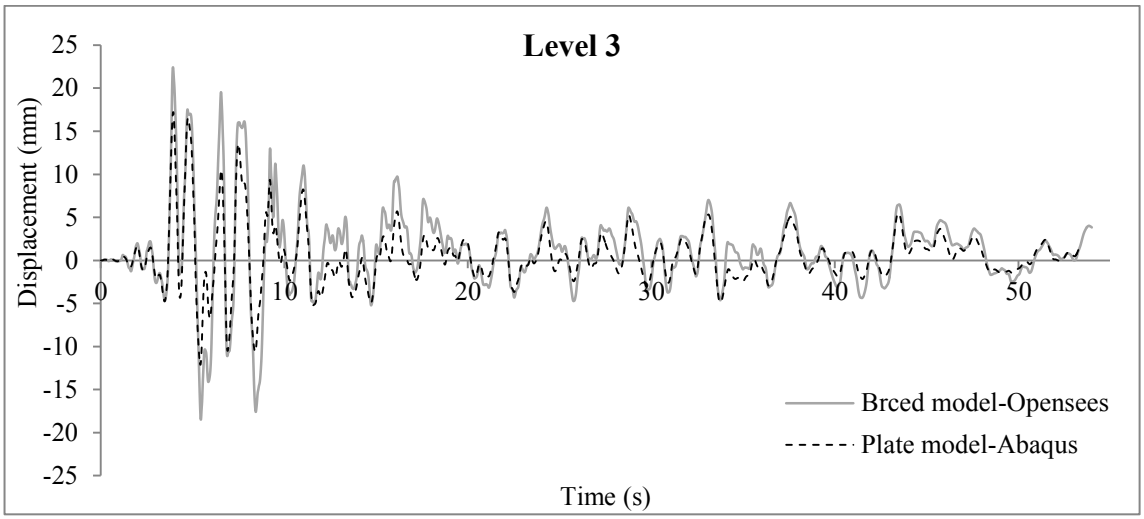
Level 3
Displacement (mm)
25
20
15
10
5
0
-5
-10
-15
-20
-25
0
10
20
30
40
50
Brced model-Opensees
Plate model-Abaqus
Time (s)

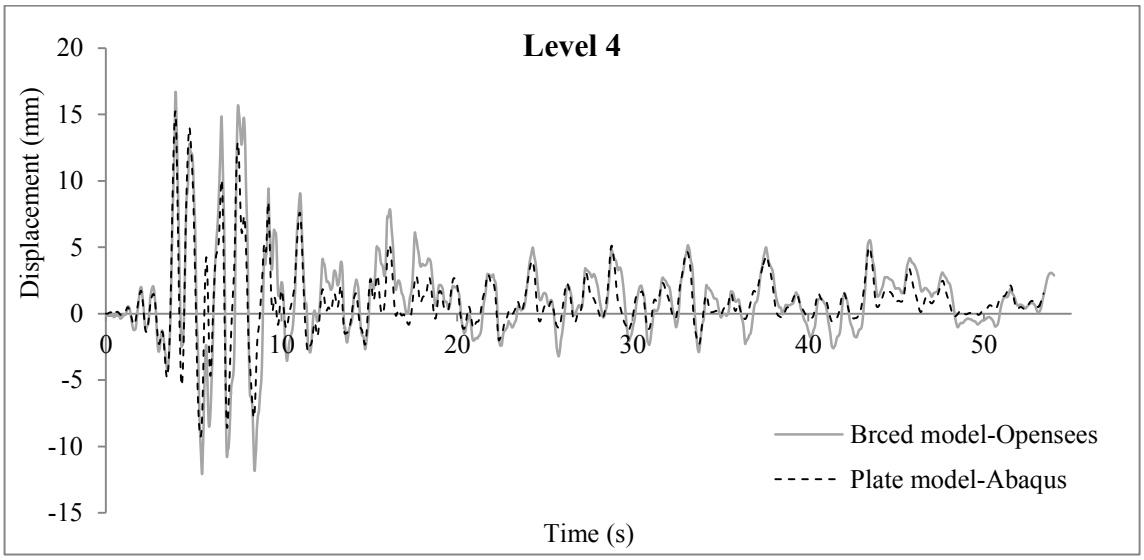
Level 4
Displacement (mm)
20
15
10
5
0
-5
-10
-15
0
10
20
30
40
50
Brced model-Opensees
Plate model-Abaqus
Time (s)

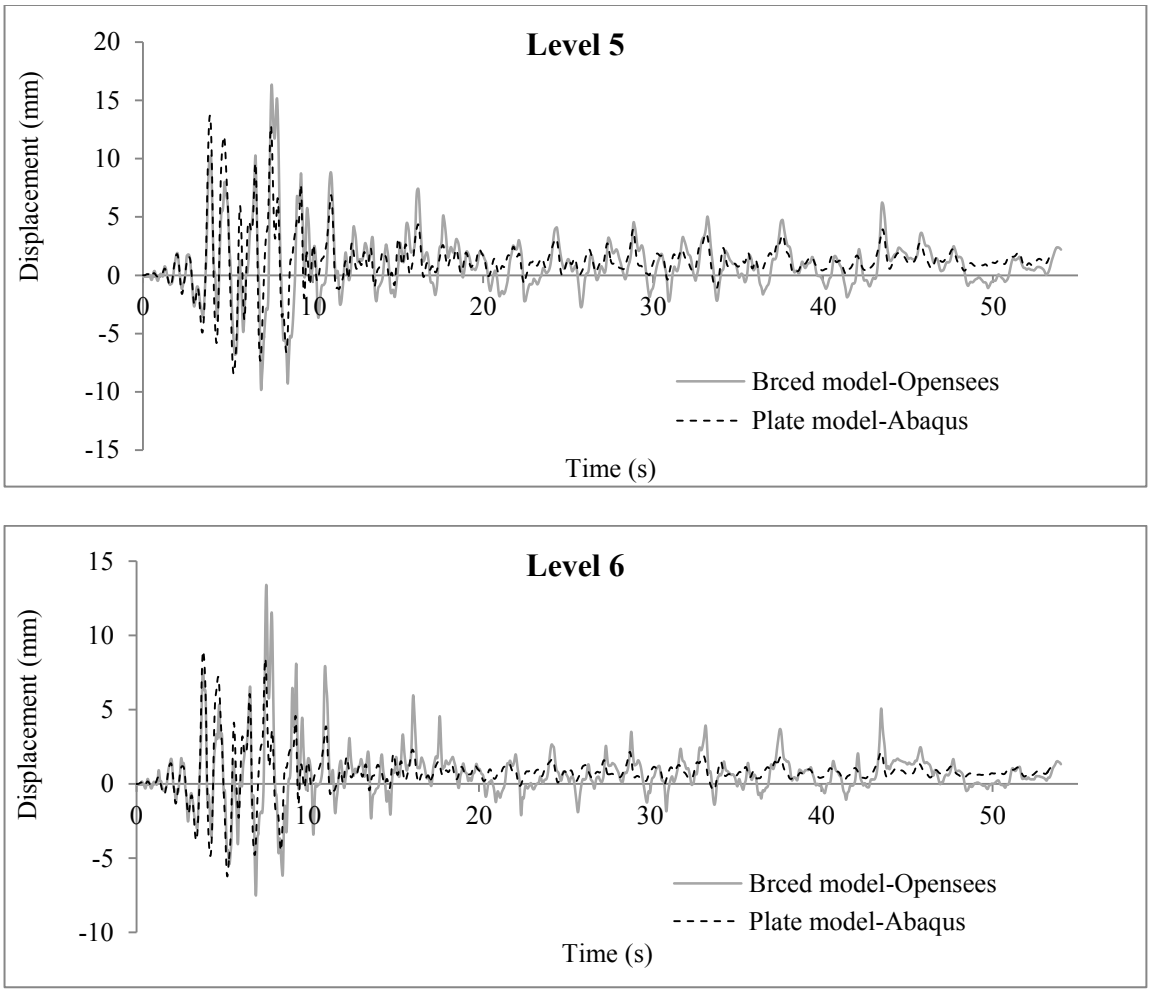

Figure II.2: Sample inter-storey drift for Earthquake Record No#2 at different storey levels as obtained from Abaqus and Opensees for 6-storey SPSW.

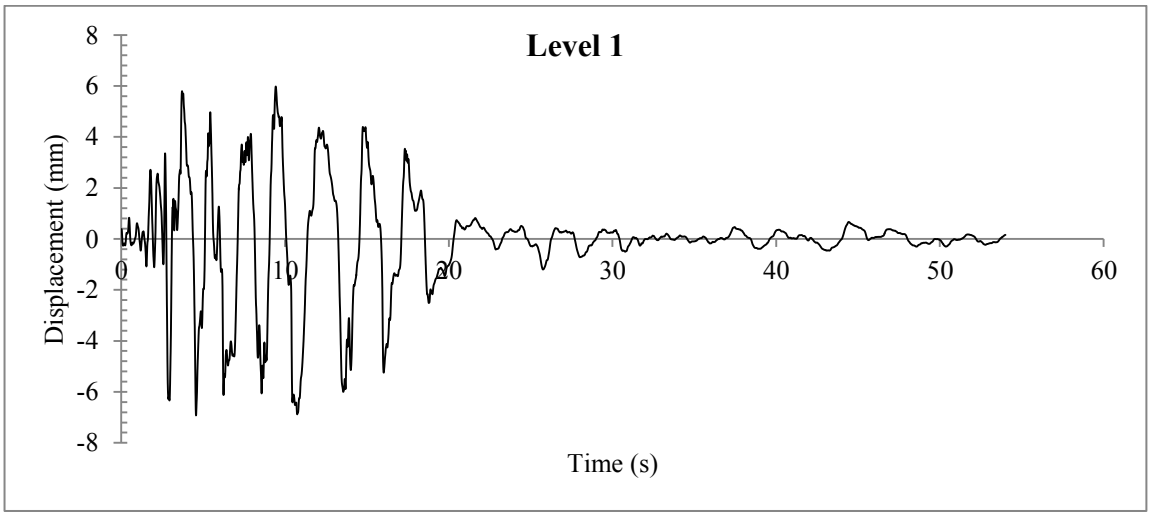

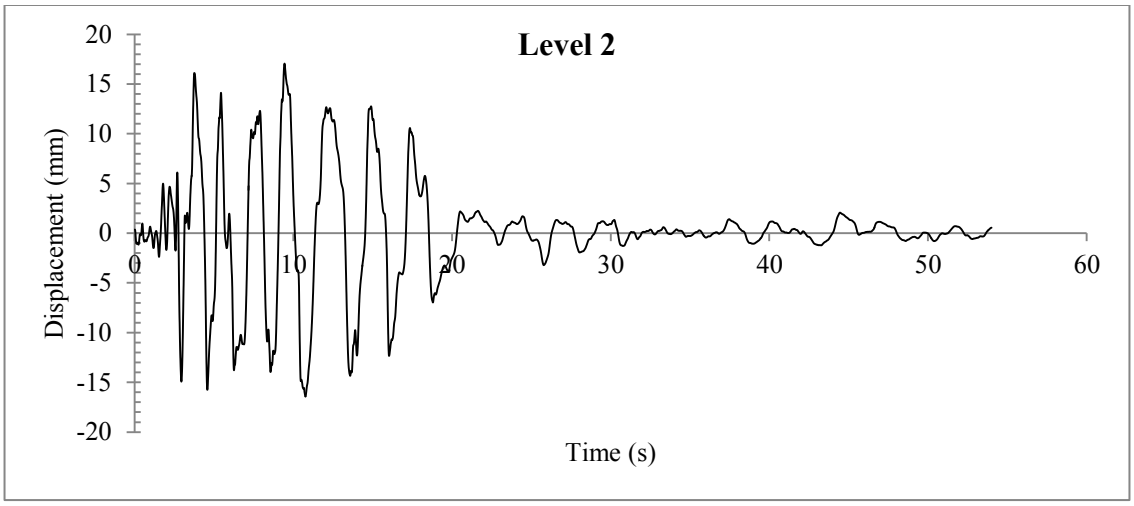
Level 2
Displacement (mm)
20
15
10
5
0
-5
-10
-15
-20
0
10
20
30
40
50
60
Time (s)

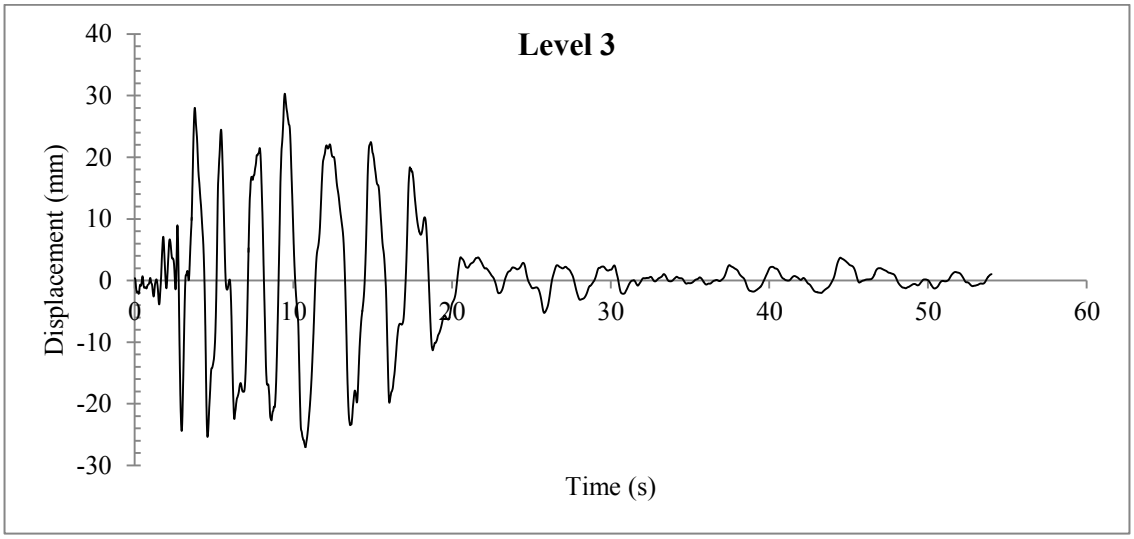
Level 3
Displacement (mm)
40
30
20
10
0
-10
-20
-30
0
10
20
30
40
50
60
Time (s)

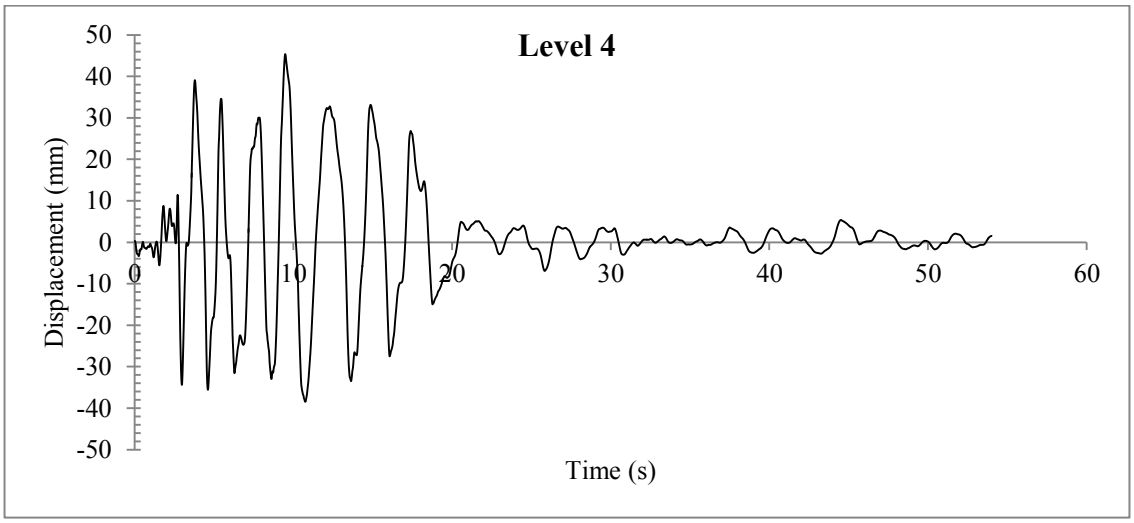
Level 4
Displacement (mm)
50
40
30
20
10
0
-10
-20
-30
-40
-50
0
10
20
30
40
50
60
Time (s)

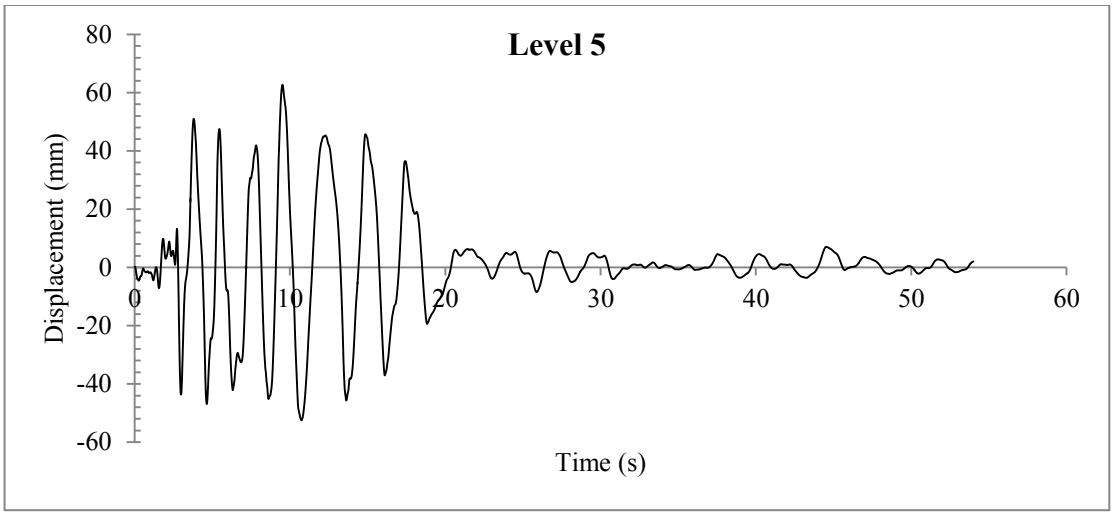
Level 5
Displacement (mm)
80
60
40
20
0
-20
-40
-60
0
10
20
30
40
50
60
Time (s)

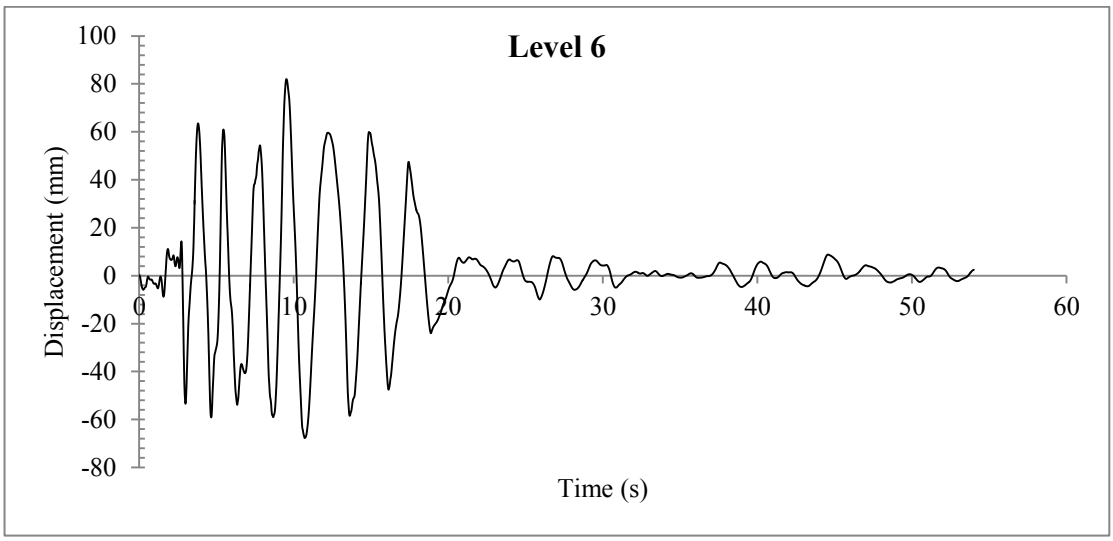
Level 6
Displacement (mm)
100
80
60
40
20
0
-20
-40
-60
-80
0
10
20
30
40
50
60
Time (s)

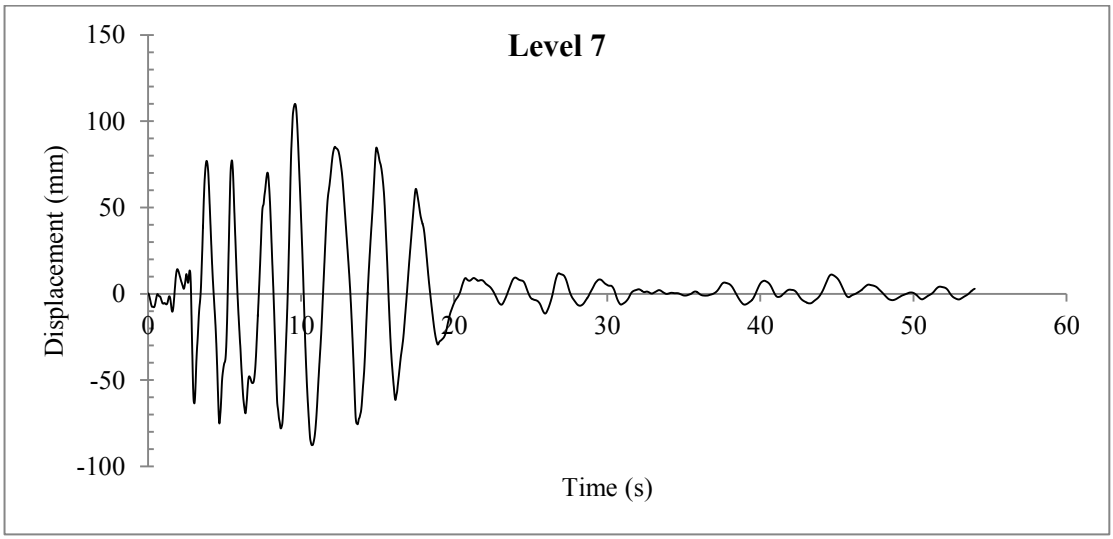
Level 7
Displacement (mm)
150
100
50
0
-50
-100
0
10
20
30
40
50
60
Time (s)

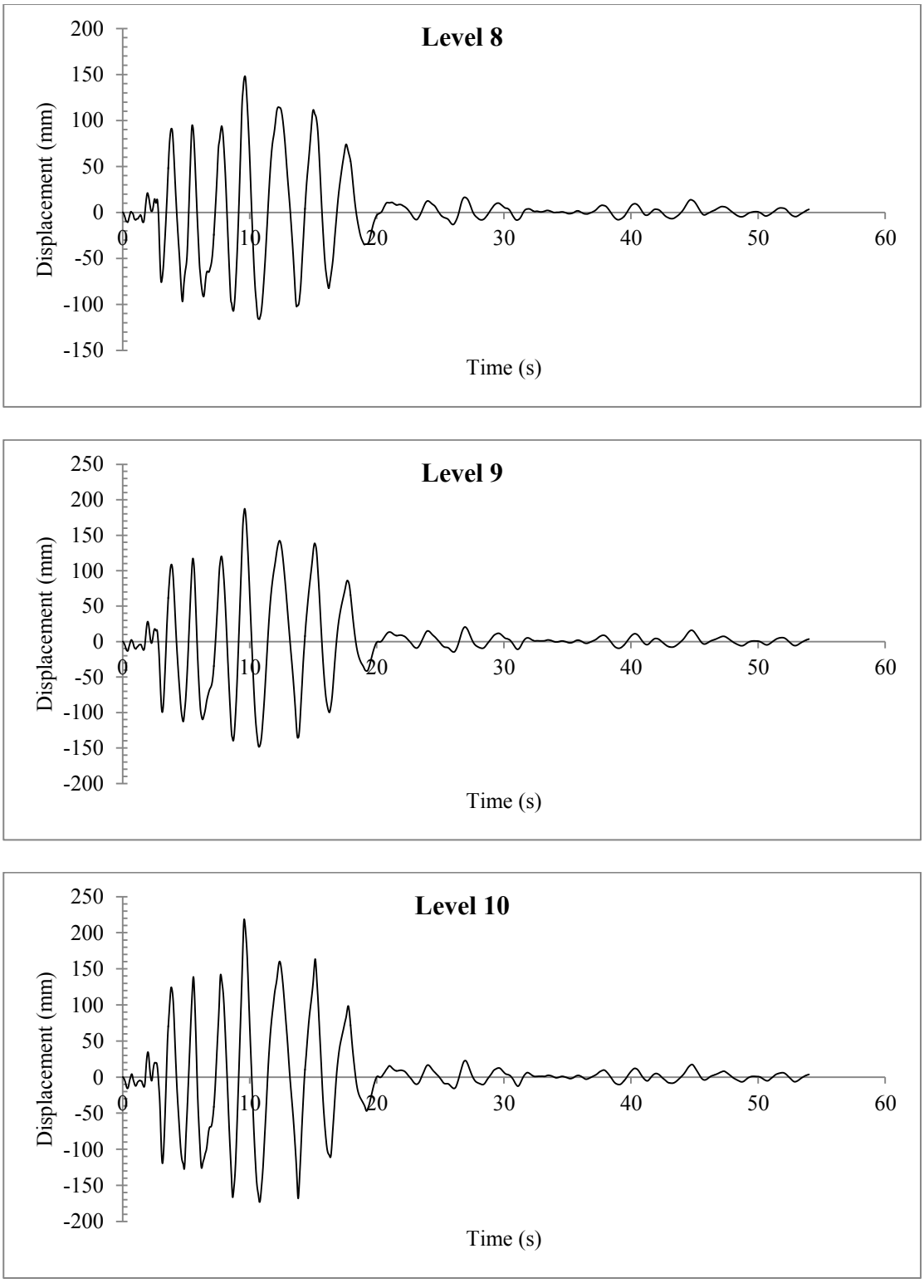

Figure II.3: Sample inter-storey drift at every storey height for 10-storey structure for Earthquake Record No#8 as obtained from Equivalent Braced Model (Opensees).